ADVANCEMENTS IN ROTOR BLADE CROSS-SECTIONAL ANALYSIS USING THE VARIATIONAL-ASYMPTOTIC METHOD

A Thesis
Presented to
The Academic Faculty

by

Anurag Rajagopal

In Partial Fulfillment
of the Requirements for the Degree
Doctor of Philosophy in the
School of Aerospace Engineering

Georgia Institute of Technology
May 2014

ADVANCEMENTS IN ROTOR BLADE CROSS-SECTIONAL ANALYSIS USING THE VARIATIONAL-ASYMPTOTIC METHOD

Approved by:

Professor Dewey H. Hodges, Advisor
School of Aerospace Engineering
Georgia Institute of Technology

Professor Olivier A. Bauchau
School of Mechanical Engineering
UM-SJTU Joint Institute

Dr. Vitali V. Volovoi
Independent Consultant

Professor Min-Feng Yu
School of Aerospace Engineering
Georgia Institute of Technology

Professor Graeme J. Kennedy
School of Aerospace Engineering
Georgia Institute of Technology

Professor Donald W. White
School of Civil and Environmental Engineering
Georgia Institute of Technology

Date Approved: 18 March 2014

To my teachers:

My parents,

Shri. Koteswara Rao,

Prof. Niranjan Naik,

Prof. Dewey Hodges,

Prof. Carl Sagan.

ACKNOWLEDGEMENTS

In writing this thesis and carrying out the corresponding research, I have been aided by several individuals. I would like to express my gratitude to all these fine people.

Under the guidance of my advisor, Prof. Hodges, I have experienced significant intellectual growth. As a structural dynamicist, he ensures his structures have eigenvalues with negative real parts, while as a mentor, he ensures that his protégés have eigenvalues with positive real parts. Several of his previous students, Drs. Ho, Yu, Volovoi and Harursampath were kind enough to dig into their past and answer my questions based on their doctoral work. In particular, I'd like to thank Prof. Yu for giving me access to the VABS source code so that I could code in and test some of the results of my developments. For introducing me to the fantastic world of engineering research and allaying my fear of the unknown, I would like to thank my undergraduate advisor, Prof. Naik.

I would like to acknowledge the efforts of my committee members, Profs. Hodges, Bauchau, Volovoi, Yu, Kennedy and White in helping me make this document more sound through their valuable feedback and insightful critique. I am also obliged to those who helped me proof-read my thesis: Phillip, Ravi, Avi and Shashank.

Coursework, while strengthening fundamentals also helps buffer the highs and lows that one experiences while doing research. I have thoroughly enjoyed attending the lectures of Profs. Bauchau, Hodges, Hanagud, Smith, Kardomateas, Lubinsky, Morley, Will, Alben, Zhou, Prasad, McCuan, Jagoda and Ozakin.

The US army VLRCOE has sponsored my education by supporting the development of VABS. While expressing my gratitude, I hope that they will support even more solid mechanics endeavors in the future. Prof. Jagoda, the AE graduate chair,

was of great help by ensuring that there were no hassles in the non-academic aspects of my graduate life. I am also much obliged to the people and government of the United States for their hospitality and for providing such wonderful educational opportunities for students like me, from all over the world.

My parents have fostered in me from a young age an appetite for knowledge and a strong ethical integrity. As with all aspects of my life, they have been the foundation for this effort too.

Over the course of several years in Atlanta, I've made some good friends: Nitesh, who was my house-mate for four years and Xin, with whom I've enjoyed several culinary adventures. I've had many technical discussions on dimensionally reducible structures with Ravi which aided my understanding of several ideas. I would also like to thank Seundo Heo and his wife for occasionally inviting me to watch movies and have dinner with them. I will miss the company of my peers in Weber 213: Ravi, Wei, Xin, Phillip, Seundo, Pezhman and Hanif. If there is only one thing I should be allowed to say without fear of contradiction, it is that all these gentlemen have bright and shiny futures ahead of them.

Finally, I'd like to unequivocally point out that should any errors be discovered in this thesis, they should be traced back to me and me alone.

TABLE OF CONTENTS

LIST OF TABLES

LIST OF FIGURES

SUMMARY

Rotor (helicopter/wind turbine) blades are typically slender structures that can be modeled as beams. Beam modeling, however, involves a substantial mathematical formulation that ultimately helps save computational costs. A beam theory for rotor blades must account for (i) initial twist and/or curvature, (ii) inclusion of composite materials, (iii) large displacements and rotations; and be capable of offering significant computational savings compared to a non-linear 3D FEA (Finite Element Analysis). The mathematical foundation of the current effort is the Variational Asymptotic Method (VAM), which is used to rigorously reduce the 3D problem into a 1D or beam problem, i.e., perform a cross-sectional analysis, without any *ad hoc* assumptions regarding the deformation. Since its inception, the VAM based cross-sectional analysis problem has been in a constant state of flux to expand its horizons and increase its potency; and this is precisely the target at which the objectives of this work are aimed. The problems addressed are the stress-strain-displacement recovery for spanwise non-uniform beams, analytical verification studies for the initial curvature effect, higher fidelity stress-strain-displacement recovery, oblique cross-sectional analysis, modeling of thin-walled beams considering the interaction of small parameters and the analysis of plates of variable thickness.

The following are the chief conclusions that can be drawn from this work:

1. In accurately determining the stress, strain and displacement of a spanwise non-uniform beam, an analysis which accounts for the tilting of the normal and the subsequent modification of the stress-traction boundary conditions is required.
2. Asymptotic expansion of the metric tensor of the undeformed state and its

powers are needed to capture the stiffnesses of curved beams in tune with elasticity theory. Further improvements in the stiffness matrix can be achieved by a partial transformation to the Generalized Timoshenko theory.

3. For the planar deformation of curved laminated strip-beams, closed-form analytical expressions can be generated for the stiffness matrix and recovery; further certain beam stiffnesses can be extracted not only by a direct 3D to 1D dimensional reduction, but a sequential dimensional reduction, the intermediate being a plate theory.
4. Evaluation of the second-order warping allows for a higher fidelity extraction of stress, strain and displacement with negligible additional computational costs.
5. The definition of a cross section has been expanded to include surfaces which need not be perpendicular to the reference line.
6. Analysis of thin-walled rotor blade segments using asymptotic methods should consider a small parameter associated with the wall thickness; further the analysis procedure can be initiated from a laminated shell theory instead of 3D.
7. Structural analysis of plates of variable thickness involves an 8×8 plate stiffness matrix and 3D recovery which explicitly depend on the parameters describing the thickness, in contrast to the simplistic and erroneous approach of replacing the thickness by its variation.

I

A LAY INTRODUCTION

> *It was kinder, gentler time in 1936, and it is interesting to read the informal beginning of Einstein's paper on gravitational lensing, which after all was published in a distinguished scientific journal: "Sometime ago RW Mandl paid me a visit, and asked me to publish the results of his little calculation, which I had made at his request. This note complies with his wish."*
>
> – Lawrence Krauss, *A Universe From Nothing*

The 20^{th} century and the first decade of the 21^{st} century have borne witness to a significant growth of science (and subsequently its applications: engineering and medicine). Mankind has crossed frontiers which seemed unimaginable and progress has been achieved by leaps and bounds. Unfortunately, while the fruits of science (by and large) have been experienced by the general public, a side-effect is that the understanding of science is increasingly alienated from the public (for example, by use of scientific jargon).

Therefore, this chapter is intended for the lay person to understand the goals and objectives of this thesis. I must add that this effort is in no way perfect; and having spent approximately 8 continuous years in engineering schools, my language has been unconsciously corrupted by engineering jargon, which obviates for me, some terms. Unfortunately, I am unable to write the rest of the thesis in this manner, the only consolation I can offer is that relevant references are provided wherever appropriate.

I would like to start this introduction from very fundamental and humble beginnings by a definition of reality (in the context of this thesis, the reality which is alluded to is 'physical reality'). When something is referred to as 'real', it can be

experienced through one of our five sense organs. Sometimes, the senses need to be enhanced, for example, using instruments such as microscopes to enhance our vision so as to see tiny organisms not visible to the naked eye. When neither of these are possible, one can resort to describing reality through models. For example, consider the Bohr model of an atom, where electrons revolve around a proton and neutron core.

Models constructed by using the scientific method have shown to best correspond to physical reality and this has been the proponent of the progress which I alluded to in the beginning.

1.1 Engineering Research

Engineering research today involves the construction of such models to capture reality. The starting point of an engineering problem is usually a system under a particular environment(s). The engineer is asked to determine certain aspects of the system which characterize its behavior in that environment. The three main stages or parts of a research initiative involve:

1. Identification of the physical mechanism that corresponds to the behavior of the system under that particular environment, which can be converted into an engineering model using mathematics.

2. Extraction of data corresponding to a prototype of the system under the pertinent environs. This will ideally involve construction of an experimental test facility.

3. Rework the model (recheck and/or relax assumptions) if its predictions do not confirm to data. In the extreme case, one might have to discard the model (which requires a good deal of mental conviction and strength).

The question naturally arises so as to why one needs to construct a model when data can be collected from an experimental test which exactly corresponds to physical reality. The reason for this is that in engineering, one needs to tweak the parameters of the model (corresponding to the features of the system) before deciding what's best. For example if I am interested in designing an aircraft wing, one of the first questions is what material should I use? Let's say I have the data of various materials and their relevant properties. To throw in another set of parameters, the client might also be interested in the behavior of the system in a range of environments. I cannot build prototype wings from each and every material and subject them to the relevant tests corresponding to each and every environment. This would be far too expensive and time-consuming. Instead I come up with an engineering model which predicts the relevant outputs of the system and to test this model I carry out the experimental studies with a limited set of materials to see how the model does. If this works, I am reasonably confident that when my model is applied to a new wing of some new material, the results confirm to reality. Of course, one can be fooled by models that are riddled with assumptions and simplifications to work only for those materials which were used in the experiment.

1.2 Structural Analysis

Aerospace engineering is a term used to collectively define the various engineering tasks where the system is an aircraft or spacecraft vehicle and the environments are its operating conditions. Fundamentally, the origins of aerospace engineering come from other disciplines, for example: fluid mechanics and propulsion systems (mechanical engineering), structural analysis (civil and material engineering) and control systems (electrical engineering); with of course an 'aerospace focus,' so to speak.

The broad category to which this work can be slotted is structural analysis. A clear definition of the terms 'structure' and 'load' follow. A structure can be a part of

the aerospace vehicle or the aerospace vehicle itself. The loads acting on the structure are forces and moments. (While force has a clear meaning, a moment is a kind of load which is generated in a small ruler if you were to hold either end in each hand and bend it). Loads are caused primarily by the fluid flow over the structure and propulsive systems such as engines, if any. Structural analysis (along with rigid-body dynamics) considers a structure under a given load and determines the final configuration of the system. As a simple example, consider a rubber eraser. Use your pen and mark two spots near the ends. Now hold one end fixed, say the left; and at the right end, bend it or stretch it and see where the right spot is. It will no longer be in the same exact position with respect to the left spot. And the more you bend or stretch the eraser, the farther the right spot will be from the left position. You could also throw the eraser across the room, in which case both spots have moved, but with their relative positions unchanged. The former is called deformation, and the latter rigid-body motion. Sometimes both occur together, for example, say you walked across the room stretching the rubber in your hands. Now rigid-body displacements can be obtained simply by Newton's laws (called rigid-body dynamics). Structural analysis is an engineering analysis which will tell you quantitatively what the deformation is. By knowing both, you can therefore know the total displacement (the final minus initial configuration of the system) of any point on the structure.

It must be pointed out that while deformation is the fundamental output of structural analysis, there are auxiliary outputs which include operation limits of the vehicle, stability boundaries, natural frequencies (when you excite a structure and leave it to itself, the rate at which it oscillates) and so on. Of course, a structural analysis model can also be used when performing a fluid-structure interaction study, commonly referred to as aeroelasticity.

Structural analysis involves three major steps:

1. A description of deformation, which usually involves the definition of quantities

called strains. The strains are written in terms of displacements.

2. A material law which relates the strains to quantities called stresses. Stress is usually some form of force per area of application.

3. A statement of Newton's law which relates the stresses.

Sometimes, it is possible to solve for these equations exactly. These solutions comprise what is known as the Theory of Elasticity (ToE). Unfortunately, the set of such solutions is quite limited and most of them can be found in the extraordinary treatise on the same subject matter by Love [76]. A more practical way of solving these set of equations is by making some assumptions on the problem, is referred to as the Strength of Materials (SM) approach. Indeed undergraduate courses on structural analysis focus on this approach. The most famous example of this method is the Euler-Bernoulli beam theory. The progress of the SM approach till 1950 has been sketched in detail by Timoshenko [110]. Another solution method involves recasting step 3 of the structural analysis procedure in energy-like terms and attempting to satisfy the equation not at every point but 'averaged' out on the structure as a whole. These are referred to as Variational Methods (VM) and it must be noted that they are only as good as the theory you base them on.

Over the past few decades, two important developments have taken in place in the field of engineering structural analysis. With the advent of significant computational resources, especially in the past few decades, it has become possible to obtain very close approximations of exact three dimensional (3D) elasticity solutions using what is known as the Finite Element Method (FEM). This method involves dividing the structure into several small parts and then applying the equations, cast in a variational form, over small parts. As the divisions get smaller and smaller, the solution is expected to get more and more precise, offset by requiring more computational resources. At the time of writing this document, the 3D FEM is the most widely

accepted method of carrying out structural analysis in academia and industry.

Traditionally aerospace vehicles were made of metals, aluminum being the primary choice. Metals are usually isotropic materials, i.e., their properties are same in all directions. This would seem a material over-indulgence in cases where loads are only along specific directions. The second significant development in structural analysis over the past few decades is the usage of composite laminated materials whose properties are different in different directions. Due to the directional nature of these materials, the properties of the structure can be tailored to suit certain requirements. The introduction of composite materials, however, has necessitated more rigor in the models developed for structural analysis (certain assumptions made might work for isotropic materials but fail in the presence of anisotropy).

Despite the advent of computational resources, there are still structures such as helicopter rotor blades for which building 3D FE models and running them will consume inordinate amounts of time and need exceptional skill. To see how complicated a blade can be, please refer to Chapter 2. Design exercises for tailoring the properties of these blades are therefore cumbersome and excruciating when done using FEM.

One feature of the helicopter blade that can be exploited by the structural analyst is that one of its dimensions is very large compared to the third. (Another feature is the 'gentleness' of curvature and twist, but I will not touch on how this can be exploited in this chapter). By using the appropriate mathematics, the 3D problem can be reduced into a 1D problem. This dimensional reduction, called a cross-sectional analysis, is achieved by evaluating the cross section (the two-dimensional surface perpendicular to the long dimension) deformation in terms of quantities (still unknown) which describe the 1D problem. This can be done analytically and only once for the entire problem (if the beam is spanwise uniform). In order for the 1D problem to be as close as possible to the 3D problem, the assumptions on the cross section deformation should be as minimal as possible. Obviously, solving a problem in 1D

will be cheaper computationally – one obvious reason being you will have far fewer divisions to make than for the 3D structure.

The dimensional reduction process described in the previous paragraph is usually accompanied by *ad hoc* assumptions regarding the deformation of the cross section. One very common example, still in use today, is that the cross-sectional surface remains rigid in its own plane, i.e. any point on the cross section will have deformed only in the 'long' direction and not in the two directions that determine the cross section itself. Unfortunately, such assumptions do not paint a picture close to reality, for complex geometry and anisotropic material. It is best if we do away with these assumptions if we are to use this model for a helicopter blade. One way of completely doing away with assumptions is to use asymptotic methods.

The primary focus of this work was the development of structural tools for the analysis of rotor blades. I would like to state at the outset that the efforts for developing these tools, now christened, VABS and GEBT (see Chapter 2) have been underway for more than 20 years. My contribution to this program was to first understand the procedure and make some refinements to add new features and test the existing capabilities of VABS. Hence the title. To understand these refinements and studies, the reader (at the very least!) needs to read Ref. [46]. I need therefore stop here lest I fall into the trap of over-simplification.

II

MOTIVATION

To tell us that every species of everything is endowed with an occult specific quantity by which it acts and produces manifest effects, is to tell us nothing; but to derive two or three general principles of motion from phenomena, and afterwards tell us how the properties and actions of all corporeal things follow from those manifest principles, would be a very great step.

– Issac Newton, *Optics*

2.1 Introduction

Rotor blades, like several critical load carrying members of an aircraft (fixed- or rotary-wing) are slender structures which are typically incorporated with a gentle curvature (usually in a direction along the length of the blade, referred to as twist). During the course of the vehicle operation, they undergo large displacements and rotations; necessitating the use of a geometrically non-linear analysis. Over the past few decades, composite materials have revolutionized the field of aerospace structural engineering due to their directional nature which lends itself to tailor properties as per the requirement; and their excellent fatigue behavior. With the introduction of composite materials, the rotor blade section has grown complex, as shown in Fig. 1. Due to the features mentioned above, a full non-linear 3D finite element analysis will be computationally intensive, and the effort grows higher if one wishes to link the structural analysis to perform an optimization or aeroelastic analysis.

The geometry of the rotor blade naturally suggests to an analyst to be modeled as a beam. A beam theory, however, involves a substantial mathematical formulation

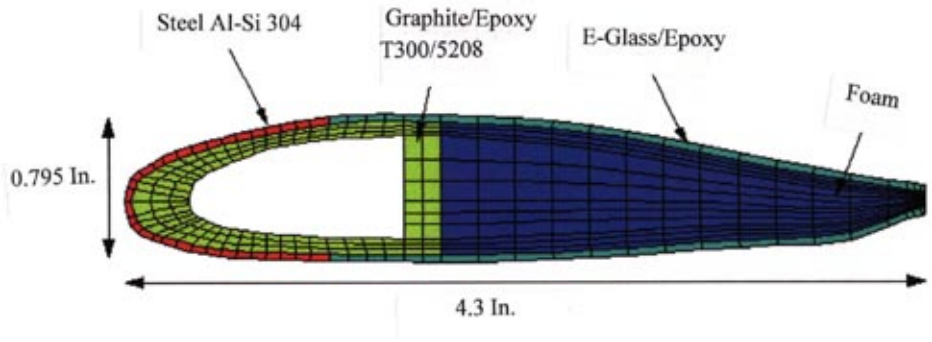

Figure 1: A typical rotor-blade cross section

that ultimately helps save computational costs. A beam theory must address the following three issues: A cross-sectional analysis which reduces the 3D problem into a 1D analysis (dimensional reduction), the equations which describe the 1D analysis, and finally a merging of the results from the 1D problem into the cross-sectional analysis to recover 3D quantities which describe the deformation of the structure (often referred to as recovery). A beam theory thus developed then should be able to able to satisfy the following requirements:

1. Include the effects of geometric non-linearity
2. Allow for the inclusion of composite materials
3. Model the effects of initial twist and curvature
4. Obtain results with accuracy equivalent to that of a fully non-linear 3D FEA analysis

The origins of the solid mechanics of beams can be traced back to the theories of Euler-Bernoulli and St. Venant, which describe the deformations of extension and bending, and torsion respectively. These were followed by the seminal developments of Timoshenko in introducing transverse shear and Vlasov [113] who showed how restrained warping effects at the boundaries penetrate into the beam interior solutions. The assumptions used in these works displays their extraordinary insight into the solid mechanics of the pertinent problems. Though these serve as very good origins

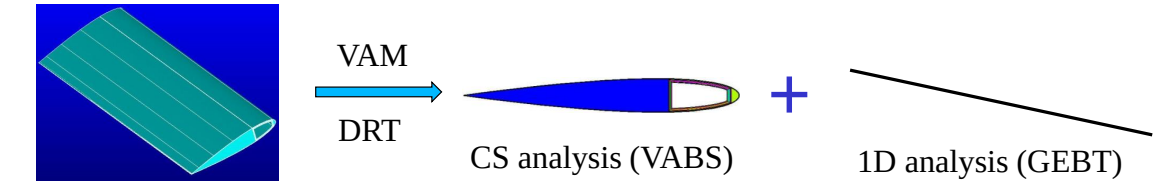

Figure 2: Structural analysis methodology for a rotor blade

for further development of beam analysis, assumptions of a nature similar to or which are inspired by the postulates of these classical works cannot be used to address the problem of rotor blades due to the requirements specified. A comprehensive review of beam theories developed till 2004 is provided by Ref. [46]. The described classification of beam theories therein still holds for the developments that one may encounter in the latest literature. *Firstly*, come the theories which make some *a priori* assumptions regarding the cross-sectional behavior and obtain equations which describe the 1D analysis; often these theories are found to have internal inconsistencies. *Secondly*, are the theories which model the structure as a 1D continuum and rely on external sources for the sectional properties. *Finally*, comes the third approach, wherein the 3D continuum mechanics of the structure is a decoupled into a 2D cross-sectional analysis and a 1D beam analysis which are consistent with each other. It is obvious by now that the third approach is far superior and complete when compared to the first two.

With respect to the third approach, it is essential to state the seminal works of Berdichevsky [15] and Danielson and Hodges [29] which introduce the ideas of the Variational Asymptotic Method (VAM) and Decomposition of the Rotation Tensor (DRT) which decouple the 3D nonlinear elasticity problem into a **linear** cross-sectional and **nonlinear** 1D analysis (see Fig. 2). A linear cross-sectional analysis suffices in most cases for rotor blades as, while they undergo large displacement and rotations,

the strains are still small [46].

Several excellent works exist concerning the geometrically exact equations pertaining to the 1D beam analysis. A representative list of such publications follows. Reissner [93] was one of the first works to present a large-displacement finite-strain beam theory. An unusual aspect of this work is the extraction of strain-displacement relations using the principle of virtual work. The Rodrigues parameters were used to describe finite rotation and the idea of intrinsic equations was touched upon. Wempner [120] extracted the equations for thin curved and twisted rods using the principle of virtual work. The works of Simo and his co-workers [101, 102] extend the classical Euler-Kirchhoff-Clebsch equations by including finite extension and shearing using a geometric mechanics approach. The 1D geometrically nonlinear beam equations of Hodges [46] have found application in the mixed-variational formulation of GEBT (Geometrically Exact Beam Theory)[126] and the intrinsic equations of NATASHA (Nonlinear Aeroelastic Trim and Stability of HALE Aircraft) [83]. These equations are also used in the beam element of the multibody dynamics tool DYMORE [12]. While literature pertaining to rotating beams mention the works of Ref. [52], followed by the well recognized Ref. [45], it has been established that the mixed variational formulation of Ref. [43] has superseded the latter.

The focus now shifts to the cross-sectional analysis problem. Several outstanding methods exist for determining the sectional constants and recovering the 3D fields once the 1D variables are solved for. Borri and his co-workers [37, 17] based their approach on linear elasticity and extracted a 6×6 cross-sectional stiffness matrix using the principle of virtual work. The tools BECAS and NABSA are based on this approach. A novel approach is introduced by Ref. [36] where the sectional properties are obtained by modeling the cross section as a slice using solid 3D finite elements. In a recent work [14], Bauchau and Han performed the cross-sectional analysis in tune with

three-dimensional elasticity based on a Hamiltonian formalism, the only approximation introduced by the finite-element discretization of the section. Another rigorous methodology of recent times in the Formal Asymptotic Method (FAM) wherein the asymptotic analysis is applied directly to the governing equations (rather than a variational equivalent of the same). The analysis begins by using the slenderness ratio to define a 'slow' and 'fast' set of coordinates; for example, the slow coordinates, would refer to the cross-sectional coordinates divided by the slenderness ratio; and the axial coordinate. Buannic and Cartaraud [18] employed the FAM to develop a theory for beams whose elastic moduli varied periodically along the beam. A recent paper [62] has shown its ability to be comparable to the VAM, at least in the case of prismatic beams. Ref. [56] presents a structural model based on a mixed force and displacement method starting from a two-dimensional shell model. The results were validated for both open and closed section beams. The method of extraction of cross-sectional anlysis properties followed by by Dong and his co-workers [32, 64, 33] is to obtain the displacements from 3D elasticity (such as Iesan's solutions [53]), from which equivalent section properties are obtained. Another idea, explained in Ref. [59] is to extract section properties using the solutions for 'fundamental states', which are loading conditions such that there is only one stress-resultant at a convenient point such as the mid-point of the beam. Another method, which performs a reduction from 3D to 1D using the ideas of an axiomatic hypothesis and an asymptotic expansion method, goes by the name of Carrera Unified Formulation (CUF). The displacement field is written as a series using Maclaurin polynomials for the cross-sectional coordinates with unknown coefficients dependent on the axial coordinate. These are then evaluated using a finite element approach. In order to reduce the computational effort, an asymptotic analysis is used to detect and eliminate the DOF which are not relevant to the problem. Various cross-sections have been studied using this method [20] and it was shown that the model was able to satisfactorily predict natural frequencies [19].

Silvestre and Camotim [99, 100] construct a Generalized Beam Theory (GBT) for composite thin-walled beams starting from classical plate theory. The kinematics are developed based on the thin plate assumptions of the Love-Kirchhoff model and the principle of virtual work is used to obtain the final governing equations of the problem. Two models are developed: a first-order theory for geometrically linear analysis and a second-order theory for linear stability analysis by including the appropriate nonlinear terms in the kinematics.

Despite the presence of the above-mentioned works, composite beam theories with *ad hoc* assumptions are continuously being churned out even today. A result-based comparison is made near-to-impossible by a shortage of benchmark problems and experimental results; agreement with these few might give even a poorly constructed theory an outward semblance of generality. A quick literature review over the last couple of years throws up several developments which can be slotted into the first category of the beam theory classification previously alluded to. Ref. [78] assumes the cross-sectional contour to be rigid and the out of plane warping to be the St. Venant solution for isotropic beams, though the development is for composite materials. The Euler-Bernoulli formula for the deflection of a simply supported beam is used for the analysis of a reinforced concrete beam with CFRP (Carbon Fiber Reinforced Polymers) [105]. Further usage of the Euler-Bernoulli beam theory is seen in Refs. [24], [67] and [121] for studies of vibration suppression, multi-scale MEMS (Micro Electrical Mechanical Systems) and smart piezo and ferro electric materials, respectively. It should be noted that the latter fails to recognize that the sectional properties are dependent on initial curvature, which is by now a well established fact [89]. This approach is also prevalent in the analyses which employ higher-order elasticity theories (couple-stress, strain gradient, and so on), for example, for micro- and nano-scale structures. Refs. [77], [27], [3] and [117] are a testament to this fact.

Apart from these one encounters in literature several another class of works which

consist of novel ideas for a pertinent problem but are not general enough. Ref. [97] uses the 'line-element less' method (a numerical technique that sets up the problem in terms of a potential involving the shear stresses instead of warping) to solve the St. Venant's problem for orthotropic beams. Ref. [106] extended Love's solution for flexure of isotropic beams to radially inhomogeneous circular cross-sections, from which the shear stiffnesses were obtained. The St. Venant torsion problem of an anisotropic non-homogeneous beam is analyzed with the shear flexibilities evaluated in terms of Prandtl's stress function of the corresponding homogeneous bar in Ref. [35]. Mathematically rigorous definitions of the shear center and center of twist are provided by Refs. [9, 10]. Ref. [72] contains studies on the free vibration of a laminated composite beam using a hyperbolic shear deformation theory. For beams with initial curvature, analytical solutions for the stresses are provided for half-elliptic [111] and composite layered beams [11]. These nevertheless serve as excellent validation tools for any cross-sectional analysis model that claims to be general. The work of Ref. [98] is representative of another line of effort, of higher order beam theories (introducing more deformation modes than the usual six: extension, twist, two bending and two shearing modes), which in this case was to address the problem of excess boundary conditions at a clamped edge for the Timoshenko beam theory.

The focus of this thesis is the cross-sectional analysis of beams. Towards the end, an important problem concerning plates is also addressed. The principal tool used to obtain the solution of these problems in this dissertation is the VAM. In a nutshell, the procedure reads thus: Set up the variational statement of the geometrically non-linear elasticity formulation. Identify small parameters which are naturally inherent to the structure. For example, in rotor blades, these would be the slenderness ratio and the gentleness of the curvature. Solve for the unknowns recursively up to an asymptotic order deemed sufficient. For a more mathematically rigorous introduction to the VAM and the various nuances in its application to dimensionally reducible structures, the

reader is encouraged to consult Sec. I, Ch. 4 of Ref. [46]. This principle has been used to construct beam models as well as plate and shell models, the latest developments (excluding the ones found in this work) of which can be found in Refs. [129] and [125] respectively.

Prof. Hodges and his co-workers have been working on the problem of rotor blade cross-sectional modeling for over two-and-a-half decades and one of the first significant publications is Ref. [22]. Their efforts to model rotor blades at Georgia Tech. (and more recently, including Utah State/Purdue) have led to the development of the computer program VABS (Variational Asymptotic Beam Section), which is based on the VAM, for the cross-sectional analysis. VABS can also recover the 3D quantities: stress, strain and displacement once the beam (1D) problem has been solved. Users of VABS include Boeing, Siemens and the US army. Over the past decade, VABS has expanded from being simply a structural tool to include other multi-physics effects such as thermal [118] and piezoelectric [95]. An example of the time required for the structural analysis of a rotor blade using VABS has been studied by Yu and Hodges [130] and is presented in Table 1. A comparison with 3D FEM (Finite Element Methods) is listed for the stress analysis of graphite-epoxy beam $[-45/+45/0/90]_{10s}$ with geometry 0.25 in. $\times$ 1 in. $\times$ 5 in. loaded with a unit tip force. The computational savings are evident.

With the increase in computing speed over the past decade, the time required to run 3D FEM models has significantly reduced. It is important to note, however, that the ratio of the times required will still be the same, i.e., there will still be a relative difference of few orders of magnitude. Therefore, savings will still be evident for design exercises wherein parametric studies need to be conducted to determine the effect of a certain geometric parameter or material property (choice of composite material and layup angle) of the cross section. Reduced order structural models are also useful in aeroelastic studies and real time monitoring of structural components.

Table 1: Computational effort for the stress analysis of an orthotropic beam: VABS vs. 3D FEM [130]

	3D FEA (ANSYS)	VABS
Elements	25600 (brick)	640 (quad)
Time	$\sim$ 1hr	0.5s

Computationally, achieving these using traditional 3D FEM might be very difficult. Also, it is typical for monitoring instruments such as strain gauges to be mounted in regions of moderate stress and based on their outputs the behavior of the entire structure (especially the regions of extreme stress) needs to ascertained. Directly mounting measuring instruments in regions of extreme stress (for example, near the root of a fixed-wing aircraft) might affect their life and the accuracy of their readings. All these are possible situations wherein the usage of beam models for predicting the structural behavior might be expedient and fastidious.

To conclude, a rotor blade analysis procedure would involve the following:

1. Providing the blade-section material and geometry with the blade initial twist and curvature to VABS, which gives the mass and stiffness matrices;
2. Input into the 1D analysis (GEBT) to get static, steady state, eigenvalue, dynamic response, etc.
3. Put the resulting 1D solutions back into VABS, to obtain the 3D stress, strain and displacement.

2.2 Scope of Present Work

Since its initiation in the early 90s, the VAM based cross-sectional analysis problem and hence, VABS, has been in a constant state of flux, in a quest to increase its potency and expand its horizons. The work that went into this thesis is another such effort in doing so. The objectives of the current effort are better put in perspective

by a brief review of the work carried out so far by Hodges and his co-workers concerning cross-sectional analysis. The VAM based cross-sectional analysis first took concrete shape with the work of Cesnik [21]. A formulation was put forth for general anisotropic twisted and curved beams for a classical (0^{th}) and 1^{st} order analysis; the latter using a least squares solution. This led to the development of VABS as a research tool. This was followed by a study by Volovoi [114] on the end effects by using dispersion curves which led to an asymptotic development of the Generalized Vlasov (GV) theory. He also put forth an analytical formulation for thin-walled beams using a novel formulation, which goes by the name of a "phantom" analysis. Significant progress was then made by Popescu [87] on the modeling of transverse shear and the trapeze effect. He also developed an oblique cross-sectional analysis formulation for the classical theory. Further studies on geometrical non-linearity in the cross-sectional analysis was accomplished by Harursampath [39]; applications of which include the Brazier effect and a non-linear extension twist coupling for pretwisted strips. Significant strides were made in the commercialization of VABS with the development of a super-efficient code by Yu [124]. He also formulated better constraints (in-tune with 3D elasticity) on the warping field and a more rigorous solution for the 1^{st} order analysis by replacing the least squares solution with a Generalized Timoshenko (GT) form which uses a perturbation technique. Finally, was the work of Ho [40], who developed a more consistent formulation for the classical and GT theories and made an attempt in modeling spanwise non-uniformity. This work picks up directly where Dr. Ho left off [40] and the specific objectives will now be listed.

2.2.1 Recovery for Spanwise Non-Uniform Beams

Rotor blades often feature regions of spanwise non-uniformity. From a structural standpoint, there are various factors which might lead to a tapered blade design. For example, the cantilevered nature of a rotor blade causes stresses to decrease outwards

and the rotation of the beam causes centrifugal forces to increase outwards. From an aerodynamics perspective the reason seems to be relatively straightforward, as Ref. [70] states "Usually small amounts of taper over the blade tip region can help significantly improve Figure of Merit (FM) in hover. The benefits, however, seem lost for higher amounts of taper." (FM is the ratio of ideal to actual power required to hover). Examples of such blades are the ONERA SPP8 and Sikorsky "Growth" blade tip. A study on the effect of spanwise non-uniformity was initiated by Hodges et al. [48] using the example of the in-plane deformation of a linearly tapered isotropic strip. They addressed the previously unknown necessity that the sectional constants are explicit functions of taper. However, as mentioned in Sec. 2.1, a complete beam theory must address, three aspects, of which the second, i.e., the 1D analysis, is made simple in this problem. Therefore the recovery of stress-strain-displacement was still left to be dealt with. In order to complete the loop, so to speak, this issue is addressed in this research, thus presenting a complete picture as to how a VAM based beam theory addresses the structural analysis of beams with spanwise non-uniformity. It should also be mentioned that Sec. 1 of Ref. [48] includes a list of other works in literature which do consider taper in the cross-sectional analysis. Few of them have the rigor associated with a VAM development. Ref. [5] stands out as one of the few works that recognize that a tapered beam cannot be considered to be a collection of cross-sections each varying in dimension. The effects of taper on the cross-sectional stiffnesses, which was subsequently used to predict lateral torsional buckling, was shown not to be negligeble.

2.2.2 Analytical Verification of the Initial Curvature Effect

Numerical validation and verification studies of VABS with 3D FEM and experimental results is a continuous and ongoing process. Several significant studies include the works of Refs. [136], and more recently [65]. Both these approaches established,

without a doubt, the accuracy and computational superiority of VABS. Numerical studies, though useful in their own right do not offer the same verification capability as problems for which closed form analytical solutions can be obtained. An analytical solution provides the researcher with a in-depth understanding of the problem for improvements in the theory and makes the process of determination of errors, if any, much more tangible. The only analytical validation [127] for VAM (and hence VABS) was carried out for isotropic, prismatic beams with rectangular and elliptic cross-sections which possess 3D elasticity solutions. Further with the work of Ref. [40], significant validation was carried out for initially twisted beams. With emphasis now on initial curvature, two different lines of approach were pursued: a numerical validation study with 3D FEM as a comparison [65] and an analytical verification study with the identification and subsequent aid of a problem which had elasticity solutions. This research task deals with the latter.

The elasticity solutions for an initially curved strip of unit thickness subjected to a bending moment and tip shear force (as depicted in Fig. 3) are given in Timoshenko and Goodier [109]. Analytical closed-form expressions for the stiffness matrix and stress-strain recovery can extracted by the development of a beam theory for the in-plane deformation of this structure using the VAM, which can be used for a vis-à-vis comparison with the corresponding elasticity solutions for a successful validation.

The successful completion of this study with the motivation from the work of Hodges et al. [47] (which extracts an analytical solution for the problem, despite it being a layered composite laminate), suggested to the author that the above verification study can be extended to a initially curved composite laminate with layers distributed through the thickness. Of course, the term 'extended' is loosely used here; it is only meant as a quest for closed-form expressions for stiffness matrix and stress-strain recovery. The development must start from scratch and no results from the isotropic case should be used in this problem. From a review of the literature, it

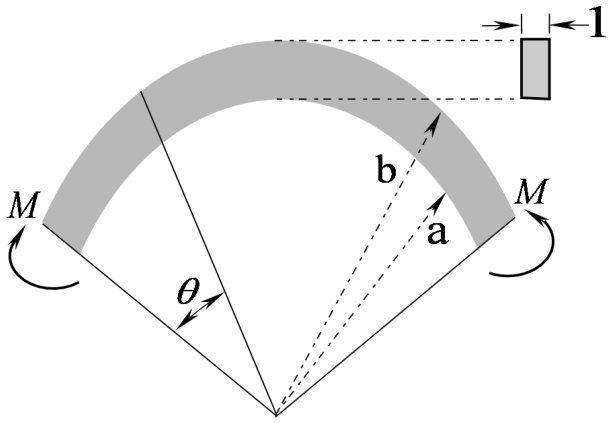

(a)

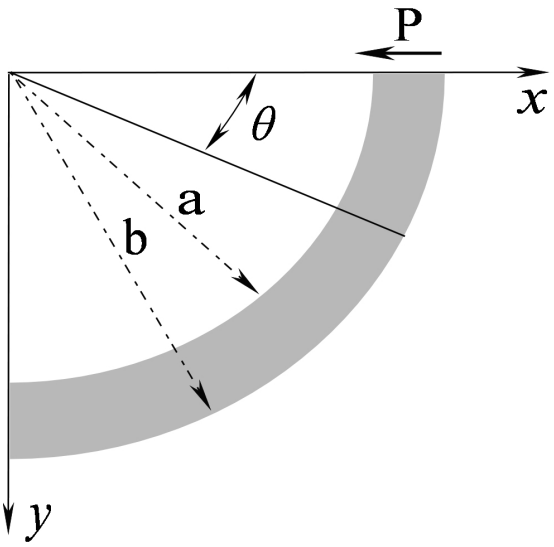

(b)

Figure 3: Strip of unit thickness with in-plane curvature subjected to (a) a constant bending moment and (b) a concentrated force at the end

was concluded that such a comprehensive treatment of laminated curved beams was clearly lacking; at best were studies like those of Ref. [75] which start from a plate theory based on the Love-Kirchoff assumptions. The study was further motivated by the findings of Ref. [8]; wherein it was reported that a wind turbine blade, one of whose features was a gentle lead-lag curvature towards the tip had an increased power output by a impressive 12%.

2.2.3 Higher Fidelity Stress-Strain-Displacement Recovery

Current capabilities of VABS include a stiffness matrix obtained from a second-order asymptotically correct strain energy and a stress-strain-displacement recovery which only incorporates the first-order warping and is hence only correct up to first-order in small parameters. Since the stiffness matrix is correct up to second-order, evaluation of the second-order warping is sufficient (without obtaining the subsequent energy which is expected to be asymptotically correct up to fourth-order) to capture the second-order terms in the final expressions for recovery. Therefore, the procedure resulting from this research task is expected to bring consistency in the analysis by raising the recovery to the same level of fidelity as the stiffness matrix. From the results of the previous problems on the tapered and initially curved isotropic strip, this procedure is seen to significantly improve the accuracy of the cross-sectional stresses, σ_{22}, σ_{23} and σ_{33}. These stresses are of paramount importance if one wishes to model the onset of damage in blades, required for the effort being pursued using VABS at Purdue University. The result of this problem is to provide VABS with second-order recovery capabilities in both the GT and GV models. To the best of the author's knowledge, this improvement in recovery is a first in beam theory development.

2.2.4 Oblique Cross-Sectional Analysis

Traditional structural analysis of beams involves the choice of a reference line and a cross section orthogonal to that reference line. However, there might be situations

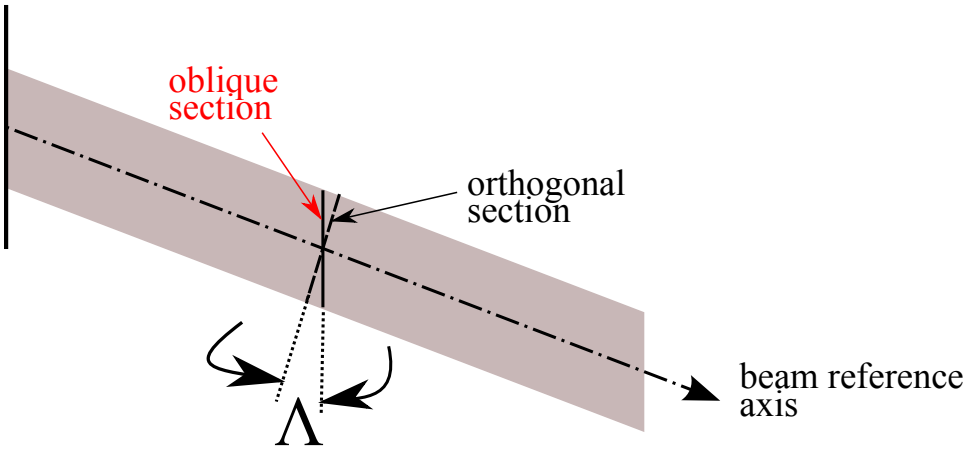

Figure 4: Schematic of swept blade or wing with normal and oblique cross sections

where an analyst might prefer a cross section which is not perpendicular to the reference line. One such frequently encountered case is rotor blades (or high $\mathcal{AR}$ wings) which are swept. A schematic of such problems is depicted in Fig. 4.

Also, for various reasons, it might be convenient for the user to use a cross section oblique to the reference line (for example, one might be interested in the variation of recovery in such a cross-sectional plane). Therefore, incorporation of the oblique cross-sectional analysis potency in VABS is of importance. A previous study successfully implemented the classical model for this problem [86]. However, due to several advantages, which include the ability to model transverse shear and capture the effects of twist and curvature, a GT model is preferred for analysis. Among the several shortcomings of the classical model is that the reference line chosen must be the locus of generalized shear centers [46], therefore a user of the current VABS must perform a normal cross-sectional analysis, gather the generalized shear center, shift the reference line and then carry out a oblique cross-sectional analysis to obtain the correct classical model. Therefore this research will address the development of the theory for incorporation of obliqueness into the GT model of VABS. In the reminder of this thesis, a cross section is taken to be orthogonal unless otherwise mentioned.

The idea of dimensional reduction using a oblique cross section was first introduced

by Borri et al. [17] who mention the possibility of "a cross section which could be tilted with respect to the reference line" and though it may be that Borri and co-workers have implemented the obliqueness feature in their cross-sectional tool, HANBA [37], to the best of the authors' knowledge an explicit formulation of such an analysis is not found in the literature. Another problem with a slight resemblance to the oblique cross-sectional analysis is the well known topic of skew plates. A large body of literature on skew plates involves the usage of an un-skewed plate theory (Love-Kirchhoff or Reissner-Mindlin) along with a transformation of the coordinate and variable to an axis system that describes the plate. Several such studies can be seen in the literature [73, 74], and to date analysis of skew plates has followed a similar approach [7, 69, 58]. It should also be noted that several of these studies use plate theories based on assumed displacement fields, unlike the more rigorous and consistent theory of Ref. [108] (which is based on asymptotic methods); and the corresponding global analysis [128]. In light of these studies it is important to note that the current analysis of oblique sections does not involve any transformations or adaptation of results from the existing VAM procedure (which goes into VABS) for orthogonal sections. The analysis for oblique cross sections will be carried out independently, from first principles.

The process is initiated by a VAM based analysis of an isotropic, prismatic strip and an isotropic prismatic beam (possessing a circular cross section) to develop a GT model. Again these cases are chosen because they have an elasticity solution [76] and since the development is expected to be analytical, it will aid in a through study of the intricacies of an orthogonal vis-à-vis a normal cross-sectional analysis. The expected outcome of these studies is to aid in the development of a fully functional GT model for VABS.

2.2.5 Thin-Walled Beams: Interaction of Small Parameters

The cross-sectional analysis which goes into VABS is a very general procedure which is not limited by considerations of geometry or material. However, in the case of cross sections which comprise of segments whose thickness (h) is small compared to a typical cross section dimension (a), also referred to as thin-walled beams, VABS produces singular stiffness matrices at moderate values of twist and curvature. For example, in the case of a graphite-epoxy strip $[45/0]_{3s}$ whose section measures 1.182 in. $\times$ 0.0579 in., and is initially curved out-of-plane (0.1 rad in.$^{-1}$), VABS outputs the bending stiffness in the hard direction to be -9.31×10^4 lb-in^2. A possible reason for this discrepancy is identified in Ref. [124], that when h/a becomes comparable to the existing small parameters of the asymptotic analysis, a/ℓ and a/R (where R =max.$(1/k_i); i = 1, 2, 3$; ℓ representing the wavelength of the deformation and k_i's representing the components of the initial curvature vector), it is necessary to take into account h/a as an additional parameter and develop the VAM based theory from scratch. The reason behind this is that in a previous work [115], where similar analysis was carried out, it was observed that terms of order h/a appear in the denominator, reducing the order of certain terms, which would otherwise be discarded as higher order. For example, terms of order $(h/a)^{-2}(a/R)^4$ which are of second-order and hence need to be considered while constructing a GT theory, might be discarded in the current analysis; yielding incorrect results. Again this problem is a specific issue concerning VABS and remains unaddressed in the current literature. It is emphasized here that this is not a 'bug' in VABS, but rather is a theory limitation, the addressing of which is fundamental problem worthy of research in its own right.

2.2.6 Plates of Variable Thickness

The results of the problem described in Sec. 2.2.1, available in literature through Refs. [48] and [50], which demonstrated that both the sectional stiffness matrix and

the recovery were explicit functions of taper, a result previously unknown, motivated the foundation of this problem. It is expected that the other class of dimensionally reducible structures, i.e., plates should also exhibit similar behavior. The VAM has also been independently used to obtain theories for plates and shells.

Leissa [71] provides a review of the analysis of plates with variable thickness till 1969. The Love-Kirchoff equations were used to analyze circular and rectangular plates with the constant h being replaced by a variable $h(r)$ and $h(x, y)$ respectively. In the former case, solutions were obtained for the case of $D = D_0 r^m$ (D being the plate flexural rigidity corresponding to classical plate theory) and the $h = h_0(1 + \alpha x)$ for the latter. Several works by Conway on the same subject, starting in early 1950s employed the same approach, i.e., solutions to the classical plate theory for a variable thickness (and hence variable D) by replacing D by $D(x, y)$. One such example is the work of Petrina and Conway [84].

Therefore the widely followed analysis methodology for plates of variable thickness can can be summarized as:

- Uniform thickness $\implies$ $D = \frac{Eh^3}{12(1-\nu^2)}$ $\implies$ Plate theory
- Variable thickness $\implies$ $D(x, y) = \frac{Eh(x,y)^3}{12(1-\nu^2)}$ $\implies$ Same plate theory as above

Since then, analysis of tapered plates has proceeded using on the same lines. Solutions have been obtained for different loadings, different boundary conditions, plates on an elastic foundation etc. but none of them acknowledge that the plate constants need to be explicit functions of taper. Bhat et al. [16] studied the effect of variable thickness on the natural frequencies of thin plates with linear taper in one direction by replacing D by $D(x)$ in the expression for potential energy for the classical plate theory. Singh and Saxena [103] studied the transverse vibration of an isotropic doubly tapered plate with various boundary conditions, replacing D by $D(x, y)$ in the expression for the potential energy of an untapred plate. Similar

studies were carried out for elliptic plates on an elastic foundation and plates made of functionally graded materials in Refs. [38] and [51] respectively. Even developments that search for analytical solutions, such as the recent work in Ref. [112], use the same approach. The authors study the axisymmetric bending of circular plates of a non-linear thickness. The cited papers only represent a sample literature in the sea of research on this topic using the current methods. Again a shortage of experimental results seems to hinder a comparison of effectiveness of these theories.

As in the case of beams, to study the effect of taper in plates, we consider an isotropic plate tapered (with different rates) along the global plate directions as shown in Fig. 70. This problem will yield a definitive insight on the effect of taper on the plate constants as well as the 3D recovery.

Plate elements can be used in bearingless rotors to model flex-beams which allow for blade pitching on account of their torsional softness. Apart from applications in rotor blades, the following are certain auxillary useful outcomes:

1. The panels (for example on a fixed wing) can be modeled as plates; and this permits modeling of these structures without restriction on their thickness.

2. Often one may model thin-walled beams using a "sequential" dimensional reduction. This means that the 3D elasticity problem is first reduced to a plate/shell problem which is further reduced to a beam problem. This has been demonstrated for the general case in Yu and Hodges [131] and later extended to include the effect of initial twist in Ref. [135]. Therefore, it might be the first step of an alternate approach on modeling spanwise non-uniformity in rotor blades.

Nevertheless the usefulness of this result from a fundamental mechanics perspective cannot be questioned.

III

RECOVERY FOR SPANWISE NON-UNIFORM BEAMS

It is a capital mistake to theorize before one has data. Insensibly one begins to twist facts to suit theories, instead of theories to suit facts.

– Sherlock Holmes, *A Scandal in Bohemia*

3.1 Introduction

It is typical in beam theory to assume that taper affects cross-sectional stiffness constants, stress and strain only from the change in section geometry along the beam axis. In other words, if for a homogeneous, isotropic beam, the bending stiffness is EI, then for a homogeneous, isotropic, tapered beam, the bending stiffness is simply written as $EI(x)$ where the area moment of inertia varies with the axial coordinate due to change in the sectional geometry arising from taper. A recent work [30] is one among a series of papers on tapered beams by the same authors that follows this methodology. In Refs. [2] and [31], the bending energy per unit length is simply written as $EI(x)\kappa^2/2$. Results in Ref. [2] were compared with those of an older work [92], both of which clearly follow this methodology. These are only a few selected examples out of the many recent works on tapered beams based on cross-sectional stiffnesses that are not corrected for taper.

An asymptotic beam theory for an isotropic strip-beam with linearly tapered width was presented in Hodges et al. [48]. Section stiffnesses for this theory depend on taper in ways other than the simplistic approach noted above. The main reason for this is the tilting of the outward-directed normal so that it has a non-zero component

This chapter was published as Hodges et al. [50].

along the beam longitudinal axis, and to be accurate the cross-sectional analysis must take this tilt into account. Because of the strip-like geometry, accuracy of the cross-sectional stiffnesses was evaluated using plane-stress elasticity solutions for extension, bending and flexure from Refs. [109] and [66] and were shown to be in excellent agreement. The plane stress problem of the in-plane deformation of an isotropic tapered strip was chosen because it is a simple example to illustrate the proposed theory. All results are closed form expressions that can be validated from corresponding elasticity solutions available in the literature.

One purpose of this chapter is to show that high fidelity information is available in beam theories based on asymptotic methods, which are no more complicated than "engineering" theories. This chapter focuses on the recovery of the stress, strain, and displacement fields for the linearly tapered isotropic strip-beam. This aspect was not addressed by Hodges et al. [48]. The recovery is performed by the VAM and is consistent with the derivation of the stiffness constants from Ref. [48]. It will be shown that to capture the recovery relations accurately, one needs to evaluate the warping one order higher than in Ref. [48]. The recovery relations are then compared with the corresponding elasticity solutions. This comparison will thus confirm that a VAM based beam theory is able to satisfactorily predict all aspects of the behavior of beam-like structures which feature regions of spanwise non-uniformity.

Section 3.2 of this chapter revisits the previous work [48] and reviews the importance of including taper in the stiffness constants. Section 3.3 provides details of the procedure to determine the recovery relations using the VAM and presents a comparison with the corresponding elasticity solutions. In Section 3.4, the range of the small parameters used in the VAM is determined for which the VAM solution is in close proximity with the elasticity solutions.

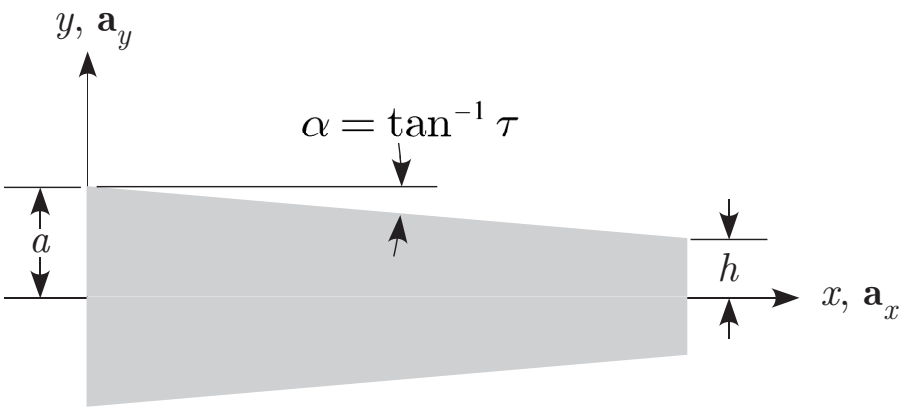

Figure 5: Schematic of the isotropic strip tapered beam

3.2 Corrected Stiffness Constants for a Tapered Beam

For better understanding of the results to be presented, a brief review of the VAM and a summary of the results from Ref. [48] is presented here. The VAM is used to perform cross-sectional analysis of beams using the principle of minimum total potential energy, exploiting the presence of small parameters. The total potential energy is developed from a general displacement field subject to a restriction to small strain. The leading terms of the energy can be obtained asymptotically in terms of the small parameters of the analysis, which can be used to obtain the equations governing in- and out-of-plane warping. This procedure can be repeated for successively higher powers of the small parameters until the desired accuracy is achieved. As a result of this analysis, the warping is expressed in terms of one-dimensional (1D) strains and can then be used to calculate the strain energy per unit length. This 1D strain energy per unit length provides the cross section constants, reducing the two-dimensional (2D) plane stress problem to 1D, and formulae that allow for recovery of stress, strain and displacement over the cross section.

An outline of the procedure to obtain the cross-sectional constants using the VAM for a tapered-strip beam as in Fig. 5 will now be presented. For further details, the

reader is encouraged to consult Hodges et al. [48]. The two small parameters of the system are a slenderness parameter $\delta = a/l$ and a taper parameter $\tau = -b'(x)$, which are assumed to be of the same asymptotic order. Considering the position vector of an arbitrary point in the undeformed and deformed configurations of the beam, the expressions for strain can be derived as

$$\begin{aligned} \Gamma_{xx} &= \overline{\epsilon} - y\overline{\kappa} + w_{x,x} \\ \Gamma_{xy} &= w_{x,y} + w_{y,x} \\ \Gamma_{yy} &= w_{y,y} \end{aligned} \tag{1}$$

where $\overline{\epsilon}$ and $\overline{\kappa}$ are the classical 1D stretching and bending strain measures, respectively. The strain energy per unit length is then

$$U = \frac{Et}{2(1-\nu^2)} \left\langle \Gamma_{xx}^2 + \Gamma_{yy}^2 + 2\nu\Gamma_{xx}\Gamma_{yy} + \frac{1-\nu}{2}\Gamma_{xy}^2 \right\rangle \tag{2}$$

where

$$\langle \bullet \rangle = \int_{-b(x)}^{b(x)} \bullet \, dx \tag{3}$$

The first step is to solve for the zeroth-order warping. For this, we identify and remove all the terms that are first and higher order in the small parameters from the strain energy. The resulting equations obtained using the principle of minimum total potential energy can be used to evaluate the zeroth-order warping, which in turn gives the zeroth-order strain energy per unit length as

$$U_0 = \frac{1}{2}EA(x)\overline{\epsilon}^2 + \frac{1}{2}EI(x)\overline{\kappa}^2 \tag{4}$$

which is the expected expression for strain energy per unit length associated with classical Euler-Bernoulli beam theory.

To refine this result it is necessary to solve for the warping corrected to first-order in δ and τ. To do so, the solution of warping previously obtained is perturbed to the next higher order. A similar procedure is preformed as described previously, the only difference being that all the terms in the energy correct through second-order in

the small parameters are retained. The first-order warping thus obtained is used to obtain the strain energy per unit length

$$U_2 = Etb(x)[1 - \frac{2}{3}(1+\nu)\tau^2]\overline{\epsilon}^2 + \frac{2}{3}Et\nu\tau b(x)^2\overline{\epsilon}\ \overline{\epsilon}' + \frac{Etb(x)^3}{9}[3 + 2(14\nu+15)\tau^2]\overline{\kappa}^2$$
$$-\frac{4}{9}Et\tau(8\nu+9)b(x)^4\overline{\kappa}\ \overline{\kappa}' + \frac{4}{15}Et(1+\nu)b(x)^5\overline{\kappa}'^2 + \frac{2}{45}Et(11\nu+12)b(x)^5\overline{\kappa}\ \overline{\kappa}'' \tag{5}$$

which is asymptotically correct through second order.

However, this strain energy per unit length is unsuitable for an engineering beam theory because it contains derivatives of the classical 1D strain measures. Hence, it is transformed into a generalized Timoshenko form as follows: First, the 1D classical strain measures are written in terms of 1D generalized Timoshenko strain measures using simple beam kinematics. A 1D shear strain measure enters into the picture through this transformation. Second, the derivatives of the 1D generalized Timoshenko strain measures are evaluated using equilibrium equations. The equilibrium equations can be simply obtained by the standard textbook approach of considering an element of the beam and writing the force and moment equilibrium.

Thus, the strain energy per unit length of a beam correct through second order, when transformed to the form of a generalized Timoshenko theory, is given by

$$U^* = \frac{1}{2}Z\epsilon^2 + \frac{1}{2}W\kappa^2 + \frac{1}{2}Y\gamma^2 + X\kappa\gamma \tag{6}$$

where

$$\begin{aligned} Z &= EA(x)\left(1 - \frac{2\tau^2}{3}\right) \\ W &= EI(x)\left[1 + \frac{(\nu-48)\nu - 45}{45(\nu+1)}\tau^2\right] \\ Y &= \frac{5}{6}GA(x) \\ X &= \frac{Et(5\nu+3)b(x)^2\tau}{9(1+\nu)} \end{aligned} \tag{7}$$

For a linearly tapered beam, τ is the tangent of the taper angle α as shown in Fig. 5. It should be noted that the stiffness associated with shear is what one obtains from

the usual Timoshenko beam theory. There is no taper correction to this term because the shear strain is already one order higher in the small parameter δ than the strains associated with 1D bending and extension measures, so that the overall contribution of the term to the strain energy per unit length is correct through second order. This theory is said to be a generalized Timoshenko theory in that it contains contributions to the strain energy associated with extension, bending and shear. However, it is not subject to any of the usual restrictions on kinematics associated with the original Timoshenko theory. Moreover, it includes a bending-shear coupling term X, which is not found in the original theory.

Validation of these stiffness constants, presented in Ref. [48], showed that the theory is only accurate when corrections associated with nonzero τ are included. Unfortunately, a review of the literature shows that there is hardly any awareness among researchers that beam stiffness constants depend on taper, as all references the authors have found to date would provide the above stiffness constants with τ set equal to zero.

An important aspect of the asymptotic theory is that bending and shear are coupled for a tapered beam; hence, the coefficient X is present in the energy. Therefore, if one takes the bending and shear stiffnesses as $EI(x)$ and $5GA(x)/6$ (i.e. only changing the sectional width in the stiffness formulae), the strain energy associated with bending-shear coupling will be missed. This can lead to significant errors in prediction of the beam deflection.

Figure 6 shows the percentage errors in extension and bending stiffnesses (Z and W from Eq. (7)) when one neglects the effect of taper and proceeds with the simplistic change in the sectional stiffnesses. It can be concluded that neglecting taper introduces an error in the beam sectional stiffnesses that can be significant, affecting deflections under load as well as natural frequencies.

To assess the importance of the bending-shear coupling term X relative to the

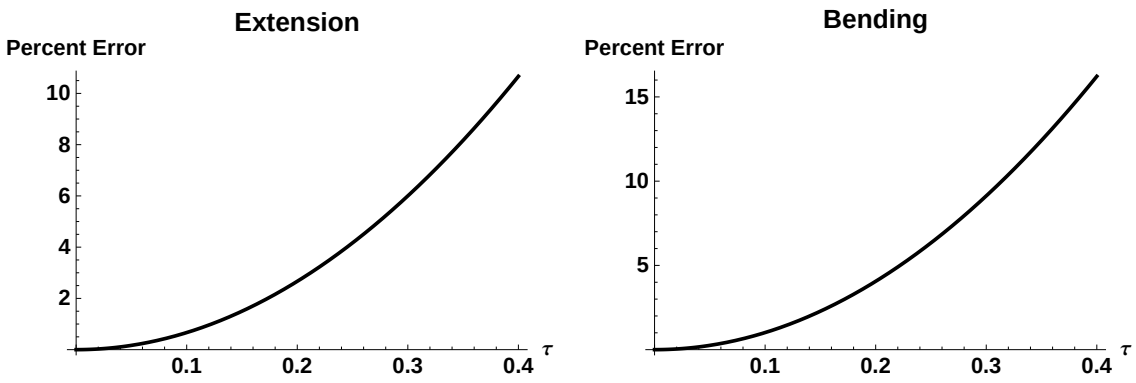

Figure 6: Percentage errors in the stiffnesses for $\nu = 0.3$

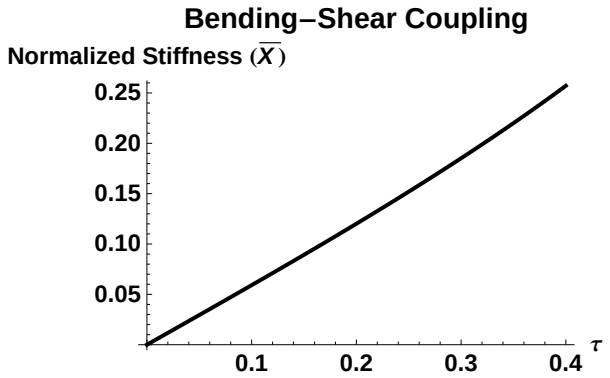

Figure 7: Normalized stiffness for bending-shear coupling, $\nu = 0.3$

pure bending and pure shear term, the coupling stiffness is normalized, such that:

$$\begin{aligned} \overline{X} &= \frac{X}{\sqrt{YW}} \\ &= \frac{(5\nu+3)\tau}{\sqrt{45(\nu+1)+(\nu^2-48\nu-45)\,\tau^2}} \end{aligned} \tag{8}$$

This normalized value can be thought of as a measure of coupling strength to be compared with unity. For a taper (τ) of 0.2, it varies from 0.0215 to 0.1367 as Poisson's ratio varies from -0.5 to 0.5. Moreover, the plot shown in Fig. 7 indicates that these values are by no means negligible compared to unity. Therefore, its absence may cause significant errors, and it is thus important to include these corrections in the stiffnesses to account correctly for the effects of taper.

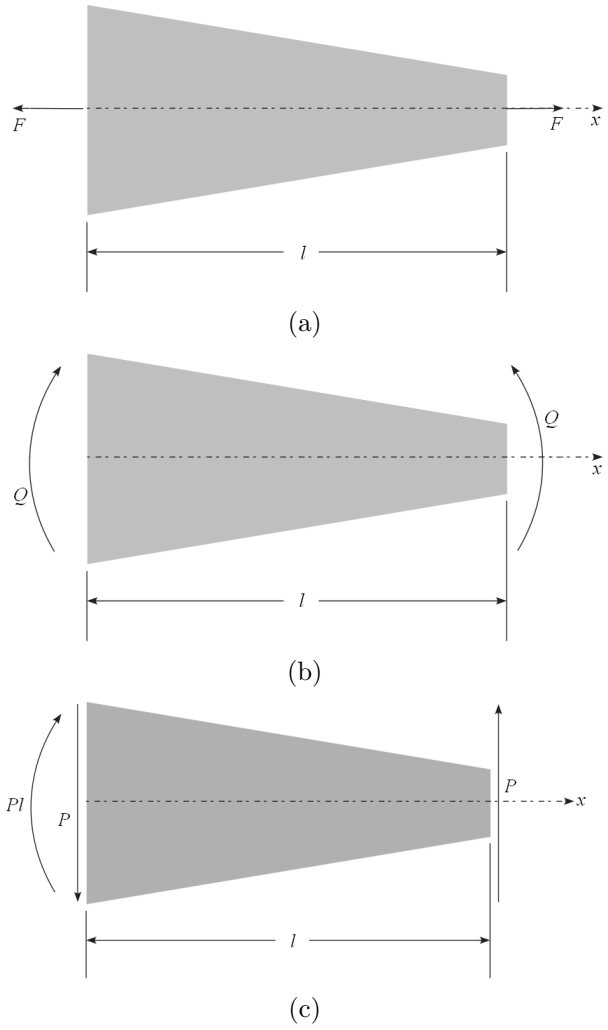

Figure 8: Schematic of beam loaded for extension (a), bending (b) and flexure (c)

3.3 Recovery Relations

This section presents strain, stress and displacement components obtained from the beam theory based on VAM and comparisons with elasticity solutions. Although the baseline elasticity solutions are not restricted to small values of the parameters δ and τ, they are compared to solutions from the beam theory, which are subject to small values of δ and τ. In particular, beam theory based on the VAM is used to analyze the problem of a tapered beam subjected to three different types of loading described as extension, bending and flexure shown in Fig. 8. These three cases correspond to

constant axial force, constant bending moment and constant shear force, respectively. As in Ref. [48], the warping and strain energy are evaluated through first and second orders, respectively.

For greater accuracy than Ref. [48], the warping is here evaluated to second-order. For this, the same procedure outlined in Sec. 3.2 is followed. The first-order warping is perturbed and from the perturbed warping, strains are obtained that are, in turn, used to evaluate the strain energy as a function of the unknown warping perturbations. Minimization of the strain energy using calculus of variations yields the expression for the second-order terms in warping as

$$\begin{aligned} w_x^{(2)} &= 0 \\ w_y^{(2)} &= A_0\overline{\epsilon} + A_1\overline{\epsilon}' + A_2\overline{\epsilon}'' + B_0\overline{\kappa} + B_1\overline{\kappa}' + B_2\overline{\kappa}'' \end{aligned} \tag{9}$$

where

$$\begin{aligned} A_0 &= \frac{1}{6b^2} y(\nu+1)\tau^2 \left[y^2(\nu+1) - b^2(\nu-3)\right] \\ A_1 &= \frac{1}{6b} y\tau \left[y^2(\nu+1)^2 - b^2\left(\nu^2+2\nu+3\right)\right] \\ A_2 &= \frac{1}{6} y\nu^2\left(b^2-y^2\right) \\ B_0 &= -\frac{1}{18}\left(8\nu^2+6\nu-3\right)\tau^2\left(b^2-3y^2\right) \\ B_1 &= \frac{1}{9} b\nu(5\nu+6)\tau\left(b^2-3y^2\right) \\ B_2 &= \frac{1}{360}\left[-b^4\left(40\nu^2+54\nu+7\right) + 30b^2y^2\left(4\nu^2+6\nu+1\right) - 15y^4(2\nu+1)\right] \end{aligned} \tag{10}$$

Thus, an expression for the warping through second order has been obtained. The derivatives of the 1D classical strain measures make it unsuitable for use in an engineering beam theory. The classical strain measures are transformed into generalized Timoshenko strain measures, whose derivatives are computed using the equilibrium equations. The required sectional stiffnesses for use in the equilibrium equations are given by Eqs. (7).

Note that the second-order warping functions are not used for obtaining stiffnesses but only for recovery of stress, strain and displacement. The expressions for strain in

Eq. (1) are restricted only by the assumption of small strain. The 1D strain measures may be used in their geometrically exact form. Herein, however, for the purpose of comparison with linear elasticity theory, they are restricted to small displacement and rotation. Care should be taken to distinguish between the 1D classical strain measures which appear in Eq. (1) and 1D generalized Timoshenko strain measures which appear in Eq. (6). The relation between the two is detailed in Ref. [46] and specialized in Ref. [48] and here as

$$\overline{\epsilon} = \epsilon \qquad \overline{\kappa} = \kappa + \gamma' \tag{11}$$

Since the problem under consideration is that of plane stress, the stresses are simply obtained from the constitutive law as

$$\left\{ \begin{array}{c} \sigma_{xx} \\ \sigma_{yy} \\ \sigma_{xy} \end{array} \right\} = \frac{E}{1-\nu^2} \left[\begin{array}{ccc} 1 & \nu & 0 \\ \nu & 1 & 0 \\ 0 & 0 & \frac{1-\nu}{2} \end{array} \right] \left\{ \begin{array}{c} \Gamma_{xx} \\ \Gamma_{yy} \\ \Gamma_{xy} \end{array} \right\} \tag{12}$$

The 2D displacements from linear beam theory are computed from subtracting the position vector of an arbitrary point on the undeformed cross-sectional plane from the corresponding position vector in the deformed cross-sectional surface, such that

$$\begin{aligned} u_x =& u - y v_{,x} + w_x \\ u_y =& v + w_y \end{aligned} \tag{13}$$

where u and v are the 1D displacement variables of the beam theory, while u_x and u_y are the 2D displacements of an arbitrary point of the cross section. These 1D displacement variables can be computed from the 1D strain measures by using the linear 1D strain-displacement equations

$$\begin{aligned} \epsilon =& u' \\ \gamma =& v' - \theta \\ \kappa =& \theta' \end{aligned} \tag{14}$$

To completely determine the 1D displacement and rotation variables, i.e. u, v and θ, the boundary condition specified at $x = 0$ sets u, v and θ to zero.

From this the stress, strain and displacement components were obtained from the beam analysis based on VAM. They are compared with the plane-stress elasticity solutions obtained from Refs. [66] and [109]. Results are presented in Figs. 9 – 11 for the three loading cases of extension, bending and flexure, respectively. The two results from the variational-asymptotic method, VAM (I) and VAM (II) correspond to the cases when warping is evaluated through first and second orders, respectively. The elasticity solutions also have been plotted for comparison purposes. For the three loading cases, the recovery relations are plotted at $x = l/2$, versus ζ, a dimensionless variable defined as $y/b(x)$.

It is clear that if the warping is accurate to second order, then the recovery relations of the beam theory agree very well with results from the elasticity solution. On the other hand, if warping is evaluated only to first order [48], some results are not in good agreement with the elasticity solutions. Note that for presentation the recovery relations were normalized by certain standard quantities. In the case of strain the normalizing quantities were $F/(ELt)$, $Q/(EL^2t)$ and $P/(ELt)$ for extension, bending and flexure, respectively. For stresses and displacements, they were the strain normalizing factors multiplied by modulus of elasticity and length of the beam, respectively. The results were generated for $\nu = 0.3$, $\tau = 0.2$ and $\delta = 0.25$. It is essential to state here that the VAM solutions are compared with the total elasticity solutions, not with the elasticity solutions expanded to a certain order in small parameters.

Asymptotic expansions of the expressions for recovered strains were carried out, and it was seen that the results are in excellent agreement with the elasticity solutions expanded through the corresponding order. For the extension case, if the warping is correct through second order, i.e. $O(b\delta^2\epsilon)$, $O(b\delta\tau\epsilon)$ and $O(b\tau^2\epsilon)$, then the strains Γ_{xx},

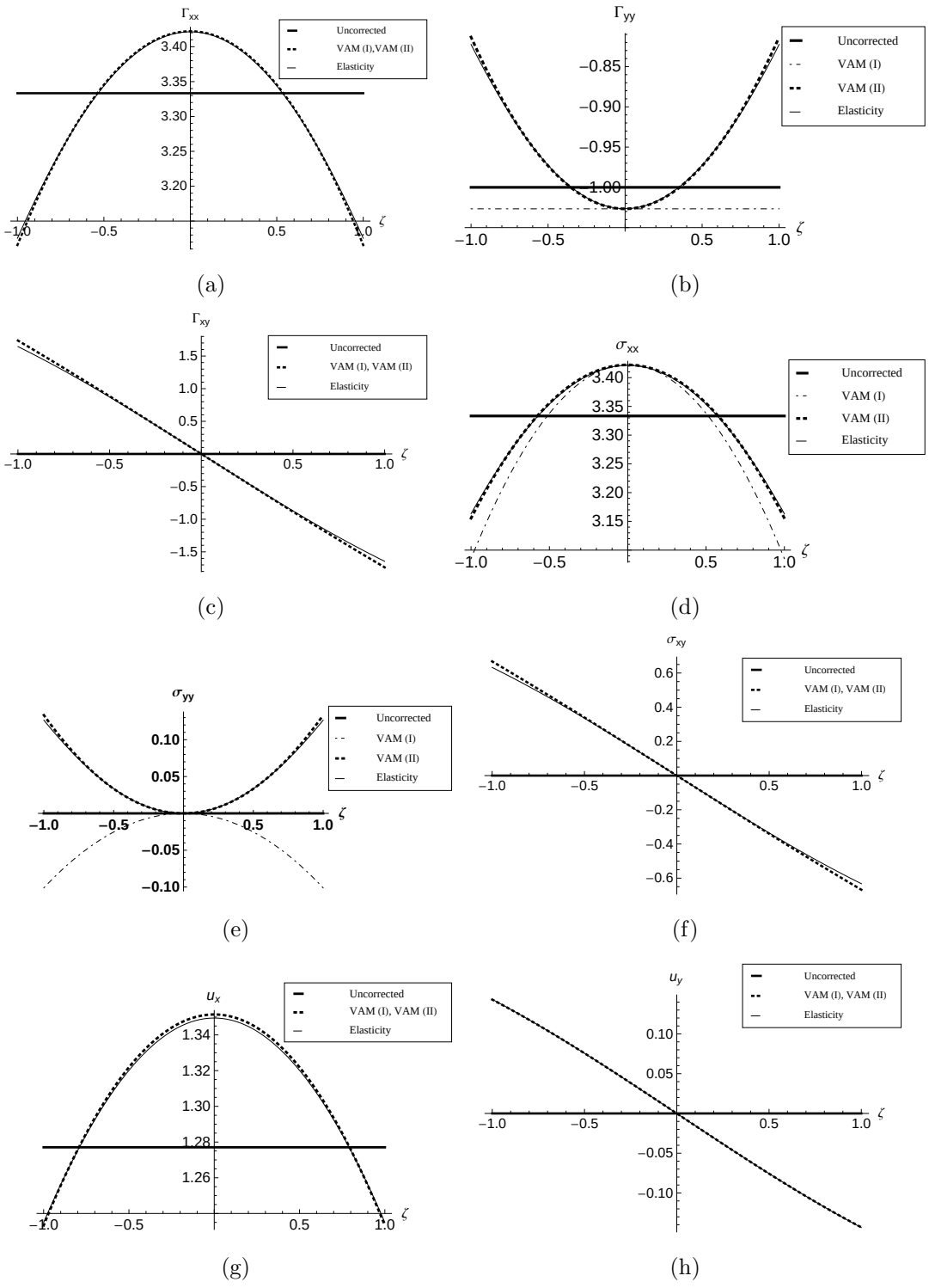

Figure 9: Comparison of the normalized VAM strains, stresses and displacements with the elasticity solutions for extension

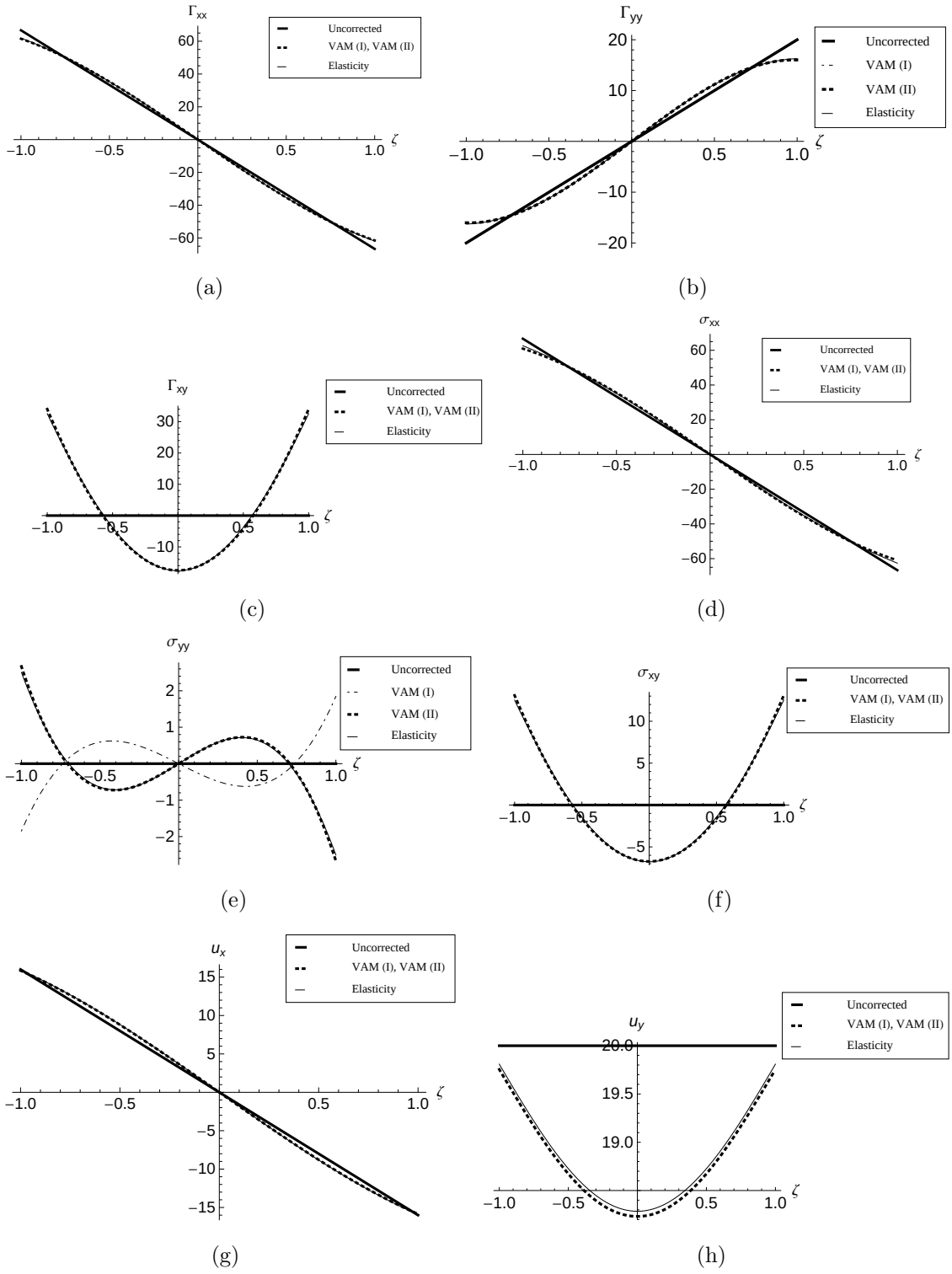

Figure 10: Comparison of the normalized VAM strains, stresses and displacements with the elasticity solutions for bending

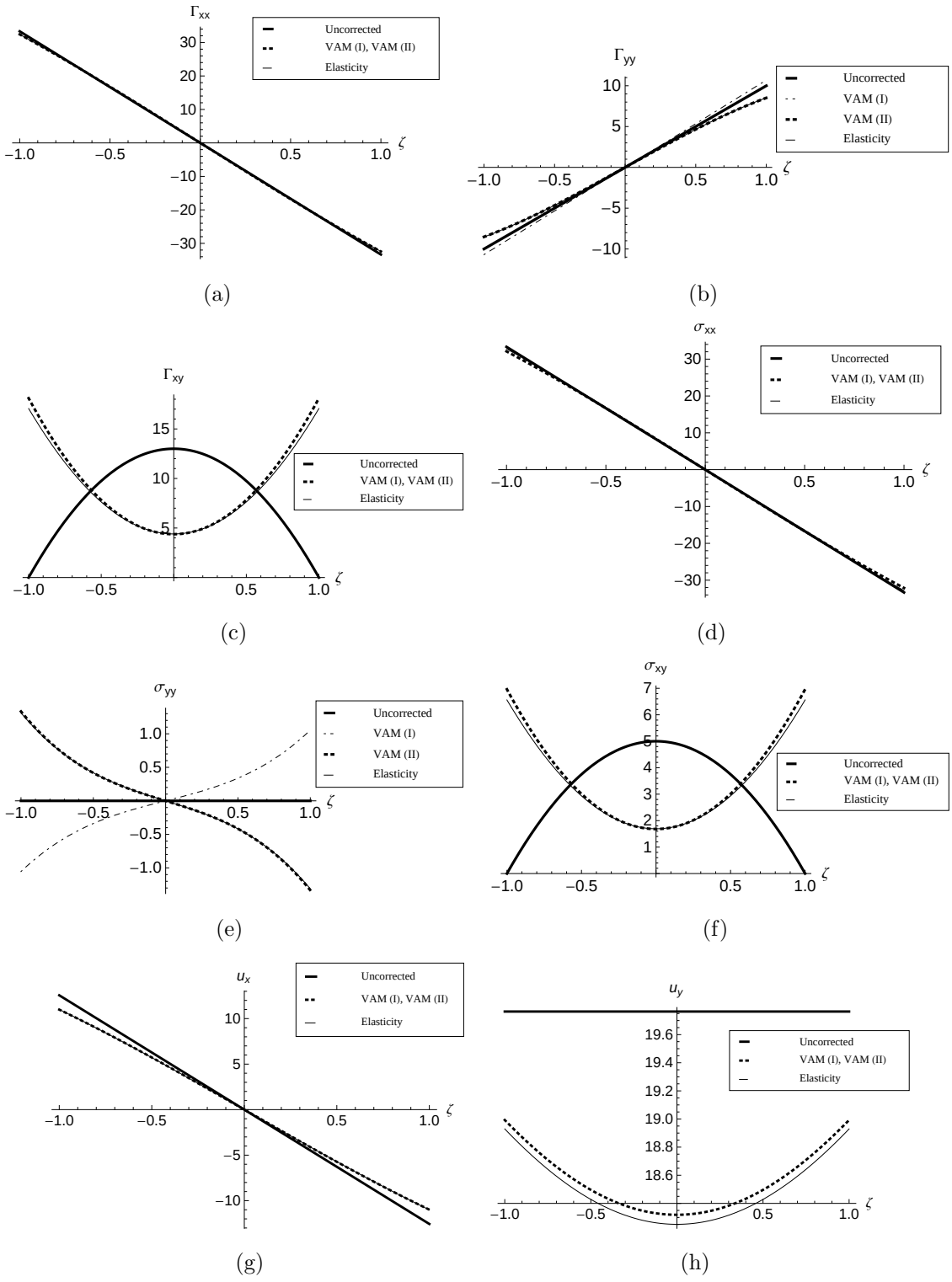

Figure 11: Comparison of the normalized VAM strains, stresses and displacements with the elasticity solutions for flexure

Table 2: Asymptotic expansions of the strains from VAM for the extension case

Strain	Expansion
Γ_{xx}	$\frac{F}{2Etb}\left[1+\frac{\tau^2}{3}\left\{2-3\zeta^2\left(2+\nu\right)\right\}\right]$
Γ_{xy}	$-\frac{\tau F\zeta(\nu+1)}{Etb}$
Γ_{yy}	$-\frac{F\nu}{2Etb}\left[1-\frac{\tau^2}{3\nu}\left\{-2\nu+3\zeta^2\left(2\nu+1\right)\right\}\right]$

Table 3: Asymptotic expansions of the strains from elasticity for the extension case

Strain	Expansion
Γ_{xx}	$\frac{F}{2Etb}\left[1+\frac{\tau^2}{3}\left\{2-3\zeta^2\left(2+\nu\right)\right\}\right]$
Γ_{xy}	$-\frac{\tau F\zeta(\nu+1)}{Etb}$
Γ_{yy}	$-\frac{F\nu}{2Etb}\left[1-\frac{\tau^2}{3\nu}\left\{-2\nu+3\zeta^2\left(2\nu+1\right)\right\}\right]$

Γ_{xy} and Γ_{yy} are expected to be correct through orders 3, 2 and 2, respectively. However, based on the trends in the evaluation of warping the third-order contribution to the warping, w_y is expected to be zero. Therefore, under these special circumstances, the strains listed in the same order as above are actually correct through orders 3, 2 and 3, respectively, relative to the leading term. Expansions of the 2D strain components for extension and bending are presented in Tables 2, 3, 4 and 5. For the case of extension, for example, the third-order terms are zero for Γ_{xx} and Γ_{yy} and hence the expansions are correct through the third order. Also, the second-order terms are zero for Γ_{xy}, and hence it is correct through second order.

Table 4: Asymptotic expansions of the strains from VAM for the bending case

Strain	Expansion
Γ_{xx}	$-\frac{3Q\zeta}{2Etb^2}\left[1-\frac{\tau^2}{5}\left\{-12-\frac{13}{3}\nu+10\left(2+\nu\right)\zeta^2\right\}\right]$
Γ_{xy}	$-\frac{3Q\tau(1+\nu)}{2Etb^2}\left(1-3\zeta^2\right)$
Γ_{yy}	$\frac{3Q\nu\zeta}{2Etb^2}\left[1-\frac{\tau^2}{5\nu}\left\{-5-12\nu-\frac{2}{3}\nu^2+10\left(1+2\nu\right)\zeta^2\right\}\right]$

Table 5: Asymptotic expansions of the strains from elasticity for the bending case

Strain	Expansion
Γ_{xx}	$-\frac{3Q\zeta}{2Etb^2}\left[1-\frac{\tau^2}{5}\left\{-12-5\nu+10\left(2+\nu\right)\zeta^2\right\}\right]$
Γ_{xy}	$-\frac{3Q\tau(1+\nu)}{2Etb^2}\left(1-3\zeta^2\right)$
Γ_{yy}	$\frac{3Q\nu\zeta}{2Etb^2}\left[1-\frac{\tau^2}{5\nu}\left\{-5-12\nu+10\left(1+2\nu\right)\zeta^2\right\}\right]$

For the flexure case, the expressions for the 2D strain are presented in Eqs. (15) and (16). In all three loading cases a good agreement is observed between the second-order expanded VAM and elasticity solutions. In the flexure results, k defined as $\tau L/b$, the ratio of the two small parameters. f and g are lengthy functions of the parameters indicated and not reproduced here for the sake of brevity. Nevertheless, it suffices to say from the VAM and elasticity agreement in Fig. 11, they are very in close proximity of each other. Care must be exercised in expanding the solutions in both the small parameters and normalizing the expressions with the appropriate lowest order terms. Any arbitary choice of non-dimensionalization while expanding the solutions will create/destroy small parameters and lead to erroneous results, such as the ones in Ref. [40].

$$
\begin{aligned}
\Gamma_{xx} =& -\frac{3PL\left(1-\eta\right)\zeta}{2Etb^2}\left[1+\frac{1}{5\left(1-\eta\right)}\left(\left\{12+\frac{13}{3}\nu-6\eta+5\left(-2+\eta\right)\left(2+\nu\right)\zeta^2\right\}\tau^2\right.\right.\\
&\left.\left.+\left\{-6-\frac{13}{3}\nu+5\left(2+\nu\right)\zeta^2\right\}\frac{\tau b}{L}\right)\right]\\
\Gamma_{xy} =& \frac{3P\left(1+\nu\right)}{2Etb\left(1-\eta k\right)}\left[1-k+\left(-1+3k-2\eta k\right)\zeta^2+f\left(k,\zeta,\eta,\nu\right)\right]\\
\Gamma_{yy} =& -\frac{3PL\left(1-\eta\right)\zeta}{2Etb^2}\left[1+\frac{1}{5\left(1-\eta\right)}\left(\left\{5+12\nu-\frac{2}{3}\nu^2-6\nu\eta+5\left(-2+\eta\right)\left(1+2\nu\right)\zeta^2\right\}\tau^2\right.\right.\\
&\left.\left.+\left\{-5-6\nu+\frac{2}{3}\nu^2+5\left(1+2\nu\right)\zeta^2\right\}\frac{\tau b}{L}\right)\right]
\end{aligned}
\tag{15}
$$

$$
\begin{aligned}
\Gamma_{xx} =& -\frac{3PL\left(1-\eta\right)\zeta}{2Etb^2}\left[1+\frac{1}{5\left(1-\eta\right)}\left(\left\{12+5\nu-6\eta+5\left(-2+\eta\right)\left(2+\nu\right)\zeta^2\right\}\tau^2\right.\right.\\
&\left.\left.+\left\{-6-5\nu+5\left(2+\nu\right)\zeta^2\right\}\frac{\tau b}{L}\right)\right]\\
\Gamma_{xy} =& \frac{3P\left(1+\nu\right)}{2Etb\left(1-\eta k\right)}\left[1-k+\left(-1+3k-2\eta k\right)\zeta^2+g\left(k,\zeta,\eta,\nu\right)\right]\\
\Gamma_{yy} =& -\frac{3PL\left(1-\eta\right)\zeta}{2Etb^2}\left[1+\frac{1}{5\left(1-\eta\right)}\left(\left\{5+12\nu-6\nu\eta+5\left(-2+\eta\right)\left(1+2\nu\right)\zeta^2\right\}\tau^2\right.\right.\\
&\left.\left.+\left\{-5-6\nu+5\left(1+2\nu\right)\zeta^2\right\}\frac{\tau b}{L}\right)\right]
\end{aligned}
\tag{16}
$$

3.3.1 Recovery relations without taper corrections

When the sectional formulae of an untapered beam are used for a tapered one, with the only effect of taper being a change in the width, it follows that taper does not enter into the expressions for strains and stresses. The stresses, strains and displacements from this type of analysis, which as mentioned in Sec. 3.2 is the starting point for most of the research on tapered beams, has been plotted along with the VAM and elasticity solutions in Figs. 9 – 11. The recovery relations are erroneous and certain trends are incorrect. The bending-shear coupling effect is not captured as expected, and it can be seen from parts (c) and (f) of Fig. 10 that the case of bending does not result in any shear stress or strain. Another example of an erroneous trend is that of σ_{xy} for flexure. The trend for a tapered beam is exactly opposite that of a prismatic beam as shown in part (f) of Fig. 11. Using merely the change in sectional width in the stiffness formulae for prismatic beams leads to erroneous stress, strain and displacement. This implies that the problem is being posed in a fundamentally incorrect way. A prominent error of this type was identified in Ref. [48], wherein it was shown that the lateral-surface boundary conditions in the typical tapered beam analysis are incorrect.

3.4 Validity of the recovery expressions

In the previous sections, the recovery relations obtained from the VAM were compared with the exact elasticity solutions. The VAM analysis was based on considering the parameters δ and τ to be small. This section addresses the definition of the "smallness" of these parameters. In other words, the values of δ and τ are increased till the point at which the VAM solution deviates from the exact elasticity solutions, thus determining the range of applicability of the VAM solution. It is important to note that from their definitions, the value of τ must always be less than or equal to the value of δ. If τ were equal to δ, this is a special case of a tapered beam, i.e. a wedge, for which a singularity exists in the case of flexure and extension, as the force applied at the end in both the cases, acts over a vanishing area. Hence, the cases for which τ is strictly less than δ will be addressed. The percentage errors for various values of δ at are plotted in Fig. 12. Error here means the maximum of the percentage errors of the recovery relations for all the three loading cases. The error of a VAM solution is obtained by comparison with the corresponding elasticity solution. Results for those combinations of τ and δ for which the maximum error was below 5% was considered to be satisfactory. It is seen that at the extreme case of $\delta = 0.4$, the results are accurate up to $\tau = 0.26$. Investigations were terminated at $\delta = 0.4$ as for higher values, it is generally expected that an engineering analysis would be done considering the structure as a plate and not a beam.

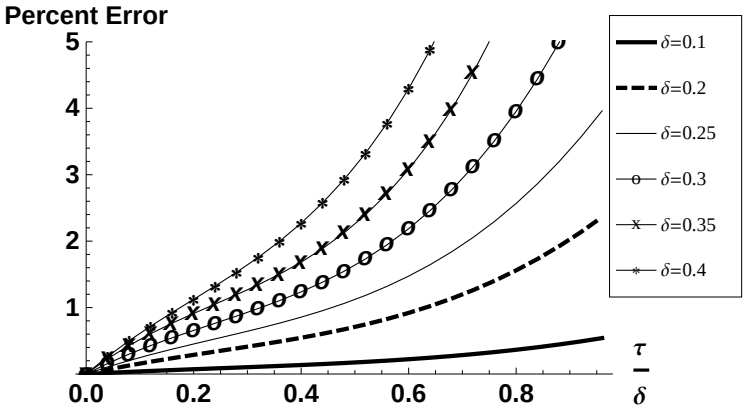

Figure 12: Percentage errors with respect to τ/δ at a given δ for the VAM recovery relations with respect to the elasticity solutions

IV

ANALYTICAL VERIFICATION OF THE INITIAL CURVATURE EFFECT

The purpose of computing is insight, not numbers.

– Richard Hamming

4.1 Introduction

For structural members with initial twist/curvature, found commonly in the field of aerospace engineering, using beam theories based on traditional approaches/ideas will not yield accurate results. Modeling of beams with initial curvature is of interest due to their presence in many engineering structures. The VAM provides a rigorous framework to model such structures without *ad hoc* assumptions regarding their deformation. Though novel ideas are not lacking in some of the beam theories in the current literature, the capability and generality of a VAM framework has maintained the superiority of VABS, subsequently making it a popular analysis tool for helicopter blades and wind turbines. Several efforts have contributed to the validation and verification of VABS (a finite-element computer program developed based on the VAM) results, and this chapter is one such effort.

The first part of this work deals with the application of the VAM to analyze the in-plane deformation of an isotropic strip with initial in-plane curvature. The current problem is chosen for two reasons: First, all of the final results, such as the sectional constants and the recovery relations for stress and strain, have closed-form analytical expressions, which enables a greater understanding and makes possible an

This chapter was published as Rajagopal et al. [89] and Rajagopal and Hodges [90].

in-depth study for improvements in the theory. Second, the problem can be verified for two specific loading cases with published elasticity solutions [109]. This purely analytical exercise also exhibits two distinct ways of improving the accuracy of the results obtained through the VAM. In the first, sectional constants are evaluated by a "partial" transformation of the second-order asymptotically correct strain energy to a Generalized Timoshenko form. In the second, the recovery relations are improved by evaluating the warping up to the second-order in the small parameters of the system. Finally, the analytical solution of this problem serves as a verification tool for certain aspects of VABS. Note that VABS is capable of analyzing beam cross sections with arbitrary geometry and materials. Thus, only a very small subset of the capabilities of VABS is addressed by the analytical solution presented herein.

Section 4.2 describes the development of a beam theory using the VAM. Sec. 4.3 compares results obtained for two loading cases from the linearized version of the beam theory from Sec. 4.2 and elasticity. Sec. 4.4 presents the verification study for VABS carried out using the beam theory. Appendix A presents a modified analysis of initially curved and twisted anisotropic beams in light of developments arising out of the current study.

Additionally, the advent of composite materials has revolutionized the field of structural engineering, most notably due to their high strength-to-weight ratio and their directional tailorability. Therefore, in the second part of this work, a beam theory is proposed to analyze the in-plane deformation of an initially curved laminated strip-beam. Recall, as mentioned in Chapter 2, a beam theory must address the following three aspects: a cross-sectional analysis leading to a stiffness matrix which is input into the 1D analysis, the 1D analysis itself, and the formulae or procedure to recover stress, strain and 3D displacement. This later half of the chapter is organized as follows: Section 4.5 outlines the theoretical development leading to the results for the first and third aspects described previously. Section 4.6 demonstrates extraction of

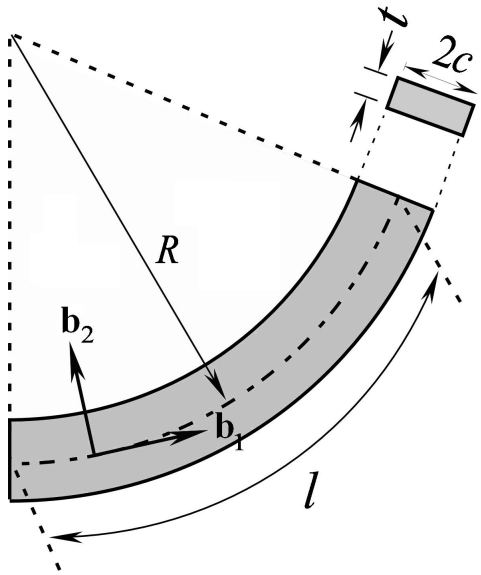

Figure 13: Schematic of the isotropic strip beam with initial in-plane curvature

some stiffness terms using an equivalent plate theory. Section 4.7 validates the current work using results from VABS. Discussion of the results is always accompanied by conclusions and suggestions arising from the study.

4.2 Analytical Development Using the VAM

In this section, a beam theory for the planar deformation of an isotropic strip with an initial curvature ($k_3 = 1/R$) as depicted in Fig. 13 is developed using the VAM. The beam theory will address the issues of the strain energy density and the cross-sectional stress-strain recovery in terms of generalized strains that depend only on the axial coordinate. The VAM procedure involves the solution of an elasticity problem in an asymptotic fashion exploiting the presence of small parameters in the system [46, 127].

The reference line is chosen as the line of section centroids, which in this case is the midline of the strip. Three different coordinate systems are used: a set of vectors $\mathbf{b}_i$ ($i = 1, 2$) associated with the undeformed configuration of the beam, i.e. along x_1 and x_2, as shown in Fig. 13; a set of vectors $\mathbf{B}_i$ ($i = 1, 2$) associated with the deformed

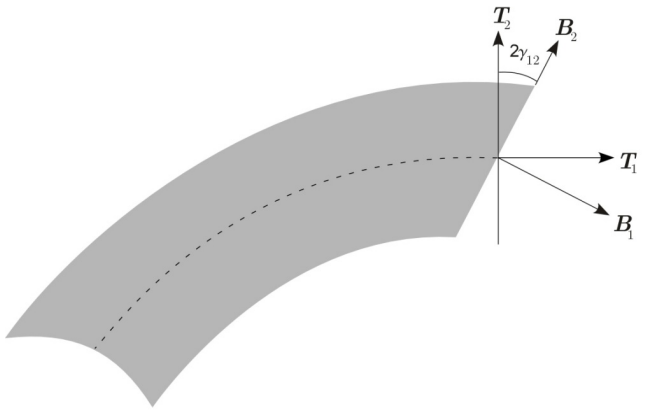

Figure 14: Relation between the **B** and **T** coordinate systems

configuration of the beam; and a set of vectors $\mathbf{T}_i$ ($i = 1, 2$), also associated with the deformed configuration of the beam. Here $\mathbf{T}_1$ and $\mathbf{B}_1$ are defined as tangent to the reference line and normal to the cross section in the deformed configuration of the beam, respectively; and $\mathbf{T}_2$ and $\mathbf{B}_2$ are in the same plane and defined to be normal to $\mathbf{T}_1$ and $\mathbf{B}_1$, respectively. The relationship between B and T frames is depicted in Fig. 14 and can be mathematically expressed as

$$\left\{ \begin{array}{c} \mathbf{B}_1 \\ \mathbf{B}_2 \end{array} \right\} = \left[\begin{array}{cc} 1 & -2\gamma_{12} \\ 2\gamma_{12} & 1 \end{array} \right] \left\{ \begin{array}{c} \mathbf{T}_1 \\ \mathbf{T}_2 \end{array} \right\} \tag{17}$$

where $2\gamma_{12}$ is the 1D shearing strain measure, defined in the latter part of this section. Note that this relation is valid for small values of $2\gamma_{12}$, which is one of the assumptions of our theory. The position vector of an arbitrary point on the undeformed beam section is

$$\hat{\mathbf{r}} = \mathbf{r} + x_2\mathbf{b}_2 \tag{18}$$

where $\mathbf{r}$ is the position vector of a point on the reference line which is at the same axial location as the chosen point. Using the curvature-angular velocity analogy [46]

one can write

$$\begin{aligned} \mathbf{b}_1' &= k_3 \mathbf{b}_2 \\ \mathbf{b}_2' &= -k_3 \mathbf{b}_1 \end{aligned} \tag{19}$$

where $(\ )'$ denotes derivative with respect to x_1. Similarly, choosing the T system, one can write the position vector for an arbitrary point on the deformed beam section as

$$\hat{\mathbf{R}} = \mathbf{R} + x_2 \mathbf{T}_2 + w_1(x_1, x_2)\mathbf{T}_1 + w_2(x_1, x_2)\mathbf{T}_2 \tag{20}$$

where $\mathbf{R} = \mathbf{r} + u\mathbf{b}_1 + v\mathbf{b}_2$, with u and v as the displacement of the beam reference line in the x_1 and x_2 directions, respectively. The unknowns in the displacement field are the warping w_1 and w_2. The displacement field is rendered unique by choosing these constraints on the warping:

$$\begin{aligned} \langle w_1 \rangle &= 0 \\ \langle w_2 \rangle &= 0 \end{aligned} \tag{21}$$

where

$$\langle \bullet \rangle = \int_{-c}^{c} \bullet \, dx_2 \tag{22}$$

Note that these constraints are not unique.

From the displacement field, one can compute the covariant and contravariant base vectors, which are the tangents to the coordinate curves and normals to the coordinate surfaces, respectively, for both the deformed and undeformed systems [46]. Then the deformation gradient tensor [81] is

$$\underline{\underline{\boldsymbol{\chi}}} = \mathbf{G}_i \mathbf{g}^i \tag{23}$$

where $\mathbf{g}^i$ and $\mathbf{G}_i$ are the contravariant and covariant base vectors associated with the undeformed and deformed configurations, respectively. While computing these vectors, the elegant definitions of the 1D strains using vector pull-back operations

[46] can be used, which may be simplified to

$$\begin{aligned}\mathbf{R}' =&(1+\overline{\gamma}_{11})\mathbf{T}_1\\ \mathbf{T}_1' =&(k_3+\overline{\kappa}_3)\mathbf{T}_2\\ \mathbf{T}_2' =&-(k_3+\overline{\kappa}_3)\mathbf{T}_1\end{aligned} \tag{24}$$

where $\overline{\gamma}_{11}$ and $\overline{\kappa}_3$ are the classical 1D generalized stretching and bending strains, respectively. Note that by definition the T frame of reference does not have a 1D shearing strain measure associated with it. After this, the polar decomposition theorem [81] is employed. Using the Jaumann-Biot-Cauchy definition of the strain tensor and assuming that both the strain and the local rotations (caused by warping) are small [46], the nonzero strain components become

$$\begin{aligned}\Gamma_{11} &= \frac{1}{\sqrt{g}}\left(\overline{\gamma}_{11} - x_2\overline{\kappa}_3 - k_3 w_2 + \frac{\partial w_1}{\partial x_1}\right)\\ \Gamma_{22} &= \frac{\partial w_2}{\partial x_2}\\ 2\Gamma_{12} &= \frac{1}{\sqrt{g}}\left(k_3 w_1 + \frac{\partial w_2}{\partial x_1}\right) + \frac{\partial w_1}{\partial x_2}\end{aligned} \tag{25}$$

where

$$g = \det\begin{bmatrix}\mathbf{g}_1\cdot\mathbf{g}_1 & \mathbf{g}_1\cdot\mathbf{g}_2\\ \mathbf{g}_2\cdot\mathbf{g}_1 & \mathbf{g}_2\cdot\mathbf{g}_2\end{bmatrix} \tag{26}$$

Since the problem under consideration is that of plane stress, the constitutive law is simply

$$\begin{Bmatrix}\sigma_{11}\\ \sigma_{22}\\ \sigma_{12}\end{Bmatrix} = \frac{E}{1-\nu^2}\begin{bmatrix}1 & \nu & 0\\ \nu & 1 & 0\\ 0 & 0 & \frac{1-\nu}{2}\end{bmatrix}\begin{Bmatrix}\Gamma_{11}\\ \Gamma_{22}\\ 2\Gamma_{12}\end{Bmatrix} \tag{27}$$

Consequently the expression for the strain energy per unit length is given by

$$U = \frac{Et}{2(1-\nu^2)}\left\langle\sqrt{g}\left[\Gamma_{11}^2+\Gamma_{22}^2+2\nu\Gamma_{11}\Gamma_{22}+\frac{1-\nu}{2}(2\Gamma_{12})^2\right]\right\rangle \tag{28}$$

The formulation until now is equivalent to that of a standard elasticity approach. If we attempt to solve the problem directly using minimization principles we will run

into the same difficulties as we would in solving an elasticity problem. The small parameters of the system are easily identified. Therefore, we turn our attention to the VAM. Firstly, the maximum strain, i.e. $\max(\overline{\gamma}_{11}, c\overline{\kappa}_3)$, is assumed to be small compared to unity and assumed to be $O(\epsilon)$. Secondly, specific to the problem are the small parameters c/l and $\delta = c/R$, which are assumed to be $O(\sigma)$. The VAM takes advantage of these small parameters to solve for the unknown warping. We will eventually ignore $O(\sigma^3)$ terms. The warping is assumed to be $O(c\epsilon)$. Its subsequent solution justifies this assumption.

The first step of the VAM is to obtain the zeroth-order solution, also referred to as the classical solution. For this the $O(\sigma)$ terms in the strain energy are ignored. The minimization of this strain energy subject to the constraints on warping given by Eqs. (21) using the standard principles of the calculus of variations leads to the solution for the zeroth-order warping

$$\begin{aligned} w_1^{(0)} =& 0 \\ w_2^{(0)} =& -\nu x_2 \overline{\gamma}_{11} + \frac{\nu\overline{\kappa}_3}{6}(3x_2^2 - c^2) \end{aligned} \tag{29}$$

Note that the order of the warping is the same as that which was assumed. It can be substituted back into the energy to obtain the zeroth-order strain energy per unit length

$$\begin{aligned} U_0 &= Ect\overline{\gamma}_{11}^2 + \frac{1}{3}Ec^3t\overline{\kappa}_3^2 \\ &= \frac{1}{2}EA\overline{\gamma}_{11}^2 + \frac{1}{2}EI_3\overline{\kappa}_3^2 \end{aligned} \tag{30}$$

The warping is then perturbed one higher order in σ, so that

$$\begin{aligned} w_1 &= w_1^{(0)} + w_1^{(1)} \\ w_2 &= w_2^{(0)} + w_2^{(1)} \end{aligned} \tag{31}$$

This implies that the first-order warping $w_i^{(1)}$ is $O(c\sigma\epsilon)$. It is substituted back into the strain energy, and all terms $O(\sigma^3)$ are disregarded. Before minimization, integration

by parts is carried out to remove the derivatives of the unknown warping functions with respect to x_1. The boundary terms can be safely ignored since we are interested in an interior solution. As before, application of the calculus of variations yields the solution to the first-order warping

$$\begin{aligned} w_1^{(1)} =& \frac{1}{6}\left\{\nu\left(3x_2^2 - c^2\right)\overline{\gamma}'_{11} + x_2\left[x_2^2(\nu+2) - c^2(5\nu+6)\right]\overline{\kappa}'_3\right\} \\ w_2^{(1)} =& \frac{1}{6}k_3\left\{\nu(\nu+1)\left(c^2 - 3x_2^2\right)\overline{\gamma}_{11} + x_2\overline{\kappa}_3\left[c^2\left(2\nu^2-3\right) + x_2^2(2\nu+1)\right]\right\} \end{aligned} \tag{32}$$

The warping is substituted back to obtain the asymptotically correct second-order strain energy

$$\begin{aligned} U_2 =& \frac{1}{2}EA\left[1 + \frac{(1+\nu)^2}{3}\delta^2\right]\ \overline{\gamma}_{11}^2 + \frac{1}{2}EI_3\left(1 + \frac{3+10\nu+5\nu^2}{3}\delta^2\right)\ \overline{\kappa}_3^2 \\ & - EI_3k_3(1+\nu)\overline{\gamma}_{11}\ \overline{\kappa}_3 + \underline{\frac{4}{15}Et(1+\nu)c^5{\overline{\kappa}'_3}^2} + \underline{\frac{2}{45}Et(11\nu+12)c^5\overline{\kappa}_3\ \overline{\kappa}''_3} \end{aligned} \tag{33}$$

Recall that $\delta = ck_3 = c/R$. The asymptotically correct second-order energy thus gives us the corrections due to the initial curvature, and other new terms (in addition to those of the zeroth-order energy) correspond to shear deformation. However, this energy expression contains derivatives of the classical 1D strain measures, which make it unsuitable from an engineering perspective. To make it usable it is desirable to convert the strain energy into the "Generalized Timoshenko" (GT) form:

$$U_{GT} = \frac{1}{2}\begin{Bmatrix} \gamma_{11} \\ \kappa_3 \\ 2\gamma_{12} \end{Bmatrix}^T \begin{bmatrix} S_{11} & S_{12} & S_{13} \\ S_{12} & S_{22} & S_{23} \\ S_{13} & S_{23} & S_{33} \end{bmatrix} \begin{Bmatrix} \gamma_{11} \\ \kappa_3 \\ 2\gamma_{12} \end{Bmatrix} \tag{34}$$

where the 1D strain measures used here are defined in the first step of the conversion procedure, known as the "Generalized Timoshenko Transformation" (GTT):

1. The classical 1D generalized strain measures $(\overline{\gamma}_{11}, \overline{\kappa}_3)$ are written in terms of the GT 1D strain measures $(\gamma_{11}, \kappa_3, 2\gamma_{12})$. The latter are the 1D strain measures obtained if one uses the B frame of reference for the deformed beam configuration. Essentially this means that we have switched from using the T frame

of reference to the B frame of reference to describe the deformed beam configuration, which will introduce $2\gamma_{12}$, a 1D shear strain measure. Following the procedure adopted by Ref. [46] and in sync with our assumption of small strain and Eq. (17), the following relation is obtained:

$$\begin{aligned} \overline{\gamma}_{11} &= \gamma_{11} \\ \overline{\kappa}_3 &= \kappa_3 + 2\gamma'_{12} \end{aligned} \tag{35}$$

These relations are used now on Eq. (33).

2. The 1D equilibrium equations are used to eliminate the derivatives of these strain measures. The stress resultants are obtained from Eq. (34) as

$$\begin{Bmatrix} F_1 \\ M_3 \\ F_2 \end{Bmatrix} = \begin{bmatrix} S_{11} & S_{12} & S_{13} \\ S_{12} & S_{22} & S_{23} \\ S_{13} & S_{23} & S_{33} \end{bmatrix} \begin{Bmatrix} \gamma_{11} \\ \kappa_3 \\ 2\gamma_{12} \end{Bmatrix} \tag{36}$$

In terms of the stress resultants, the 1D equilibrium equations are [46]

$$\begin{aligned} F'_1 - k_3 F_2 &= 0 \\ M'_3 + F_2 &= 0 \\ F'_2 + k_3 F_1 &= 0 \end{aligned} \tag{37}$$

Using these equilibrium equations, one can solve for the derivatives of the generalized strains in terms of the generalized strains themselves.

Using the resulting relations, one arrives at a set of equations to solve for the 3×3 stiffness matrix in Eq. (34). This is then solved using a perturbation solution, exploiting the fact that the stiffnesses need to be correct up to a certain order. This can be obtained by recognizing the fact that $\gamma_{11}, c\kappa_3$ and $2\gamma_{12}$ have orders of $O(\epsilon), O(\epsilon)$ and $O(c\epsilon/l)$, respectively. The details of the solution are too lengthy to be presented here, but suffice it to say one can obtain it using symbolic manipulation software such

as Mathematica. The strain energy in the GT form can be obtained as

$$\begin{aligned} U_{GT} =& \frac{1}{2}EA\left[1+\frac{(1+\nu)(1+25\nu)}{75}\delta^2\right]\gamma_{11}^2+\frac{1}{2}EI_3\left(1+\frac{15+60\nu+37\nu^2}{75}\delta^2\right)\kappa_3^2 \\ & -EI_3k_3\left(1+\frac{6}{5}\nu\right)\gamma_{11}\kappa_3+\underline{\frac{1}{2}\left(\frac{5}{6}GA\right)(2\gamma_{12})^2} \end{aligned} \tag{38}$$

It must be remarked here that apart from the presence of derivatives, there is another troublesome aspect of the asymptotically correct second-order energy: the boundary conditions. The classical (i.e. zeroth-order) and the GT theories have a consistent number of boundary conditions. These boundary conditions affect the displacement, section rotation, bending moment and shear force in the usual ways. However, the asymptotically correct second-order energy has additional boundary conditions, the physical interpretations of which are rather obscure. For example, the higher-order derivative terms involve boundary-layer phenomena, which are not involved at all in either the classical or GT theories. Decay lengths associated with these phenomena are extremely short, making it feasible to capture the dominant deformations with the simpler GT theory.

It is important, however, to note that the GT energy is no longer accurate up to second order. The asymptotic exactness has been lost during the conversion process. To obtain an energy that is closer to the asymptotically correct second-order energy we make the following observation: The underlined term in Eq. (38) is obtained from the underlined terms in Eq. (33). Therefore, if we perform a "partial" conversion by converting only the underlined terms in Eq. (33), we will obtain a partially converted GT form (pGT)

$$\begin{aligned} U_{pGT} =& \frac{1}{2}EA\left(1+\frac{(1+\nu)^2}{3}\delta^2\right)\gamma_{11}^2+\frac{1}{2}EI_3\left(1+\frac{3+10\nu+5\nu^2}{3}\delta^2\right)\kappa_3^2 \\ & -EI_3k_3(1+\nu)\gamma_{11}\kappa_3+\frac{1}{2}\left(\frac{5}{6}GA\right)(2\gamma_{12})^2 \end{aligned} \tag{39}$$

This turns out to be the energy given by Eq. (33), with the underlined terms replaced by the underlined term of Eq. (38). This energy is also not asymptotically correct up to the second order, but it is a slightly better approximation than the GT form.

The importance of an analytical solution is highlighted here as it was possible to keep track of the terms during the process and define a pGT form that preserves the second-order exactness to a somewhat greater extent than the GT form. Were a numerical solution obtained using the VAM as in Ref. [136], it would be very cumbersome to identify the terms and define a pGT form.

In either the GT/pGT forms above, the correction due to the small parameter c/l appears through the term associated with the shearing deformation and the corrections due to δ through the first three terms involving extension and bending deformation. As mentioned previously, the 1D generalized shearing strain is of order $O(c\epsilon/l)$; and, hence, the energy associated with shearing deformation is of order $O(\sigma^2)$. Consequently, the shearing stiffness does not contain any higher-order terms.

At this point it is necessary to emphasize that, unlike many of the beam theories in literature with the same or similar names, neither the classical model nor the pGT/GT model make any of the myriad assumptions about beam deformation.

Once the strain energy per unit length is obtained, the second aspect of the beam theory is now addressed: the cross-sectional stress and strain recovery relationships. The asymptotically correct warping is known up to first order. The classical strain measures can be transformed to the GT ones, and their derivatives evaluated using the stiffness terms obtained in the GT/pGT forms. The warping is then used in Eq. (25) to recover strains. This can be used in Eq. (27) to recover the stresses. By solving the 1D problem, one can also recover the displacements point-wise in the cross section. For an example of how this is done, the reader is encouraged to consult Ref. [50] wherein cross-sectional recovery of stress, strain, and displacement is carried out for a tapered strip using the VAM.

However, obtaining stress and strain this way will result in the recovery relationships being asymptotically correct only up to the first order. To improve this

situation, second-order warping functions, viz. $w_1^{(2)}$and $w_2^{(2)}$, are evaluated. The procedure for this mirrors the evaluation of the first-order warping, and the details are not presented here because the expressions obtained are very lengthy. However, they are easily obtained and used with symbolic manipulation software. The warping, when evaluated as described and correct up to second-order, can be used to obtain a more accurate evaluation of the stress and strain, in fact asymptotically correct up to the second order. It should be noted, however, that one need not evaluate a higher order energy (4^{th}) associated with correction of the warping to the second order. Derivatives of the 1D strain measures contained in the second-order warping expressions can be evaluated using the equilibrium equations and cross-sectional stiffnesses obtained from the GT/pGT form since the strain energy based on those stiffnesses is itself close to the asymptotically correct second-order strain energy. So, this way, the recovery relations are as close to second-order accuracy as the GT/pGT forms are. In addition to improving the consistency of the beam theory, evaluation of the second-order warping guarantees the recovery relations will be more accurate for larger values of the small parameters. With this, a complete beam theory has been proposed for the isotropic strip with initial in-plane curvature using the principles of the VAM.

4.3 Comparison with Classical Elasticity Solutions

The beam theory developed in the previous section will be now be applied to solve two classical problems, solutions of which are obtained through linear elasticity theory [109]. The two loading cases are for a strip with initial in-plane curvature of unit thickness subjected to (1) a bending moment M at its ends and (2) a concentrated tip force P at one end. These two loading cases are depicted in Fig. 3. The solutions obtained from the VAM-based beam theory will be verified against those obtained from Ref. [109].

Recall that in the VAM-based beam theory, the only assumptions were smallness of strain and the parameters δ and a/l. However, the theory of elasticity solutions require that the displacements and rotations associated with the deformation be small as well. Therefore, in what follows we too make this assumption to facilitate comparisons between the two results. This requires us to linearize our beam theory before comparing its results with the elasticity solutions, so that results from VAM should be interpreted as results from the linearized VAM beam theory.

For loading case (1), it is obvious that the 1D equilibrium yields stress resultants with values

$$F_1 = 0 \qquad F_2 = 0 \qquad M_3 = M \tag{40}$$

Employing Eq. (36) and using the stiffnesses from both the GT and pGT forms, the values of M/γ_{11} and M/κ_3 are presented in Table 6. The shearing strain measure turns out to be zero. Recall that the solutions from the VAM are for obtained using $t = 1$ so as to compare with the elasticity solutions.

For the loading case (2), 1D equilibrium in terms of the stress resultants will yield the following distribution:

$$F_1 = -P\cos(\phi) \qquad F_2 = P\sin(\phi) \qquad M_3 = PR\cos(\phi); \tag{41}$$

where $\phi = x_1/l$. Table 6 presents the values of P/γ_{11} and P/κ_3 at $x_1 = 0$ and $P/2\gamma_{12}$ at $x_1 = l$ obtained using both the GT and pGT forms. The results will now be developed from the elasticity solutions given in Ref. [109]. For the loading case (1), the stresses in terms of polar coordinates r and θ, defined in Fig. 3 are given by

$$\begin{aligned}
\sigma_r &= \frac{4M}{N}\left(\frac{a^2b^2}{r^2}\log\frac{b}{a} + b^2\log\frac{r}{b} + a^2\log\frac{a}{r}\right) \\
\sigma_\theta &= -\frac{4M}{N}\left(-\frac{a^2b^2}{r^2}\log\frac{b}{a} + b^2\log\frac{r}{b} + a^2\log\frac{a}{r} + b^2 - a^2\right) \\
\sigma_{r\theta} &= 0
\end{aligned} \tag{42}$$

where

$$N = \left(b^2 - a^2\right)^2 - 4a^2b^2\left(\log\frac{b}{a}\right)^2 \tag{43}$$

From the stresses, the following operations are performed in order to get the 1D generalized strains:

1. The strains are obtained using the constitutive law for plane stress.

2. The displacement field is obtained using the strain-displacement relations and some appropriate geometric boundary conditions.

3. An appropriate coordinate transformation is done. Also the quantities a and b used are expressed in terms of c and R. One thus obtains, $u_1(x_1, x_2)$ and $u_2(x_1, x_2)$.

4. The displacement field is expressed in terms of the displacement of the reference line and warping functions using Eqs. (18) and (20).

$$\hat{\mathbf{R}} - \hat{\mathbf{r}} = \hat{\mathbf{u}} = u_1\mathbf{b}_1 + u_2\mathbf{b}_2 \tag{44}$$

Assuming small displacements and rotations, this reduces to

$$\begin{aligned} u_1 &= u - x_2 v' + w_1 \\ u_2 &= v + w_2 \end{aligned} \tag{45}$$

5. The constraints on warping are then utilized to obtain the displacement components of the reference line:

$$\begin{aligned} u &= \langle u_1 \rangle \\ v &= \langle u_2 \rangle \end{aligned} \tag{46}$$

6. A 1D section rotation variable θ_3 is defined that minimizes the average distance between the warped cross section of the deformed beam and the cross section rigidly translated by $u\mathbf{b}_1 + v\mathbf{b}_2$ and rotated by θ_3. It is easily shown that

$$\theta_3 = -\frac{3}{2c^3}\langle x_2 u_1 \rangle \tag{47}$$

7. The 1D generalized strains are obtained from the above displacement and rotation variables as explained in Sec. 4.2. Note that the 1D variables are now defined with respect to the B frame of reference. If one assumes small displacements and rotations, these generalized strains are

$$\begin{aligned} \gamma_{11} &= u' - k_3 v \\ 2\gamma_{12} &= v' + k_3 u - \theta_3 \\ \kappa_3 &= \theta_3' \end{aligned} \tag{48}$$

It is to be noted that the choice of geometric boundary conditions in step 2 should not affect the 1D strains obtained. We choose the displacement components of the reference line and the section rotation (defined in steps 5 and 6 above) to be zero at the left end of the beam where $x_1 = 0$. The results thus obtained are truncated to the second order in the small parameter (δ) and tabulated with the corresponding results from the VAM in Table 6. A similar procedure can be carried out for loading case (2). From a detailed comparison of results in Table 6 of the VAM and elasticity, it is obvious that both GT and pGT are in very good agreement with the elasticity results though the pGT form does a better job than the GT form in accurately capturing the sectional constants. Also, recall that the transformation of U_2 to U_{GT}/U_{pGT} does not preserve asymptotic exactness; and, hence, there is a minor difference in the value of $P/2\gamma_{12}$ from the GT/pGT approaches when compared to the elasticity solution.

The second part of the verification consists of cross-sectional stress and strain recovery. The elasticity expressions for the stress and strain [109] (with appropriate coordinate transformations) and the corresponding ones from the VAM-based beam theory are obtained as explained towards the end of Sec. 4.2. The expressions from elasticity are to be truncated within the second order of small parameters. As an example, Table 7 presents the analytical expressions for σ_{11} for the loading case (1). The boxed terms in the GT/pGT rows are those that can be obtained only if the warping is evaluated up to second order. Two very straightforward conclusions can

Table 6: Stiffnesses from VAM and elasticity for a curved-strip beam for the loading cases in Fig. 3

Stiffness	VAM (pGT)	VAM (GT)	Elasticity
M/γ_{11}	$-\frac{2c^2E}{(1+\nu)\delta}$	$-\frac{2c^2E}{(1+\frac{6}{5}\nu)\delta}$	$-\frac{2c^2E}{(1+\nu)\delta}$
M/κ_3	$\frac{2}{3}c^3E(1-\frac{2}{15}\delta^2)$	$\frac{2}{3}c^3E\left[1-\frac{2}{15}(1-\frac{\nu^2}{10})\delta^2\right]$	$\frac{2}{3}c^3E(1-\frac{2}{15}\delta^2)$
P/γ_{11}	$\frac{2cE}{\nu}$	$\frac{5cE}{3\nu}$	$\frac{2cE}{\nu}$
P/κ_3	$\frac{2c^2E}{3}\delta$	$\frac{2c^2E}{3}\delta$	$\frac{2c^2E}{3}\delta$
$P/2\gamma_{12}$	$\frac{5cE}{6(1+\nu)}$	$\frac{5cE}{6(1+\nu)}$	$\frac{10cE}{12+11\nu}$

Table 7: σ_{11} recovered by VAM and elasticity for a curved-strip beam for loading case (1)

Case	σ_{11}
VAM (GT)	$-\frac{3Mx_2}{2c^3}-\frac{M((1+\frac{\nu}{5})c^2-3x_2^2)}{2c^4}\delta+\boxed{\frac{7Mx_2(3(1+\frac{2\nu}{21}+\frac{4\nu^2}{35})c^2-5x_2^2)}{2c^4}\delta^2}$
VAM (pGT)	$-\frac{3Mx_2}{2c^3}-\frac{M(c^2-3x_2^2)}{2c^4}\delta+\boxed{\frac{7Mx_2(3c^2-5x_2^2)}{2c^4}\delta^2}$
Elasticity	$-\frac{3Mx_2}{2c^3}-\frac{M(c^2-3x_2^2)}{2c^4}\delta+\frac{7Mx_2(3c^2-5x_2^2)}{2c^4}\delta^2$

be put forth: First, the pGT form gives a result that is much closer to the elasticity solutions than that of the GT form. Second, introduction of the second-order warping makes the recovery process accurate to the next order, which essentially means larger values of the small parameters can be used. It is also trivial to note that the VAM-based beam theory results are in excellent agreement with those from elasticity.

A sample of the stress and strain recovery that has been carried out for the two loading cases, and results for the stresses for each loading case are presented in Fig. 15. The plots were generated for $\delta = 0.15$ and Poisson's ratio of 0.3. The stresses were normalized by M/c^2 for loading case (1) and P/c for loading case (2). Recall, the thickness of the strips is taken to be unity in the elasticity solution [109]. It must be emphasized here that the elasticity solutions used for comparison are the complete expressions, not expanded and truncated to a certain order; this is in contrast to the

treatment above, which was done for comparison purposes. The two results from the variational-asymptotic method, VAM (I) and VAM (II) correspond to the cases when warping is evaluated through first and second orders, respectively. Though there is a difference analytically between the GT and pGT forms, hardly any differences were observed numerically; and, hence, they have not been graphed separately. The stresses are plotted against $\zeta = x_2/c$, a dimensionless coordinate along x_2. For the load case (1), the stresses are independent of x_1, while for case (2), the plots are generated for $x_1 = l/2$.

It can be observed that for σ_{11}, there is no visible difference between the various approaches for both the loading cases, while for σ_{22}, there is an appreciable difference between the plot for the VAM solution from the first- and second-order warping, the latter being obviously closer to the elasticity solution. A similar trend can be observed for the plot of σ_{12} as well, especially near the boundaries. All the approaches confirm $\sigma_{12} = 0$ for loading case (1) and thus are not plotted.

Therefore, from the results presented in this section, the linearized version of the asymptotic beam theory proposed in Sec. 4.2 has been successfully verified up to $O(\sigma^3)$ using the results from plane stress elasticity. This exercise also verifies the accuracy of the results that can be predicted by such an approach to solve beam-like structures.

4.4 Verification for Initial Curvature Effect in VABS

The asymptotic beam theory developed in Sec. 4.2, which has been successfully verified using classical elasticity solutions, was used for the purpose of verifying VABS [136, 23], a computer program used in rotor blade modeling and design. VABS is a very general FEM-based code that uses the VAM to perform the cross-sectional analysis of beam-like structures. Since the procedure employed is the same as that of our beam theory, it is expected that identical results are produced from VABS.

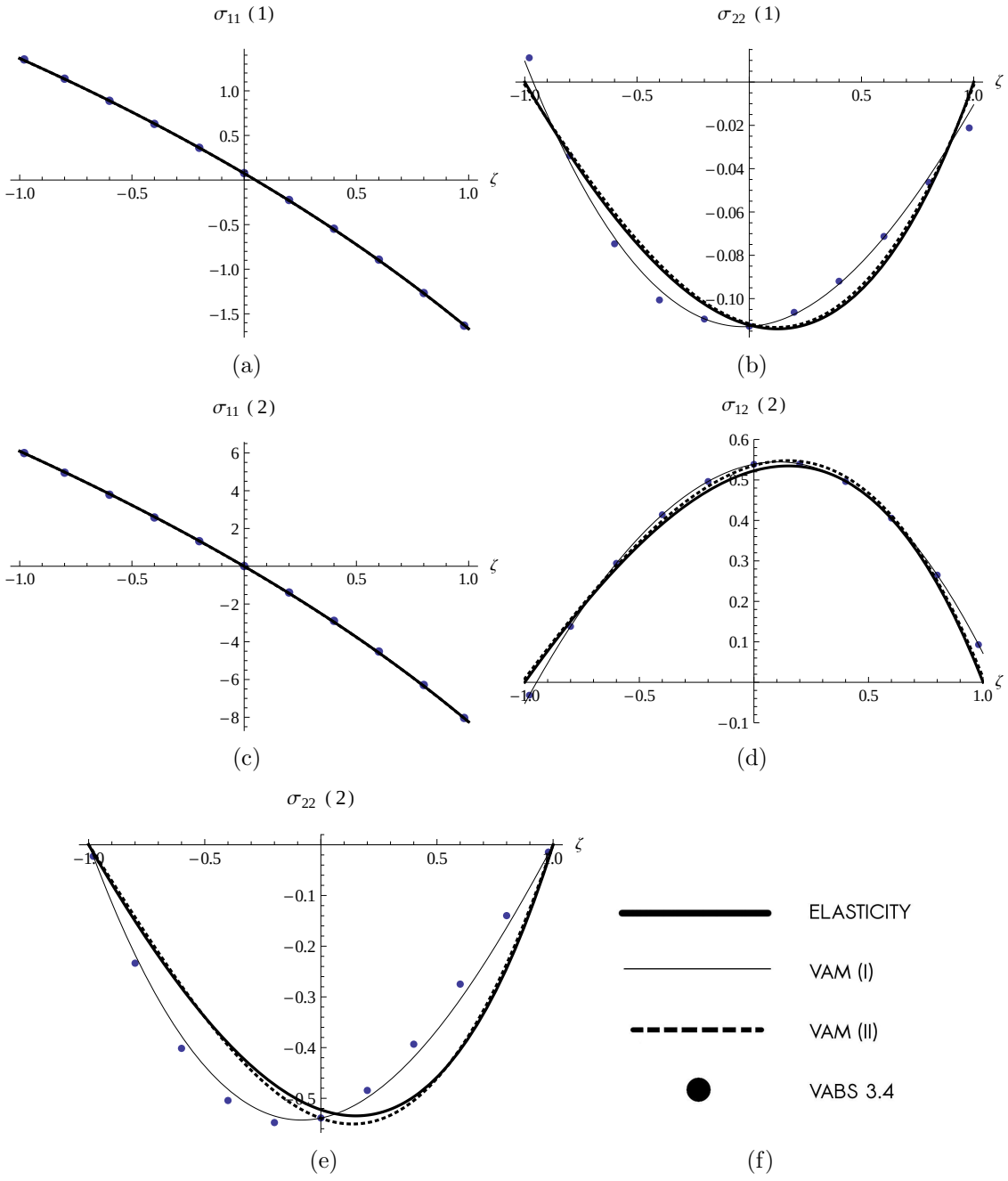

Figure 15: Comparison of the normalized VAM stresses and those from VABS 3.4 with the elasticity solutions for the loading cases in Fig. 3; (a) and (b) are for loading case (1); (c), (d) and (e) are for loading case (2)

The test case chosen was that of a 10×1 isotropic strip with properties $E = 0.26 \times 10^{10}$ and $\nu = 0.3$. The curvature values (k_3) were taken up to 0.05. The stiffness matrices obtained from VABS 3.3 were compared with the beam theory, which exhibited a discrepancy in the extensional stiffness. Upon investigation, two major differences were identified between the analyses behind VABS 3.3 and the above beam theory. First, the VABS 3.3 analysis treats the terms accompanying the generalized strains and their derivatives in the second order asymptotically correct strain energy as constants and not explicit functions of k_3; second, it does not asymptotically expand g (defined in Sec. 4.2) or its powers. It was established using Mathematica that the former does not lead to any change in the stiffness values. For the latter, an analytical solution was generated as in Sec. 4.2, the only difference being the restriction of expansion of g and its powers. It was found that not expanding $\sqrt{g}$ terms in the strains and strain energy leads to certain terms being missed while truncating the expression for the strain energy density beyond the second-order terms. This leads to erroneous terms in the expressions for the first-order warping and, consequently, the second-order energy and the subsequent expressions for the stiffnesses. Using this approach, the second order energy when transformed to a GT form is given by:

$$\begin{aligned} U^g_{GT} =& \frac{1}{2}EA\left(1+\frac{-119-84\nu+25\nu^2}{75}\delta^2\right)\gamma_{11}^2+\frac{1}{2}EI_3\left(1+\frac{15+60\nu+37\nu^2}{75}\delta^2\right)\kappa_3^2 \\ & - EI_3k_3\left(1+\frac{6}{5}\nu\right)\gamma_{11}\kappa_3+\frac{1}{2}\left(\frac{5}{6}GA\right)(2\gamma_{12})^2 \end{aligned} \tag{49}$$

The discrepancy in the extensional stiffness is clearly noted by comparing the above expression with Eq. 38. Once this restriction of the expansion of g and its powers was lifted in the VABS code, the corrected version (VABS 3.4) produced stiffnesses that were in agreement with the predictions of our beam theory. The corrections to the VABS theoretical formulation are given in Appendix A.

The stiffnesses from various approaches are plotted versus k_3 in Figs. 16 – 19.

VAM (GT) and VAM (pGT) are the solutions from the beam theory detailed in Sec. 4.2 from the GT and pGT forms, respectively. VAM (g) is the solution from the same beam theory imposing the restriction that g and its powers are not expanded. It can be concluded that the VAM (g) results are close to that of VABS 3.3 and VAM (GT) is close to VABS 3.4 (within minor numerical differences). This proves the conclusion made above.

For example, if one looks at the extensional stiffness, as in Fig. 16, the VABS 3.3 predictions decrease with k_3, but the results from the above beam theory, both the GT and pGT ones increase with k_3. If we perform the same analysis as in Sec. 4.2 without expanding $\sqrt{g}$ asymptotically, one ends up with the exact same prediction as by VABS 3.3. But obviously, since our beam theory has been successfully verified using elasticity, the predictions from VABS 3.3 can be concluded to be faulty. When this term $\sqrt{g}$ was expanded in VABS (and hence VABS 3.4), they were close agreement with those obtained from GT/pGT results. A similar observation can be made about the bending and extension-bending stiffness. Only in Fig. 19, the elasticity solution is plotted separately as the expression for $P/2\gamma_{12}$ from Table 6 slightly differs from the ones obtained by the GT/pGT approach, which means that the shear stiffness is not exactly the same. The slight discrepancy is because when the GTT process is done, the energy is no longer exact up to second order. The shear stiffness as obtained by VABS is not expected to have any corrections as explained in the previous section. For all other values in Table 6, the pGT and elasticity solutions give identical results; hence, the stiffnesses other than shear are not plotted separately.

VABS 3.4 was also used to perform the sectional stress-strain recovery for the same values of the parameters as in Sec. 4.3 and the results are included in Fig. 15. It can be seen that the results from VABS exactly coincide with those obtained from VAM (I). Though these results are in close agreement with the elasticity solutions, they can be further improved if the warping is evaluated up to second-order as shown

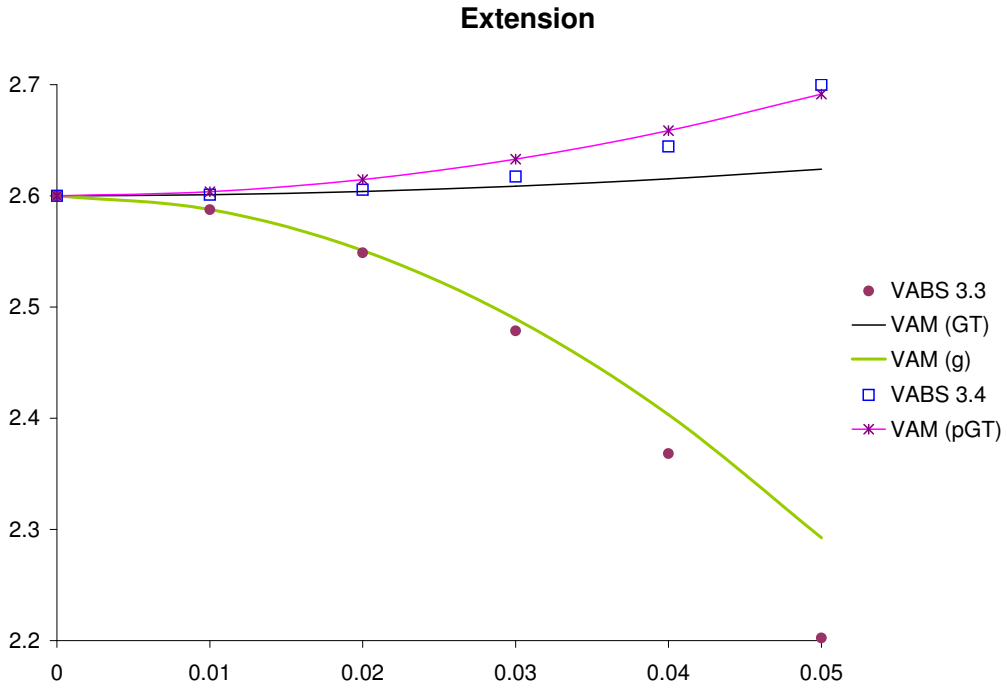

Figure 16: Extensional stiffness vs. k_3 for a 10×1 isotropic strip with initial in-plane curvature obtained from various approaches. Stiffness is scaled down by 10^{10}

by VAM (II).

To conclude, the VAM based beam theory of Sec. 4.2 has served as a very useful verification tool for VABS, a software being extensively used in the rotorcraft and wind turbine industry. It has helped uncover an error in the analysis of curved beams, which could be significant for some structures. The next few sections pertain to the second half of this verification study and extends the analysis for laminated beams with initial curvature.

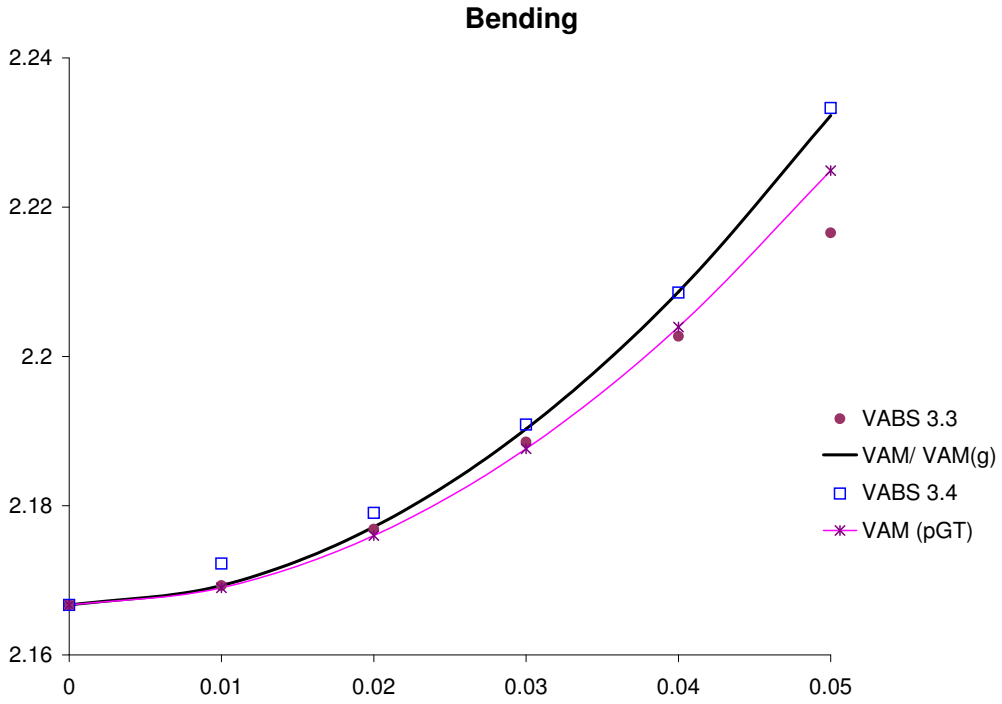

Figure 17: In-plane bending stiffness vs. k_3 for a 10×1 isotropic strip with initial in-plane curvature obtained from various approaches. Stiffness is scaled down by 10^{11}

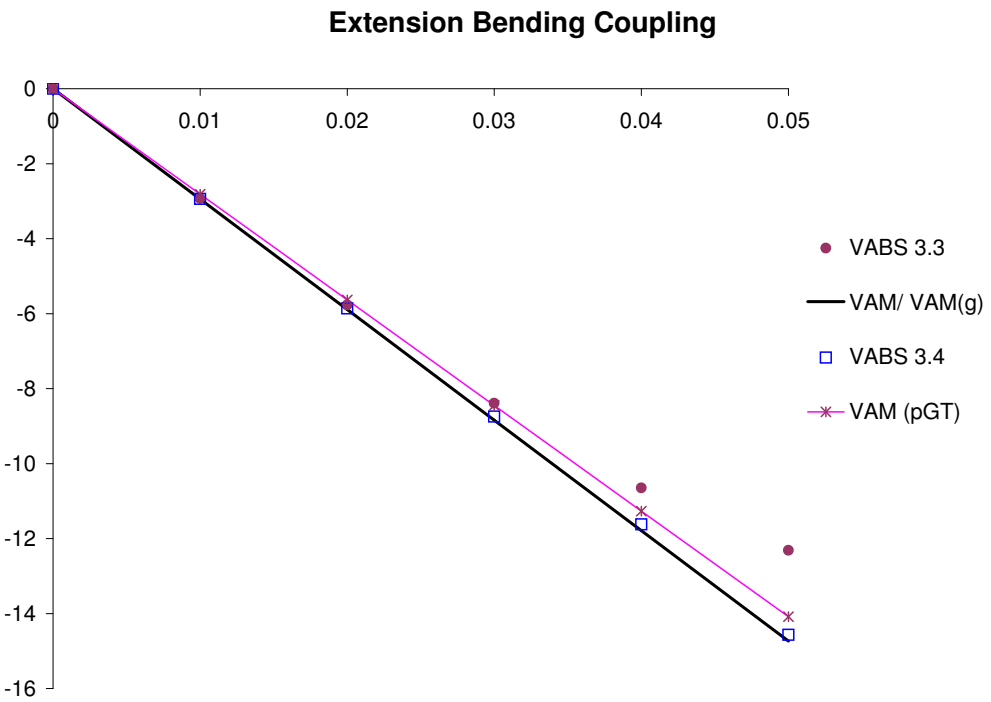

Figure 18: Extension-inplane bending coupling stiffness vs. k_3 for a 10×1 isotropic strip with initial in-plane curvature obtained from various approaches. Stiffness is scaled down by 10^9

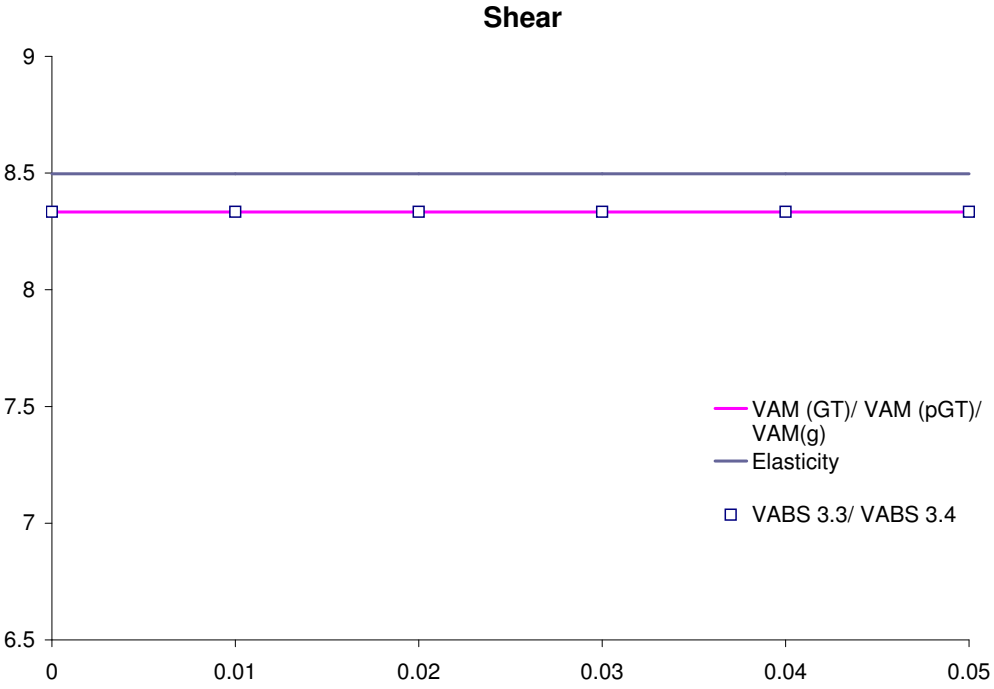

Figure 19: In-plane shear stiffness vs. k_3 for a 10×1 isotropic strip with initial in-plane curvature obtained from various approaches. Stiffness is scaled down by 10^9

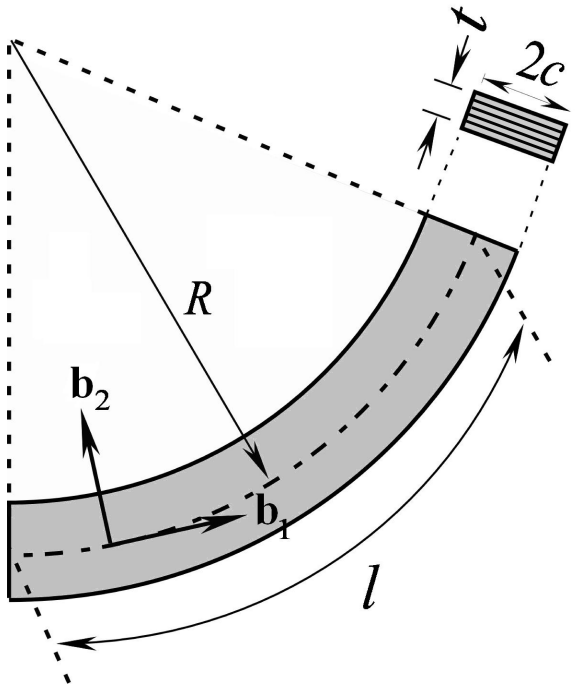

Figure 20: Schematic of the composite strip beam with initial in-plane curvature

4.5 Laminated Strips: Beam Theory

Consider a laminated strip beam with initial curvature $k_3 = 1/R$ as shown in Fig. 20. This section deals with the development of a beam theory to describe the in-plane deformation of such a structural member. In the undeformed configuration, for a given axial coordinate (x_1), the unit vectors $\mathbf{b}_1$ and $\mathbf{b}_2$ are defined to be tangent to the reference line and perpendicular to it as shown.

Two frames of reference are used in the analysis to describe the deformed configuration. The 1D generalized strain measures associated with the frame of reference in which one of its unit vectors is tangent to the reference line are $\overline{\gamma}_{11}$ and $\overline{\kappa}_3$. On the other hand, those associated with the frame of reference in which one of its unit vectors is normal to the cross section are γ_{11}, κ_{11} and $2\gamma_{12}$; geometrically exact expressions for both of these measures may be found in Ref. [46]. The kinematics development parallels that of Sec. 4.2, and the reader is advised to go through this

section for a complete description of the kinematics of this problem. Consequently, the strain expressions

$$\begin{aligned}\Gamma_{11} &= \frac{1}{\sqrt{g}}\left(\overline{\gamma}_{11} - x_2\overline{\kappa}_3 - k_3 w_2 + \frac{\partial w_1}{\partial x_1}\right)\\ \Gamma_{22} &= \frac{\partial w_2}{\partial x_2}\\ 2\Gamma_{12} &= \frac{1}{\sqrt{g}}\left(k_3 w_1 + \frac{\partial w_2}{\partial x_1}\right) + \frac{\partial w_1}{\partial x_2}\end{aligned} \tag{50}$$

are obtained, where the square root of the metric tensor of the undeformed state is given by

$$\sqrt{g} = 1 - x_2 k_3 \tag{51}$$

where w_1 and w_2 are the unknown warping displacements. The problem we are dealing with is a plane stress problem; hence,

$$\begin{Bmatrix} \sigma_{11} \\ \sigma_{22} \\ \sigma_{12} \end{Bmatrix} = \begin{bmatrix} C_{11} & C_{12} & C_{16} \\ C_{12} & C_{22} & C_{26} \\ C_{16} & C_{26} & C_{66} \end{bmatrix} \begin{Bmatrix} \Gamma_{11} \\ \Gamma_{22} \\ 2\Gamma_{12} \end{Bmatrix} \tag{52}$$

Consequently the strain energy per unit length is

$$\mathcal{U} = \frac{1}{2}\left\langle \sqrt{g} \begin{Bmatrix} \sigma_{11} \\ \sigma_{22} \\ \sigma_{12} \end{Bmatrix}^T \begin{Bmatrix} \Gamma_{11} \\ \Gamma_{22} \\ 2\Gamma_{12} \end{Bmatrix} \right\rangle \tag{53}$$

where $\langle\ \rangle$ denotes an integration over the cross section. Now define: $A_{ij} = \int_{-t/2}^{t/2} C_{ij}\, \mathrm{d}x_3$, i.e., an integration through the thickness, which can also be written as a summation over the various layers of the laminate (after appropriate coordinate transformations). One therefore can write the strain energy per unit length to be

$$\mathcal{U} = \int_{-c}^{c} \frac{1}{2}\sqrt{g} \begin{Bmatrix} \Gamma_{11} \\ \Gamma_{22} \\ 2\Gamma_{12} \end{Bmatrix}^T \begin{bmatrix} A_{11} & A_{12} & A_{16} \\ A_{12} & A_{22} & A_{26} \\ A_{16} & A_{26} & A_{66} \end{bmatrix} \begin{Bmatrix} \Gamma_{11} \\ \Gamma_{22} \\ 2\Gamma_{12} \end{Bmatrix} \mathrm{d}x_2 \tag{54}$$

This completes the formulation of the variational aspect of the problem. The current unknowns in the problem are the warping field. An attempt to solve this using standard variational principles will lead to the same difficulties as the corresponding elasticity problem. The solution of the problem is now carried out using asymptotic methods. One does this by identifying the inherent small parameters of the system: c/l and ck_3 which are assumed to be $O(\sigma)$. Also the maximum strain ($\max(\overline{\gamma}_{11}, c\overline{\kappa}_3) = O(\epsilon)$) is assumed to be small compared to unity. Before we proceed further, we define the following quantities which will be used in later analysis:

$$\begin{gathered}
\overline{A}_{11} = A_{11} + \frac{A_{22}A_{16}^2 - 2A_{12}A_{16}A_{26} + A_{12}^2 A_{66}}{A_{26}^2 - A_{22}A_{66}} \\
\tilde{A}_{11} = A_{22}A_{66} - A_{26}^2; \quad \tilde{A}_{22} = A_{11}A_{66} - A_{16}^2; \quad \tilde{A}_{66} = A_{11}A_{22} - A_{12}^2; \\
\tilde{A}_{12} = A_{16}A_{26} - A_{12}A_{66}; \quad \tilde{A}_{16} = A_{12}A_{26} - A_{16}A_{22}; \quad \tilde{A}_{26} = A_{12}A_{16} - A_{26}A_{11}
\end{gathered} \tag{55}$$

The first step of the VAM is a zeroth-order or classical analysis where all terms $O(\sigma)$ are ignored in the strain energy. The warping is assumed to be of order $O(c\epsilon)$, and its subsequent solution justifies this assumption. Standard procedures of calculus of variations yield the warping as

$$\begin{aligned}
w_1^{(0)} &= \frac{\tilde{A}_{16}}{\tilde{A}_{11}} \left(x_2 \overline{\gamma}_{11} + \frac{c^2 - 3x_2^2}{6} \overline{\kappa}_3 \right) \\
w_2^{(0)} &= \frac{\tilde{A}_{12}}{\tilde{A}_{11}} \left(x_2 \overline{\gamma}_{11} + \frac{c^2 - 3x_2^2}{6} \overline{\kappa}_3 \right)
\end{aligned} \tag{56}$$

The classical strain energy per unit length is thus

$$\mathcal{U}_0 = \frac{1}{2} \left\{ \begin{array}{c} \overline{\gamma}_{11} \\ \overline{\kappa}_3 \end{array} \right\}^T \left[\begin{array}{cc} 2c\overline{A}_{11} & 0 \\ 0 & \frac{2c^3}{3}\overline{A}_{11} \end{array} \right] \left\{ \begin{array}{c} \overline{\gamma}_{11} \\ \overline{\kappa}_3 \end{array} \right\} \tag{57}$$

We then proceed to an analysis one order higher. This is done by perturbing the warping with terms of $O(\sigma c\epsilon)$. The resulting minimization problem leads to a set of

Euler-Lagrange equations, which can be solved for the first-order warping

$$
\begin{aligned}
w_1^{(1)} =& \frac{\tilde{A}_{16}\tilde{A}_{12}}{6\tilde{A}_{11}^2}k_3(c^2-3x_2^2)\overline{\gamma}_{11} + \frac{x_2k_3}{6\tilde{A}_{11}}\left[\left(2\overline{A}_{11}A_{26}-\tilde{A}_{16}-\tilde{A}_{26}\right)c^2+\left(\tilde{A}_{26}-\tilde{A}_{16}\right)x_2^2\right]\overline{\kappa}_3 \\
&+ \frac{A_{22}\overline{A}_{11}-\tilde{A}_{66}+\tilde{A}_{12}}{6\tilde{A}_{11}}\overline{\gamma}'_{11} \\
&+ \frac{x_2}{6\tilde{A}_{11}}\left[\left(-\overline{A}_{11}A_{22}-\tilde{A}_{12}+\tilde{A}_{66}\right)(c^2-x_2^2)+\overline{A}_{11}A_{22}(-3c^2+x_2^2)\right]\overline{\kappa}'_3 \\
w_2^{(1)} =& \frac{\tilde{A}_{12}}{\tilde{A}_{11}}\left(\frac{\tilde{A}_{12}}{\tilde{A}_{11}}-1\right)k_3(c^2-3x_2^2)\overline{\gamma}_{11} - \frac{x_2k_3}{6\tilde{A}_{11}}\left[\left(2\overline{A}_{11}A_{66}+\tilde{A}_{22}\right)c^2+\left(2\tilde{A}_{12}-\tilde{A}_{22}\right)x_2^2\right]\overline{\kappa}_3 \\
&- \frac{\tilde{A}_{12}\tilde{A}_{16}}{6\tilde{A}_{11}^2}(c^2-3x_2^2)\overline{\gamma}'_{11} + \frac{x_2}{6\tilde{A}_{11}^2}\left[\tilde{A}_{12}\tilde{A}_{16}(c^2-x_2^2)-\overline{A}_{11}\tilde{A}_{11}A_{26}(x_2^2-3c^2)\right]\overline{\kappa}'_3
\end{aligned}
\tag{58}
$$

Once the first-order warping is determined, the asymptotically correct second-order strain energy per unit length can be obtained

$$
\begin{aligned}
\mathcal{U}_2 =& \frac{1}{2}(S_{110}+S_{112}k_3^2)\overline{\gamma}_{11}^2 + S_{121}k_3\overline{\gamma}_{11}\overline{\gamma}'_{11} + \frac{1}{2}S_{220}\overline{\gamma}_{11}'^2 + S_{141}k_3\overline{\gamma}_{11}\overline{\kappa}_3 + \frac{1}{2}(S_{440}+S_{442}k_3^2)\overline{\kappa}_3^2 \\
&+ \frac{1}{2}S_{550}\overline{\kappa}_3'^2 + S_{240}\overline{\gamma}'_{11}\overline{\kappa}_3 + S_{451}k_3\overline{\kappa}_3\overline{\kappa}'_3 + S_{460}\overline{\kappa}_3\overline{\kappa}''_3
\end{aligned}
\tag{59}
$$

The terms in the above equation are defined as

$$
\begin{aligned}
&S_{110} = 2c\overline{A}_{11};\ S_{112} = \frac{2c^3}{3}\overline{A}_{11}\left(1-\frac{\tilde{A}_{12}}{\tilde{A}_{11}}\right)^2;\ S_{121} = \frac{2c^3}{3}\overline{A}_{11}\frac{\tilde{A}_{16}}{\tilde{A}_{11}}\left(1-\frac{\tilde{A}_{12}}{\tilde{A}_{11}}\right); \\
&S_{220} = \frac{2c^3}{3}\overline{A}_{11}\left(\frac{\tilde{A}_{16}}{\tilde{A}_{11}}\right)^2;\ S_{141} = -\frac{2c^3}{3}\overline{A}_{11}\left(1-\frac{\tilde{A}_{12}}{\tilde{A}_{11}}\right);\ S_{440} = \frac{2c^3}{3}\overline{A}_{11} \\
&S_{550} = \frac{2c^5}{45}\overline{A}_{11}\left(\frac{5\overline{A}_{11}A_{22}+\tilde{A}_{66}}{\tilde{A}_{11}}\right);\ S_{240} = -\frac{2c^3}{3}\overline{A}_{11}\left(\frac{\tilde{A}_{16}}{\tilde{A}_{11}}\right); \\
&S_{460} = \frac{2c^5}{45}\overline{A}_{11}\left(\frac{\tilde{A}_{12}+7\overline{A}_{11}A_{22}-\tilde{A}_{66}}{\tilde{A}_{11}}\right);\ S_{451} = \frac{2c^5}{45}\overline{A}_{11}\left(\frac{6\tilde{A}_{16}-5\overline{A}_{11}A_{26}+\tilde{A}_{26}}{\tilde{A}_{11}}\right); \\
&S_{442} = \frac{2c^5}{45}\overline{A}_{11}\left(9-\frac{10\tilde{A}_{12}+5\overline{A}_{11}A_{66}+\tilde{A}_{22}}{\tilde{A}_{11}}\right);
\end{aligned}
\tag{60}
$$

It can be remarked here that the asymptotically correct strain energy has the

derivatives of the 1D generalized strains which make it unsuitable from an engineering perspective. To overcome this shortcoming, a Generalized Timoshenko (GT) transformation is carried out. The details are similar to those of [89] and are not repeated here. The final GT model can be written as

$$\begin{aligned}\mathcal{U}_{GT} =& \frac{1}{2}\begin{Bmatrix}\gamma_{11}\\ \kappa_3\\ 2\gamma_{12}\end{Bmatrix}^T \begin{bmatrix}X_{11} & X_{12} & X_{13}\\ X_{12} & X_{22} & X_{23}\\ X_{13} & X_{23} & X_{33}\end{bmatrix}\begin{Bmatrix}\gamma_{11}\\ \kappa_3\\ 2\gamma_{12}\end{Bmatrix}\\ =& \frac{1}{2}\begin{Bmatrix}\gamma_{11}\\ \kappa_3\\ 2\gamma_{12}\end{Bmatrix}^T \begin{bmatrix}X_{110}+X_{112}k_3^2 & X_{121}k_3 & X_{130}\\ X_{121}k_3 & X_{220}+X_{222}k_3^2 & X_{231}k_3\\ X_{130} & X_{231}k_3 & X_{330}\end{bmatrix}\begin{Bmatrix}\gamma_{11}\\ \kappa_3\\ 2\gamma_{12}\end{Bmatrix}\end{aligned} \tag{61}$$

The stiffness matrix in the above equation contains terms which are zeroth, first and second order in k_3. The formula for each set is sequentially listed below in the order mentioned.

$$X_{110} = S_{110} + \frac{S_{240}^2}{S_{550}};\ X_{220} = S_{440};\ X_{130} = \frac{S_{240}S_{440}}{S_{550}};\ X_{330} = \frac{S_{440}^2}{S_{550}} \tag{62}$$

$$\begin{aligned}X_{231} &= S_{240} + \frac{S_{440}S_{451} - S_{240}S_{460}}{S_{550}}\\ X_{121} &= S_{141} + \frac{S_{240}S_{451}}{S_{550}} + \frac{1}{S_{440}}\left(\frac{S_{240}^2}{S_{550}} - S_{110}\right)(S_{550} - S_{460})\end{aligned} \tag{63}$$

$$\begin{aligned}X_{222} &= S_{442} + \frac{S_{451}^2}{S_{550}} + \frac{S_{460} - S_{550}}{S_{440}}\left[2\left(S_{141} - \frac{S_{240}S_{451}}{S_{550}}\right) + \frac{1}{S_{440}}(S_{460} - S_{550})\left(\frac{S_{240}^2}{S_{550}} + 2S_{110}\right)\right]\\ X_{112} &= \frac{1}{S_{110}^2 S_{440}^3 S_{550}^2}(\alpha_1 + \alpha_2 + \alpha_3 + \alpha_4 + \alpha_5 + \alpha_6)\end{aligned} \tag{64}$$

where

$$\alpha_1 = -S_{240}^8 + \left[\left(-2S_{141} + S_{220} - 2S_{440}\right) S_{440} - 4S_{110}S_{460}\right] S_{240}^6 + 2S_{110}S_{440}S_{451}S_{240}^5$$

$$\alpha_2 = 2S_{110}S_{240}S_{440}S_{550}\left\{S_{110}S_{451}\left(S_{141}S_{440} + S_{110}S_{460}\right) + S_{121}S_{440}\left[S_{440}\left(S_{141} + S_{440}\right) + S_{110}S_{460}\right]\right\}$$

$$\alpha_3 = 2S_{110}S_{440}S_{240}^3\left[S_{440}S_{451}\left(S_{141} + S_{440}\right) + 2S_{110}S_{460}S_{451} + S_{121}S_{440}S_{550}\right]$$

$$\alpha_4 = S_{240}^4\Big[2S_{460}S_{550}S_{110}^2 + S_{141}^2S_{440}^2 + \left(S_{440}^2 + 2S_{110}S_{460}\right)^2 - 2S_{220}\left(S_{440}^3 + S_{110}S_{460}S_{440}\right)$$
$$+ 2S_{141}S_{440}\left(S_{440}^2 - S_{220}S_{440} + 2S_{110}S_{460} + S_{110}S_{550}\right)\Big]$$

$$\alpha_5 = S_{110}^2S_{550}^2\left\{S_{112}S_{440}^3 + S_{110}S_{550}\left[S_{110}\left(S_{550} - 2S_{460}\right) - 2S_{141}S_{440}\right]\right\}$$

$$\alpha_6 = S_{240}^2\Bigg(S_{220}S_{440}\left(S_{440}^2 + S_{110}S_{460}\right)^2 + 2S_{141}S_{440}\left[S_{220}\left(S_{440}^3 + S_{110}S_{460}S_{440}\right) - 3S_{110}^2S_{460}S_{550}\right] -$$
$$S_{110}^2\left\{\left[S_{451}^2 + 2S_{550}\left(S_{442} + S_{550}\right)\right]S_{440}^2 + 2S_{110}S_{550}\left(3S_{460}^2 - 2S_{550}S_{460} + S_{550}^2\right)\right\} + S_{141}^2S_{220}S_{440}^3\Bigg) \tag{65}$$

This completes the formulation of the beam theory. Eq. (61) provides the stiffness matrix that can be used in the 1D beam analysis. Once the generalized strains are determined, the strain can be recovered by substituting Eqs. (56) and (58) into Eq. (50). The stresses follow from Eq. (52), completing the recovery aspect. Before closing, it is important to make several observations. First, no *ad hoc* assumptions were used regarding the beam deformation. Second, with emphasis on the fact that the beam is constituted of composite materials, the entire development is analytical. The author wishes to emphasize the latter point as the unique aspect and perhaps the most singular contribution of this part of the chapter to existing literature on beam theory.

4.6 Extraction of Extension-Shear Coupling from Plate Theory

When casting the second-order asymptotically correct strain energy into a GT form, one has to solve a set of nonlinear, algebraic equations. In the course of this process,

Figure 21: Composite Strip with $k_3 = 0$, subjected to a tip force P as shown

it is observed that the equation for the extension-shear coupling term, X_{130} yields no information by being indeterminate (it is satisfied for all values of X_{130}). It is to be noted that X_{130} describes the extension-shear coupling stiffness for the beam without initial curvature ($k_3 = 0$). Since the theory has been obtained using a rigorous dimensional reduction of 3D elasticity, one should be able to recover this term from the corresponding plate theory. Consider the beam of Fig. 21 subjected to a load P as shown.

Classical Laminated Plate Theory (CLPT) yields:

$$\begin{Bmatrix} N_{11} \\ N_{22} \\ N_{12} \end{Bmatrix} = \begin{bmatrix} A_{11} & A_{12} & A_{16} \\ A_{12} & A_{22} & A_{26} \\ A_{16} & A_{26} & A_{66} \end{bmatrix} \begin{Bmatrix} \epsilon_{11} \\ \epsilon_{22} \\ 2\epsilon_{12} \end{Bmatrix} \tag{66}$$

The N_{ij} and ϵ_{ij} are the membrane stress-resultants and strains respectively. For further details on this subject, the reader is advised to refer to Ref. [133]. Now since the member is also qualified to be modeled as a beam, we can reduce the above model by setting $N_{22} = 0$

$$\begin{Bmatrix} N_{11} \\ N_{12} \end{Bmatrix} = \begin{bmatrix} A_{11} - \frac{A_{12}^2}{A_{22}} & A_{16} - \frac{A_{12}A_{26}}{A_{22}} \\ A_{16} - \frac{A_{26}A_{12}}{A_{22}} & A_{66} - \frac{A_{26}^2}{A_{22}} \end{bmatrix} \begin{Bmatrix} \epsilon_{11} \\ 2\epsilon_{12} \end{Bmatrix} \tag{67}$$

For this case, we can use $\int_{-c}^{c} N_{11}\,\mathrm{d}x_2 = P$, $\int_{-c}^{c} N_{12}\,\mathrm{d}x_2 = 0$, $\int_{-c}^{c} \epsilon_{11}\,\mathrm{d}x_2 = 2c\gamma_{11}$ and $\int_{-c}^{c} \epsilon_{12}\,\mathrm{d}x_2 = 2c\gamma_{12}$. Upon solving for γ_{11} and γ_{12} and comparing the results from the beam GT model (setting $k_3 = 0$), we obtain two equations for the three unknowns, X_{110}, X_{330} and X_{130}. Extraction of the first two quantities from the GT

transformation process presents no difficulties and the these values satisfy the first equation (equality of γ_{11}). The second equation (equality of $2\gamma_{12}$) is used to extract the extension-shear coupling term.

$$\begin{aligned} X_{130} =& -\frac{10c\overline{A}_{11}\tilde{A}_{16}}{5\overline{A}_{11}A_{22}+\tilde{A}_{66}} \\ =& \frac{S_{240}S_{440}}{S_{550}} \end{aligned} \tag{68}$$

This extraction clearly demonstrates the mathematical rigor of the VAM. Since the VAM performs the dimensional reduction with no *ad hoc* assumptions, for a given structural member, a plate (2D) and the corresponding beam (1D) theory will be consistent with not only the starting point which is 3D elasticity, but between themselves as well.

4.7 Validation of Results with VABS

The beam theory developed in Section 4.5 will now be validated using the computer program VABS. The consistency of VABS with 3D FEM has been established in several studies in literature [136, 65]. Validation will be presented in the form of cross-sectional stiffness and stress recovery for a composite beam with a given layup configuration.

The test case is that a cross section manufactured from AS5/3501-6 graphite epoxy with cross-sectional dimensions 1.182 in. $\times$ 0.0579 in., consisting of a $[45\,^\circ/0\,^\circ]_{3s}$ layup. This case was chosen because it has been validated and verified for VABS using 3D FEM [65, 122]. In all the plots that follow, the solid black line denotes the results of the current beam theory (obtained using Mathematica®) and the discrete squares/circles, those of VABS. The stiffness values have been normalized as follows

$$\begin{aligned} \overline{X}_{ii} &= \frac{X_{ii}}{(X_{ii})_{k_3=0}} \\ \overline{X}_{ij} &= \frac{X_{ij}}{\sqrt{(X_{ii}X_{jj})_{k_3=0}}} \quad (i \neq j) \end{aligned} \tag{69}$$

For consistency, the normalizing values were chosen to be those from VABS, i.e., the quantities in the denominator of the above equation were VABS inputs. The six different stiffnesses for this case are plotted in Fig. 22. It can be seen that there is an excellent agreement between the results of VABS and from the current approach. It is observed that there is a slight discrepancy between the results of the extension-bending coupling stiffness. Upon curve fitting the VABS results, it was determined that the difference was a term cubic in k_3. Thus VABS has picked up some cubic terms whose accuracy cannot be trustworthy as our GT model is extracted from a second-order asymptotically correct strain energy. This is due to the fact that during the GT transformation VABS considers the terms accompanying the generalized strains and their derivatives in the second order asymptotically correct strain energy as numbers (without the explicit dependence on k_3). However this difference is small when compared to the actual correction.

The stress recovery is carried out for two different loading cases, the first with the beam subjected to a unit bending moment (1 lb-in), and the second with it subjected to a unit tip force (1 lb) as shown in Fig. 4.7. The stress recovery was carried out at the section at the middle of the beam, i.e., at $x_1 = l/2$ and along $x_3 = 0$ and for $k_3 = 0.2$ in^{-1}. A choice of the loading cases is from Ref. [109] where the corresponding results for the isotropic case were studied in and used for the VAM validation in Ref. [89].

The stress variations for these two cases are presented in Fig. 24. Again, we observe an excellent agreement between the current and VABS results. Agreement of stresses implies that the strain and displacement (when the appropriate geometric boundary conditions are applied, e.g, for the second case, the left end is fixed) are in good agreement as well. Validation studies also have been carried out for another layup configuration. To prevent cluttering of results and subsequent confusion for the reader, it suffices to say that the results from the two approaches were in good

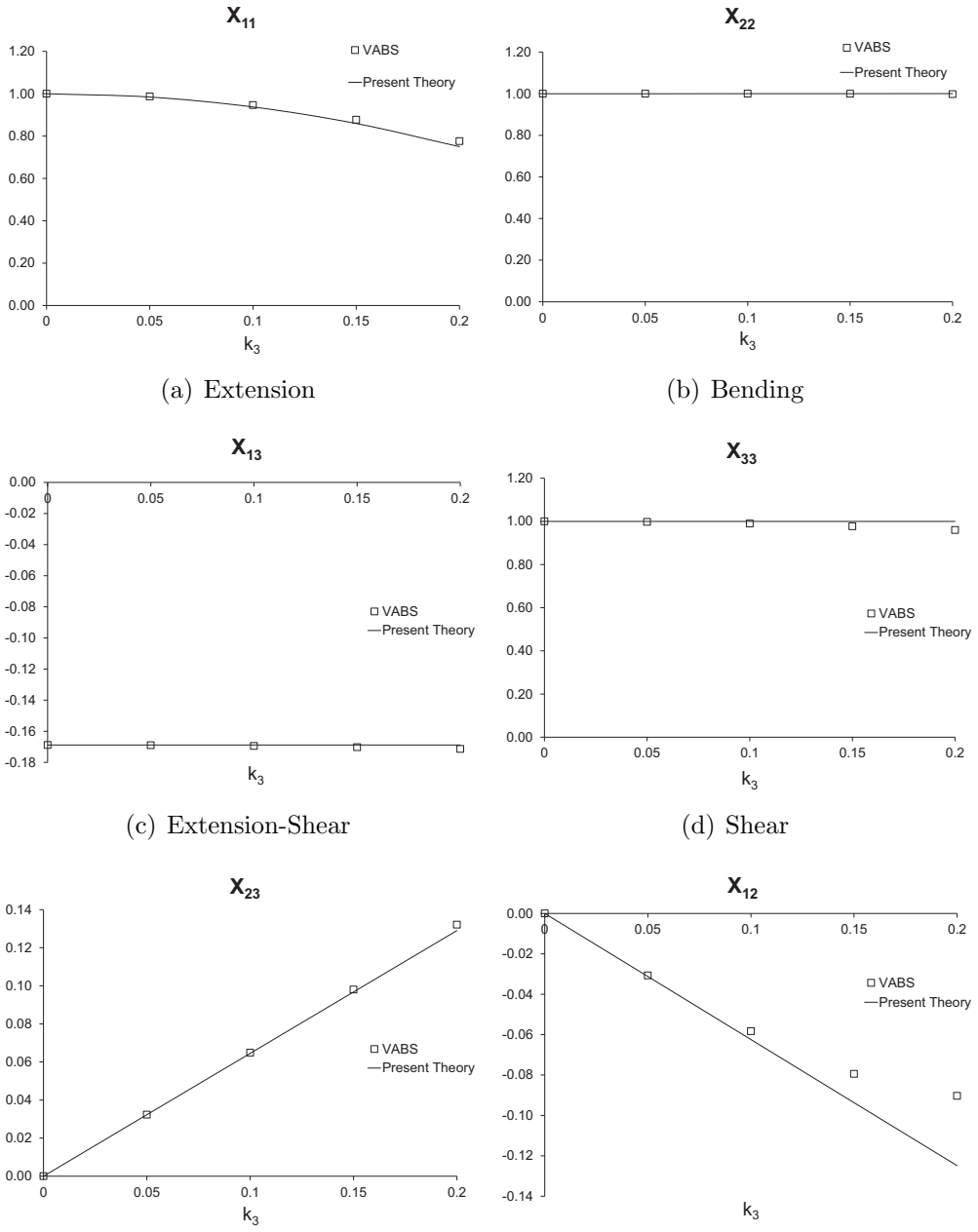

(a) Extension (b) Bending

(c) Extension-Shear (d) Shear

(e) Bending-Shear (f) Extension-Bending

Figure 22: Normalized in-plane stiffnesses versus in-plane curvature k_3 (with units in^{-1}) for a 1.182 in. $\times$ 0.0579 in. graphite-epoxy strip; layup: $[45\,^\circ/0\,^\circ]_{3s}$, VABS vs. current approach

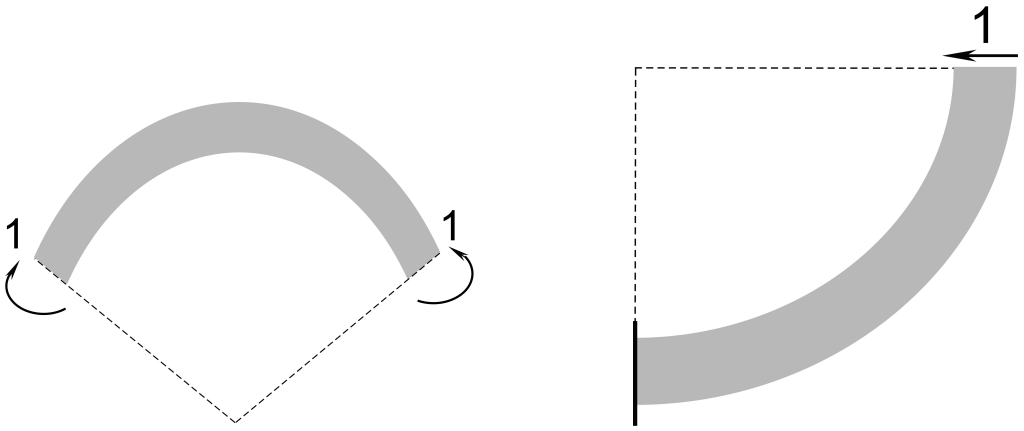

(a) Loading Case 1 (b) Loading Case 2

Figure 23: Composite Strip subjected to (a) Constant Bending Moment and (b) Tip Shear Force

agreement. The current test case drives home the point desired to be made.

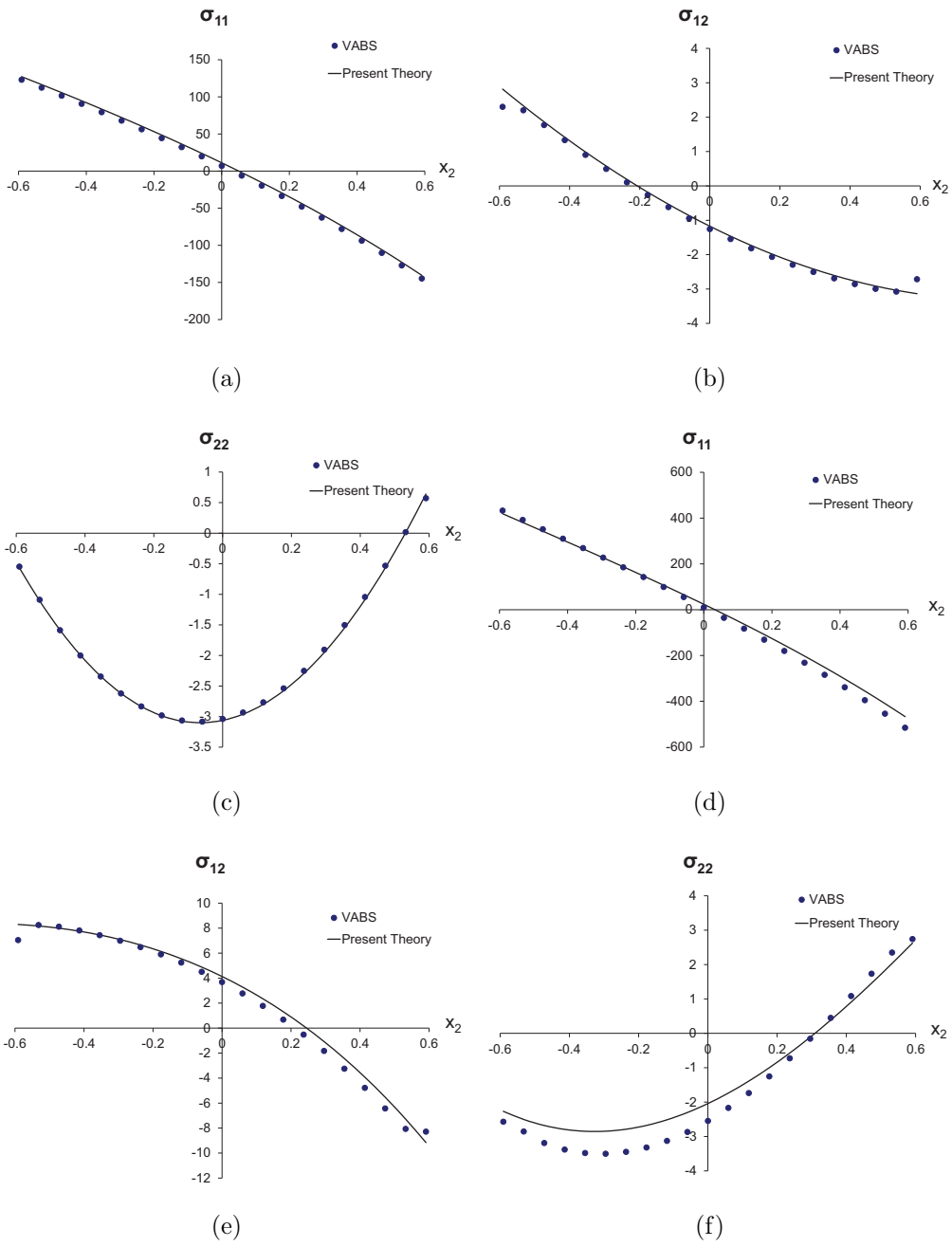

Figure 24: Cross-sectional stress (psi) recovery for a 1.182 in. $\times$ 0.0579 in. graphite-epoxy strip with layup $[45\,^\circ/0\,^\circ]_{3s}$ at $x_1 = l/2$ and for $k_3 = 0.2$ in^{-1}; (a)$-$(c) are for loading case 1; (d)$-$(f) are for loading case 2

V

HIGHER FIDELITY STRESS-STRAIN-DISPLACEMENT RECOVERY

Courage is not the absence of fear, but rather the ability to understand, rationalize and triumph over fear.

– Various

From Chapters 3 and 4, an important conclusion established was the usefulness in perturbing the warping to the second-order and the subsequent evaluation of the stress, strain and displacement to a higher fidelity. The thus recovered 3D quantities would be accurate up to second order in small parameters since the stiffness matrix is currently extracted from a second-order asymptotically correct strain energy. It is therefore desirable to implement this feature in the general VABS finite-element procedure for anisotropic beams with initial twist and curvature. In principle, the procedure is simple enough: perturb the existing first-order warping to one order higher in small parameters and obtain the resulting strain energy. Using the standard procedures of calculus of variations and keeping in mind the constraints on the warping field, the Euler-Lagrange equations and boundary conditions are obtained, which can be solved for the warping field. The formulation presented in this chapter remains consistent with the zeroth- and first-order formulation – the latest version of which is presented in Appendix A. The final expression for the second-order warping reduces to, albeit, after a series of remarkable cancellations, a relatively simple one.

This chapter contains all the equations needed for obtaining a higher-order recovery of stress, strain and displacement in VABS. The procedure can be considered to be of two parts: evaluating the second order warping and obtaining the final recovery by

evaluation of the derivatives of the 1D strain measures. Finally, some results from the updated version of VABS are presented to demonstrate the capturing of second-order terms and any possible advantages over the previously existing first-order recovery.

5.1 Evaluating Second-Order Warping

The finite-element procedure to determine second order warping for VABS is now detailed. The $\sqrt{g}$ correction outlined in Chapter 4 has complicated the process by significantly increasing the number of terms (impaled by one's own sword!). One begins with the expansion of the relevant powers of g

$$\begin{aligned}
\sqrt{g} &= \beta_{11} - y_2 k_3 + y_3 k_2 = g_0 + g_1 \\
\frac{1}{\sqrt{g}} &= \frac{1}{\beta_{11}} + \frac{y_2 k_3 - y_3 k_2}{\beta_{11}^2} + \frac{(y_2 k_3 - y_3 k_2)^2}{\beta_{11}^3} + \frac{(y_2 k_3 - y_3 k_2)^3}{\beta_{11}^4} + \frac{(y_2 k_3 - y_3 k_2)^4}{\beta_{11}^5} + O(k_i^5) \\
&= \gamma g_0 + \gamma g_1 + \gamma g_2 + \gamma g_3 + \gamma g_4 + O(k_i^5)
\end{aligned} \tag{70}$$

The strain is defined in the usual way

$$\Gamma = \Gamma_{a\beta}\ w + \Gamma_\epsilon\ \bar{\epsilon} + \Gamma_R\ w + \Gamma_l\ w' \tag{71}$$

The operators used in Eq. (71) are now defined.

$$\begin{aligned}
\Gamma_\beta &= \sum_{i=0}^{4} \Gamma_{\beta_i} \\
\Gamma_{\beta_i} &= -\gamma g_i \left(\beta_{12} \frac{\partial}{\partial y_2} + \beta_{13} \frac{\partial}{\partial y_3} \right)
\end{aligned} \tag{72}$$

$$\Gamma_{a\beta} = \begin{bmatrix} \Gamma_\beta & 0 & 0 \\ \frac{\partial}{\partial y_2} & \Gamma_\beta & 0 \\ \frac{\partial}{\partial y_3} & 0 & \Gamma_\beta \\ 0 & \frac{\partial}{\partial y_2} & 0 \\ 0 & \frac{\partial}{\partial y_3} & \frac{\partial}{\partial y_2} \\ 0 & 0 & \frac{\partial}{\partial y_3} \end{bmatrix} = \sum_{i=0}^{4} \Gamma_{a\beta_i}; \qquad \Gamma_{a\beta_i} = \begin{bmatrix} \Gamma_{\beta_i} & 0 & 0 \\ \frac{\partial}{\partial y_2} & \Gamma_{\beta_i} & 0 \\ \frac{\partial}{\partial y_3} & 0 & \Gamma_{\beta_i} \\ 0 & \frac{\partial}{\partial y_2} & 0 \\ 0 & \frac{\partial}{\partial y_3} & \frac{\partial}{\partial y_2} \\ 0 & 0 & \frac{\partial}{\partial y_3} \end{bmatrix} \tag{73}$$

$$\Gamma_\epsilon = \frac{1}{\sqrt{g}} \begin{bmatrix} \beta_{11} & 0 & y_3 & -y_2 \\ \beta_{12} & -y_3 & 0 & 0 \\ \beta_{13} & y_2 & 0 & 0 \\ 0 & 0 & 0 & 0 \\ 0 & 0 & 0 & 0 \\ 0 & 0 & 0 & 0 \end{bmatrix} = \frac{1}{\sqrt{g}} \overline{\Gamma}_\epsilon = \sum_{i=0}^{4} \gamma g_i \overline{\Gamma}_\epsilon \tag{74}$$

$$\Gamma_\ell = \frac{1}{\sqrt{g}} \begin{bmatrix} 1 & 0 & 0 \\ 0 & 1 & 0 \\ 0 & 0 & 1 \\ 0 & 0 & 0 \\ 0 & 0 & 0 \\ 0 & 0 & 0 \end{bmatrix} = \frac{1}{\sqrt{g}} \overline{\Gamma}_\ell = \sum_{i=0}^{3} \gamma g_i \overline{\Gamma}_\ell \tag{75}$$

$$\Gamma_R = \frac{1}{\sqrt{g}} \begin{bmatrix} \Gamma_{hR} & -k_3 & k_2 \\ k_3 & \Gamma_{hR} & -k_1 \\ -k_2 & k_1 & \Gamma_{hR} \\ 0 & 0 & 0 \\ 0 & 0 & 0 \\ 0 & 0 & 0 \end{bmatrix} = \frac{1}{\sqrt{g}} \overline{\Gamma}_R = \sum_{i=0}^{3} \gamma g_i \overline{\Gamma}_R \tag{76}$$

where

$$\Gamma_{hR} = k_1 \left(y_3 \frac{\partial}{\partial y_2} - y_2 \frac{\partial}{\partial y_3} \right) \tag{77}$$

In the absence of obliqueness (i.e. $\beta_{1\alpha} = 0$), then $\Gamma_{a\beta} = \Gamma_{a\beta_0}$. The strain energy per unit length is

$$\begin{aligned} 2U =& \langle\langle \sigma^T \Gamma \rangle\rangle \\ \langle\langle \bullet \rangle\rangle =& \langle \bullet \sqrt{g} \rangle \end{aligned} \tag{78}$$

where $\langle \bullet \rangle$ denotes an integration over the beam cross section. The expression for the strain energy can be rewritten using the finite element discretization of the warping

field [46]

$$\begin{aligned} w\left(x_1, x_2, x_3\right) &= S\left(x_2, x_3\right) V\left(x_1\right) \\ w &= \lfloor w_1 \quad w_2 \quad w_3 \rfloor^T \end{aligned} \tag{79}$$

where $S(x_2, x_3)$ are the finite-element shape functions.

$$\begin{aligned} 2U =& V^T E V + 2V^T (D_{a\epsilon}\overline{\epsilon} + D_{aR}V + D_{a\ell}V') + \overline{\epsilon}^T D_{\epsilon\epsilon}\overline{\epsilon} + V^T D_{RR} V \\ &+ V'^T D_{\ell\ell} V' + 2V^T D_{R\epsilon}\overline{\epsilon} + 2V'^T D_{\ell\epsilon}\overline{\epsilon} + 2V^T D_{R\ell} V' \end{aligned} \tag{80}$$

The matrices in the above equation are defined as

$$\begin{aligned} D_{a\epsilon} &= \sum_{i=0}^{4} D_{a\epsilon_i} \\ D_{a\epsilon_i} &= \langle (\Gamma_{a\beta_i} S)^T D\overline{\Gamma}_{\epsilon} \rangle \end{aligned} \tag{81}$$

$$\begin{aligned} D_{aR} &= \sum_{i=0}^{3} D_{aR_{i+1}} \\ D_{aR_{i+1}} &= \langle (\Gamma_{a\beta_i} S)^T D\overline{\Gamma}_{R} S \rangle \end{aligned} \tag{82}$$

$$\begin{aligned} D_{a\ell} &= \sum_{i=0}^{4} D_{a\ell_{i+1}} \\ D_{a\ell_{i+1}} &= \langle (\Gamma_{a\beta_i} S)^T D\overline{\Gamma}_{\ell} S \rangle \end{aligned} \tag{83}$$

$$\begin{aligned} D_{\epsilon\epsilon} &= \sum_{i=0}^{4} D_{\epsilon\epsilon_i} \\ D_{\epsilon\epsilon_i} &= \langle \gamma g_i \overline{\Gamma}_{\epsilon}^T D\overline{\Gamma}_{\epsilon} \rangle \end{aligned} \tag{84}$$

$$\begin{aligned} D_{RR} &= \sum_{i=0}^{2} D_{RR_{i+2}} \\ D_{RR_{i+2}} &= \langle \gamma g_i (\overline{\Gamma}_{R} S)^T D\overline{\Gamma}_{R} S \rangle \end{aligned} \tag{85}$$

$$\begin{aligned} D_{\ell\ell} &= \sum_{i=0}^{2} D_{\ell\ell_{i+2}} \\ D_{\ell\ell_{i+2}} &= \langle \gamma g_i (\overline{\Gamma}_{\ell} S)^T D\overline{\Gamma}_{\ell} S \rangle \end{aligned} \tag{86}$$

$$D_{R\epsilon} = \sum_{i=0}^{3} D_{R\epsilon_{i+1}} \tag{87}$$
$$D_{R\epsilon_{i+1}} = \langle \gamma g_i (\overline{\Gamma}_R S)^T D \overline{\Gamma}_\epsilon \rangle$$

$$D_{\ell\epsilon} = \sum_{i=0}^{3} D_{\ell\epsilon_{i+1}} \tag{88}$$
$$D_{\ell\epsilon_{i+1}} = \langle \gamma g_i (\overline{\Gamma}_\ell S)^T D \overline{\Gamma}_\epsilon \rangle$$

$$D_{R\ell} = \sum_{i=0}^{2} D_{R\ell_{i+2}} \tag{89}$$
$$D_{R\ell_{i+2}} = \langle \gamma g_i (\overline{\Gamma}_R S)^T D \overline{\Gamma}_\ell S \rangle$$

$$\begin{aligned} E =& \sum_{i=0}^{4} E_i \\ E_i =& g_0 K_i + g_1 K_{i-1} \\ K_i =& \sum_{m=0}^{4} \sum_{n=0}^{4} (\Gamma_{a\beta_n} S)^T D (\Gamma_{a\beta_m} S) \\ & \forall m, n \in \mathbb{Z};\ m+n=i;\ 0 \le m, n \le 4 \end{aligned} \tag{90}$$

In the last equation, it should be noted that that by definition, one sets $K_{-1} = 0 = K_5$. The total strain energy that is to be considered is therefore

$$\begin{aligned} 2U =& (V_0+V_1+V_2)^T (E_0+E_1+E_2+E_3+E_4)(V_0+V_1+V_2) \\ &+ 2(V_0+V_1+V_2)^T (D_{a\epsilon_0}+D_{a\epsilon_1}+D_{a\epsilon_2}+D_{a\epsilon_3}+D_{a\epsilon_4})\overline{\epsilon} \\ &+ 2(V_0+V_1+V_2)^T (D_{aR_1}+D_{aR_2}+D_{aR_3}+D_{aR_4})(V_0+V_1+V_2) \\ &+ 2(V_0+V_1+V_2)^T (D_{a\ell_1}+D_{a\ell_2}+D_{a\ell_3}+D_{a\ell_4})(V_0'+V_1'+V_2') \\ &+ \overline{\epsilon}^T (D_{\epsilon\epsilon_0}+D_{\epsilon\epsilon_1}+D_{\epsilon\epsilon_2}+D_{\epsilon\epsilon_3}+D_{\epsilon\epsilon_4})\overline{\epsilon} \\ &+ (V_0+V_1+V_2)^T (D_{RR_2}+D_{RR_3}+D_{RR_4})(V_0+V_1+V_2) \\ &+ (V_0'+V_1'+V_2')^T (D_{\ell\ell_2}+D_{\ell\ell_3}+D_{\ell\ell_4})(V_0'+V_1'+V_2') \\ &+ 2(V_0+V_1+V_2)^T (D_{R\epsilon_1}+D_{R\epsilon_2}+D_{R\epsilon_3}+D_{R\epsilon_4})\overline{\epsilon} \\ &+ 2(V_0'+V_1'+V_2')^T (D_{\ell\epsilon_1}+D_{\ell\epsilon_2}+D_{\ell\epsilon_3}+D_{\ell\epsilon_4})\overline{\epsilon} \\ &+ 2(V_0+V_1+V_2)^T (D_{R\ell_2}+D_{R\ell_3}+D_{R\ell_4})(V_0'+V_1'+V_2') \end{aligned} \tag{91}$$

The terms are now split into orders for the asymptotic analysis. Note that the definitions of the terms are such that the order of any term is the sum of all the numbers that appear as subscripts in that term. While minimizing the strain energy, one needs to also consider the constraints due to warping

$$V^T D_c = 0 \tag{92}$$

The kernel of $\Gamma_{a\beta_0}$, ψ, also comes in handy during the development

$$\begin{aligned} \Gamma_{a\beta_0}\psi = 0 \implies E_0\Psi = 0 \\ \psi = S\Psi \end{aligned} \tag{93}$$

5.1.1 Zeroth-Order Analysis

From Eq. (91), the zeroth-order energy can be obtained.

$$2U_0 = V_0^T E_0 V_0 + 2V_0^T D_{a\epsilon_0}\overline{\epsilon} + \overline{\epsilon}^T D_{\epsilon\epsilon_0}\overline{\epsilon} \tag{94}$$

Keeping track of the warping constraints, the final equation for zeroth-order warping is therefore

$$E_0 V_0 + D_{a\epsilon_0}\overline{\epsilon} = 0 \tag{95}$$

After considering singularities of E_0 [46], the final solution is

$$V_0 = \hat{V}_0\overline{\epsilon} \tag{96}$$

5.1.2 First-Order Analysis

The relevant terms in the strain energy are those up to second-order. However, the zeroth-order strain energy is a constant and does not feature in the first-order warping calculation.

$$\begin{aligned} 2U_1 = &\overline{\epsilon}^T D_{\epsilon\epsilon_1}\overline{\epsilon} + (\cancel{2V_1^T D_{a\epsilon_1}} + 2V_0^T D_{a\epsilon_1} + V_0'^T D_{\ell\epsilon_1} + V_0^T D_{R\epsilon_1})\overline{\epsilon} \\ &2V_0^T D_{aR_1} V_0 + \cancel{V_1^T E_0 V_0} + V_0^T E_1 V_0 + \cancel{V_0^T E_0 V_1} + 2V_0^T D_{a\ell_1} V_0' \end{aligned} \tag{97}$$

$$
\begin{aligned}
2U_2 =&\bar{\epsilon}D_{\epsilon\epsilon_2}\bar{\epsilon} + (\cancel{2V_2^T D_{a\epsilon_0}} + 2V_1^T D_{a\epsilon_1} + 2V_0^T D_{a\epsilon_2} + 2V_1'^T D_{\ell\epsilon_1} + 2V_0'^T D_{\ell\epsilon_2} \\
&+ 2V_1^T D_{R\epsilon_1} + 2V_0^T D_{R\epsilon_2})\bar{\epsilon} + 2V_1^T D_{aR_1}V_0 + 2V_0^T D_{aR_2}V_0 + V_0^T D_{RR_2}V_0 \\
&+ \cancel{V_2^T E_0 V_0} + V_1^T E_1 V_0 + V_0^T E_2 V_0 + 2V_0^T D_{aR_1}V_1 + V_1^T E_0 V_1 + V_0^T E_1 V_1 \\
&+ \cancel{V_0^T E_0 V_2} + 2V_1^T D_{a\ell_1}V_0' + 2V_0^T D_{a\ell_2}V_0' + V_0^T D_{\ell\ell_2}V_0' + 2V_0^T D_{R\ell_2}V_0' + 2V_0^T D_{a\ell_1}V_1'
\end{aligned} \tag{98}
$$

The canceled terms in the above two equations are results of Eq. (95). As expected the second-order warping plays no part in the second-order strain energy (a fact stated in Ref. [124]). After considerations of the warping constraints, the final equation for V_1 is

$$
\begin{aligned}
E_0 V_1 =&(D_c(\Psi^T D_c)^{-1}\Psi^T - \Delta)(D_R\bar{\epsilon} + D_S\bar{\epsilon}') \\
D_R =&E_1\hat{V}_0 + D_{a\epsilon_1} + (D_{aR_1} + D_{aR_1}^T)\hat{V}_0 + D_{R\epsilon_1} \\
D_S =&(D_{a\ell_1} - D_{a\ell_1}^T)\hat{V}_0 - D_{\ell\epsilon_1}
\end{aligned} \tag{99}
$$

The solution after removing the singularities of E_0 may be written as

$$
V_1 = V_{1R}\bar{\epsilon} + V_{1S}\bar{\epsilon}' \tag{100}
$$

5.1.3 Second-Order Analysis

The relevant terms in the strain energy are those up to fourth-order. The algebra is very tedious. However since our interest is only to evaluate the second-order warping and not the final energy, the following simplifications (not assumptions!) are made. One, there the terms up to second order are constant and do not enter into V_2 computation. Second, the terms in the third- and fourth-order strain energy can be simplified to exclude the terms that do not contain V_2 for the same reason. Thus,

$$
\begin{aligned}
2U_3 =&(2V_2^T D_{a\epsilon_1} + 2V_2'^T D_{\ell\epsilon_1} + 2V_2^T D_{R\epsilon_1})\bar{\epsilon} + 2V_2^T D_{aR_1}V_0 + V_2^T E_1 V_0 + V_2^T E_0 V_1 \\
&+ 2V_0^T D_{aR_1}V_2 + V_1^T E_0 V_2 + V_0^T E_1 V_2 + 2V_2^T D_{a\ell_1}V_0' + 2V_0^T D_{a\ell_1}V_2' \\
=&2V_2^T(E_0 V_1 + D_R\bar{\epsilon} + D_S\bar{\epsilon}')
\end{aligned} \tag{101}
$$

The above simplification comes from Eq. (99)

$$
\begin{aligned}
2U_4 =&(2V_2^T(D_{a\epsilon_2}+D_{R\epsilon_2})+2V_2'^T D_{\ell\epsilon_2})\overline{\epsilon}+2V_2^T D_{aR_2}V_0+V_2^T D_{RR_2}V_0+V_2^T E_2 V_0\\
&+2V_2^T D_{aR_1}V_1+V_2^T E_1 V_1+2V_1^T D_{aR_1}V_2+2V_0^T D_{aR_2}V_2+V_0^T D_{RR_2}V_2\\
&+V_2^T E_0 V_2+V_1^T E_1 V_2+V_0^T E_2 V_2+V_2^T D_{a\ell_2}V_0'+V_2'^T D_{\ell\ell_2}V_0'+2V_2^T D_{R\ell_2}V_0'\\
&+2V_2^T D_{a\ell_1}V_1'+2V_1^T D_{a\ell_1}V_2'+2V_0^T D_{a\ell_2}V_2'+V_0'^T D_{\ell\ell_2}V_2'+2V_0^T D_{R\ell_2}V_2'\\
=&V_2^T E_0 V_2+2V_2^T\{[D_{a\epsilon_2}+D_{R\epsilon_2}+(D_{aR_2}+D_{RR_2}+E_2+D_{aR_2}^T)\hat{V}_0\\
&+(E_1+D_{aR_1}+D_{aR_1}^T)V_{1R}]\overline{\epsilon}+[-D_{\ell\epsilon_2}+(D_{a\ell_2}-D_{a\ell_2}^T+D_{R\ell_2}-D_{R\ell_2}^T)\hat{V}_0\\
&+(E_1+D_{aR_1}+D_{aR_1}^T)V_{1S}+(D_{a\ell_1}-D_{a\ell_1}^T)V_{1R}]\overline{\epsilon}'+[(D_{a\ell_1}-D_{a\ell_1}^T)V_{1S}-D_{\ell\ell_2}\hat{V}_0]\overline{\epsilon}''\}
\end{aligned}
\tag{102}
$$

The final function to be minimized is therefore

$$
\begin{aligned}
\mathcal{F} =&V_2^T E_0 V_2+2V_2^T(D_0\overline{\epsilon}+D_1\overline{\epsilon}'+D_2\overline{\epsilon}'')+2V_2^T D_c\Lambda\\
&+2V_2^T(E_0V_1+D_R\overline{\epsilon}+D_S\overline{\epsilon}')
\end{aligned}
\tag{103}
$$

The matrices above are defined as

$$
\begin{aligned}
D_0 &= D_{a\epsilon_2}+D_{R\epsilon_2}+(D_{aR_2}+D_{RR_2}+E_2+D_{aR_2}^T)\hat{V}_0+(E_1+D_{aR_1}+D_{aR_1}^T)V_{1R}\\
D_1 &= -D_{\ell\epsilon_2}+(D_{a\ell_2}-D_{a\ell_2}^T+D_{R\ell_2}-D_{R\ell_2}^T)\hat{V}_0+(E_1+D_{aR_1}+D_{aR_1}^T)V_{1S}\\
&\quad+(D_{a\ell_1}-D_{a\ell_1}^T)V_{1R}\\
D_2 &= (D_{a\ell_1}-D_{a\ell_1}^T)V_{1S}-D_{\ell\ell_2}\hat{V}_0
\end{aligned}
\tag{104}
$$

The third-order terms cancel out after determination of the Lagrange multiplier in the usual way and subsequent substitution for V_1. After considerations of the warping constraints, the final equation for second-order warping can be written as

$$
E_0V_2=[D_c(\Psi^T D_c)^{-1}\Psi^T)-\Delta](D_0\overline{\epsilon}+D_1\overline{\epsilon}'+D_2\overline{\epsilon}'')
\tag{105}
$$

After elimination of the singularities associated with E_0 in the usual way, the final expression for the second-order warping is

$$
V_2=V_{20}\overline{\epsilon}+V_{21}\overline{\epsilon}'+V_{22}\overline{\epsilon}''
\tag{106}
$$

5.2 Final Recovery

At the x_1 location of the recovery, the following are needed:

1. 1D displacements
2. Direction cosine matrix
3. Stress resultants
4. Distributed forces and moments and their first, second and *third* derivatives

The expression for strain reads

$$\begin{aligned}\Gamma =&\Gamma_{a\beta}w + \Gamma_{\epsilon}\overline{\epsilon} + \Gamma_R w + \Gamma_\ell w' \\ =&\Gamma_{a\beta}S(V_0+V_1+V_2) + \Gamma_{\epsilon}\overline{\epsilon} + \Gamma_R S(V_0+V_1+V_2) + \Gamma_\ell(V_0'+V_1'+V_2') \\ =&\left[(\Gamma_{a\beta}+\Gamma_R)S(\hat{V_0}+V_{1R}+V_{20}) + \Gamma_\epsilon\right]\overline{\epsilon} + \left[(\Gamma_{a\beta}+\Gamma_R)SV_{22} + \Gamma_\ell S(V_{1S}+V_{21})\right]\overline{\epsilon}'' \\ &+\left[(\Gamma_{a\beta}+\Gamma_R)S(V_{1S}+V_{21}) + \Gamma_\ell S(\hat{V_0}+V_{1R}+V_{20})\right]\overline{\epsilon}' + \Gamma_\ell S V_{22}\overline{\epsilon}'''\end{aligned} \tag{107}$$

The final expression for stress is simply

$$\sigma = D\Gamma \tag{108}$$

Finally, one can ascertain the displacement to be

$$U_i = u_i + x_\alpha[C_{\alpha i} - \delta_{\alpha i}] + C_{ji}w_j \tag{109}$$

where w_j can be obtained from

$$w = S\left[(\hat{V_0}+V_{1R}+V_{20})\overline{\epsilon} + (V_{1S}+V_{21})\overline{\epsilon}' + V_{22}\overline{\epsilon}''\right] \tag{110}$$

Now all that is left is the evaluation of the 1D strain derivatives. A quick summary of the various notations for the 1D strain measures and the relations between them

follows

$$\begin{aligned}
\overline{\epsilon} &= \lfloor \overline{\gamma}_{11} \quad \overline{\kappa}_1 \quad \overline{\kappa}_2 \quad \overline{\kappa}_3 \rfloor^T \\
\epsilon &= \lfloor \gamma_{11} \quad \kappa_1 \quad \kappa_2 \quad \kappa_3 \rfloor^T \\
\gamma_s &= \lfloor 2\gamma_{12} \quad 2\gamma_{13} \rfloor^T \\
\varepsilon &= \lfloor \gamma_{11} \quad 2\gamma_{12} \quad 2\gamma_{13} \quad \kappa_1 \quad \kappa_2 \quad \kappa_3 \rfloor^T \\
\overline{\epsilon} &= \epsilon + Q\gamma_s' + P\gamma_s
\end{aligned} \tag{111}$$

Hence, to determine $\overline{\epsilon}$, one needs ϵ and ϵ'. Hence the strain recovery needs ε, ε', ε'', ε''' and $\varepsilon^{(IV)}$. After lumping the inertial terms with the applied loads, the 1D beam equations can be written as

$$\begin{aligned}
\mathcal{F}' + \mathcal{R}\mathcal{F} + \phi &= 0 \\
\mathcal{F} &= \lfloor F_1 \quad F_2 \quad F_3 \quad M_1 \quad M_2 \quad M_3 \rfloor^T \\
\mathcal{R} = \mathcal{R}(\varepsilon) &= \begin{bmatrix} \tilde{K} & 0 \\ \tilde{e_1} + \tilde{\gamma} & \tilde{K} \end{bmatrix} \\
\phi &= \begin{Bmatrix} f \\ m \end{Bmatrix}
\end{aligned} \tag{112}$$

Note that the $\mathcal{F}$ is not to be confused with the minimization functional used in the previous section. The 6×6 cross-sectional flexibility matrix (Φ) of the GT model is employed as follows:

- $\varepsilon = \Phi\mathcal{F} \implies \mathcal{R}$ can be evaluated
- $\mathcal{F}' = -\mathcal{R}\mathcal{F} - \phi$; $\varepsilon' = \Phi\mathcal{F}' \implies \mathcal{R}'$ can be evaluated
- $\mathcal{F}'' = -\mathcal{R}'\mathcal{F} - \mathcal{R}\mathcal{F}' - \phi'$; $\varepsilon'' = \Phi\mathcal{F}'' \implies \mathcal{R}''$ can be evaluated
- $\mathcal{F}''' = -\mathcal{R}''\mathcal{F} - \mathcal{R}\mathcal{F}'' - 2\mathcal{R}'\mathcal{F}' - \phi''$; $\varepsilon''' = \Phi\mathcal{F}''' \implies \mathcal{R}'''$ can be evaluated
- $\mathcal{F}^{(IV)} = -\mathcal{R}'''\mathcal{F} - 3\mathcal{R}''\mathcal{F}' - 3\mathcal{R}'\mathcal{F}'' - \mathcal{R}\mathcal{F}''' - \phi'''$; $\varepsilon^{(IV)} = \Phi\mathcal{F}^{(IV)}$

In case of recovery using the Vlasov model, the derivatives of the strain measures are not extracted from the equilibrium equations or any such method. Instead they come from the 1D analysis and the user is expected to input $\bar{\epsilon}$, $\overline{\kappa}_1'$, $\overline{\kappa}_1''$ and $\overline{\kappa}_1'''$. From this, one obtains the derivatives as $\bar{\epsilon}' = [0\ \overline{\kappa}_1'\ 0\ 0]^T$ and so on. With this the formulation for the second-order stress, strain and displacement recovery from VABS for general anisotropic and curved and/or twisted beams is complete.

5.3 Results

The above mentioned formulation has been coded up and is present in VABS versions 3.6 and later. A first test to ensure that second order effects are indeed being picked up will be to regenerate Fig. 15 additionally using VABS 3.6 and verify that the solutions coincide with the corresponding second-order analytical development. This is presented in Fig. 25, and it can be concluded from the plots of σ_{12} and σ_{22} that VABS is indeed capturing the second order effects.

Now, a test is performed on the CAS1 cross section. The geometry and material of this cross section are detailed in Ref. [124]. For a cantilevered beam of length 10 in., two cases are considered: one prismatic and another with initial twist (k_1) of 0.05 rad. in.$^{-1}$. The free end is subjected to a load such that at the mid-span of the beam, the only non-zero stress resultants are $F_3 = 1$ lb. and $M_2 = -5$ lb-in. For the prismatic case, this would require simply a unit F_3 at the free end; and for the twisted beam, the loading might be more complex. This kind of loading is chosen so as to ascertain the effect of k_1 on the cross-sectional stress recovery alone (by keeping out the effects of initial twist from the 1D analysis). The stress is recovered at the mid-span for the right-wall. For the untwisted case, it is evident from Fig. 26 that the second-order recovery offers very little advantages compared to the first-order results. In the solution of the second order warping, two out of three terms, i.e., V_{20} and V_{21} are zero for first prismatic beams. Recall that a VAM solution is fundamentally

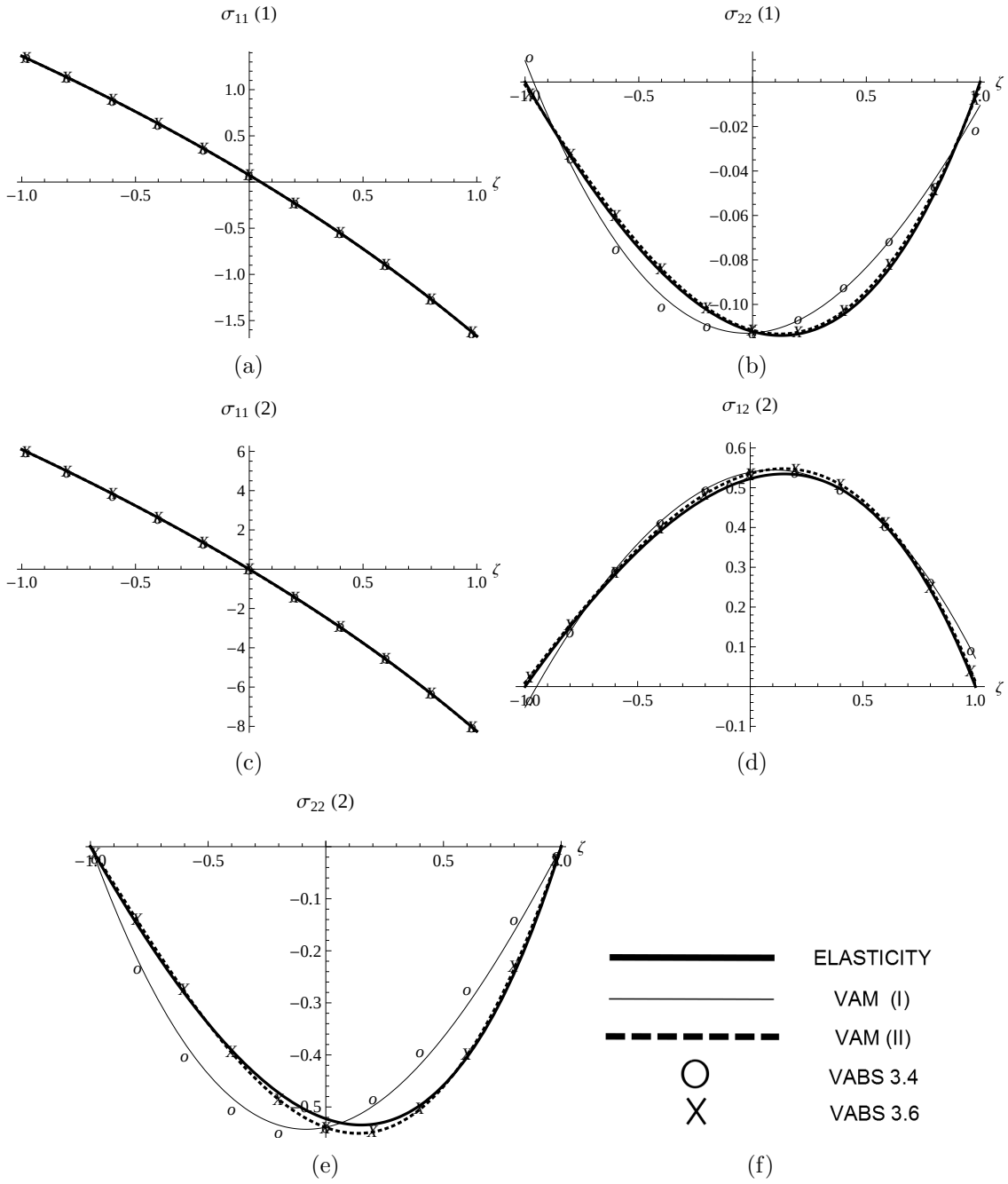

Figure 25: Comparison of the normalized VAM stresses and those from VABS 3.4 and VABS 3.6 with elasticity solutions for the loading cases in Fig. 3; (a) and (b) are for loading case (1); (c), (d) and (e) are for loading case (2)

nothing but the elasticity solution expanded in terms of small parameters. Therefore, an interesting conclusion from this result is that possibly an exact elasticity solution has been achieved if there is very less difference between and n^{th} and $(n+1)^{th}$ order solution, n being 1 in this case.

However, for the case of initial twist, an appreciable difference is observed for the cross-sectional stresses σ_{22}, σ_{23} and σ_{33}. One must also realize that the CAS1 section has an interface at the top and bottom ends of the right-wall where layers go from being stacked horizontally to being stacked vertically and vice-versa. Therefore traditional 3D finite-element procedures may be not be the best judge of whether the beam solutions are close to the actual values. Wan-Lee Yin [123] presents an analysis with approximate analytical solutions for problems of this kind. The spikes in the plots may be result of the well known singularities in such structures. Therefore, an analysis of the type done in Ref. [123] is required validate the stress-recovery plots for the CAS1 section obtained using VABS.

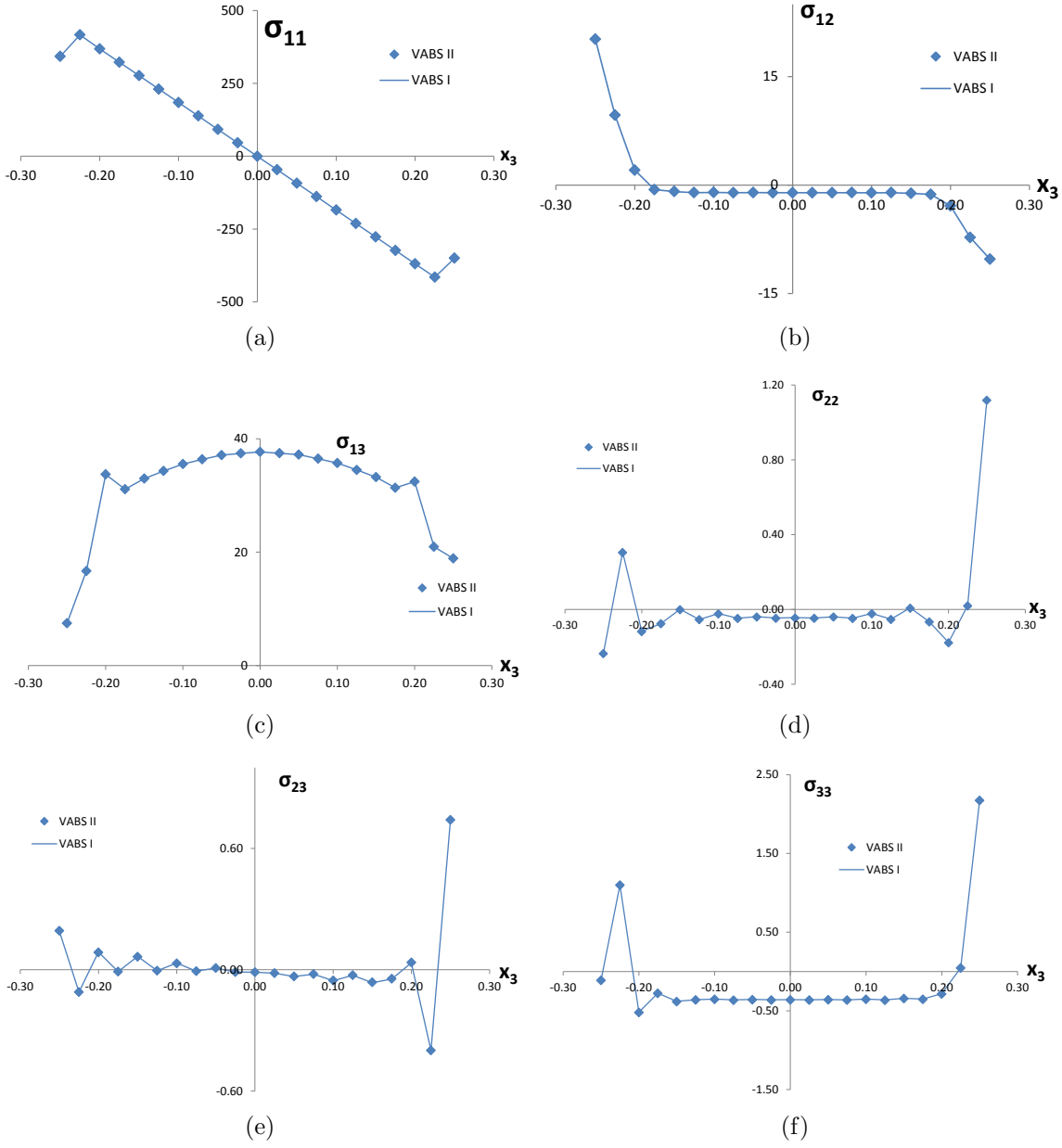

Figure 26: Stress distributions (in psi.) on the right wall of the CAS1 section at mid-span for a tip transverse force. VABS I and II represent the first and second-order recoveries.

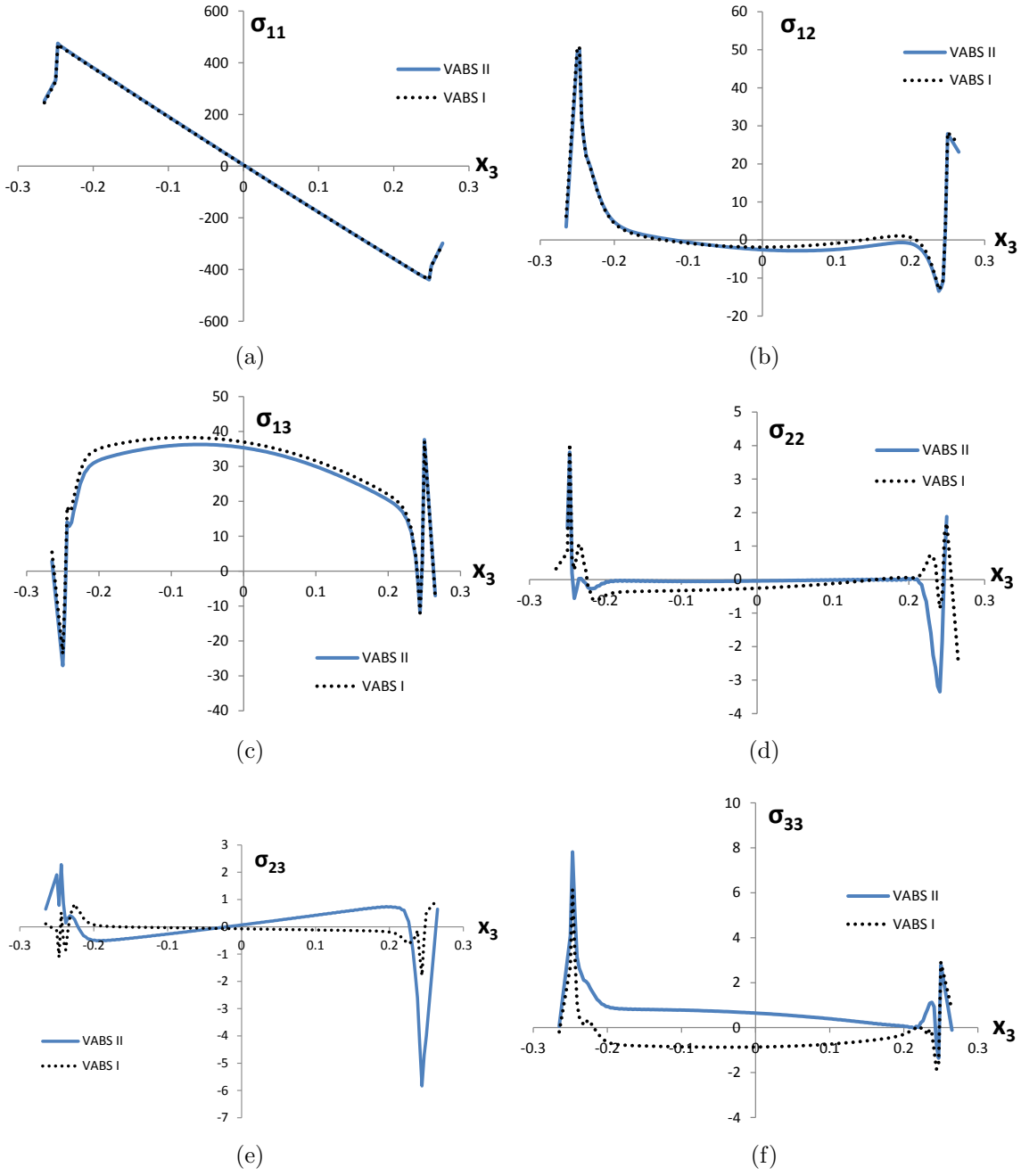

Figure 27: Stress distributions (in psi.) on the right wall of the pretwisted CAS1 section at mid-span for a tip transverse force. VABS I and II represent the first and second-order recoveries.

VI

OBLIQUE CROSS-SECTIONAL ANALYSIS

Johannes Kepler preferred the hardest of truths to his illusions. And that is the heart of science.

– Carl Sagan, *Cosmos*

6.1 Introduction

In beam theory, a natural choice of the reference cross-sectional plane is the one normal to the reference line. In fact, most beam theories in literature constrain the user's choice of the reference cross section to be perpendicular to the reference line. In certain cases, particularly when the user happens to possess the properties of a section which is not orthogonal to the blade reference axis, the limitations of such a restriction lead to a significant expenditure of time because calculations must be made to transform the geometry and material properties of the oblique section to that of an orthogonal section. The latter is compounded because of the presence of composite materials at varying fiber orientations. An oblique cross-sectional analysis is therefore a dimensional reduction that uses a cross section that is not constrained to be perpendicular to the reference line.

It should be pointed out here that one could carry out the regular cross-sectional analysis (using a cross section perpendicular to the reference line) and use tensorial and vectorial rotation formulae to obtain 3D quantities (stress, strain and displacement). An oblique cross-sectional analysis is merely a convenience, which is significant

The first part of this chapter was published as Rajagopal and Hodges [91]. The second part has been accepted for presentation at the 70^{th} annual AHS forum.

especially in cases where the cross section geometry and material is complex such as rotorcraft blades.

The current obliqueness model in VABS [86] is limited to classical theory which does not model transverse shear or restrained warping. This chapter presents details of the various studies undertaken by the author in solving this problem. The first effort consisted of developing a beam theory for an oblique cross-sectional analysis of in-plane deformation of a prismatic, isotropic strip. A second effort was an analysis of the full 3D deformation of an isotropic beam in the form of a solid, circular cylinder. The choice of these problems was determined by two considerations:

- The results of the beam theory (i.e., cross-sectional stiffness matrix and stress-strain recovery relations) should be closed-form analytical expressions. Such studies have been undertaken by the author to study the effects of span-wise non-uniformity [50] and initial curvature [89, 90]. These serve as validation tools for VABS in the same sense that elasticity validates FEM.

- The presence of elasticity solutions for several loading cases [109, 76], which shall be described in detail.

These considerations facilitate in-depth study of the problem and consequently will aid in a thorough understanding of the intricacies of an oblique cross-sectional analysis vis-à-vis an orthogonal cross-sectional analysis. These, as will be shown, demonstrate that an oblique cross-sectional analysis is capable of accurately capturing transverse shear effects for isotropic, prismatic rods, as long as the obliqueness angle is not assumed to be arbitrarily large.

The precise objective of this work is to add to the existing oblique cross-sectional model in VABS, the ability to capture the effects of transverse shear and restrained warping (important for flex-beams) for initially curved and/or twisted beams made of generally anisotropic material. This chapter is organized as follows: First, we expand

on the idea of the importance of possessing an oblique cross-sectional analysis and the advantages it offers users; then following the analytical studies, present a brief overview of the theory and the equations pertaining to the obliqueness model and their implementation in VABS. After this, several validation studies are provided for beams using results from experiments and 3D FEM. These studies ensure that the latest oblique cross-sectional model of VABS is able to accurately both (a) obtain the cross-sectional stiffness matrix and (b) recover the 3D stress. The final outcome of this work is a version of VABS in which the user has the freedom to choose a reference cross section that is not orthogonal to the reference line.

6.2 Motivation

In this section, several scenarios are presented wherein the concept and application of an oblique cross-sectional analysis might be greatly beneficial to the VABS user. These include, but are not limited to:

1. *The presence of sweep in a wing or blade*: In classical aeroelasticity, the problem of a swept wing (see Fig. 4) is analyzed considering an approximate structure by "rotating the wing about the root" [49]. Further calculations are needed to show that bending and torsion are coupled for such a problem. On the other hand if one can use a cross section along the stream-wise direction, i.e., oblique to the reference line, coupling between bending and torsion stems directly from the stiffness matrix (as we shall establish shortly), and there is no need to undertake any special analysis – or even define a chordwise direction.
2. *Composite laminates at various fiber orientations*: Because it is commonplace to encounter composite laminates at various fiber orientations in the section of a rotor blade, the alignment of the cross section along or perpendicular to fiber directions may result in the stiffness matrix having a much simpler form. Consider for example, Fig. 28, if one chooses the cross section to be at $90 - \Lambda$

with respect to the reference line, the fibers will all seem to be at 0° orientation. Two cautionary remarks must be made here: This is not of a nature similar to what is done in aeroelastic tailoring. The global behavior of the structure here obviously remains the same; only an intermediate result, i.e., the stiffness matrix, is simpler. Second, in colloquial terms when two measures of beam deformation are referred to as coupled, these are usually defined with reference to an orthogonal reference section. Therefore, when using the concept of oblique cross-sectional analysis, care should be taken in interpreting the results.

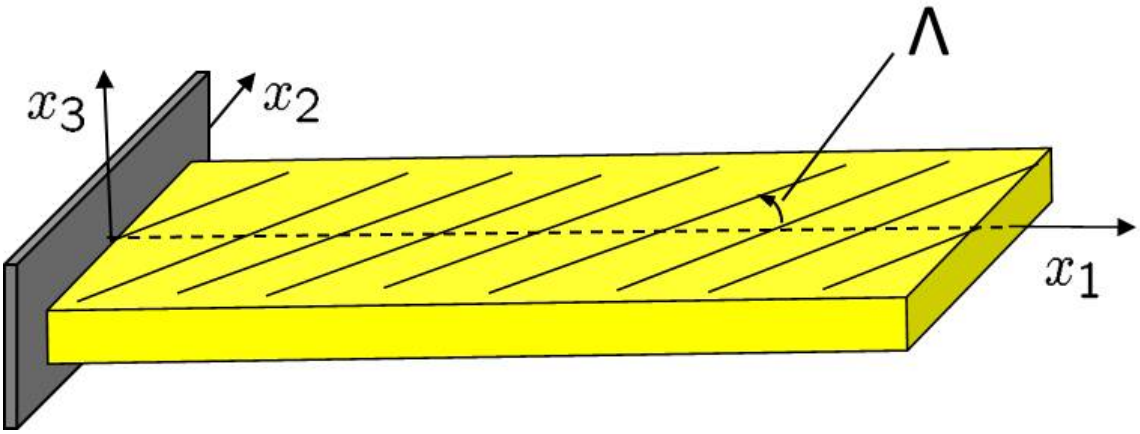

Figure 28: Composite laminate with non-zero fiber orientation

3. *When recovering 3D stress, strain or displacement in a nonorthogonal plane as shown in Fig. 29*: To achieve this using a section perpendicular to the reference line, the user would have to solve the 1D problem at various axial locations as shown and at each location run VABS recovery to obtain the 3D quantity at a point on the oblique plane corresponding to that particular axial location. On the other hand, an oblique cross-sectional analysis entails a single run to obtain the recovery.
4. *Readily available properties for a reference surface that is not perpendicular to the reference line*: An instance of this occurs when the ribs of a wing structure are not perpendicular to its axis. A representative rotor blade section is shown

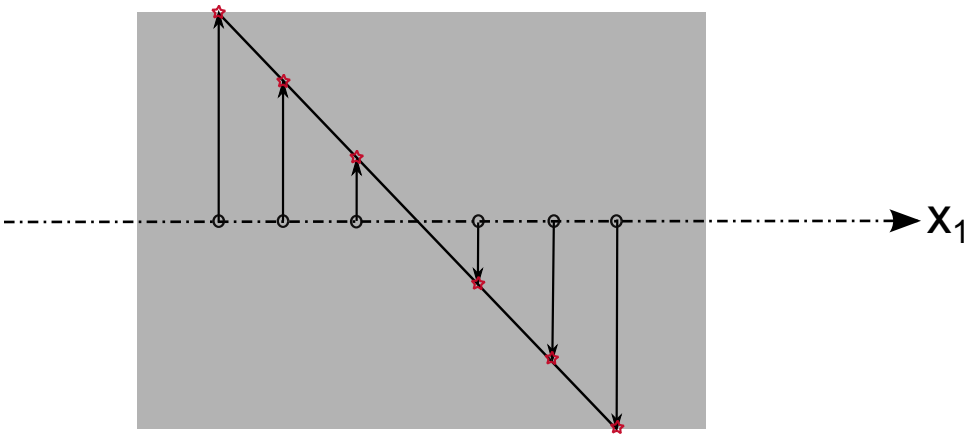

Figure 29: Recovering 3D quantities on an nonorthogonal plane: oblique vs. orthogonal cross-sectional analysis

in Fig. 30. If this were, for example, a section not perpendicular to the axis, generation of the corresponding orthogonal section would involve a transformation of the geometry and material properties. While the geometry transformation is relatively simple and can be obtained readily from the rotation parameters relating the two sections, material transformations are quite involved. The material transformation, which is not so simple [54], is further complicated when the blade is made of different composite materials with differing stacking sequences in different walls of the blade section. This will involve significant effort for a section such as the one in Fig. 30.

6.3 Reference Frames

Before undertaking the analysis, the various frames of reference used in the solution procedure are introduced in this section. For the analysis of the deformation of any structure, at least two frames of reference are required: one to describe the deformed state and another the undeformed state. The term "corresponding normal section" is used to denote a cross section orthogonal to the beam reference axis at the same axial coordinate (x_1) as that of the oblique section. Latin indices range from 1 to 3, and Greek from 2 to 3. We will refer to the following frames of reference (listed

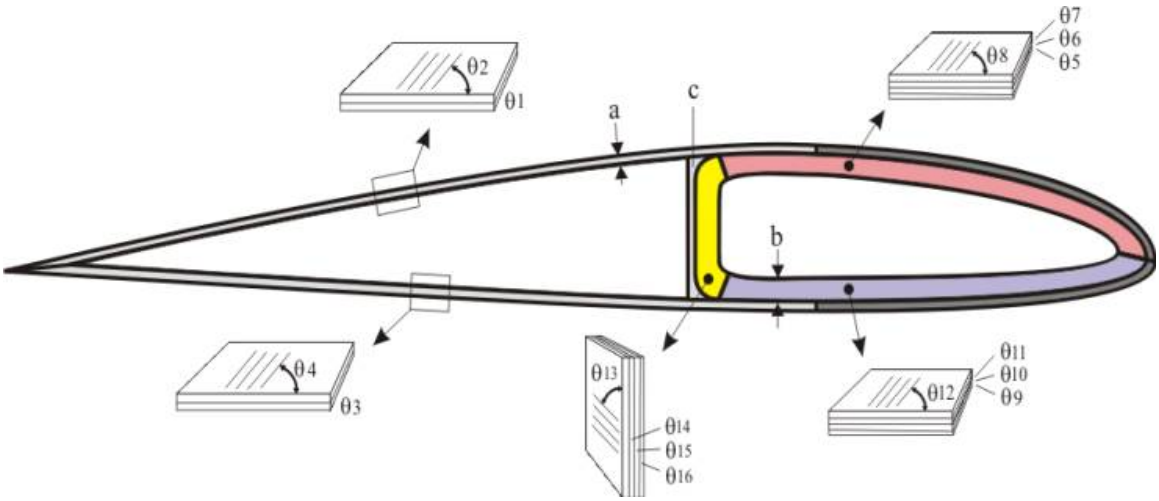

Figure 30: A typical rotor blade section made of composite and generally anisotropic materials with varying fiber orientation

with the corresponding orthonormal vectors describing the frames) during the course of this development:

1. Frame b with unit vectors $\mathbf{b}_i\,(x_1)$: $\mathbf{b}_1$ is tangent to the undeformed reference line and $\mathbf{b}_\alpha$ are in the plane of the corresponding normal section

2. Frame a with unit vectors $\mathbf{a}_i(x_1)$: $\mathbf{a}_1$ is normal to and $\mathbf{a}_\alpha$ are in the plane of the oblique section

3. Frames T with unit vectors $\mathbf{T}_i\,(x_1)$ and B with unit vectors $\mathbf{B}_i\,(x_1)$: $\mathbf{T}_1$ is tangent to the deformed reference line and $\mathbf{B}_1$ is a normal to the deformed surface associated with the corresponding normal section

4. Frames A with unit vectors $\mathbf{A}_i\,(x_1)$ and N with unit vectors $\mathbf{N}_i\,(x_1)$, such that $\underline{\mathbf{C}}^{Aa} = \underline{\mathbf{C}}^{Tb}$ and $\underline{\mathbf{C}}^{Na} = \underline{\mathbf{C}}^{Bb}$, where $\underline{\mathbf{C}}^{Bb}$ refers to the dyadic associated with the finite rotations from b to B, etc.

Note that the development in Ref. [46] for the orthogonal section uses frames b (undeformed beam), T and B (deformed beam). One of the frames used for the deformed configuration brings transverse shear strain explicitly into the formulation (B), while

the other (T) does not. The precise orientation of the in-plane unit vectors is user-defined for the undeformed case and is obtained by imposing constraints on the unknown warping field for the deformed case. It is emphasized here that the frames of reference used for the description of the deformed configuration do not represent the total deformation; they still have an unknown warping which is evaluated using the VAM. For the development of the oblique cross-sectional analysis, the frames a (undeformed), A and N (deformed) will be used. Classical theory is developed in terms of the 1D strains associated with frame A, while the GT theory is developed in terms of the 1D strains of N. A measure of the obliqueness of the section is defined by the parameters β_{1i}:

$$\mathbf{b}_1 = \beta_{1i}\mathbf{a}_i \tag{113}$$

Using the above relation and the fact that a rotation about the beam reference line does not create an oblique section, the following relation between the frames b and a can be developed by means of the standard Euler rotation [57]

$$\begin{Bmatrix} \mathbf{b}_1 \\ \mathbf{b}_2 \\ \mathbf{b}_3 \end{Bmatrix} = \begin{bmatrix} \beta_{11} & \beta_{12} & \beta_{13} \\ -\beta_{12} & 1-\frac{\beta_{12}^2}{1+\beta_{11}} & -\frac{\beta_{12}\beta_{13}}{1+\beta_{11}} \\ -\beta_{13} & -\frac{\beta_{12}\beta_{13}}{1+\beta_{11}} & 1-\frac{\beta_{13}^2}{1+\beta_{11}} \end{bmatrix} \begin{Bmatrix} \mathbf{a}_1 \\ \mathbf{a}_2 \\ \mathbf{a}_3 \end{Bmatrix} \tag{114}$$

From the definitions of frames A and N, it can also be shown that the above equation holds when $\mathbf{b}_i$ and $\mathbf{a}_i$ are replaced by $\mathbf{T}_i$ and $\mathbf{A}_i$, or $\mathbf{B}_i$ and $\mathbf{N}_i$, respectively. In the problems of interest in this paper, the oblique section is obtained by rotating the corresponding normal section by Λ about $\mathbf{b}_3$, for which the frames a and b are depicted in Fig. 31. Note in the problem schematics (Figs. 32 and 38), $\mathbf{b}_3$ is directed out of the plane of the paper. For this case, the obliqueness parameters are: $\beta_{11} = \cos(\Lambda)$, $\beta_{12} = -\sin(\Lambda)$ and $\beta_{13} = 0$.

The beam or 1D generalized strains associated with each of the deformed beam frames are listed in Table 8, the meanings and applicability of which will become clear in later sections. It should be stated here that kinematics can be employed to relate

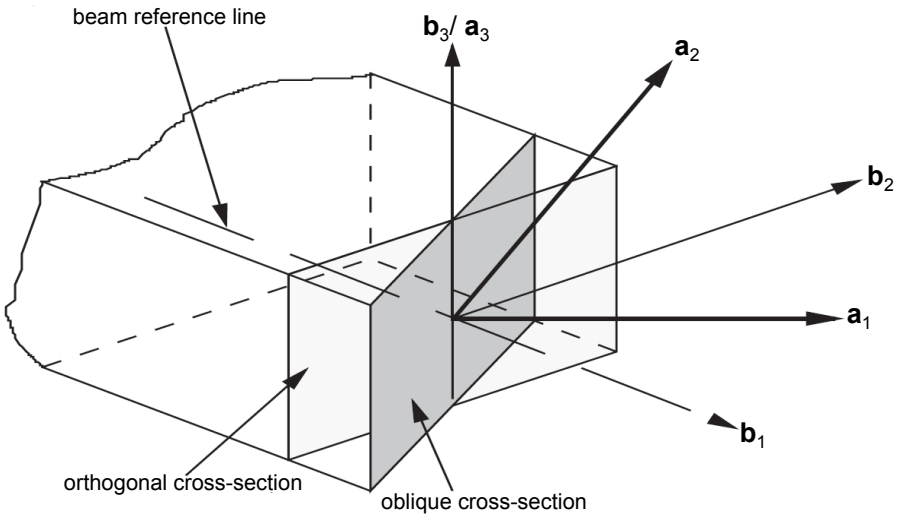

Figure 31: Reference frames used in the cross-sectional analysis

Table 8: 1D generalized strains for various reference frames

Frame	Extension	Twisting	Bending	Transverse Shear
T	$\overline{\gamma}_{11}$	$\overline{\kappa}_1$	$\overline{\kappa}_\alpha$	$-$
B	γ_{11}	κ_1	κ_α	$2\gamma_{1\alpha}$
A	$\overline{\gamma}^o_{11}$	$\overline{\rho}_1$	$\overline{\rho}_\alpha$	$2\overline{\gamma}^o_{1\alpha}$
N	γ^o_{11}	ρ_1	ρ_α	$2\gamma^o_{1\alpha}$

the two sets of strain measures of Table 8.

6.4 Isotropic Strip: In-plane Deformation

The first problem of interest is the development of a beam theory to analyze in-plane deformation of an isotropic strip using an oblique cross section as shown in Fig. 32. The beam theory formulation will be carried out using the VAM. The reference line is chosen as the line of section centroids. The position vector of an arbitrary point P in the undeformed configuration, can be written as:

$$\hat{\mathbf{r}} = \mathbf{r} + \boldsymbol{\xi} \tag{115}$$

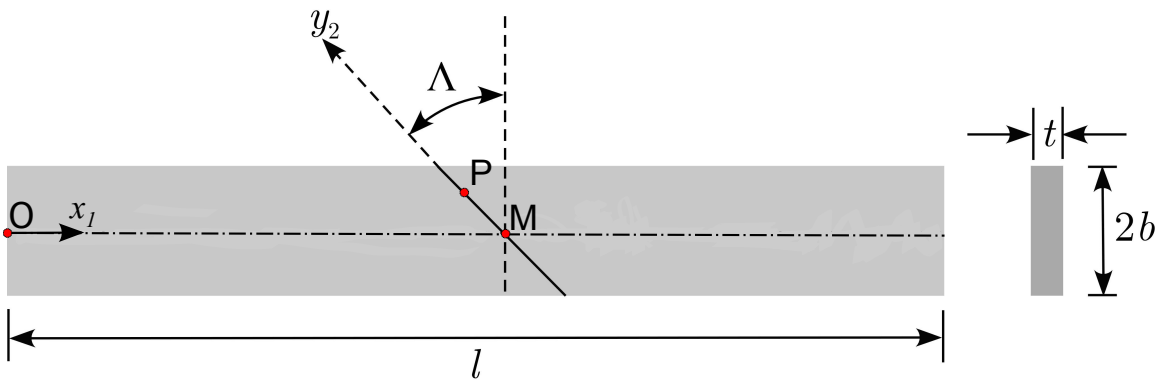

Figure 32: Schematic of the isotropic strip

where $\mathbf{r}$ is the position vector from the reference point (O) to the point on the reference axis (M), and $\boldsymbol{\xi} = y_2\mathbf{a}_2$ is the position vector from M to P. After deformation, the point P is now at:

$$\hat{\mathbf{R}} = \mathbf{R} + y_2\mathbf{A}_2 + w_1(x_1, y_2)\mathbf{A}_1 + w_2(x_1, y_2)\mathbf{A}_2 \tag{116}$$

where $\mathbf{R}$ is the position vector to the point M after deformation, and w_1 and w_2 represent the unknown warping. These expressions are used to form the covariant ($\mathbf{G}_i$) and contravariant ($\mathbf{g}^i$) base vectors of the deformed and undeformed states, respectively. In doing so, one uses the elegant definitions of the 1D strains [46] as:

$$\begin{aligned} \mathbf{R}' &= (1 + \overline{\gamma}_{11})\mathbf{T}_1 = [1 + \overline{\gamma}_{11}(x_1)][\cos(\Lambda)\mathbf{A}_1 - \sin(\Lambda)\mathbf{A}_2] \\ \mathbf{A}_i' &= \overline{\rho}_3(x_1)\mathbf{A}_3 \times \mathbf{A}_i \end{aligned} \tag{117}$$

In what follows $(\bullet)' = d(\bullet)/dx_1$. Note that even though an oblique section is being used, it makes more sense to define the stretch of the reference line in a direction along the beam reference axis. The next step is to form the deformation gradient tensor [81]

$$\underline{\boldsymbol{\chi}} = \mathbf{G}_i\mathbf{g}^i \tag{118}$$

Under the assumptions of the smallness of strains and local rotation [29] (caused by warping), the Jaumann-Biot-Cauchy strains turn out to be:

$$\begin{aligned} \Gamma_{ij} &= \frac{\chi_{ij} + \chi_{ji}}{2} - \delta_{ij} \\ \chi_{ij} &= \mathbf{A}_i . \underline{\boldsymbol{\chi}} . \mathbf{a}_j \end{aligned} \tag{119}$$

where δ_{ij} is the Kronecker delta. The nonzero measures of the strains, when written out explicitly, reduce to

$$\begin{aligned} \Gamma_{11} &= \overline{\gamma}_{11} - y_2 \sec(\Lambda)\overline{\rho}_3 + \tan(\Lambda) w_{1,2} + \sec(\Lambda) w_1' \\ 2\Gamma_{12} &= w_{1,2} + \sec(\Lambda)\left[w_2' + \sin(\Lambda) w_{2,2} - \sin(\Lambda)\overline{\gamma}_{11}\right] \\ \Gamma_{22} &= w_{2,2} \end{aligned} \tag{120}$$

Note the square root of the magnitude of the metric tensor for the undeformed state, $\sqrt{g} = \cos(\Lambda)$. Since the problem of interest is the planar deformation of a strip, the stress-strain relations correspond to those of plane stress, and hence,

$$\begin{Bmatrix} \sigma_{11} \\ \sigma_{22} \\ \sigma_{12} \end{Bmatrix} = \frac{E}{1-\nu^2} \begin{bmatrix} 1 & \nu & 0 \\ \nu & 1 & 0 \\ 0 & 0 & \frac{1-\nu}{2} \end{bmatrix} \begin{Bmatrix} \Gamma_{11} \\ \Gamma_{22} \\ 2\Gamma_{12} \end{Bmatrix} \tag{121}$$

The sectional strain energy can therefore be obtained as

$$\mathcal{U} = \langle\langle \frac{1}{2} \sigma^T \Gamma \rangle\rangle \tag{122}$$

where $\langle\langle \bullet \rangle\rangle = \langle \bullet \sqrt{g} \rangle$ and $\langle\rangle$ denotes an integration over the oblique-section. For a complete solution of the problem, it is necessary to pose constraints to render the displacement field (introduced in Eq. (116)) unique, which are:

$$\langle w_1 \rangle = \langle w_2 \rangle = 0 \tag{123}$$

The formulation up to now has cast the elasticity problem in a form suitable for a variational analysis. Therefore, if an attempt is made to solve it directly, one encounters the same difficulties as in solving any other elasticity problem. An asymptotic

method will now be employed to circumvent this obstacle. A small parameter is easily identified as the inverse of the slenderness ratio, b/l, of order δ. As usual, the orders of the 1D strains are $O(\overline{\gamma}_{11}, b\overline{\rho}_3) = \epsilon$, where ϵ is of the order of the maximum strain in the structure; and the orders of warping, obtained by equating the orders of the leading bilinear and quadratic terms in the unknowns, are $b\epsilon$.

Throwing away all the terms of order $O(\delta)$ in the strain energy density, and solving for the zeroth-order warping, using the standard principles of calculus of variations, one obtains

$$\begin{aligned} w_1^{(0)} =& \frac{1}{12}\sin(\Lambda)\sec^2(\Lambda)\Big\{-12y_2(1+\nu)\cos(\Lambda)^3\overline{\gamma}_{11} \\ & - \left[b^2 - 3y_2^2\cos(\Lambda)^2\right]\left[(3+\nu)+(1+\nu)\cos(2\Lambda)\right]\overline{\rho}_3\Big\} \\ w_2^{(0)} =& \frac{1}{6}\left[\nu\cos(\Lambda)^2 - \sin(\Lambda)^2\right]\sec(\Lambda)\left\{-6y_2\cos(\Lambda)\overline{\gamma}_{11} + \left[-b^2 + 3y_2^2\cos(\Lambda)^2\right]\overline{\rho}_3\right\} \end{aligned} \tag{124}$$

This can be substituted back in the expression for $\mathcal{U}$ and integrated to obtain the classical strain energy:

$$\mathcal{U}_0 = \frac{1}{2}\begin{Bmatrix} \overline{\gamma}_{11} \\ \overline{\rho}_3 \end{Bmatrix}^T \begin{bmatrix} 2Ebt & 0 \\ 0 & \frac{2}{3}Etb^3 \end{bmatrix} \begin{Bmatrix} \overline{\gamma}_{11} \\ \overline{\rho}_3 \end{Bmatrix} \tag{125}$$

As mentioned previously, the stretching strain measure corresponding to T has been used. If one used that of A, an additional shearing strain measure would have been introduced because:

$$\mathbf{R}' = [\cos(\Lambda) + \overline{\gamma}_{11}^o]\mathbf{A}_1 + [-\sin(\Lambda) + 2\overline{\gamma}_{12}^o]\mathbf{A}_2 \tag{126}$$

However, this would not be an independent 1D variable as can be ascertained by a comparison with the first of Eq. (117), which yields:

$$\begin{aligned} \overline{\gamma}_{11}^o &= \cos(\Lambda)\overline{\gamma}_{11} \\ 2\overline{\gamma}_{12}^o &= -\sin(\Lambda)\overline{\gamma}_{11} \end{aligned} \tag{127}$$

To go to the next level of the asymptotic analysis, the warping is perturbed one order higher ($O(\delta b\epsilon)$), and all terms $O(\delta^3)$ are discarded in the strain energy density. Before minimization, integration by parts is carried out to remove the derivatives of the unknown warping functions with respect to x_1. The boundary terms can be safely ignored since we are interested in an interior solution. As with the zeroth-order solution, taking the warping constraints into considerations, one obtains the first-order warping as:

$$\begin{aligned}
w_1^{(1)} =& \frac{1}{96}\sec(\Lambda)^2\Bigg\{8\cos(\Lambda)\left[(\nu+1)\cos(2\Lambda)-3\nu-1\right]\left[b^2-3y_2^2\cos(\Lambda)^2\right]\overline{\gamma}'_{11} \\
&+2y_2\Big(-12b^2(\nu+1)+(\nu+3)y_2^2+\cos(2\Lambda)\left[(3\nu+7)y_2^2-4b^2(5\nu+7)\right] \\
&+\cos(4\Lambda)\left[(3\nu+5)y_2^2-8b^2(\nu+1)\right]+(\nu+1)y_2^2\cos(6\Lambda)\Big)\overline{\rho}'_3\Bigg\} \\
w_2^{(1)} =& -\frac{1}{12}\sec(\Lambda)\tan(\Lambda)\Bigg\{2\left[b^2-3y_2^2\cos(\Lambda)^2\right]\left[\nu\cos(\Lambda)^2-\sin(\Lambda)^2\right]\overline{\gamma}'_{11} \\
&+y_2\cos(\Lambda)\Big(-4b^2(2\nu+1)+(3\nu+1)y_2^2+2\cos(2\Lambda)\left[(2\nu+1)y_2^2-4b^2(\nu+1)\right] \\
&+(\nu+1)y_2^2\cos(4\Lambda)\Big)\overline{\rho}'_3\Bigg\}
\end{aligned} \tag{128}$$

Employing this expression for warping in Eq. (122) and subsequent integration over the oblique section yields the second-order asymptotically correct strain energy per unit length:

$$\begin{aligned}
\mathcal{U}_2 =& Ebt\overline{\gamma}_{11}^2+\frac{1}{3}Eb^3t\overline{\rho}_3^2+\frac{2}{3}Eb^3t\tan(\Lambda)\overline{\gamma}'_{11}\overline{\rho}_3+\frac{2}{45}b^5Et\sec^2(\Lambda)\left[(3\nu+2)\cos(2\Lambda)+3\nu+4\right]\overline{\rho}_3'^2 \\
&+\frac{1}{3}b^3Et\tan(\Lambda)^2\overline{\gamma}_{11}'^2+\frac{1}{45}b^5Et\sec^2(\Lambda)[(11\nu+15)\cos(2\Lambda)+11\nu+9]\overline{\rho}_3\overline{\rho}''_3
\end{aligned} \tag{129}$$

The second-order strain energy contains the derivatives of the 1D generalized strains which make it unsuitable from an engineering perspective. Apart from the presence of derivatives, another troublesome aspect of the asymptotically correct second-order

energy is the difficulty in the interpretation of the boundary conditions. For these reasons, the energy is cast into a readily usable form called the GT energy. The transformation procedure involves the following steps:

1. The classical strain measures of Eqs. (117) are written in terms of the classical strain-measures for the corresponding normal section by using the appropriate transformation. Note the stretching strain is already that of the T frame. For the strip, the planar bending measures of the A and T frame are equal, i.e. $\overline{\rho}_3 = \overline{\kappa}_3$. This can be obtained from the frame developments in Sec. 6.3, the second of Eqs. (117), and recognizing that $\mathbf{T}_i' = \overline{\kappa}_3(x_1)\mathbf{T}_3 \times \mathbf{T}_i$.

2. These classical (T) strain measures are written in terms of the GT (B) strain measures, which introduces a 1D shear strain. From the definition of the T and B frames, one can derive [46]

$$\begin{aligned} \overline{\gamma}_{11} &= \gamma_{11} \\ \overline{\kappa}_3 &= \kappa_3 + (2\gamma_{12})' \end{aligned} \tag{130}$$

3. The 1D equilibrium equations are used to eliminate the derivatives of these strain measures. For the strip, in terms of the beam stress resultants, i.e., sectional forces ($\mathcal{F}_1(x_1)$ and $\mathcal{F}_2(x_1)$) and moment ($\mathcal{M}_3(x_1)$) the equations are simply

$$\begin{aligned} \mathcal{F}_1' &= 0 \\ \mathcal{F}_2' &= 0 \\ \mathcal{M}_3' + \mathcal{F}_2 &= 0 \end{aligned} \tag{131}$$

If the GT form of the strain energy can be written as

$$\mathcal{U}_{GT} = \frac{1}{2} \left\{ \begin{array}{c} \gamma_{11} \\ 2\gamma_{12} \\ \kappa_3 \end{array} \right\}^T \left[\begin{array}{ccc} S_{11} & S_{12} & S_{13} \\ S_{12} & S_{22} & S_{23} \\ S_{13} & S_{23} & S_{33} \end{array} \right] \left\{ \begin{array}{c} \gamma_{11} \\ 2\gamma_{12} \\ \kappa_3 \end{array} \right\} \tag{132}$$

then the equilibrium equations reduce to

$$\begin{aligned}(S_{11}\gamma_{11} + S_{12}2\gamma_{12} + S_{13}\kappa_3)' &= 0\\ (S_{12}\gamma_{11} + S_{22}2\gamma_{12} + S_{23}\kappa_3)' &= 0\\ (S_{13}\gamma_{11} + S_{23}2\gamma_{12} + S_{33}\kappa_3)' + (S_{12}\gamma_{11} + S_{22}2\gamma_{12} + S_{23}\kappa_3) &= 0\end{aligned} \tag{133}$$

which can be used to solve for the derivatives of the generalized strain measures. These can be substituted into $\mathcal{U}_2$, and the final result must be the same as $\mathcal{U}_{GT}$, leading to a set of nonlinear algebraic equations for the S_{ij}'s.

4. The GT strain energy which is now in terms of the B strain measures can be cast into a form associated with the strain measures that correspond to the frame that describes the deformed oblique section, i.e., N. We therefore develop the kinematical equations relating the strains of the N and B frames. Following, Refs. [46] and [86], the derivative of $\mathbf{R}$ with respect to x_1 can be written in two different ways:

$$\begin{aligned}\mathbf{R}' &= (1+\gamma_{11})\mathbf{B}_1 + 2\gamma_{12}\mathbf{B}_2\\ \mathbf{R}' &= [\cos(\Lambda) + \gamma^o_{11}]\,\mathbf{N}_1 + [-\sin(\Lambda) + 2\gamma^o_{12}]\,\mathbf{N}_2\end{aligned} \tag{134}$$

Following the development in Sec. 6.3, the following relations are obtained:

$$\begin{aligned}\gamma^o_{11} &= \cos(\Lambda)\gamma_{11} + \sin(\Lambda)2\gamma_{12}\\ 2\gamma^o_{12} &= -\sin(\Lambda)\gamma_{11} + \cos(\Lambda)2\gamma_{12}\end{aligned} \tag{135}$$

Using an analysis similar to step 1 of the GT transformation, it can be proven that $\rho_3 = \kappa_3$.

Note that steps 1 and 4 are not absolutely necessary. However the equilibrium equations with the oblique-section force resultants will involve Λ. In other words, they are simplest when written for the normal-section resultants. The existing GT procedure even for the simpler case is quite involved [132]. Instead of further increasing the length and the complexity of the expressions in the GT procedure by introducing

terms associated with obliqueness, before and after the actual derivative elimination process using the equations of equilibrium, the energy is transformed forth and back in terms of the oblique-section strain measures, which, as demonstrated involved simple kinematical transformations.

Also, the second-order energy, when cast into the GT form, loses its asymptotic exactness. This is not unique for the section being oblique; indeed, it is also true for the usual VAM dimensional reduction involving an orthogonal section. Carrying out the procedure as described above, the sectional strain energy reduces to (in the B strain measures):

$$\begin{aligned}\mathcal{U}_{GT} =& \frac{1}{2}\begin{Bmatrix}\gamma_{11}\\ 2\gamma_{12}\\ \kappa_3\end{Bmatrix}^T X_{GT}^{(B)} \begin{Bmatrix}\gamma_{11}\\ 2\gamma_{12}\\ \kappa_3\end{Bmatrix}\\ X_{GT}^{(B)} =& \begin{bmatrix} 2Ebt & 0 & 0\\ 0 & \frac{5Ebt}{6(1+\nu)+2\tan(\Lambda)^2} & 0\\ 0 & 0 & \frac{2}{3}Eb^3t\end{bmatrix}\end{aligned} \tag{136}$$

This strain energy is also suitable for direct comparison with existing results (which have been shown to be equivalent to 3D elasticity [127]) because the strain measures are those of the corresponding orthogonal section. The stiffnesses associated with extension and bending are correctly captured. For a rectangular cross section, the elasticity solution for shear stiffness in the stiff-direction is shown to approach $5GA/6$ (where G is the shear modulus of the material and A is the area of the corresponding orthogonal section) when the aspect ratio of the rectangle is very large, which is by definition a strip. A plot of the shear stiffness in Fig. 33, shows a divergence from the elasticity result at large obliqueness angles, the reason for which can be attributed to a natural "reminder" to the analyst from the dimensional reduction procedure that the obliqueness angle cannot be too large, following which the definition of a cross section breaks down. Such an effect is not observed in the stiffnesses associated

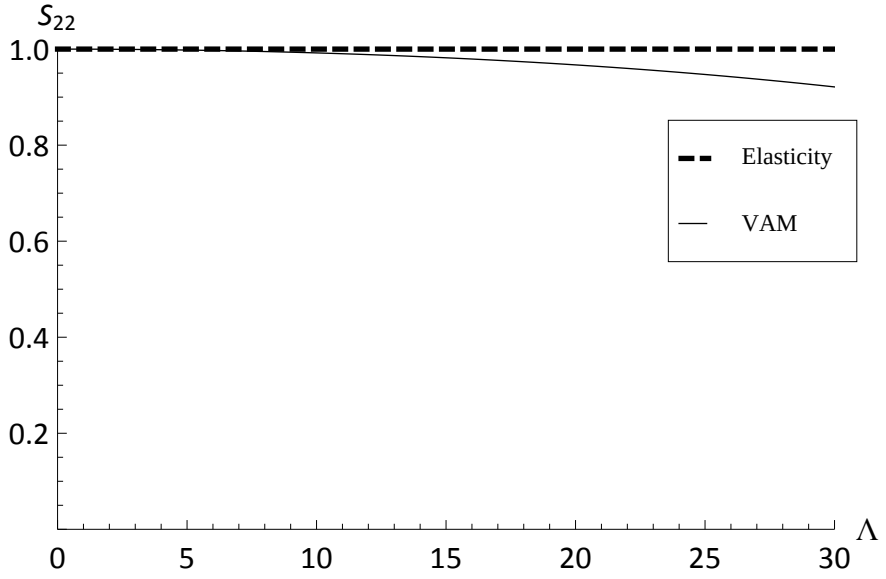

Figure 33: In-plane shear stiffness of the strip vs. obliqueness angle (in degrees) for $\nu = 0.3$. Shear stiffnesses have been normalized by the corresponding elasticity values

with the classical strain measures. This is fundamentally because the classical strain measures are of order ϵ, whose ratio to the order of the shear strain measure is the slenderness ratio. Therefore, it is only when the inverse of the slenderness ratio factors into the analysis, does the mathematical procedure spit out a warning concerning the extent of obliqueness.

Finally, in terms of the strain measures of the deformed oblique section (N), the GT sectional strain energy can be written as:

$$\mathcal{U}_{GT} = \frac{1}{2} \begin{Bmatrix} \gamma_{11}^o \\ 2\gamma_{12}^o \\ \rho_3 \end{Bmatrix}^T X_{GT}^{(N)} \begin{Bmatrix} \gamma_{11}^o \\ 2\gamma_{12}^o \\ \rho_3 \end{Bmatrix}$$

$$X_{GT}^{(N)} = \begin{bmatrix} \frac{3Ebt\cos(\Lambda)^2\left[4+4\nu+3\tan(\Lambda)^2\right]}{2[3+3\nu+\tan(\Lambda)^2]} & -\frac{Ebt\sin(2\Lambda)\left[7+12\nu+4\tan(\Lambda)^2\right]}{4[3+3\nu+\tan(\Lambda)^2]} & 0 \\ -\frac{Ebt\sin(2\Lambda)\left[7+12\nu+4\tan(\Lambda)^2\right]}{4[3+3\nu+\tan(\Lambda)^2]} & \frac{Ebt\cos(\Lambda)^2\left[5+12(1+\nu)\tan(\Lambda)^2+4\tan(\Lambda)^4\right]}{2[3+3\nu+\tan(\Lambda)^2]} & 0 \\ 0 & 0 & \frac{2}{3}Eb^3t \end{bmatrix} \tag{137}$$

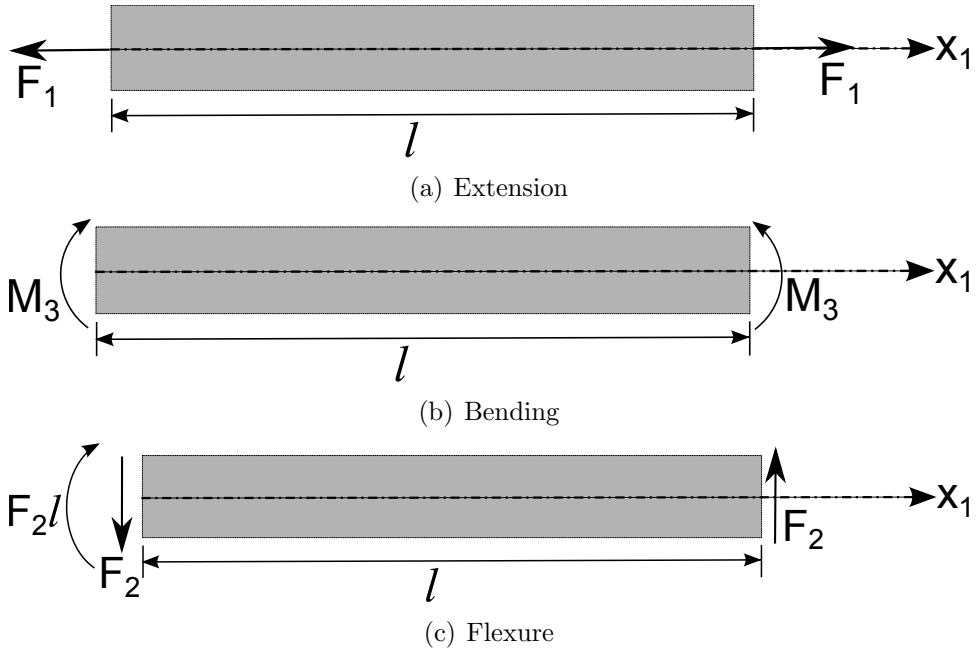

(a) Extension

(b) Bending

(c) Flexure

Figure 34: Various loading cases for the strip which possess elasticity solutions

The final aspect of the beam theory is to recover the cross-sectional stress, strain and displacement. This can be done by using the expressions for warping from Eqs. (124) and (128) in the strain measures developed in Eqs. (120). The derivatives of the generalized strain measures can be evaluated now using the 1D equilibrium equations, as in step 3 of the GT transformation, with the knowledge of the final section constants. The 1D generalized strains can be computed using solvers such as GEBT [126], which are based on a set of 1D beam equations [46] consistent with the current VAM based cross-sectional analysis. Also, since most 1D solvers work with the generalized strains of the corresponding normal section, it is preferred (again, not necessary) to set up the expressions in terms of the B generalized strain measures. Once the strains are known, the cross-sectional stress can be obtained from Eq. (121). Using Eq. (116) and the essential boundary conditions of the problem, the displacement field can be determined.

The recovery is validated against elasticity for three different loading cases as shown in Fig. 34. The elasticity solutions for these are quite simple, and can be

Table 9: Stresses: VAM vs. elasticity for the loading case of extension

Stress	VAM/Elasticity
σ_{11}	$\dfrac{F_1 \cos(\Lambda)^2}{2Ebt}$
σ_{12}	$-\dfrac{F_1 \sin(\Lambda)\cos(\Lambda)}{2Ebt}$
σ_{22}	$\dfrac{F_1 \sin(\Lambda)^2}{2Ebt}$

found in any standard elasticity text [109]. One could choose other loading cases too for which elasticity solutions exist, but that would needlessly complicate the process. This is because though the current loading cases are simple, they form a complete validation set as they involve all three modes pertaining to the planar deformation pertaining to the strip: extension, bending and shearing. It should be stated here that the only assumptions in the VAM were the smallness of local rotation and strains. But elasticity solutions assume small (total) rotations and displacements. Therefore the beam theory is specialized to the linear case before comparing it with the elasticity solutions. Each loading case will have three strains, three stresses and two displacements, making it a total of eight recovery quantities. If the stresses are in good agreement, this implies so will the strains and a consistent set of essential boundary conditions will ensure agreement in displacement as well. Therefore each loading case, the expressions for stress from the VAM and elasticity are presented in Tables 9, 10 and 11. The VAM recovers the quantities in the oblique cross section, so the elasticity solutions will be have to be transformed by using the well known tensorial and vectorial rotation formulae.

For the cases of extension and bending, the VAM predicts the stresses to be exactly the same as the elasticity solution. Excellent agreement is observed even for the flexure case, except for a minor difference involving the coefficient of b^2. Apart from this, the cross-sectional variation of the stress for both elasticity and VAM are in

Table 10: Stresses: VAM vs. elasticity for the loading case of bending

Stress	VAM/Elasticity
σ_{11}	$-\dfrac{3M_3 y_2 \cos(\Lambda)^3}{2Eb^3t}$
σ_{12}	$\dfrac{3M_3 y_2 \cos(\Lambda)^2 \sin(\Lambda)}{2Eb^3t}$
σ_{22}	$-\dfrac{3M_3 y_2 \cos(\Lambda) \sin(\Lambda)^2}{2Eb^3t}$

Table 11: Stresses: VAM vs. elasticity for the loading case of flexure

Stress		Theory
σ_{11}	VAM	$\dfrac{3F_2 \cos(\Lambda)}{2b^3t}\left[\dfrac{4}{3}\sin(\Lambda)b^2 - y_2\cos(\Lambda)^2\left(l - x_1 + 2y_2\sin(\Lambda)\right)\right]$
	Elasticity	$\dfrac{3F_2 \cos(\Lambda)}{2b^3t}\left[\sin(\Lambda)b^2 - y_2\cos(\Lambda)^2\left(l - x_1 + 2y_2\sin(\Lambda)\right)\right]$
σ_{12}	VAM	$\dfrac{3F_2}{4b^3t}\left[\dfrac{1}{3}\left(1 - 4\cos(2\Lambda)\right)b^2 + \cos(\Lambda)\cos(3\Lambda)y_2^2 - 2y_2\cos(\Lambda)^2\sin(\Lambda)\left(l - x_1\right)\right]$
	Elasticity	$\dfrac{3F_2}{4b^3t}\left[-\cos(2\Lambda)b^2 + \cos(\Lambda)\cos(3\Lambda)y_2^2 - 2y_2\cos(\Lambda)^2\sin(\Lambda)\left(l - x_1\right)\right]$
σ_{22}	VAM	$\dfrac{3F_2\sin(2\Lambda)}{4b^3t}\left[-(1 - \dfrac{1}{3}\tan(\Lambda)^2)b^2 - y_2^2\cos(2\Lambda) - \left(l - x_1\right)y_2\sin(\Lambda)\right]$
	Elasticity	$\dfrac{3F_2\sin(2\Lambda)}{4b^3t}\left[-b^2 - y_2^2\cos(2\Lambda) - \left(l - x_1\right)y_2\sin(\Lambda)\right]$

perfect agreement. The minor decrease possibly can be attributed to the reason given for the shear stiffness variation with Λ. A quantitative comparison of the solutions can be ascertained by plotting the stresses for various obliqueness angles as shown in Figs. 35, 36 and 37. While the stresses have been made dimensionless by F_2/bt, ζ is a dimensionless width defined as $y_2 \cos(\Lambda)/b$. The b/l value for all the cases is chosen to be 0.1, which implies that the ratio of beam's width to length is 0.2, which is a reasonably "stout" beam. From the plots, it can be seen as the section gets oblique, there is a significant change in the behavior of σ_{12} and σ_{22} over the width. For $\Lambda = 15°$, the results are in excellent agreement, and as Λ is increased to 30°, there is a minor difference in the stress distributions, and as mentioned previously, is a reminder that the obliqueness angle cannot be arbitrarily large.

It must be stated here that the patterns of the stress distribution, especially at higher obliqueness angles can be used to bring to light the fact that traditional beam assumptions regarding the deformation and variation of cross-sectional stresses will not work when trying to construct a beam theory using an oblique cross section as in the current problem. Only an approach that adheres closely to elasticity will yield true. None of the analysis steps, such as using the warping constraints or equilibrium equations to eliminate the strain derivatives, impose any *ad hoc* restrictions on the deformation. To conclude this section, a beam theory has been proposed for the in-plane deformation of an isotropic strip using an oblique section. A cross-sectional stiffness matrix was derived and the stress recovery was demonstrated for loading cases which involved all three possible in-plane deformations. Both these quantities were shown to be in agreement with elasticity.

6.5 Isotropic Prismatic Beam: 3D Deformation

The second problem of interest is the development of a beam theory for a prismatic, isotropic beam whose orthogonal cross section is a solid circle. The oblique-section

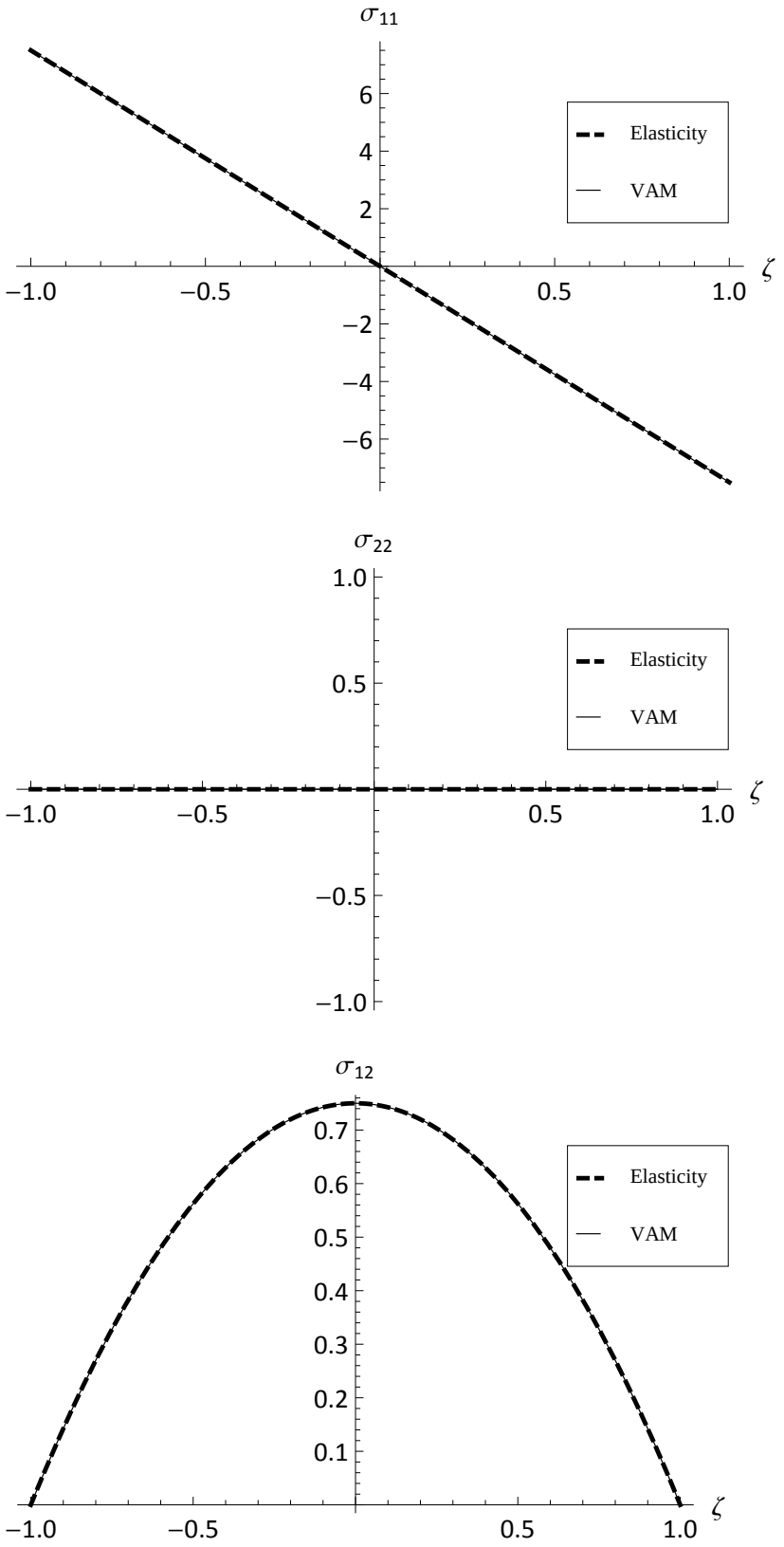

Figure 35: Variation of cross-sectional stresses for flexure; $b/l = 0.1$ and $\Lambda = 0^\circ$.

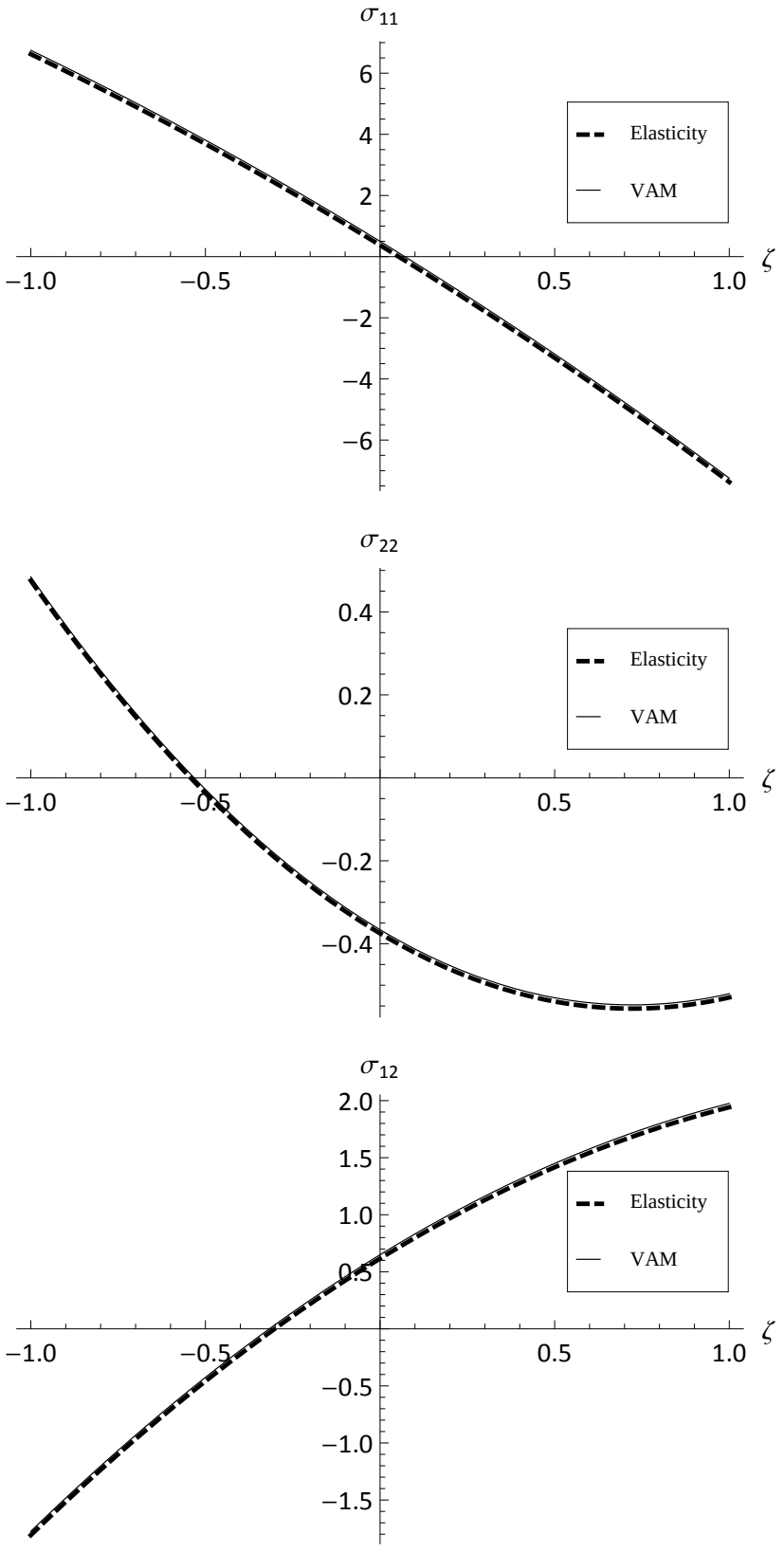

Figure 36: Variation of cross-sectional stresses for flexure; $b/l = 0.1$ and $\Lambda = 15^\circ$

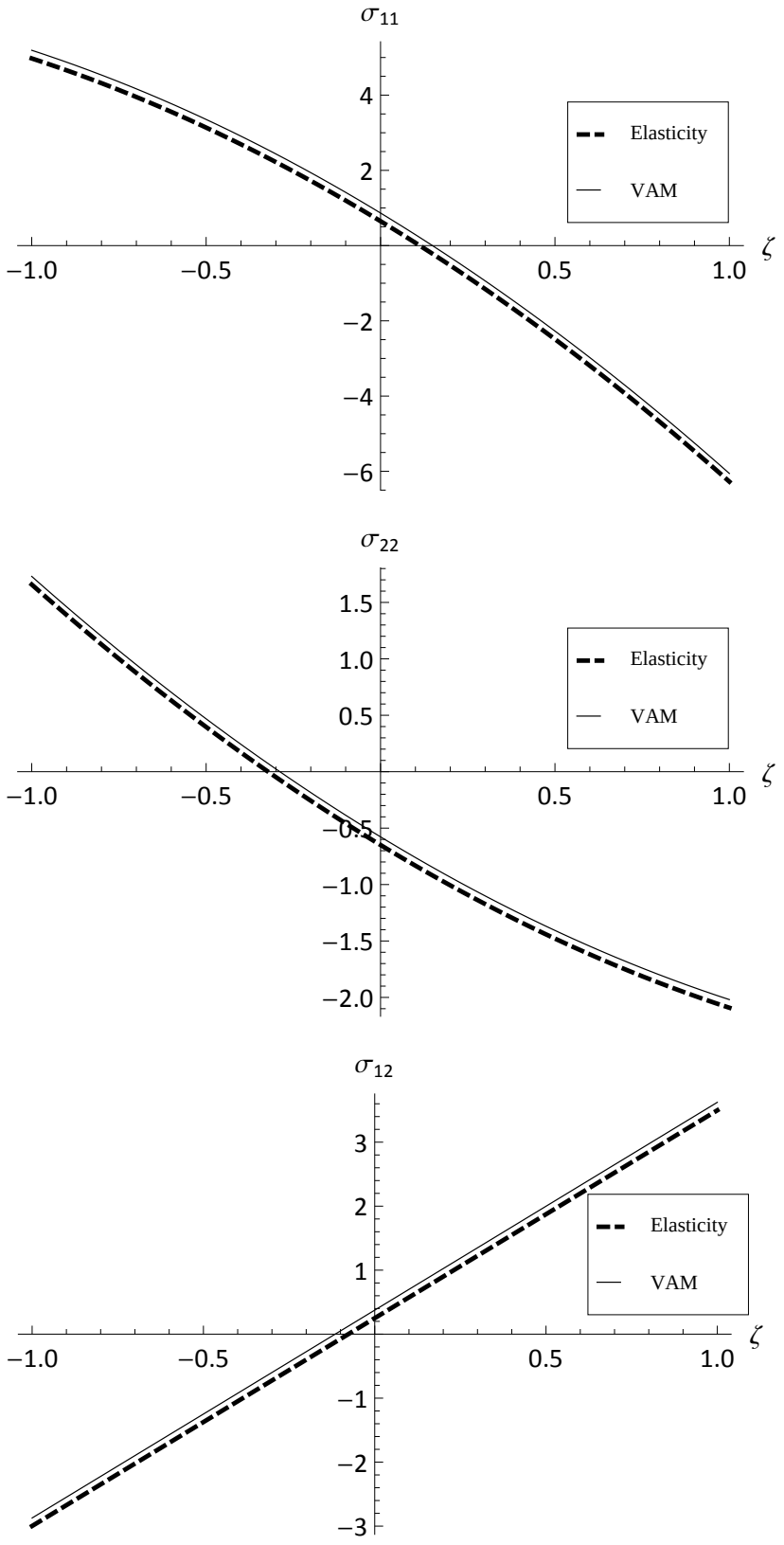

Figure 37: Variation of cross-sectional stresses for flexure; $b/l = 0.1$ and $\Lambda = 30^\circ$

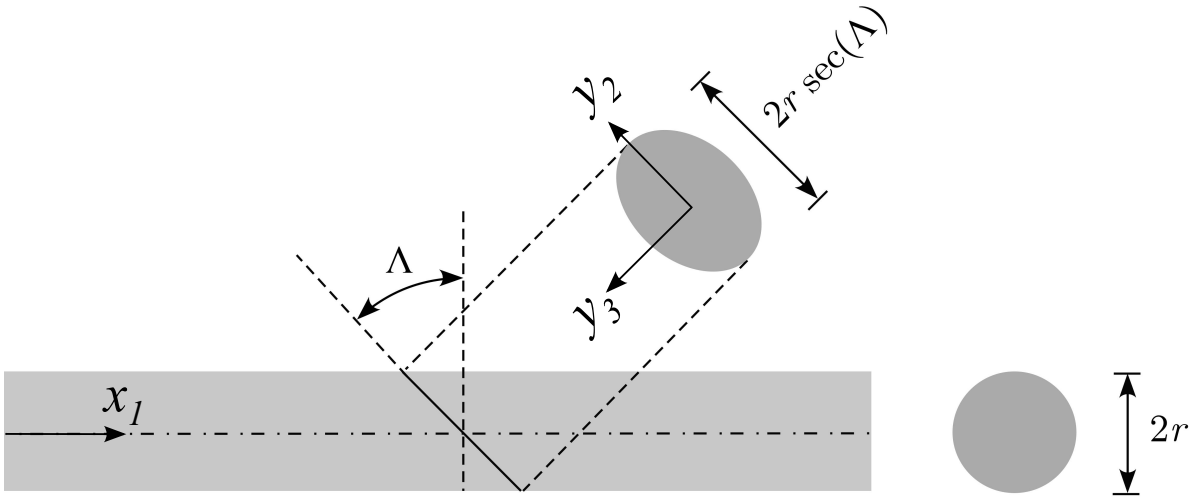

Figure 38: Schematic of a prismatic, isotropic beam with a circular cross section

used for the VAM based dimensional reduction will therefore be an ellipse as shown in Fig. 38. Again for this case, an obvious choice of the reference line will be the line of section centroids.

The VAM procedure follows along the lines corresponding to the development of the strip, the chief difference being that the cross section is two dimensional in this case; and the deformation will include all possible modes, which will become evident as the theory is developed. Therefore for the purpose of brevity, the description of the problem will be limited to the places where there is significant departure from the previous problem. The equations presented will involve quantities with the same interpretation as in Sec. 6.4, but applied to the problem of current interest. As always, the solution of the problem begins with writing the geometrically exact expressions for the position of a generic point in the undeformed section and its corresponding position in the deformed section, viz.,

$$\hat{\mathbf{r}} = \mathbf{r} + y_2\mathbf{a}_2 + y_3\mathbf{a}_3$$

$$\hat{\mathbf{R}} = \mathbf{R} + y_2\mathbf{A}_2 + y_3\mathbf{A}_3 + w_1(x_1, y_2, y_3)\mathbf{A}_1 + w_2(x_1, y_2, y_3)\mathbf{A}_2 + w_3(x_1, y_2, y_3)\mathbf{A}_3 \tag{138}$$

The beam strains used for the development of the classical analysis are:

$$\begin{aligned}\mathbf{R}' &= [1+\overline{\gamma}_{11}(x_1)]\mathbf{T}_1 \\ \mathbf{A}_i' &= \overline{\rho}_j(x_1)\mathbf{A}_j \times \mathbf{A}_i\end{aligned} \tag{139}$$

Subsequently, the expressions for the 3D strains are:

$$\begin{aligned}\Gamma_{11} &= \sec(\Lambda)\left[w_1' + y_3\overline{\rho}_2 - y_2\overline{\rho}_3 + \cos(\Lambda)\overline{\gamma}_{11}\right] + \tan(\Lambda)w_{1,2} \\ 2\Gamma_{12} &= \sec(\Lambda)\left[-y_3\overline{\rho}_1 - \sin(\Lambda)\overline{\gamma}_{11} + w_2'\right] + w_{1,2} + \tan(\Lambda)w_{2,2} \\ 2\Gamma_{13} &= \sec(\Lambda)\left(y_2\overline{\rho}_1 + w_3'\right) + w_{1,3} + \tan(\Lambda)w_{3,2} \\ \Gamma_{22} &= w_{2,2} \\ 2\Gamma_{23} &= w_{2,3} + w_{3,2} \\ \Gamma_{33} &= w_{3,3}\end{aligned} \tag{140}$$

From the constitutive law of 3D elasticity, the stress-strain relations for an isotropic material may be expressed as

$$\begin{Bmatrix}\sigma_{11}\\ \sigma_{12}\\ \sigma_{13}\\ \sigma_{22}\\ \sigma_{23}\\ \sigma_{33}\end{Bmatrix} = \frac{E}{(1-2\nu)(1-\nu)}\begin{bmatrix}1-\nu & 0 & 0 & \nu & 0 & \nu\\ 0 & \frac{1-2\nu}{2} & 0 & 0 & 0 & 0\\ 0 & 0 & \frac{1-2\nu}{2} & 0 & 0 & 0\\ \nu & 0 & 0 & 1-\nu & 0 & \nu\\ 0 & 0 & 0 & 0 & \frac{1-2\nu}{2} & 0\\ \nu & 0 & 0 & \nu & 0 & 1-\nu\end{bmatrix}\begin{Bmatrix}\Gamma_{11}\\ 2\Gamma_{12}\\ 2\Gamma_{13}\\ \Gamma_{22}\\ 2\Gamma_{23}\\ \Gamma_{33}\end{Bmatrix} \tag{141}$$

which can be used to obtain an expression for the sectional strain energy in terms of the unknown warping. The displacement field introduced in Eq. (138) is rendered unique by the following constraints on the unknown warping:

$$\begin{aligned}\langle w_i\rangle &= 0 \\ \langle\cos(\Lambda)\left(w_{2,3} - w_{3,2}\right) + \sin(\Lambda)w_{1,3}\rangle &= 0\end{aligned} \tag{142}$$

The first three constraints are obtained from stipulating that the position of the reference line ($\mathbf{R}$) is the average over the cross section of the positions of all particles

that make up the oblique section. The fourth constraint is obtained from vanishing of the average local rotation about $\mathbf{T}_1$, which is a necessity for the VAM procedure to be in sync with 3D elasticity [132]. Thus, one can formulate the exact elasticity problem using variational principles. Estimating orders as was done in Sec. 6.4, an asymptotic procedure can be carried out. The solution of the zeroth order warping turns out to be

$$
\begin{aligned}
w_1^{(0)} =& \frac{1}{8}\Bigg\{ -4y_2 \sin(\Lambda)\left[2\left(1+\nu\right)\cos(\Lambda)\overline{\gamma}_{11} + \nu y_3 \sin(2\Lambda)\overline{\rho}_1 + 2y_3\left(1+\nu\cos(\Lambda)^2\right)\overline{\rho}_2\right] \\
&+ \left[\left(-r^2 - 4y_3^2\nu + \left(\nu+5\right)y_2^2\right)\sin(\Lambda) + \left(1+\nu\right)y_2^2\sin(3\Lambda) - r^2\sec(\Lambda)\tan(\Lambda)\right]\overline{\rho}_3 \Bigg\} \\
w_2^{(0)} =& \frac{1}{8}\Bigg\{ -8y_2\left[\left(\nu\cos(\Lambda)^2 - \sin(\Lambda)^2\right)\overline{\gamma}_{11} + y_3\sin(\Lambda)\left(-1+\nu\cos(\Lambda)^2\right)\overline{\rho}_1 + y_3\nu\cos(\Lambda)^3\overline{\rho}_2\right] \\
&+ \left[-4\cos(\Lambda)\left(\nu y_3^2 + \left(-\nu\cos(\Lambda)^2 + \sin(\Lambda)^2\right)y_2^2\right) + r^2\sin(\Lambda)\tan(\Lambda)\right]\overline{\rho}_3 \Bigg\} \\
w_3^{(0)} =& \frac{1}{8}\Bigg\{ -8\nu y_3\overline{\gamma}_{11} + \sin(\Lambda)\left[r^2\left(1+\sec(\Lambda)^2\right) - 4\nu y_3^2 + 2y_2^2\left(-3+\nu+\left(-1+\nu\right)\cos(2\Lambda)\right)\right]\overline{\rho}_1 \\
&+ \left[-4\nu y_3^2\cos(\Lambda) + 4y_2^2\cos(\Lambda)\left(\sin(\Lambda)^2 + \nu\cos(\Lambda)^2\right) - r^2\sin(\Lambda)\tan(\Lambda)\right]\overline{\rho}_2 \\
&+ 8y_2y_3\nu\cos(\Lambda)\overline{\rho}_3 \Bigg\}
\end{aligned}
\tag{143}
$$

and the corresponding sectional strain energy is

$$
\mathcal{U}_0 = \frac{1}{2}\begin{Bmatrix} \overline{\gamma}_{11} \\ \overline{\rho}_1 \\ \overline{\rho}_2 \\ \overline{\rho}_3 \end{Bmatrix}^T \begin{bmatrix} E\pi r^2 & 0 & 0 & 0 \\ 0 & \frac{E\pi r^4}{4(1+\nu)}\left(1+\nu\sin(\Lambda)^2\right) & \frac{E\pi r^4\sin(2\Lambda)}{8(1+\nu)} & 0 \\ 0 & \frac{E\pi r^4\sin(2\Lambda)}{8(1+\nu)} & \frac{E\pi r^4}{4(1+\nu)}\left(1+\nu\cos(\Lambda)^2\right) & 0 \\ 0 & 0 & 0 & \frac{1}{4}E\pi r^4 \end{bmatrix} \begin{Bmatrix} \overline{\gamma}_{11} \\ \overline{\rho}_1 \\ \overline{\rho}_2 \\ \overline{\rho}_3 \end{Bmatrix}
\tag{144}
$$

Note that the classical theory is described using the stretching strain of the T frame and the curvature strain measures of the A frame. If the stretching strain of the A frame were used, the shearing strain measures will enter into the picture and they

are not independent strain measures for this theory. They can be related using the kinematical equations and frame relations outlined in Sec. 6.3.

$$\begin{aligned}
\mathbf{R}' &= (1+\overline{\gamma}_{11})[\cos(\Lambda)\mathbf{A}_1 - \sin(\Lambda)\mathbf{A}_2] \\
\mathbf{R}' &= [\cos(\Lambda)+\overline{\gamma}^o_{11}]\mathbf{A}_1 + [-\sin(\Lambda)+2\overline{\gamma}^o_{12}]\mathbf{A}_2 + 2\overline{\gamma}^o_{13}\mathbf{A}_3 \\
\implies & \overline{\gamma}^o_{11} = \cos(\Lambda)\overline{\gamma}_{11};\ 2\overline{\gamma}^o_{12} = -\sin(\Lambda)\overline{\gamma}_{11};\ 2\overline{\gamma}^o_{13} = 0
\end{aligned} \tag{145}$$

For these reasons and the fact that the stretching strain is more natural when it is expressed along the longitudinal axis, the classical analysis is carried out in terms of $\overline{\gamma}_{11}$. The analytical evaluation of the warping perturbed one order higher turns out to be very challenging, so terms which are expected to contribute to the Generalized Vlasov energy (another model obtained from the second-order asymptotically correct strain energy [46]) and those which are expected to vanish with application of the equilibrium equations (recall from Sec. 6.4 that this is one of the steps of the GT transformation) are dropped, and the final expressions for the first-order warping

become

$$
\begin{aligned}
w_1^{(1)} =& \frac{1}{96}\Bigg\{ -6y_3\Big[2(2\nu+1)r^2\sec(\Lambda)+\cos(\Lambda)\left(-2(6\nu+7)r^2-4\nu y_2^2+y_2^2+4y_3^2\right) \\
&+(4\nu+3)y_2^2\cos(3\Lambda)\Big]\left(\sin(\Lambda)\overline{\rho}_1'+\cos(\Lambda)\overline{\rho}_2'\right) \\
&+y_2\Big[12r^2\sec^2(\Lambda)-4\cos(2\Lambda)\left(3(3\nu+4)r^2+3(2\nu-1)y_3^2-5y_2^2\right) \\
&-3\left(4(\nu+3)r^2+(2\nu+1)\left(y_2^2-4y_3^2\right)\right)+(6\nu+7)y_2^2\cos(4\Lambda)\Big]\overline{\rho}_3'\Bigg\} \\
w_2^{(1)} =& \frac{1}{96}\tan(\Lambda)\Bigg\{ 6y_3\Big[2r^2\sec(\Lambda)+\cos(\Lambda)\left(-2(6\nu+7)r^2+12\nu y_2^2+y_2^2+4y_3^2\right) \\
&+(4\nu+3)y_2^2\cos(3\Lambda)\Big]\left(\sin(\Lambda)\overline{\rho}_1'+\cos(\Lambda)\overline{\rho}_2'\right) \\
&+y_2\Big[12(3\nu+2)r^2-(6\nu+7)y_2^2\cos(4\Lambda)-(18\nu+5)y_2^2+12(2\nu-1)y_3^2 \\
&-12\cos(2\Lambda)\left(-(3\nu+4)r^2+2\nu\left(y_2^2-y_3^2\right)+y_2^2+y_3^2\right)\Big]\overline{\rho}_3'\Bigg\} \\
w_3^{(1)} =& \frac{1}{24}\Bigg\{ y_2\Big[-3r^2\tan(\Lambda)\sec(\Lambda)+3\sin(\Lambda)\left((2\nu+1)\,r^2+(1-\nu)\,y_2^2+4\nu y_3^2\right) \\
&-(3\nu+1)y_2^2\sin(3\Lambda)\Big]\left(\sin(\Lambda)\overline{\rho}_1'+\cos(\Lambda)\overline{\rho}_2'\right) \\
&+6\nu y_3\left(r^2\tan(\Lambda)-2y_2^2\sin(2\Lambda)\right)\overline{\rho}_3'\Bigg\}
\end{aligned}
\tag{146}
$$

which can be used to obtain the second-order asymptotically correct sectional strain energy, $\mathcal{U}_2$. The resulting expression is too lengthy to be included here. However, all quantities needed for its computation have been explicitly presented, and results can be obtained by using symbolic manipulation software, such as Mathematica. The expression $\mathcal{U}_2$ involves the derivatives of the 1D generalized strain measures and is thus not in a form suitable for use in an engineering beam theory. The derivatives are eliminated using the GT transformation as outlined in Sec. 6.4. The pertinent equations used in each of the four steps of the transformation are sequentially listed

below

$$\left\{\begin{array}{c}\overline{\gamma}_{11}\\ \overline{\rho}_1\\ \overline{\rho}_2\\ \overline{\rho}_3\end{array}\right\}=\left[\begin{array}{cccc}1 & 0 & 0 & 0\\ 0 & \cos(\Lambda) & \sin(\Lambda) & 0\\ 0 & -\sin(\Lambda) & \cos(\Lambda) & 0\\ 0 & 0 & 0 & 1\end{array}\right]\left\{\begin{array}{c}\overline{\gamma}_{11}\\ \overline{\kappa}_1\\ \overline{\kappa}_2\\ \overline{\kappa}_3\end{array}\right\} \tag{147}$$

$$\begin{aligned}\overline{\gamma}_{11} =&\gamma_{11}\\ \overline{\kappa}_1 =&\kappa_1\\ \overline{\kappa}_2 =&\kappa_2-(2\gamma_{13})'\\ \overline{\kappa}_3 =&\kappa_3+(2\gamma_{12})'\end{aligned} \tag{148}$$

$$\begin{aligned}\mathcal{F}_1'=0\\ \mathcal{F}_2'=0\\ \mathcal{F}_3'=0\\ \mathcal{M}_1'=0\\ \mathcal{M}_2'-\mathcal{F}_3=0\\ \mathcal{M}_3'+\mathcal{F}_2=0\end{aligned} \tag{149}$$

$$\left\{\begin{array}{c}\gamma_{11}\\ 2\gamma_{12}\\ 2\gamma_{13}\\ \kappa_1\\ \kappa_2\\ \kappa_3\end{array}\right\}=\left[\begin{array}{cccccc}\cos(\Lambda) & -\sin(\Lambda) & 0 & 0 & 0 & 0\\ \sin(\Lambda) & \cos(\Lambda) & 0 & 0 & 0 & 0\\ 0 & 0 & 1 & 0 & 0 & 0\\ 0 & 0 & 0 & \cos(\Lambda) & -\sin(\Lambda) & 0\\ 0 & 0 & 0 & \sin(\Lambda) & \cos(\Lambda) & 0\\ 0 & 0 & 0 & 0 & 0 & 1\end{array}\right]\left\{\begin{array}{c}\gamma_{11}^o\\ 2\gamma_{12}^o\\ 2\gamma_{13}^o\\ \rho_1\\ \rho_2\\ \rho_3\end{array}\right\} \tag{150}$$

The final forms of the stiffness matrices of the GT sectional strain energy associated

with the B and N frames of reference are therefore:

$$\mathcal{S}_{GT}^{(B)} = \begin{bmatrix} E\pi r^2 & 0 & 0 & 0 & 0 & 0 \\ 0 & \frac{3E\pi r^2(1+\nu)}{7+14\nu+8\nu^2+3(1+\nu)\tan(\Lambda)^2} & 0 & 0 & 0 & 0 \\ 0 & 0 & \frac{3E\pi r^2(1+\nu)}{7+14\nu+8\nu^2+2(1+\nu)\tan(\Lambda)^2} & 0 & 0 & 0 \\ 0 & 0 & 0 & \frac{E\pi r^4}{4(1+\nu)} & 0 & 0 \\ 0 & 0 & 0 & 0 & \frac{1}{4}E\pi r^4 & 0 \\ 0 & 0 & 0 & 0 & 0 & \frac{1}{4}E\pi r^4 \end{bmatrix} \tag{151}$$

$$\mathcal{S}_{GT}^{(N)} = \begin{bmatrix} S_\gamma & 0_{3\times3} \\ 0_{3\times3} & S_\rho \end{bmatrix} \tag{152}$$

where the 3×3 matrix S_ρ is defined as

$$\mathcal{S}_\rho = \begin{bmatrix} \frac{E\pi r^4}{4(1+\nu)}\left[1+\nu\sin(\Lambda)^2\right] & \frac{E\pi r^4\sin(2\Lambda)}{8(1+\nu)} & 0 \\ \frac{E\pi r^4\sin(2\Lambda)}{8(1+\nu)} & \frac{E\pi r^4}{4(1+\nu)}\left[1+\nu\cos(\Lambda)^2\right] & 0 \\ 0 & 0 & \frac{1}{4}E\pi r^4 \end{bmatrix} \tag{153}$$

and the nonzero elements of the S_γ matrix are

$$\begin{aligned} (\mathcal{S}_\gamma)_{11} =& E\pi r^2\cos(\Lambda)^2\left[1+\frac{3(1+\nu)\tan(\Lambda)^2}{7+14\nu+8\nu^2+3(1+\nu)\tan(\Lambda)^2}\right] \\ (\mathcal{S}_\gamma)_{12} =& \frac{E\pi r^2\sin(2\Lambda)}{2}\left[-1+\frac{3(1+\nu)}{7+14\nu+8\nu^2+3(1+\nu)\tan(\Lambda)^2}\right] \\ (\mathcal{S}_\gamma)_{22} =& E\pi r^2\cos(\Lambda)^2\left[\tan(\Lambda)^2+\frac{3(1+\nu)}{7+14\nu+8\nu^2+3(1+\nu)\tan(\Lambda)^2}\right] \\ (\mathcal{S}_\gamma)_{33} =& \frac{3E\pi r^2(1+\nu)}{7+14\nu+8\nu^2+2(1+\nu)\tan(\Lambda)^2} \end{aligned} \tag{154}$$

Using orthogonal (i.e., traditional) cross-sectional analysis, Ref. [127] presents a 6×6 stiffness matrix for an elliptical section, which was verified against elasticity solutions. For this case, the corresponding normal section for the oblique cross section is a circle. Eq. (151) is based on the strain measures of the corresponding normal section and hence can be used for comparison, when the ellipse is specialized to a circle. When this comparison is made, it can be seen that the stiffnesses associated with extension,

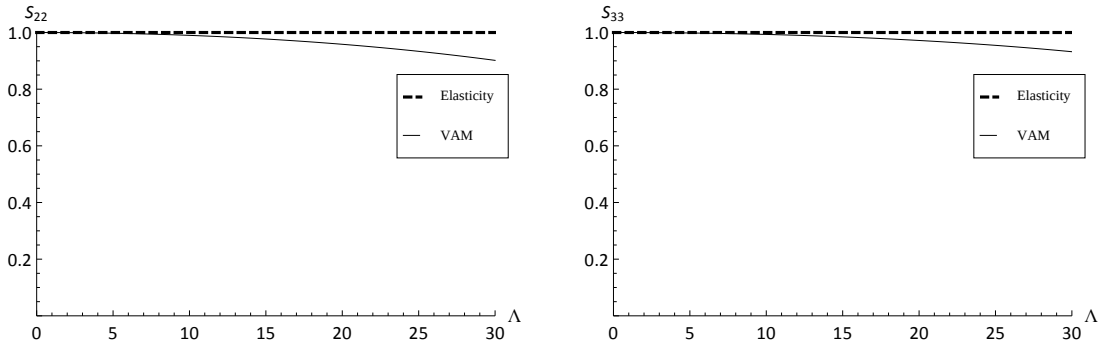

(a) 2-shear (b) 3-shear

Figure 39: Shear stiffnesses associated with $S_{GT}^{(B)}$ vs. obliqueness angle, Λ(deg.) for $\nu = 0.3$. All values are normalized by the corresponding elasticity solutions

twist and bending (in either direction) are correctly captured. The shear stiffness for the circular section in either direction is $3(1+\nu)E\pi r^2/(8\nu^2+14\nu+7)$; and therefore the only departure from the exact solution for the current oblique-sectional analysis are the terms involving $\tan(\Lambda)$. The qualitative aspect of this result is demonstrated in Fig. 39.

As with the strip, there is a departure from the elasticity solution which becomes predominant at large values of Λ, indicating that the cross section cannot be tilted at an arbitrarily large angle. A clearer picture the effects of this departure can be gleaned when an recovery comparison is carried out; which shall be our next recourse.

The generic procedure for the recovery that is outlined in Sec. 6.4 is followed in principle to obtain the cross-sectional stress, strain and displacement. Prior to comparison with the elasticity solutions, the VAM beam theory is specialized for small displacement and (total) rotation. The loading cases which will be considered are depicted in Fig. 40 - they total to six in number. The loading cases which involve the same deformation along multiple axes will be referred to in short by 'direction-deformation'. For example, the F_3 loading case will be referred to as 3-flexure. The elasticity solutions to these problems are often attributed to St. Venant [76]. Again,

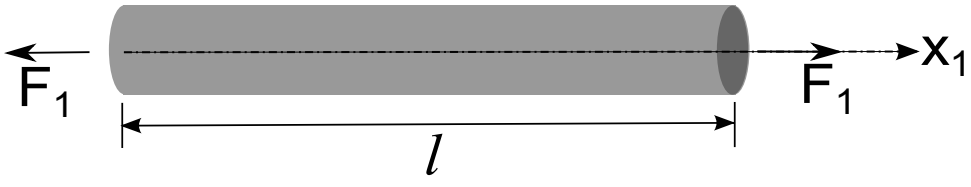

(a) Extension

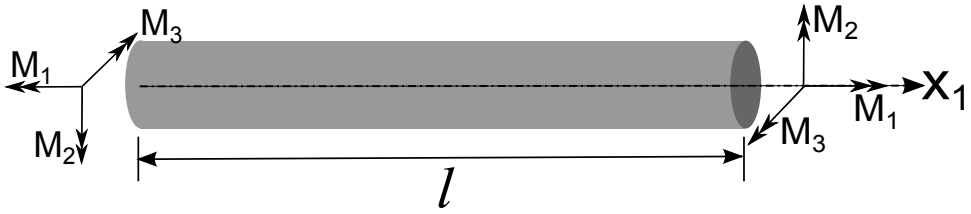

(b) Twisting, Bending (2)

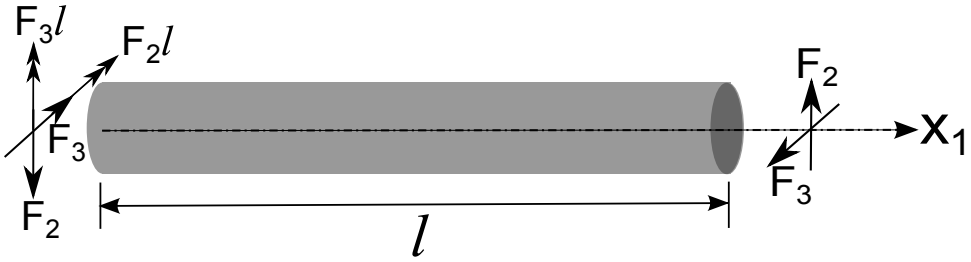

(c) Flexure (2)

Figure 40: Loading cases for which the beam has elasticity solutions. Some of the figures have multiple loading cases depicted on them.

Table 12: Stresses: VAM vs. elasticity for the loading case of extension

Stress	VAM/Elasticity
σ_{11}	$\frac{F_1 \cos(\Lambda)^2}{\pi r^2}$
σ_{12}	$-\frac{F_1 \sin(\Lambda)\cos(\Lambda)}{\pi r^2}$
σ_{22}	$\frac{F_1 \sin(\Lambda)^2}{\pi r^2}$
$\sigma_{13}, \sigma_{23}, \sigma_{33}$	0

Table 13: Stresses: VAM vs. elasticity for the loading case of twisting

Stress	VAM/Elasticity
σ_{11}	$-\frac{2M_1 y_3 \sin(2\Lambda)}{\pi r^4}$
σ_{12}	$-\frac{2M_1 y_3 \cos(2\Lambda)}{\pi r^4}$
σ_{13}	$\frac{2M_1 y_2 \cos(\Lambda)^2}{\pi r^4}$
σ_{22}	$\frac{4M_1 y_3 \cos(\Lambda)\sin(\Lambda)}{\pi r^4}$
σ_{23}	$-\frac{2M_1 y_2 \cos(\Lambda)\sin(\Lambda)}{\pi r^4}$
σ_{33}	0

there is a possibility the beam might have elasticity solutions for a more complex loading case. But the intent of this problem is to ensure that all the six possible deformation modes of the beam- extension, torsion, bending and shearing in either directions are captured in sync with the elasticity solution. Therefore the set of the problems considered forms a complete validation set for the GT theory, introducing the minimum level of complexity.

Table 14: Stresses: VAM vs. elasticity for the loading case of 2-bending

Stress	VAM/Elasticity
σ_{11}	$\frac{4M_2y_3\cos(\Lambda)^2}{\pi r^4}$
σ_{12}	$-\frac{4M_2y_3\sin(\Lambda)\cos(\Lambda)}{\pi r^4}$
σ_{22}	$\frac{4M_2y_3\sin(\Lambda)^2}{\pi r^4}$
$\sigma_{13},\sigma_{23},\sigma_{33}$	0

Table 15: Stresses: VAM vs. elasticity for the loading case of 3-bending

Stress	VAM/Elasticity
σ_{11}	$-\frac{4M_3y_2\cos(\Lambda)^3}{\pi r^4}$
σ_{12}	$\frac{4M_3y_2\sin(\Lambda)\cos(\Lambda)^2}{\pi r^4}$
σ_{22}	$-\frac{4M_3y_2\sin(\Lambda)^2\cos(\Lambda)}{\pi r^4}$
$\sigma_{13},\sigma_{23},\sigma_{33}$	0

Table 16: Stresses: VAM vs. elasticity for the loading case of 3-flexure

Stress	VAM/Elasticity
σ_{11}	$-\frac{2F_3y_3\cos(\Lambda)^2}{\pi r^4(1+\nu)}\left[2(1+\nu)(l-x_1)+y_2\sin(\Lambda)(3+4\nu)\right]$
σ_{12}	$\frac{F_3y_3\cos(\Lambda)}{\pi r^4(1+\nu)}\left[-y_2\cos(2\Lambda)(3+4\nu)+2(1+\nu)\left(y_2+2\sin(\Lambda)\left(l-x_1\right)\right)\right]$
σ_{13}	$\frac{F_3\cos(\Lambda)}{2\pi r^4(1+\nu)}\left[y_2^2\cos(\Lambda)^2(2\nu-1)+(2\nu+3)(r^2-y_3^2)\right]$
σ_{22}	$\frac{F_3y_3\sin(\Lambda)}{\pi r^4(1+\nu)}\left[-y_2+y_2\cos(2\Lambda)(3+4\nu)-4(1+\nu)\sin(\Lambda)(l-x_1)\right]$
σ_{23}	$\frac{F_3\sin(\Lambda)}{2\pi r^4(1+\nu)}\left[y_2^2\cos(\Lambda)^2(1-2\nu)+(2\nu+3)(y_3^2-r^2)\right]$
σ_{33}	0

Table 17: Stresses: VAM vs. elasticity for the loading case of 2-flexure

Stress		Theory
σ_{11}	VAM	$\frac{F_2\cos(\Lambda)}{(1+\nu)\pi r^4}\left[\sin(\Lambda)\left((2\nu-1)\,y_3^2+(4+3\nu)\,r^2\right)-y_2\cos(\Lambda)^2\left(4\,(1+\nu)\,(l-x_1)+y_2\sin(\Lambda)\,(7+6\nu)\right)\right]$
	Elasticity	$\frac{F_2\cos(\Lambda)}{(1+\nu)\pi r^4}\left[\sin(\Lambda)\left((2\nu-1)\,y_3^2+(3+2\nu)\,r^2\right)-y_2\cos(\Lambda)^2\left(4\,(1+\nu)\,(l-x_1)+y_2\sin(\Lambda)\,(7+6\nu)\right)\right]$
σ_{12}	VAM	$\frac{F_2}{8(1+\nu)\pi r^4}\left[2\cos(2\Lambda)\left(2\,(-1+2\nu)\,y_3^2-(3+2\nu)\,y_2^2+(6+4\nu)r^2\right)+y_2\left((1+2\nu)y_2-y_2(7+6\nu)\cos(4\Lambda)+32\,(l-x_1)\,(1+\nu)\cos(\Lambda)^2\sin(\Lambda)\right)-8r^2(1+\nu)\sin(\Lambda)^2\right]$
	Elasticity	$\frac{F_2}{8(1+\nu)\pi r^4}\left[2\cos(2\Lambda)\left(2\,(-1+2\nu)\,y_3^2-(3+2\nu)\,y_2^2+(6+4\nu)r^2\right)+y_2\left((1+2\nu)y_2-y_2(7+6\nu)\cos(4\Lambda)+32\,(l-x_1)\,(1+\nu)\cos(\Lambda)^2\sin(\Lambda)\right)\right]$
σ_{13}	VAM	$-\frac{F_2y_2y_3(1+2\nu)\cos(\Lambda)^2}{\pi r^4(1+\nu)}$
	Elasticity	$-\frac{F_2y_2y_3(1+2\nu)\cos(\Lambda)^2}{\pi r^4(1+\nu)}$
σ_{22}	VAM	$-\frac{F_2\sin(2\Lambda)}{4\pi r^4(1+\nu)}\left[2\,(2\nu-1)\,y_3^2+(2\nu+1)\,y_2^2+\left(6+4\nu-2\,(1+\nu)\tan(\Lambda)^2\right)r^2+y_2\left(-y_2\,(7+6\nu)\cos(2\Lambda)+8\,(l-x_1)\,(1+\nu)\sin(\Lambda)\right)\right]$
	Elasticity	$-\frac{F_2\sin(2\Lambda)}{4\pi r^4(1+\nu)}\left[2\,(2\nu-1)\,y_3^2+(2\nu+1)\,y_2^2+(6+4\nu)\,r^2+y_2\left(-y_2\,(7+6\nu)\cos(2\Lambda)+8\,(l-x_1)\,(1+\nu)\sin(\Lambda)\right)\right]$
σ_{23}	VAM	$\frac{F_2y_2y_3(1+2\nu)\cos(\Lambda)\sin(\Lambda)}{\pi r^4(1+\nu)}$
	Elasticity	$\frac{F_2y_2y_3(1+2\nu)\cos(\Lambda)\sin(\Lambda)}{\pi r^4(1+\nu)}$
σ_{33}	VAM	0
	Elasticity	0

The stress recovered from VAM is compared with the six loading cases in Tables 12-17. The VAM recovers stresses in an oblique cross section, and thus elasticity solutions must be expressed in this system by tensorial laws of rotation. It can be seen that the oblique cross-sectional analysis recovers the same stress as the elasticity solution for the loading cases of extension, twist, bending and 3-flexure. For the 2-flexure case, σ_{13}, σ_{23} and σ_{33} are in perfect agreement. Even for the cases of σ_{11}, σ_{12} and σ_{22}, the cross-sectional distribution of the stresses are in perfect agreement. The minor difference comes through the coefficient of the constant term (associated with r^2), which is attributed to the slight decrease in shear stiffness; the reason for this was stated previously. A qualitative measure of this difference can be obtained by plotting the stress distribution over the cross section, as shown in Figs. 41 and 42. The stresses are normalized by F_2/r^2, and the dimensionless coordinates are defined as $\zeta_\alpha = y_\alpha/r$, respectively. For σ_{13}, σ_{23} and σ_{33}, the recovery expressions are perfectly coincident, and this is captured in the plots. As mentioned previously, the other three stresses (σ_{11}, σ_{12} and σ_{22}) differ by very minor constants (approximately 0.13, 0.08 and 0.04, respectively – and thus negligible compared to the corresponding representative stress values). This is established by a side-by-side display of the solutions from VAM and elasticity; the difference between either is hardly discernible.

This completes the development and validation of an oblique cross-sectional analysis based beam theory for the problem of interest using the VAM. A 6×6 cross-sectional matrix was presented associated with the strain measures of a deformed oblique section. The stress recovery is presented for six different loading cases to validate all the six deformation modes of the beam. Both the stiffness matrix and recovery were shown to be in good agreement with the corresponding results obtained from 3D elasticity.

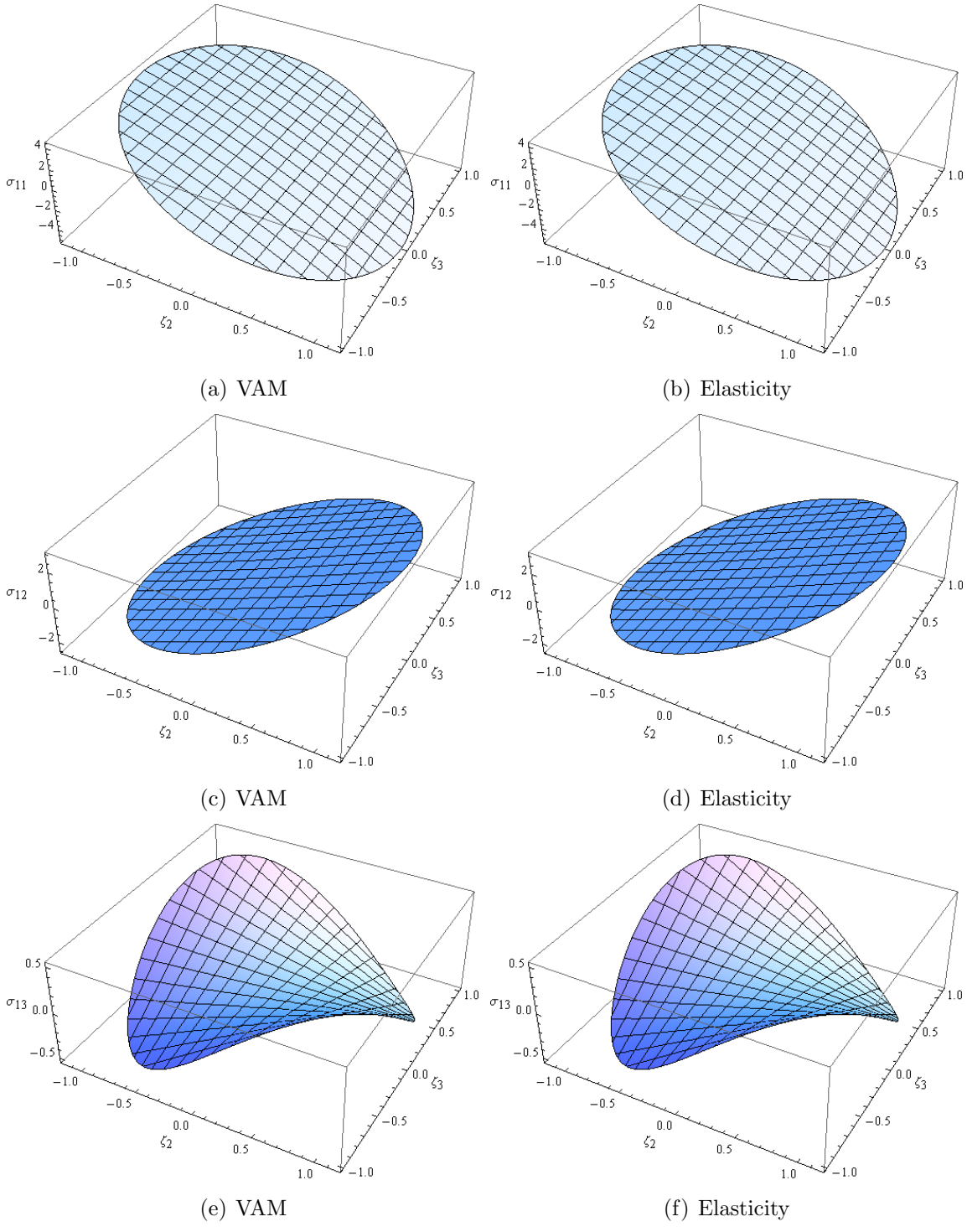

(a) VAM (b) Elasticity

(c) VAM (d) Elasticity

(e) VAM (f) Elasticity

Figure 41: Variation of cross-sectional stresses (σ_{11}, σ_{12} and σ_{13}) for 2-flexure: VAM vs. elasticity for $r/l = 0.1$ and $\Lambda = 30°$

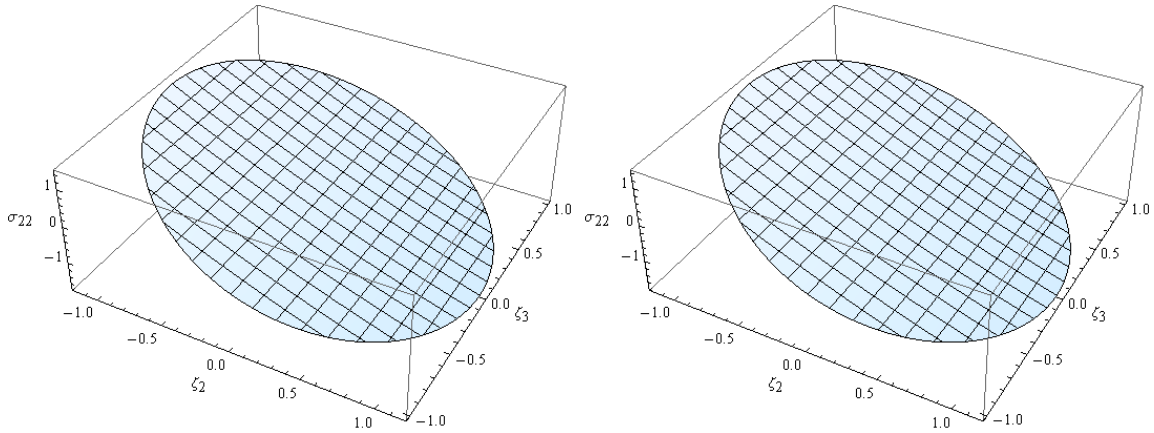

(a) VAM (b) Elasticity

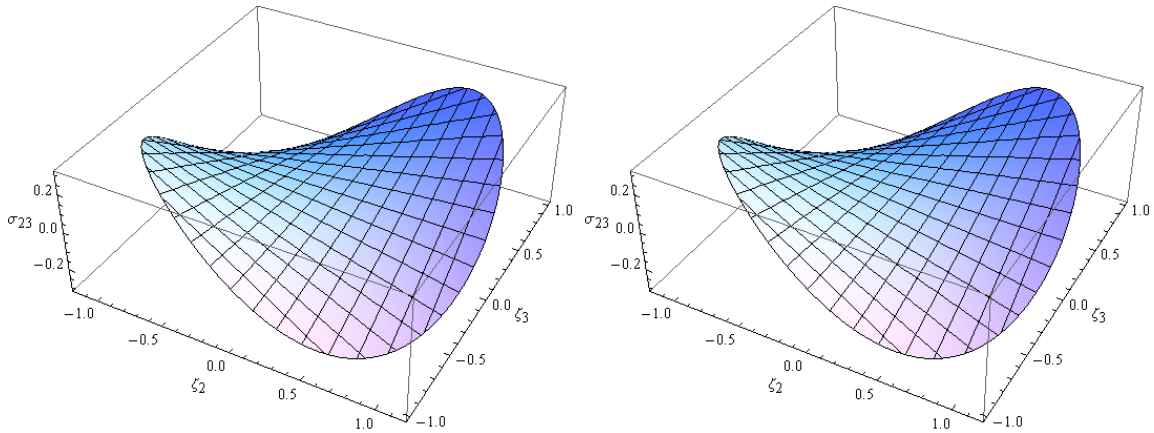

(c) VAM (d) Elasticity

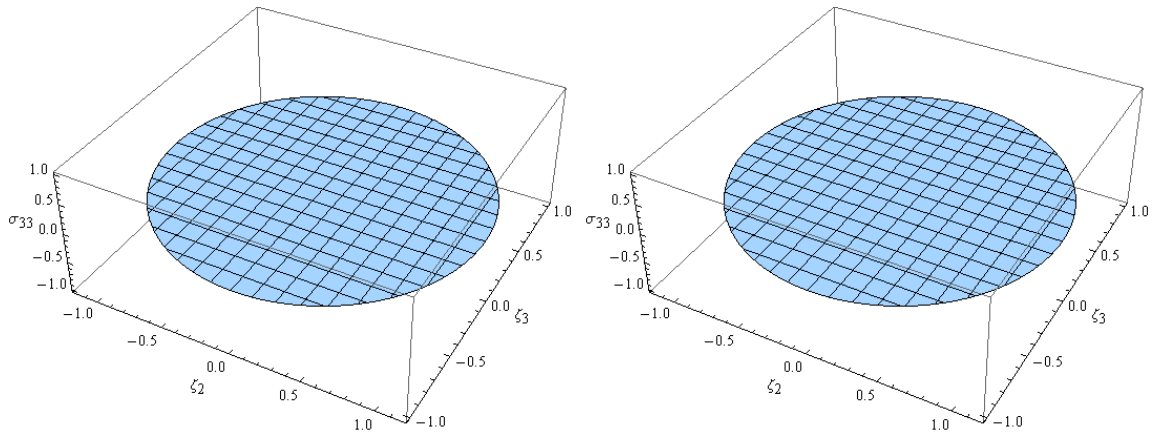

(e) VAM (f) Elasticity

Figure 42: Variation of cross-sectional stresses (σ_{22}, σ_{23} and σ_{33}) for 2-flexure: VAM vs. elasticity for $r/l = 0.1$ and $\Lambda = 30°$

6.6 Conclusions From the Analytical Developments

An oblique cross-sectional analysis based beam theory was developed for the in-plane deformation of an isotropic strip and the full 3D deformation of an isotropic solid cylinder. The theory was developed using the VAM, viz., minimization of the total potential energy using an asymptotic method. Results from these problems were conclusively demonstrated to coincide with those of 3D elasticity. These problems have been used to develop the formulation for the general case (including anisotropic material and initial twist and/or curvature), which are being implemented in VABS. Since a VAM based theory is devoid of any *ad hoc* assumptions regarding the deformation, extending it to the general case can be accomplished without any significant alterations of the theories developed above.

The analytical solutions for the two problems presented in this paper provide valuable tools for the development of the general theory to test the formulation at each stage. For this reason and because the problems have been validated with elasticity theory, the departure points of the differences when carrying out an oblique cross-sectional analysis (vis-à-vis the existing orthogonal cross-sectional analysis currently in VABS) can be clearly identified. The following aspects of the general cross-sectional analysis associated with the GT model have been modified/added to account for obliqueness:

- Obtaining the direction cosine matrix from the user-defined obliqueness parameters (see Eq. (114))
- The measures of the 3D strain tensor
- The magnitude of the metric tensor in the undeformed state
- The constraints associated with warping
- The kernel of the matrix used to solve for the nodal values of the warping (VABS

is a finite element program)

- Transformation of the 1D generalized strain measures before and after the GT transformation (if the beam is initially twisted and/or curved, the measure numbers of the curvature vector have to be expressed in the b frame for use in the existing GT transformation. Since it is natural for the user to specify the measure numbers in the a frame, this conversion process is facilitated).

- The solver for the Y matrix (the part of the stiffness matrix that couples the classical to the transverse shear strain measures) is now least-squares based.

These prove to be of immense aid in developing the equations for the general case for anisotropic beams with initial twist and/or curvature. The VAM procedure remains the same, except that the warping is now numerically evaluated using a finite-element approach.

6.7 Theory for the General Case

This section describes the theory pertaining to obtaining the sectional mass and stiffness matrices and finally recovering the 3D quantities. As usual [132], the 3D problem is dimensionally reduced to 1D using the VAM without *ad hoc* assumptions. The schematic of deformation is depicted in Fig. 43. Frames a and N are used to describe the undeformed and deformed oblique sections respectively with an intermediate frame A. For the corresponding orthogonal section, the frames are b and B with an intermediate frame T. For further information on various frames of reference used and the generalized strains associated with them, the reader is encouraged to consult Sec. 6.3. While x_1 is the usual axial curvilinear coordinate, the section is described using y_α. The obliqueness of the section (depicted green in Fig. 43) is quantified by relating its unit vectors with the unit vectors of the corresponding orthogonal section (black outline in Fig. 43) using the obliqueness parameters β_{1i}.

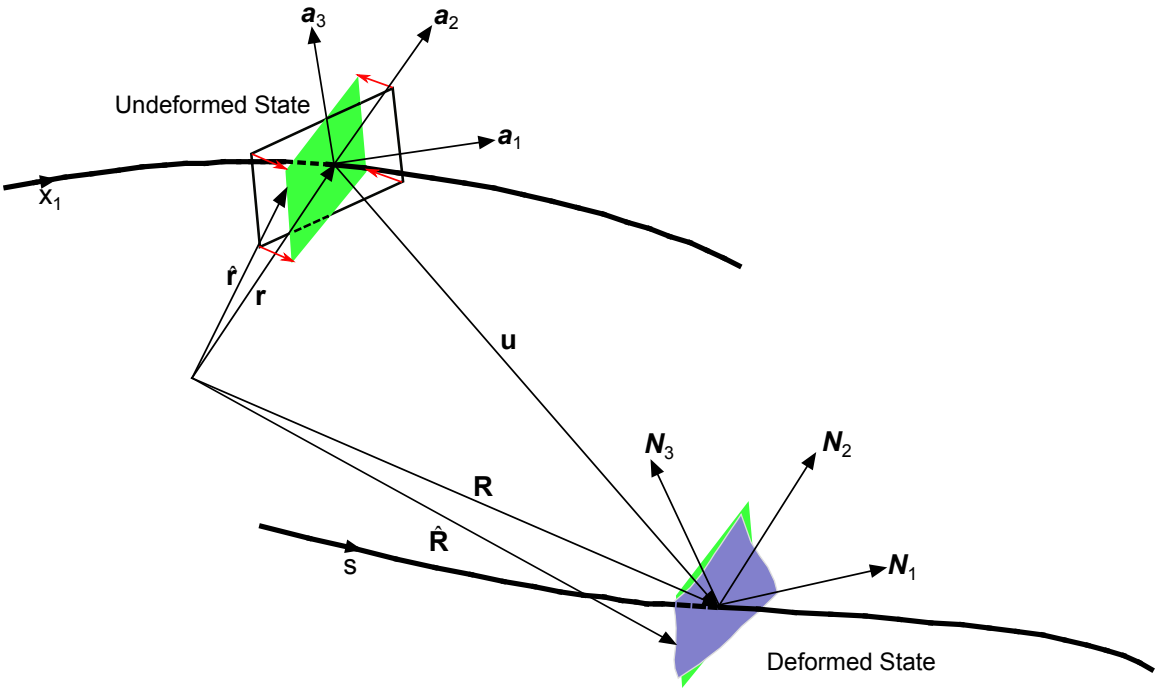

Figure 43: Schematic of beam deformation using an oblique cross section

Using geometrically exact expressions for the displacement of a generic point in the undeformed and deformed sections, and the assumptions of smallness of local rotations, the expression for the strain tensor is obtained to be

$$\begin{aligned} \Gamma &= \Gamma_{a\beta} w + \Gamma_{\epsilon} \bar{\epsilon} + \Gamma_R w + \Gamma_{\ell} w' \\ w &= \lfloor w_1 \quad w_2 \quad w_3 \rfloor^T \\ \bar{\epsilon} &= \lfloor \overline{\gamma}_{11} \quad \overline{\rho}_1 \quad \overline{\rho}_2 \quad \overline{\rho}_3 \rfloor^T \end{aligned} \tag{155}$$

where w represents the unknown warping functions, $\overline{\gamma}_{11}$ and $\overline{\rho}_i$'s are the geometrically exact strain measures for stretch (along the reference line instead of perpendicular to the section because the latter introduces non-independent shear strains) and sectional curvatures of the oblique section. The matrices in Eq. (155) are now explicitly defined

as

$$\Gamma_{a\beta} = \begin{bmatrix} \Gamma_\beta & 0 & 0 \\ \frac{\partial}{\partial y_2} & \Gamma_\beta & 0 \\ \frac{\partial}{\partial y_3} & 0 & \Gamma_\beta \\ 0 & \frac{\partial}{\partial y_2} & 0 \\ 0 & \frac{\partial}{\partial y_3} & \frac{\partial}{\partial y_2} \\ 0 & 0 & \frac{\partial}{\partial y_3} \end{bmatrix}$$

$$\Gamma_\epsilon = \frac{1}{\sqrt{g}} \begin{bmatrix} \beta_{11} & 0 & y_3 & -y_2 \\ \beta_{12} & -y_3 & 0 & 0 \\ \beta_{13} & y_2 & 0 & 0 \\ 0 & 0 & 0 & 0 \\ 0 & 0 & 0 & 0 \\ 0 & 0 & 0 & 0 \end{bmatrix} \tag{156}$$

$$\Gamma_R = \frac{1}{\sqrt{g}} \begin{bmatrix} \tilde{k} + I_3 k_1 \left(y_3 \frac{\partial}{\partial y_2} - y_2 \frac{\partial}{\partial y_3} \right) \\ 0_{3\times 3} \end{bmatrix}$$

$$\Gamma_\ell = \frac{1}{\sqrt{g}} \begin{bmatrix} I_3 \\ 0_{3\times 3} \end{bmatrix}$$

where $\Gamma_\beta = -\frac{1}{\sqrt{g}} \left(\beta_{12} \frac{\partial}{\partial y_2} + \beta_{13} \frac{\partial}{\partial y_3} \right)$, $\sqrt{g} = \beta_{11} - y_2 k_3 + y_3 k_2$ and k_i are the measure numbers of the initial curvature vector. Assuming the material operates in a linear elastic regime, the 3D stresses are simply $\sigma = D\Gamma$. The redundancies in the displacement field are removed by introducing constraints on the warping:

$$\begin{aligned} \langle w_i \rangle &= 0 \\ \langle \beta_{11} (w_{2,3} - w_{3,2}) + \beta_{13} w_{1,2} - \beta_{12} w_{1,3} \rangle &= 0 \end{aligned} \tag{157}$$

where $\langle \bullet \rangle$ represents integration over the cross section. These constraints specify that the 1D displacements (see Ref. [46]) are the average of the displacements of all the material points that make up the section and that the average local rotation in

a direction tangent to the deformed reference axis is zero. One can now set up a variational statement of the problem by the usual definition of the strain energy

$$\mathcal{U} = \frac{1}{2}\langle\sqrt{g}\sigma^T\Gamma\rangle \tag{158}$$

The warping is discretized using finite element shape functions $S(y_2, y_3)$ as

$$w(x_1, y_2, y_3) = S(y_2, y_3)V(x_1) \tag{159}$$

The unknown nodal values of warping $V(x_1)$ are now recursively solved for in an asymptotic manner using standard procedures of the calculus of variations. For the asymptotic method, the small parameters used are a/ℓ and ak_i, where ℓ is the maximum wavelength of deformation. The solutions for the zeroth, first and second order warping are obtained as

$$V = \underbrace{V_0\overline{\epsilon}}_{0} + \underbrace{V_{1R}\overline{\epsilon} + V_{1S}\overline{\epsilon}'}_{1} + \underbrace{V_{20}\overline{\epsilon} + V_{21}\overline{\epsilon}' + V_{22}\overline{\epsilon}''}_{2} \tag{160}$$

The zeroth- and first-order expressions for warping, when substituted back in the strain energy, yield the classical and second-order asymptotically correct strain energies, respectively, viz.,

$$\begin{aligned} 2U_0 =& \overline{\epsilon}^T A_{cl}\overline{\epsilon} \\ 2U_2 =& \overline{\epsilon}^T A\overline{\epsilon} + 2\overline{\epsilon}^T B\overline{\epsilon}' + \overline{\epsilon}'^T C\overline{\epsilon}' + 2\overline{\epsilon}^T D\overline{\epsilon}'' \end{aligned} \tag{161}$$

The latter is converted to a Generalized Timoshenko form or a Generalized Vlasov form by either using the equilibrium equations or neglecting all the strain derivatives except the derivative of the torsion variable of the corresponding orthogonal section. The final strain energies yield the stiffness matrices for these two theories in terms of the generalized strains of B (the deformed corresponding orthogonal section) as

$$\begin{aligned} 2\mathcal{U}_{GT} &= \epsilon^T S_{GT}\epsilon; \quad \epsilon = \lfloor\gamma_{11} \quad 2\gamma_{1\alpha} \quad \kappa_i\rfloor^T \\ 2\mathcal{U}_{GV} &= \epsilon_V^T \hat{S}\ \epsilon_V; \quad \epsilon_V = \lfloor\gamma_{11} \quad \kappa_i \quad \kappa_1'\rfloor^T \end{aligned} \tag{162}$$

While both these stiffnesses correct for initial twist and/or curvature, the GT theory incorporates transverse shear while GV captures the end effect due to restrained warping. The latter is important for thin-walled beams with open sections, such as rotorcraft flex-beams. As mentioned in Sec. 6.6, the solution for the Y matrix, i.e., the matrix that couples classical and transverse shear strain measures, is now based on a least-squares solver. For further details, see Appendix B.

The kinetic energy can be obtained with sufficient accuracy in a much simpler manner, using the assumptions that corresponding orthogonal section remains plane and rigid during deformation

$$2K = \begin{Bmatrix} V \\ \Omega \end{Bmatrix}^T M \begin{Bmatrix} V \\ \Omega \end{Bmatrix} \tag{163}$$

where V and Ω are again the velocity and angular velocity of the corresponding orthogonal section. The 1D variables chosen so that the VABS outputs can be directly input into GEBT [126]. In calculating the mass matrix, the following transformation is needed to obtain the coordinates of the corresponding orthogonal section from the given coordinates of the oblique section

$$\lfloor x_2 \quad x_3 \rfloor = \lfloor y_2 \quad y_3 \rfloor \begin{bmatrix} 1 - \frac{\beta_{12}^2}{1+\beta_{11}} & -\frac{\beta_{12}\beta_{13}}{1+\beta_{11}} \\ -\frac{\beta_{12}\beta_{13}}{1+\beta_{11}} & 1 - \frac{\beta_{13}^2}{1+\beta_{11}} \end{bmatrix} \tag{164}$$

The mass and stiffness matrices are now input into the 1D solver GEBT, and upon obtaining the solution of the 1D variables, VABS can be used to recover the 3D stress, strain and displacement variables. The following are the user inputs for VABS recovery:

1. the 1D displacements (a frame)
2. the rotation matrix (C^{Na})
3. sectional force and moment resultants and the distributed and inertial loads (B frame)

GEBT outputs the 1D displacements in the b frame, the force and moment resultants in the B frame and quantities that be used to calculate C^{Bb}. To obtain the required VABS outputs, the measure numbers of the 1D displacements in a frame can be simply obtained using C^{β}, which defines the rotation from a to b (C^{ba}) and is known in terms of the obliqueness parameters, β_{1i}'s. It is defined in Eq. 114.

GEBT also outputs quantities which can be used to calculate C^{Bb}. From this C^{Na} can be obtained using the formula given in Ref. [91]. Given the sectional forces and moments and the distributed and inertial loads, VABS recovery calculates the strain measures (and their derivatives) of B, converts them into the strain measures of T [46], then finally gets the strain measures of A using the obliqueness parameters. These can be then used to obtain the 3D stress and strain using Eqs. (155) and (160). The displacement is then recovered using

$$\begin{aligned} U_i =& u_i(x_1) + y_\alpha \left[C^{Aa}_{\alpha i}(x_1) - \delta_{\alpha i}\right] + C^{Aa}_{ji} w_j \\ C^{Aa} =& C^{AN} C^{Na} \\ C^{AN} =& C^{\beta^T} C^{TB} C^{\beta} \end{aligned} \tag{165}$$

From Ref. [46], C^{TB} is

$$C^{TB} = \begin{bmatrix} 1 & 2\gamma_{12} & 2\gamma_{13} \\ -2\gamma_{12} & 1 & 0 \\ -2\gamma_{13} & 0 & 1 \end{bmatrix} \tag{166}$$

Thus concludes the determination of the sectional properties and 3D quantities by VABS for an oblique cross-sectional analysis. In the subsequent sections the results from a VABS obliqueness model and GEBT will be verified against solutions from experiments, 3D FEM and other beam analyses in a quest to demonstrate its functionality and accuracy.

6.8 VABS Verification and Validation

Static and dynamic results of various kinds of cross sections are available in literature [107, 104, 26, 25, 55, 56, 6, 60, 62, 61, 80, 134, 63, 76] for ready comparison of the outputs from an oblique cross-sectional analysis. Because these results are from completely different approaches such as experiments, FEM and unrelated beam procedures, they serve as adequate and unbiased validation cases. One important point must be made at this juncture: the blade is obviously the same, so it is not "aware" that the analysis is being carried out with an oblique section, so the global behavior of the structure remains the same. Again, it is iterated here that the obliqueness feature in VABS ONLY offers the user a flexibility of modeling blades using a nonorthogonal cross section. So, analyzing a structure with an orthogonal section or oblique sections (at various oblique angles) should lead to the same results and, as shall be seen shortly, it does.

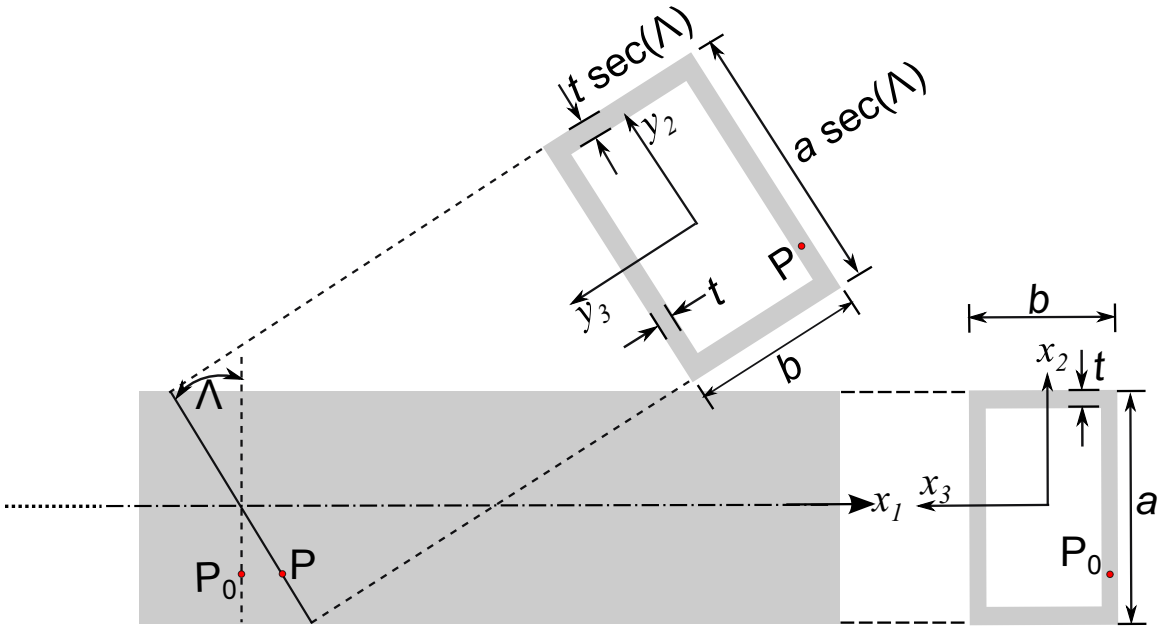

Figure 44: Generating the properties of an oblique section given the properties of an orthogonal section

Most of the works cited from the literature readily provide the properties of the

orthogonal section. Therefore, there is a need to generate the properties of a section not perpendicular to the reference line. For example, in the thin-walled box beam shown in Fig. 44, if the geometry and material of a point P_0 in the orthogonal section is known, the corresponding point on the oblique section, P, the coordinates of which can be determined using Eq. (164). The 6×6 material matrix at P can be determined from the 6×6 material matrix at P_0 using material transformation laws outlined in Ref. [54] bearing in mind the wall orientation, fiber angle and the obliqueness of the section (defined by Λ). In the examples to follow, we consider the oblique section as defined in Fig. 44, i.e., a rotation of Λ about x_3, which results in $\beta_{11} = \cos(\Lambda)$, $\beta_{12} = -\sin(\Lambda)$ and $\beta_{13} = 0$.

6.8.1 The CUS and CAS Sections

Fundamentally, there are only two types of composite cross sections: The Circumferentially Uniform Section (CUS) and the Circumferentially Asymetric Section (CAS). While the former exhibits extension-twist and bending-shear couplings, the latter exhibits extension-shear and bending-twist couplings. The other two types of coupling, viz., extension-bending and shear-twist are caused by picking a reference line which differs from the lines of tension centers and generalized shear centers respectively. Therefore, the ability to accurately predict the behavior of the CUS and CAS sections inherently implies that the methodology holds for any thin-walled composite cross section.

The properties of Fig. 45 are provided in Tables 18 and 19 with $\theta = -15°$. The properties of the oblique CUS section are provided for a representative obliquity angle of $\Lambda = 30°$. It can be seen that the oblique section possesses the characteristics of having truly anisotropic materials. Therefore, this validation should serve as a test for the ability of VABS to capture generally anisotropic behavior as well.

In what follows, the results are presented from runs of the obliqueness model of VABS, i.e., VABS(Λ) and GEBT and compared with the results obtained from other

Table 18: Section properties for the orthogonal CAS and CUS sections

Geometry	Material
$a = 0.953$ in.	$E_l = 20.59 \times 10^6$ psi
$b = 0.537$ in.	$E_t = 1.42 \times 10^6$ psi
$t = 0.03$ in.	$G_{lt} = 8.9 \times 10^5$ psi
	$G_{tn} = 6.96 \times 10^5$ psi
	$\nu_{lt} = 0.42$
	$\nu_{tn} = 0.5$
	$\rho = 1.352 \times 10^{-4}$ lb-in^{-4}-s^2

Table 19: Section properties for the oblique ($\Lambda = 30°$) CUS section. Listed below are the Material Properties (MP) corresponding to 6×6 material matrix D

MP (psi)	M_1	M_2	M_3	M_4
D_{11}	7.4192E6	1.2061E7	1.9229E7	1.2061E6
D_{12}	−4.9193E6	−5.3841E6	−4.3586E6	−5.3841E6
D_{13}	0	−2.8647E6	−2.8647E6	2.8647E6
D_{14}	5.6392E5	4.0901E6	2.3502E6	4.0901E6
D_{15}	0	1.6054E6	0	−1.6054E6
D_{16}	1.1366E6	2.0214E6	1.2381E6	2.0214E6
D_{22}	5.2754E6	3.7290E6	1.9863E6	3.7290E6
D_{23}	0	1.6003E6	0	−1.6003E6
D_{24}	−4.9193E6	−2.0909E6	−5.6073E5	−2.0909E6
D_{25}	0	−9.5197E5	0	9.5197E5
D_{26}	−1.1726E5	−5.6948E5	−5.8627E4	−5.6948E5
D_{33}	7.93E5	1.6670E6	8.77E5	1.6670E6
D_{34}	0	−9.6074E5	0	9.6074E5
D_{35}	7.4192E6	−5.5311E5	−4.85E4	−5.5311E5
D_{36}	0	−4.8560E5	0	4.8560E5
D_{44}	7.4192E6	3.4297E6	2.1877E6	3.4297E6
D_{45}	0	6.0318E5	0	−6.0318E5
D_{46}	1.1366E6	1.3638E6	1.0350E6	1.3638E6
D_{55}	7.93E5	1.0283E6	7.09E5	1.0283E6
D_{56}	0	2.8036E5	0	−2.8036E5
D_{66}	1.9660E6	2.1877E6	1.9660E6	2.1877E6

methods. Table 20 presents the stiffnesses for the CUS section with respect to the strain measures of the orthogonal section. Again it is emphasized here that because the beam remains the same, the strain energy per unit length must be the same, and if the same strain measures are used to write the potential energy, the stiffnesses must be the same. The reason for a slight discrepancy for the shear related terms with larger obliqueness angles has been discussed in detail in Ref. [91]. Note that NABSA is a code based on Ref. [37] (developed by Prof. Bauchau).

In what follows, all rotations of the blade refer to rotations about x_3 or y_3. Flap and lag deformations are those corresponding to the deformations in the x_3 and x_2 directions respectively. We will now discuss the dynamic results of the CUS section. Table 21 lists the first five natural frequencies from experiments and other analyses, even with an earlier version of VABS. From Fig. 46, lag frequencies are not significantly affected by the rotor angular speed for small hub radii or in the absence of hinge offsets; centrifugal lead-lag stiffening is nearly cancelled out by the "negative spring" term in lead-lag motion. Considering Fig. 47, two conclusions can be gleaned: The stretch is less than 0.01 even for an angular speed of 10000 RPM (which may entail only academic interest), validating the small strain analysis. Second, as Ω increases, the mode shape begins to resemble a straight line with an area of large curvature at the root, caused by the root boundary conditions of zero displacement and rotation. The first two natural frequencies are plotted as a function of the slenderness ratio (defined here as the ratio of length to height) and compared with the corresponding FEM results. Figs. 49, 50, 51 and 52 present the mode shapes corresponding to the CUS section for a slenderness ratio equal to 60. The mode shapes are normalized such that the maximum displacement or rotation variable corresponding to that particular mode is unity at the tip. It is interesting to note the extension-twist and bending shear couplings and the equal contributions of flap and lag displacements to the eighth mode.

Table 20: Stiffnesses for the CUS section

Stiffness	VABS($\Lambda = 0°$)	VABS($\Lambda = 15°$)	VABS($\Lambda = 30°$)	NABSA	Ref. [56]
S_{11} (lb.)	1.4441E6	1.4441E6	1.4441E6	1.4380E6	1.4310E6
S_{14} (lb-in.)	1.0686E5	1.0686E5	1.0686E5	1.0750E5	1.0640E5
S_{22} (lb.)	9.0354E4	8.9984E4	8.8662E4	9.0180E4	9.0890E4
S_{25} (lb-in.)	−5.2098E4	−5.1885E4	−5.1123E4	−5.2040E4	−5.3910E4
S_{33} (lb.)	3.9741E4	3.9642E4	3.8477E4	3.9320E4	3.8220E4
S_{36} (lb-in.)	−5.5787E4	−5.5396E4	−5.4014E4	−5.6370E4	−5.6050E4
S_{44} (lb-in.^{2})	1.7085E4	1.7085E4	1.7086E4	1.6780E4	1.6620E4
S_{55} (lb-in.^{2})	6.8490E4	6.8367E4	6.7929E4	6.6220E4	6.8370E4
S_{66} (lb-in.^{2})	1.7331E5	1.7276E5	1.7082E5	1.7260E5	1.7280E5

Table 21: Natural frequencies (Hz) for the CUS section. L=33.25 in. and rotor rotational speed about x_3 (or y_3) Ω=1002 RPM

Mode	Ref. [25]	Ref. [107]	Ref. [104]	Ref. [55]	VABS(2005)	VAPAS[1]	VABS ($\Lambda = 0°$) +GEBT	VABS ($\Lambda = 15°$) +GEBT	VABS ($\Lambda = 30°$) +GEBT
Flap 1	33.60	34.63	36.49	33.99	34.10	33.20	34.14	34.14	34.14
Lag 1	46.60	47.31	53.73	45.68	45.90	45.10	45.95	45.95	45.95
Flap 2	184.00	188.00	202.20	184.80	181.60	180.60	183.82	183.87	183.81
Lag 2	–	287.20	328.20	285.30	277.90	278.80	280.54	280.63	280.57
Torsion 1	–	513.20	493.70	495.50	503.20	491.70	499.62	499.99	499.59

[1]Variational Asymptotic Plate And Shell; 2D analysis carried out using DYMORE [12]

Moving on to static results, deflections, geometrically exact slopes and sectional rotations are presented for various loading cases in Figs. 53, 54, 55 and 56. Displacement results are in inches and rotations in radians; all values normalized as indicated in each figure.

Dynamic results of the CAS section are now alluded to. Table 22 presents the natural frequency comparison similar to what Table 21 did for the CUS section. If the fiber layup angle is changed from 15°, the dynamic results corresponding to the first three modes are shown in Fig. 57. Only in the case of the second flap mode of the 45° case is there a slight discrepancy between the experimental and theoretical results, which can be possibly be attributed to a nonlinearity in the shearing deformation. Due the bending-twist coupling, their effective stiffnesses or rigidities, defined as the inverse of the corresponding flexibility coefficients are presented in Fig. 58. This concludes a validation of the obliqueness model for VABS for the CUS and CAS sections.

6.8.2 Anisotropic I-beams

While the CUS and CAS sections serve as sufficient validation for thin-walled closed section beams, open section beams, such as the ones employed in flex-beams of rotorcraft need a separate verification because end effects pertaining to restrained warping become significant in the central beam solutions. For this purpose, consider an I-beam, whose orthogonal section is shown in Fig. 59. For this kind of cross section, the Generalized Vlasov model needs to be used in the cross-sectional analysis. Two cases are considered: one isotropic and one orthotropic as outlined in Table 23. The value of α for the orthotropic case is taken to be 15°. The properties of the oblique section can be generated in a manner similar to the procedure outlined the previous section. Two important parameters that govern the behavior of these kind of cross sections are the torsional and warping rigidity which are the coefficients of κ_1^2 and

$\kappa_1'^2$ in the sectional strain energy. These results are listed in Table 24 corresponding to the strain measures of the corresponding orthogonal section in lb-in.^{2} and lb-in.^{4} respectively. Because the strain energy per unit length is not dependent on the choice of a reference cross-sectional plane, if the same 1D strain measures are used, the results are expected to be identical with sufficient accuracy, which can be seen in the results. Agreement with an earlier version of VABS [134], wherein the solutions were shown to produce results equivalent to 3D FEM imply that the obliqueness model in VABS models the GV theory correctly.

6.8.3 Initial Twist

The next feature to be validated is the effect of initial twist and curvature on the cross-sectional analysis. For this consider a pre-twisted strip as shown in Fig. 60. When using an orthogonal section to model this structure, it needs to be analyzed with a non-zero initial twist. On the other hand, modeling this with an oblique section requires a non-zero initial twist and curvature. Mathematically, this is easier to comprehend because initial twist and curvature are simply measure numbers of the same initial curvature vector. If x_3 is the cross-sectional coordinate corresponding to the thickness variable of the strip, the initial curvature vector has the following measure numbers in the orthogonal and oblique sections respectively: $\lfloor k_1 \quad 0 \quad 0 \rfloor$ and $\lfloor k_1 \cos(\Lambda) \quad -k_1 \sin(\Lambda) \quad 0 \rfloor$. The strip has cross section dimensions 10×1 and is made up of isotropic material of $E = 2.6 \times 10^7$ and $\nu = 0.3$. All the inputs and outputs are assumed to be in a consistent system of units. The stiffness results for the classical corrected stiffnesses are presented in Fig. 61. The extensional, extension-torsion and torsional stiffnesses (again for the oblique section, they are converted into those of the corresponding orthogonal section) are affected by k_1 and the exact solutions for these stiffnesses are provided by Ref. [63]. Again, an excellent agreement is observed.

6.8.4 Stress Recovery

The final aspect of the VABS oblique cross-sectional model is to demonstrate accurate recovery of 3D stress, strain and displacement. In this section, stress recovery is alluded to and it is presumed that the reader is familiar with standard elasticity procedures of extracting 3D strain and displacement (given the appropriate essential boundary conditions) from the stress and hence can concur that agreement in stress implies an agreement in the other nine quantities as well. Consider an isotropic prismatic rod as shown in Fig. 38. For the six different loading cases shown in Fig. 40, Ref. [76] provides the exact elasticity solutions. These solutions, after appropriate vectorial and tensorial transformations of the stresses and coordinates, form the basis of comparison of the VABS results over an oblique plane as shown in Fig. 38. In what follows, the stresses are normalized by F_i/r^2 or M_i/r^3 and plotted with respect to the cross-sectional coordinates: ζ $(y_2 \cos(\Lambda)/r)$ or η (y_3/r), and along $y_3 = 0$ and $y_2 = 0$ respectively. The flexure loading cases necessitates stress plotting along $y_3 = y_2 \cos(\Lambda)$; in those cases ζ^* is $(y_3 + y_2 \cos(\Lambda))/\left(\sqrt{2}r\right)$. Only the non-zero variations and a bare-minimum number of plots sufficient to establish all the stress variations over the cross section are sufficiently captured are plotted. The obliqueness angle, Λ, is chosen to be 30°, while r/l is 0.15. From the results displayed in Figs. 62, 63, 64, 65, 66, 67 and 68, an excellent agreement of the VABS obliqueness model with respect to exact elasticity solutions is observed. The slight divergence from elasticity solutions for the loading case of F_2 can be attributed to the fact that a large obliqueness angle might lead to errors when shearing deformations are involved. This is because the small parameter associated with the inverse of the slenderness ratio is no longer small at large obliqueness angles. This concludes a successful and rigorous validation of the oblique cross-sectional analysis using VABS.

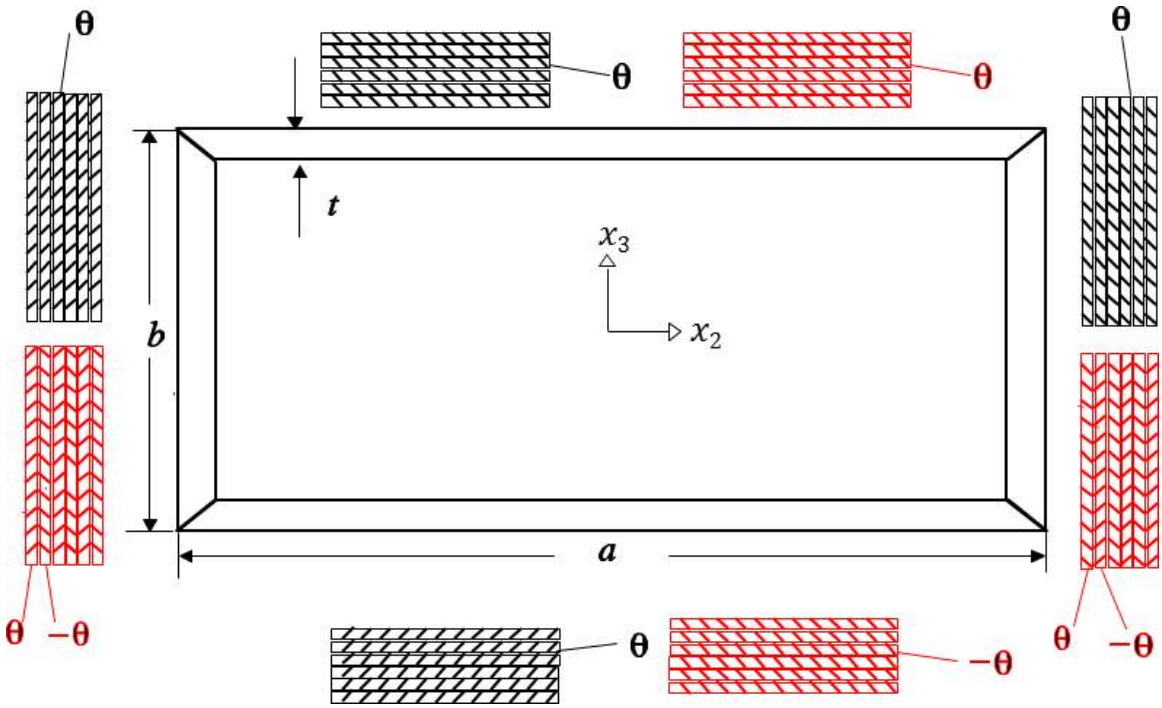

(a) Orthogonal. CAS orientations are in red.

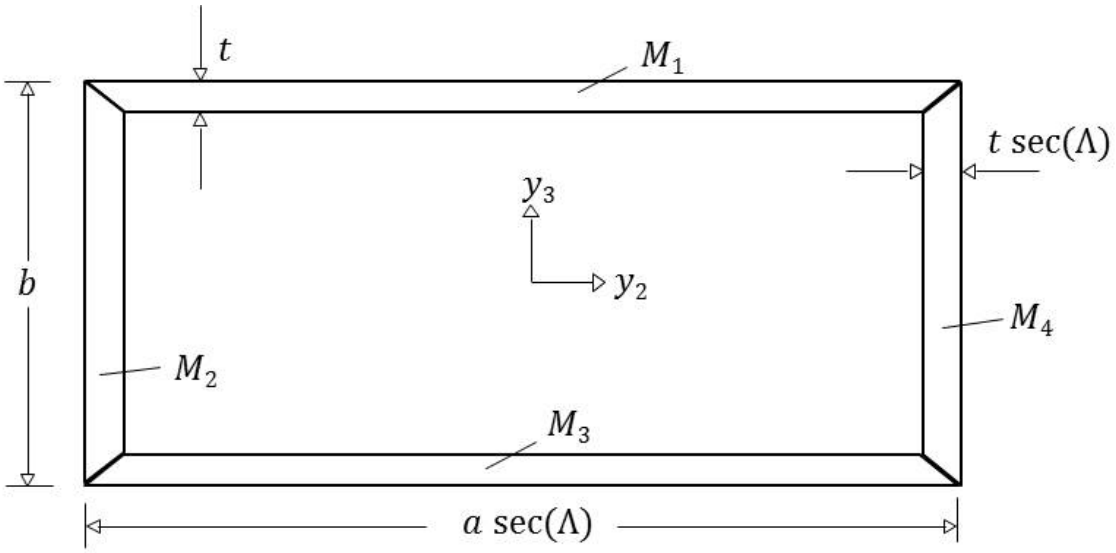

(b) Oblique

Figure 45: Orthogonal CUS and CAS sections and the oblique CUS section. Fiber orientations are defined with respect to the local normal

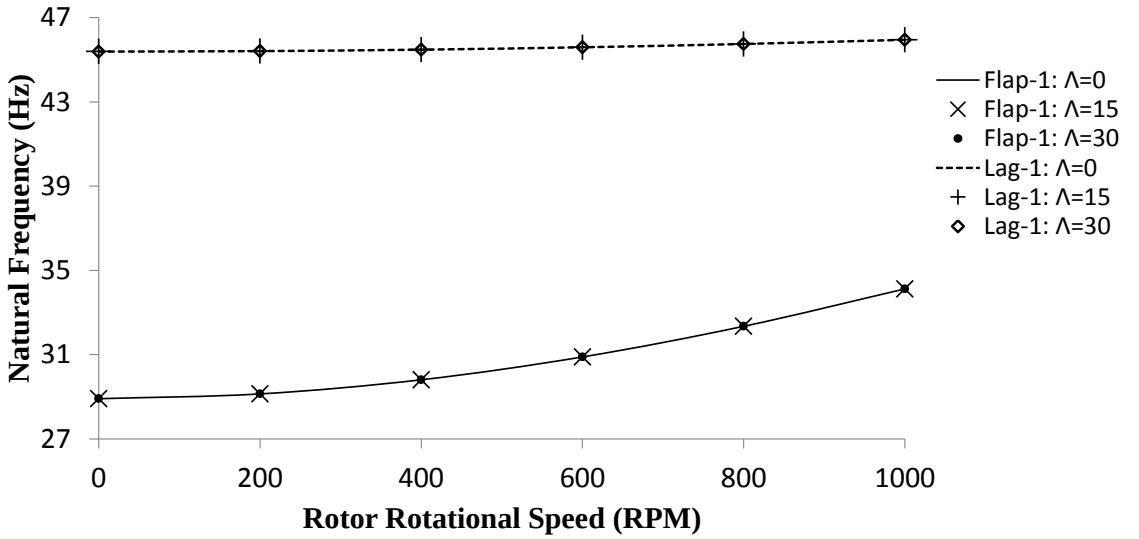

Figure 46: Variation of the first flap and lag frequencies of a CUS section (Hz) with rotor rotational speed

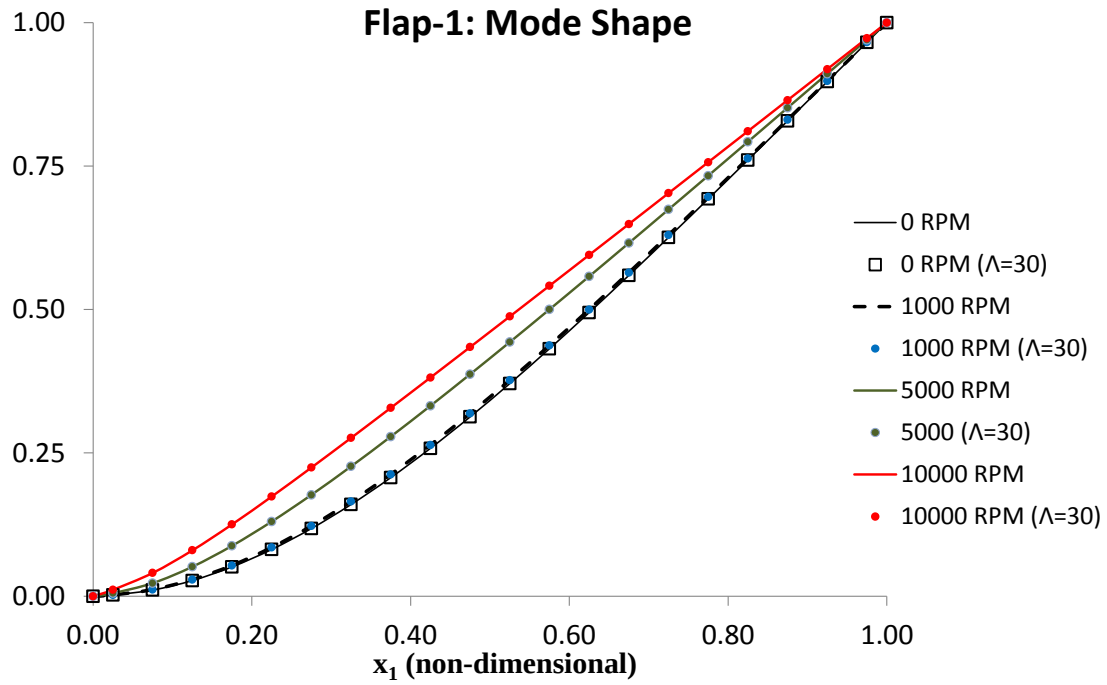

Figure 47: Variation of the first normalized flap mode shape of a CUS section (Hz) with rotor rotational speed

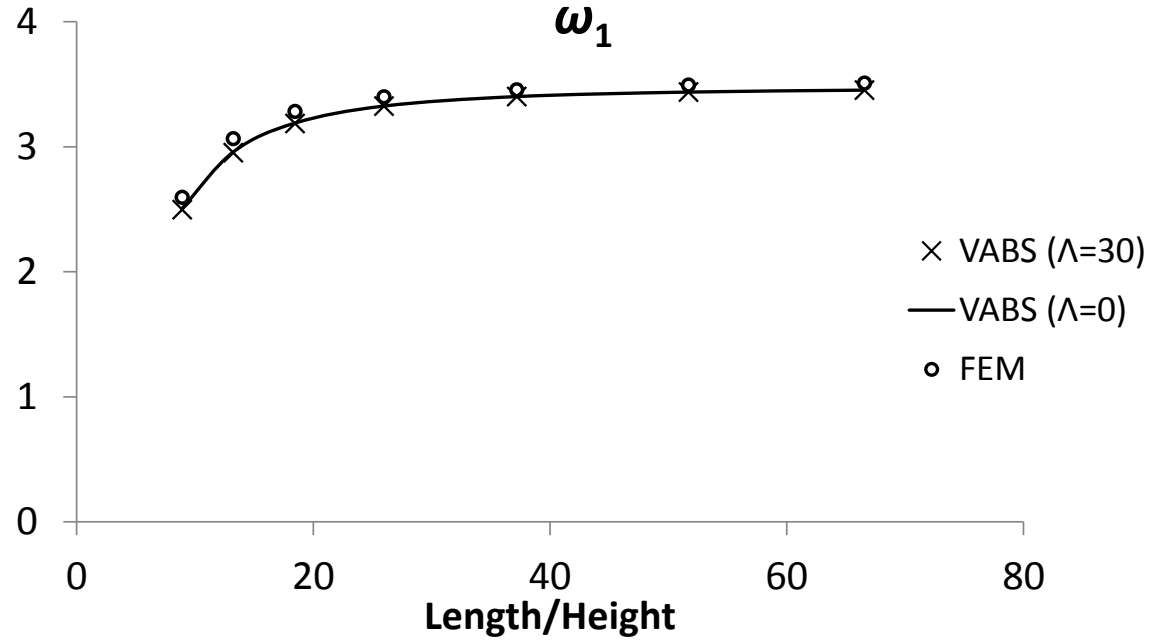

(a)

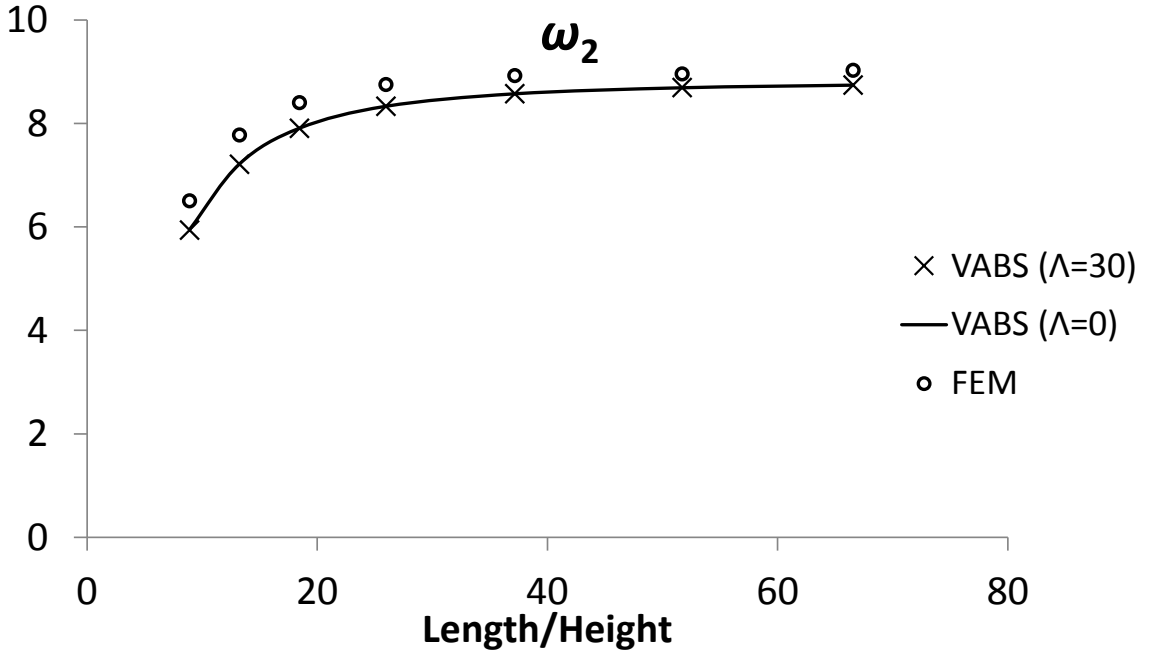

(b)

Figure 48: Normalized $(\times(L/h)^4/E_l)$ 1st two natural frequencies vs. slenderness ratio for the CUS section

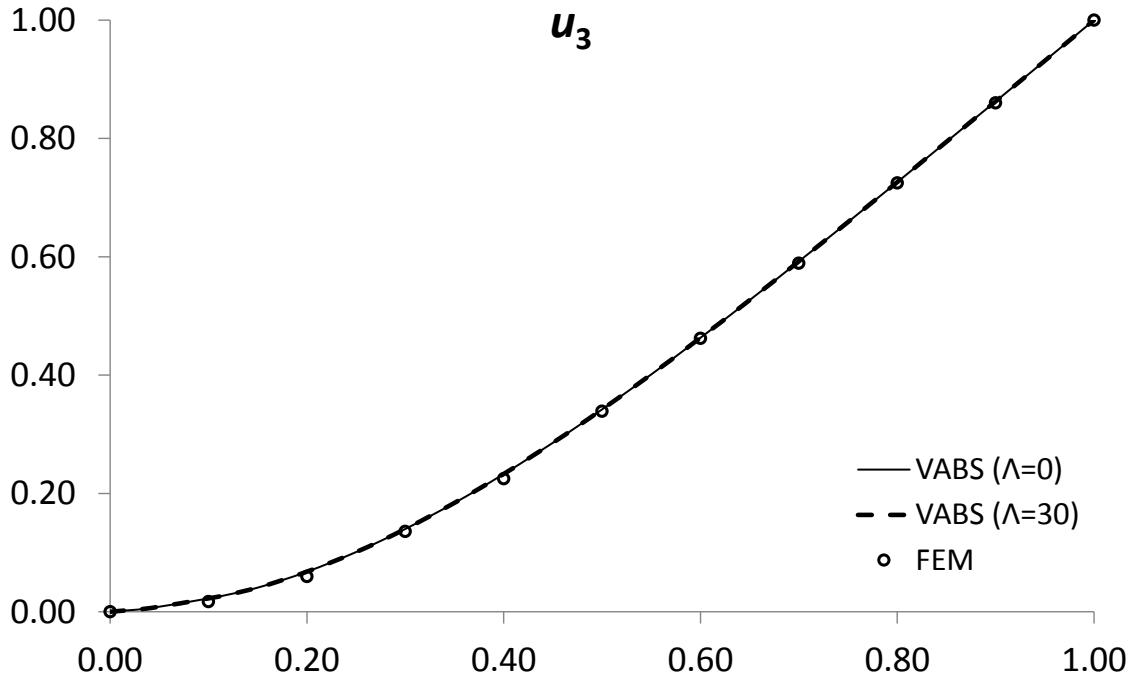

(a) u_3

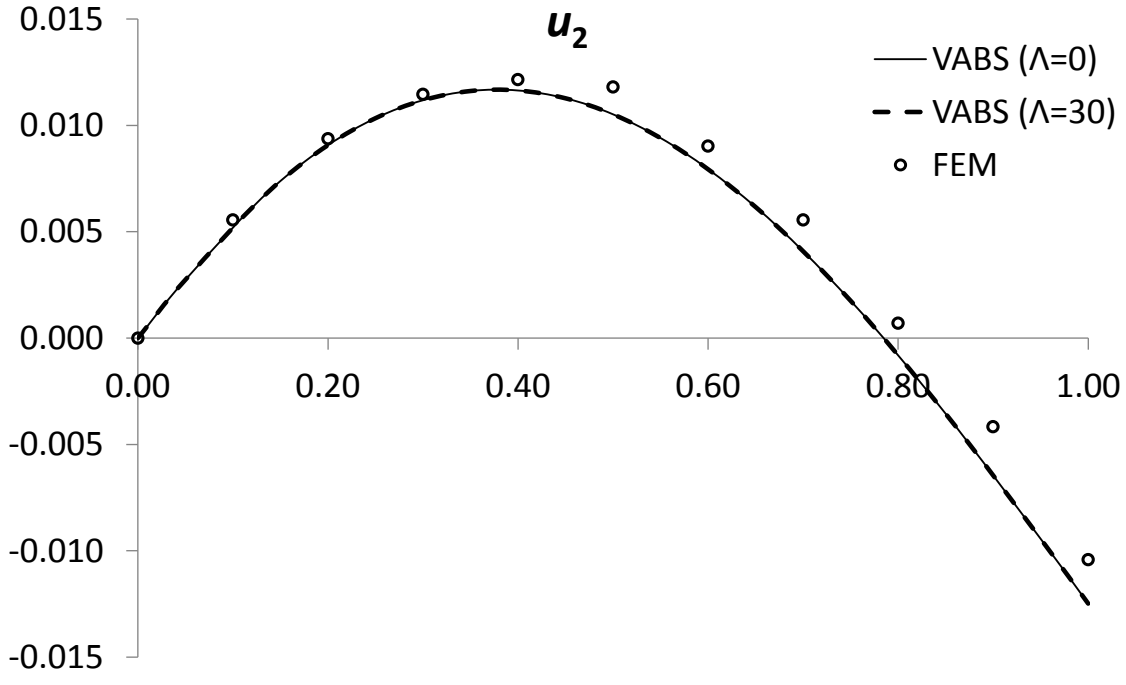

(b) u_2

Figure 49: Normalized first mode shape for the CUS section

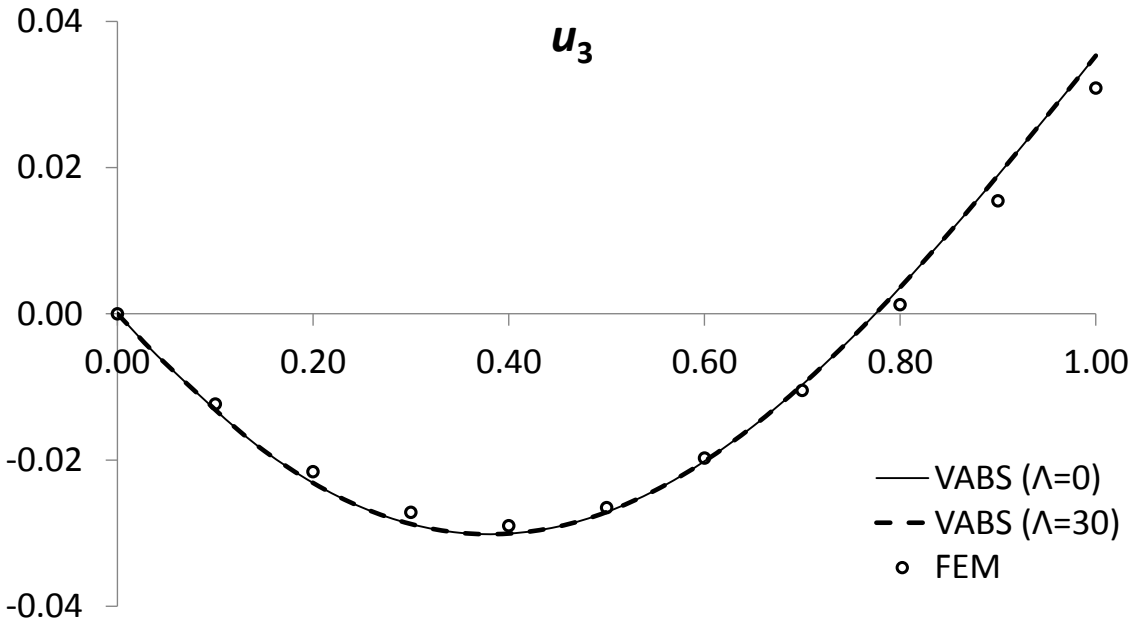

(a) u_3

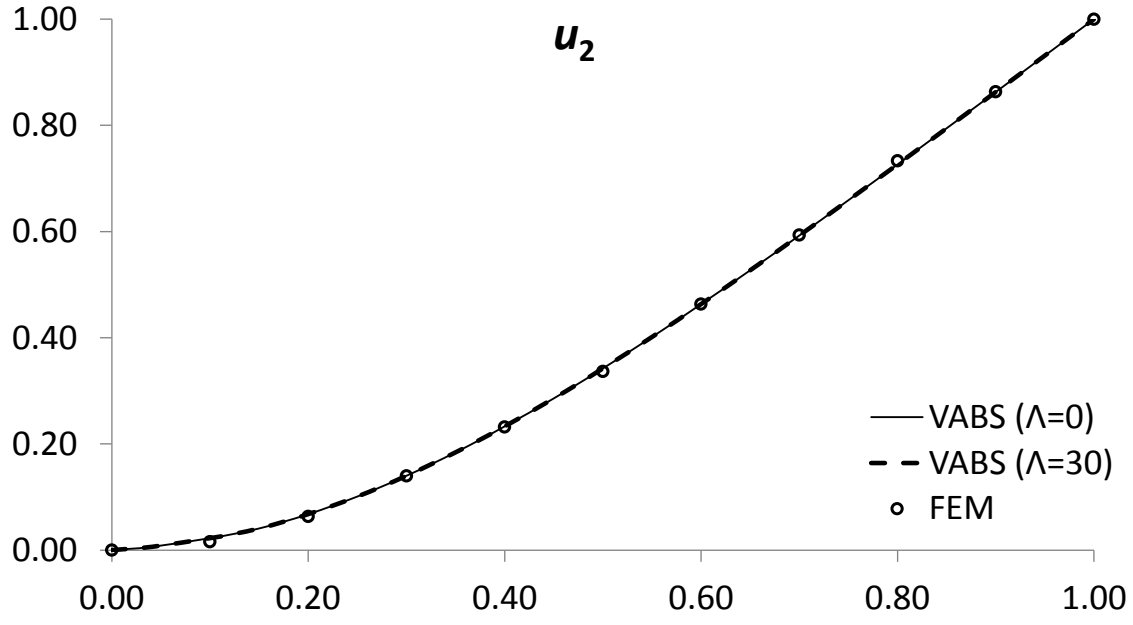

(b) u_2

Figure 50: Normalized second mode shape for the CUS section

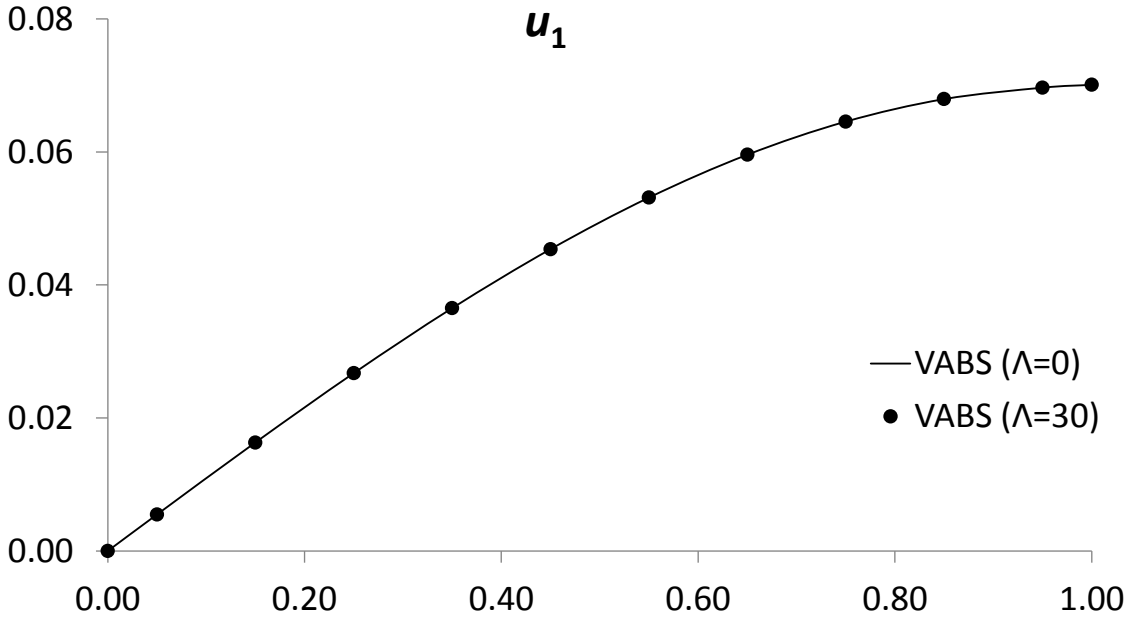

(a) u_1

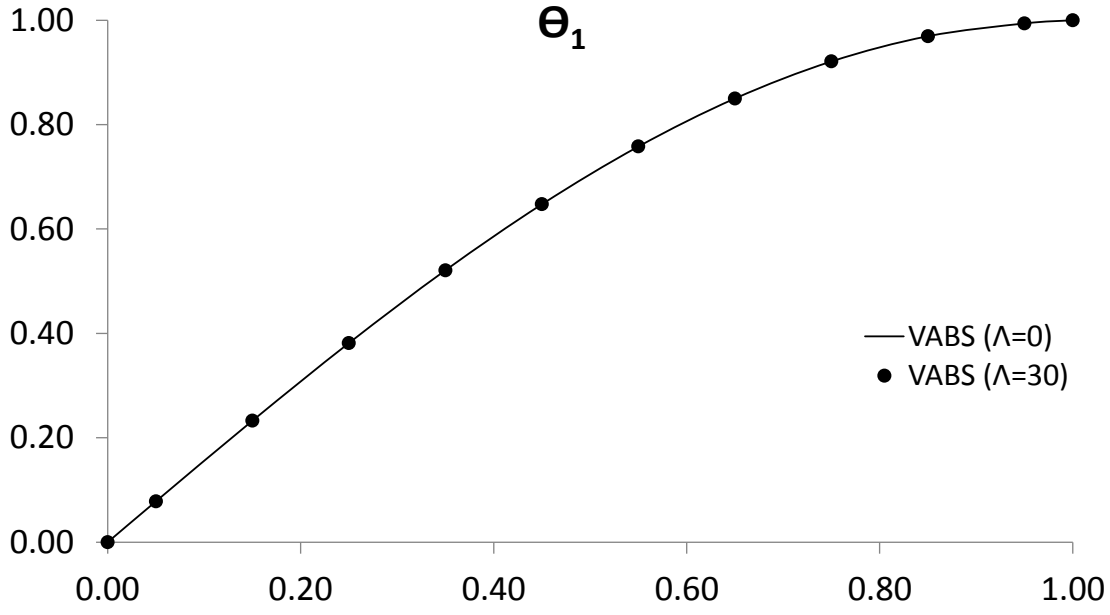

(b) θ_1

Figure 51: Normalized fifth mode shape for the CUS section

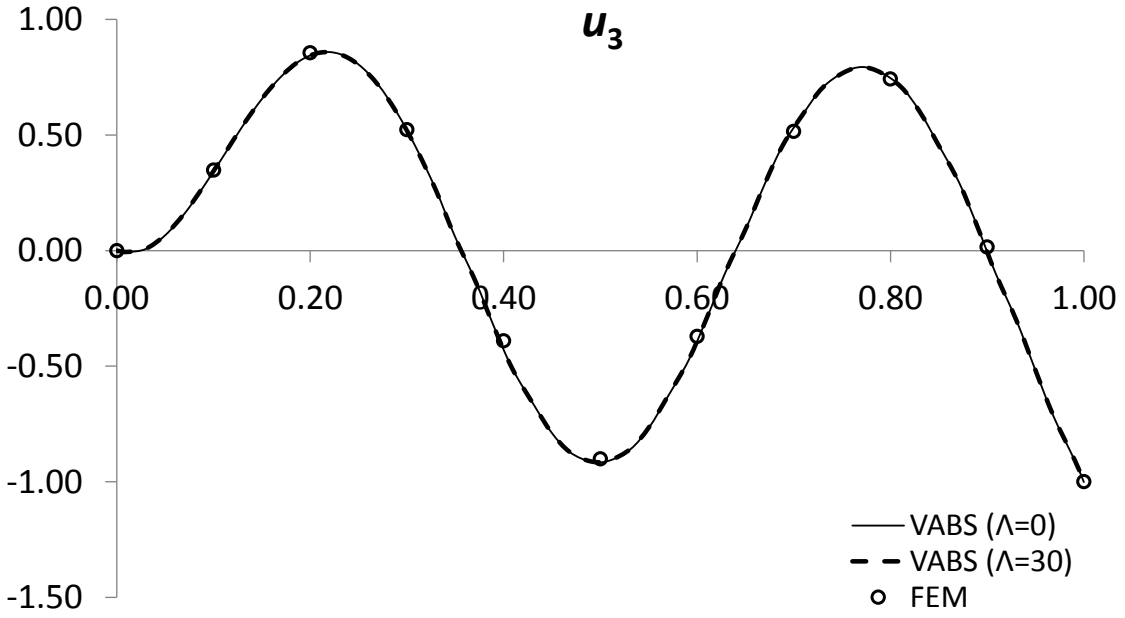

(a) u_3

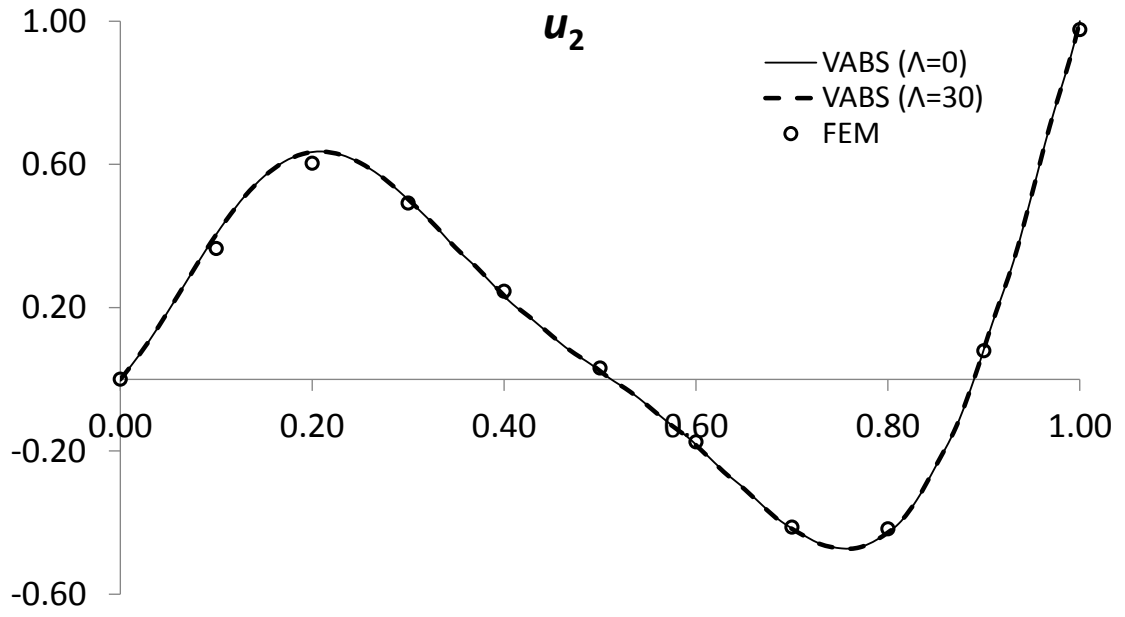

(b) u_2

Figure 52: Normalized eighth mode shape for the CUS section

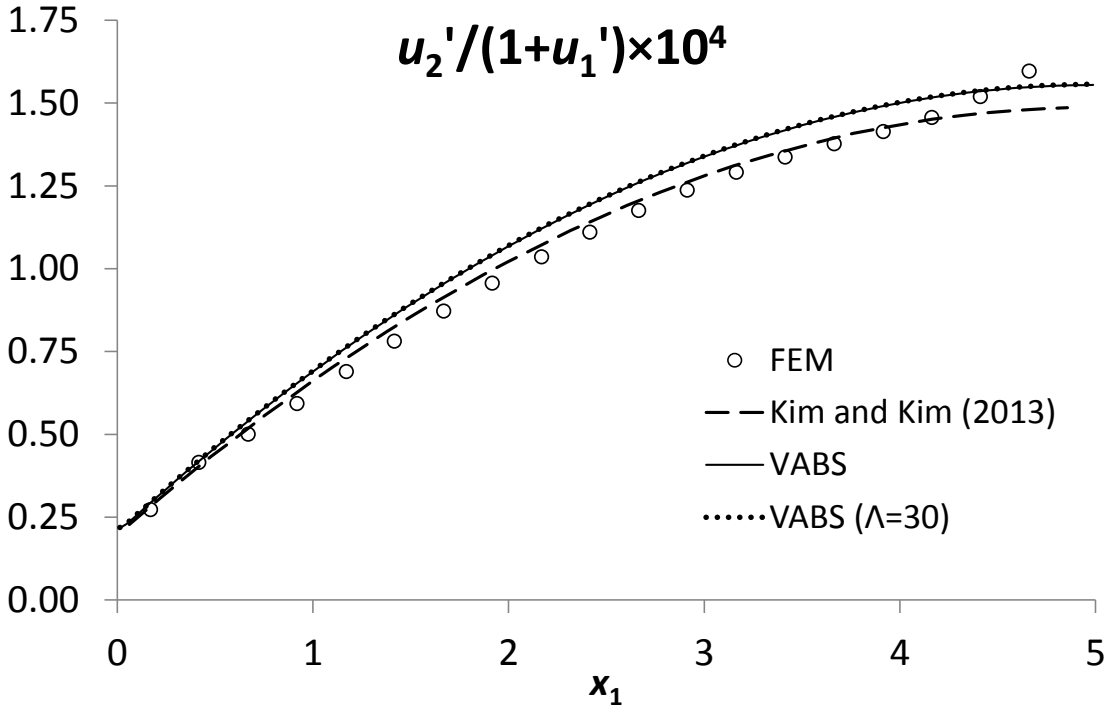

(a) Lag bending slope, L=5 in.

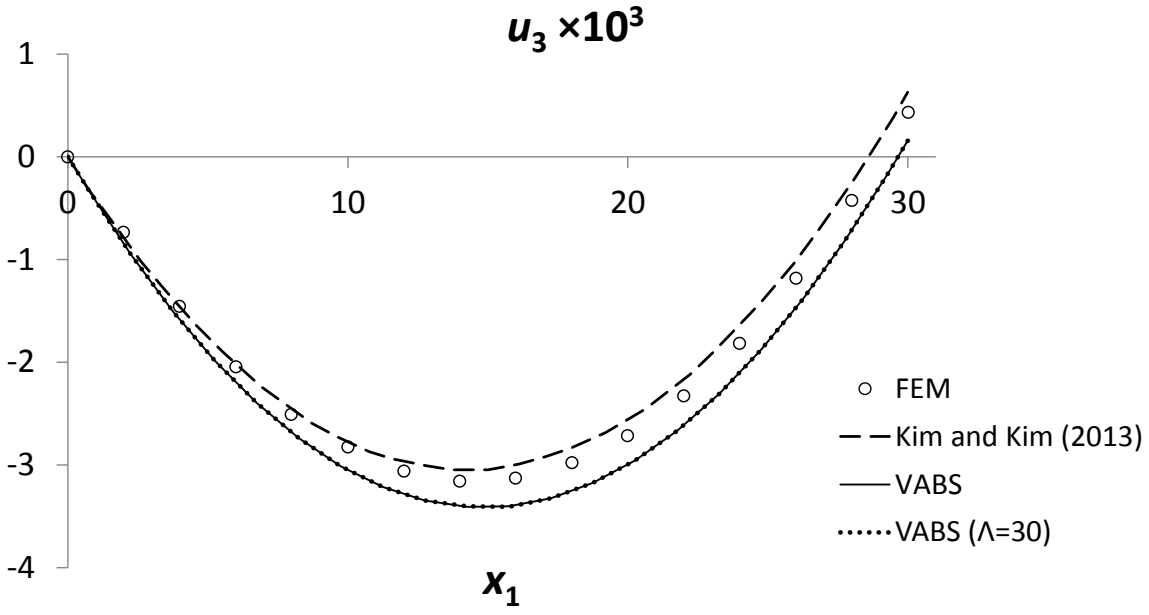

(b) Flap deflection, L=30 in.

Figure 53: Geometrically exact static results for CUS under tip load, F_2=1 lb.

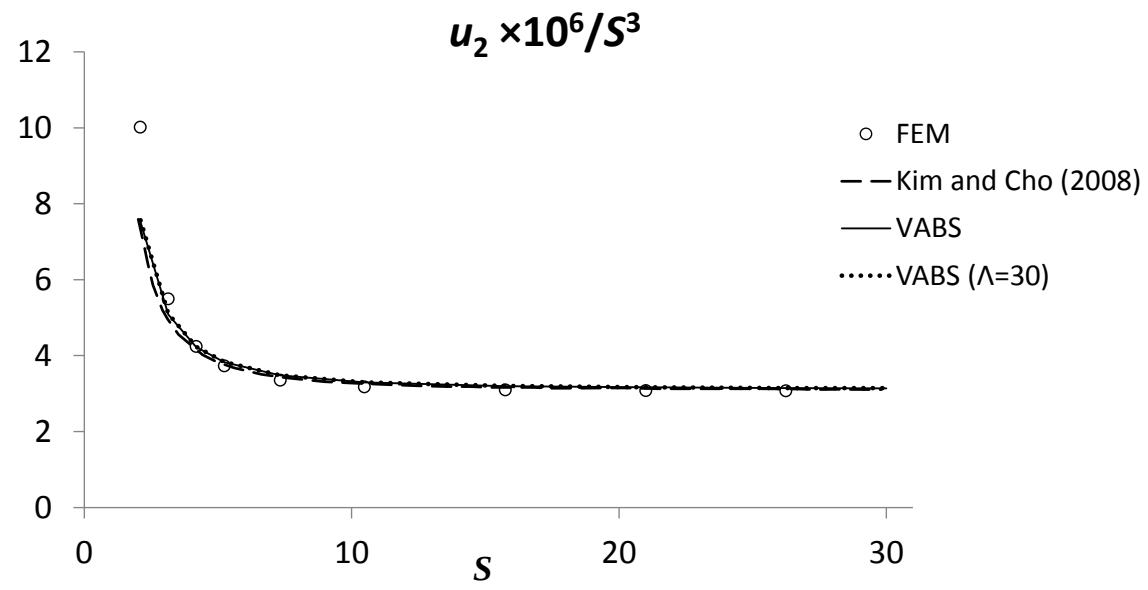

(a) Lag defection at $x_1 = L$

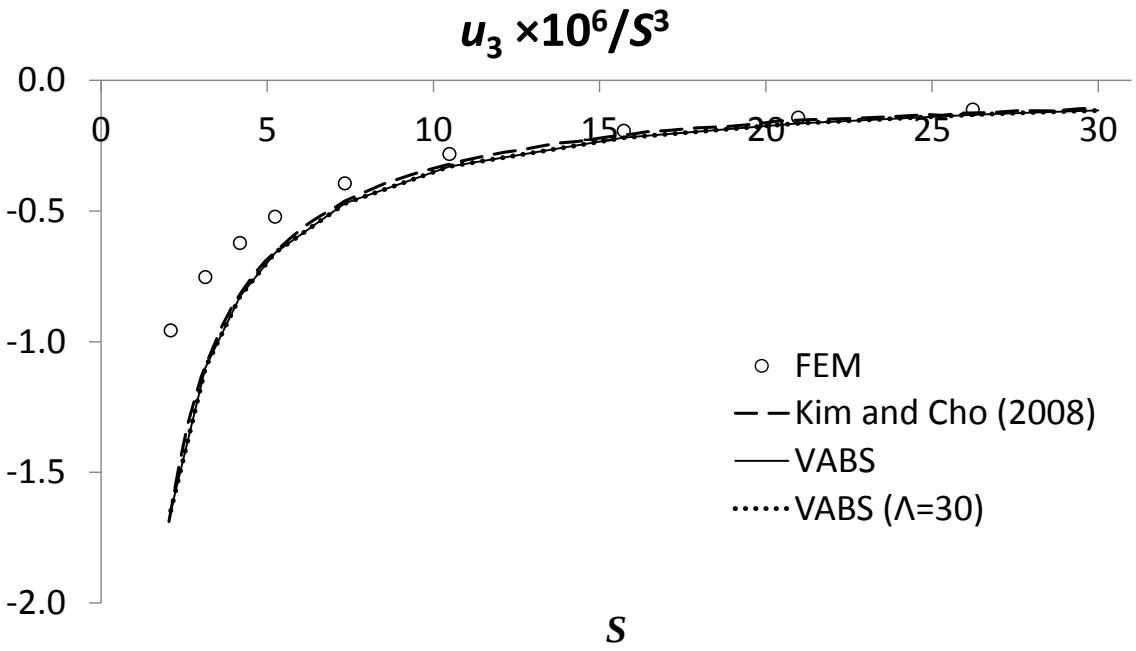

(b) Flap deflection at $x_1 = L/2$

Figure 54: Geometrically exact static results vs. slenderness ratio (S=length/width) under tip load for CUS, F_2=1 lb.

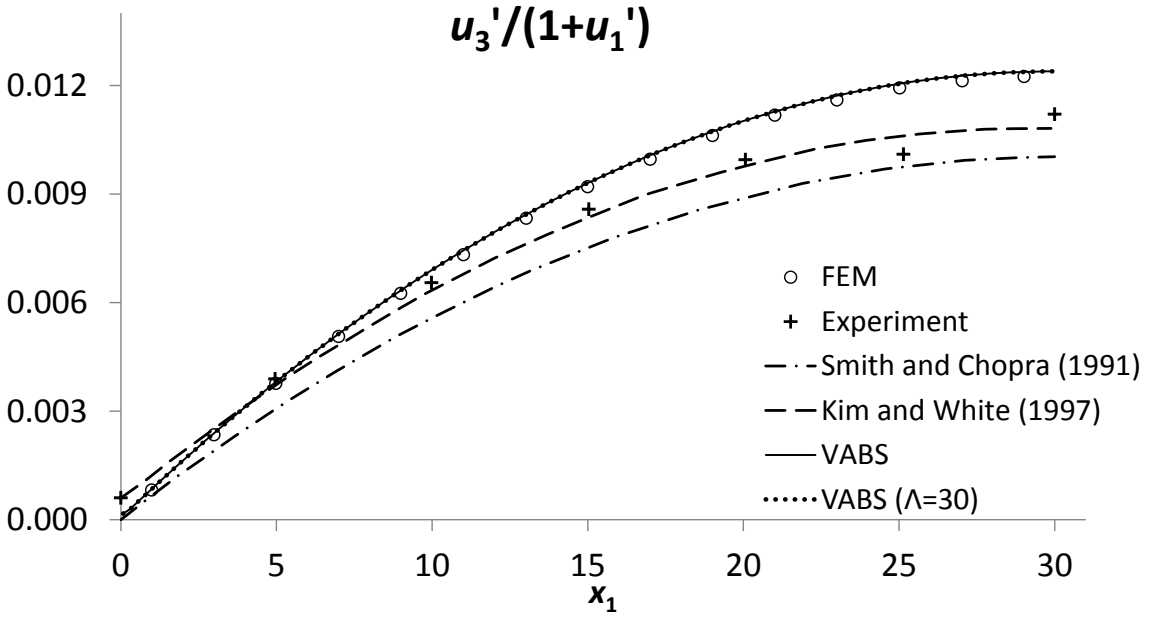

Figure 55: Geometrically exact flap bending slope for $L = 30$ in. under tip load for CUS, F_3=1 lb.

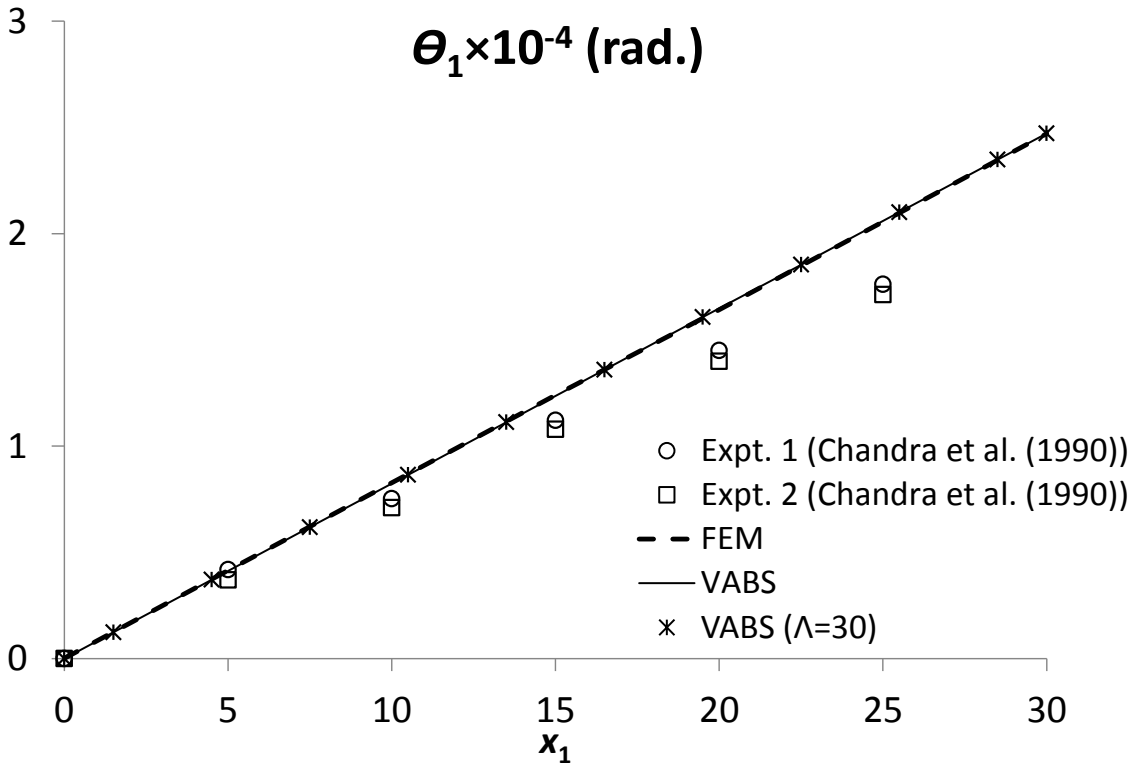

(a) $F_1 = 1$ lb.

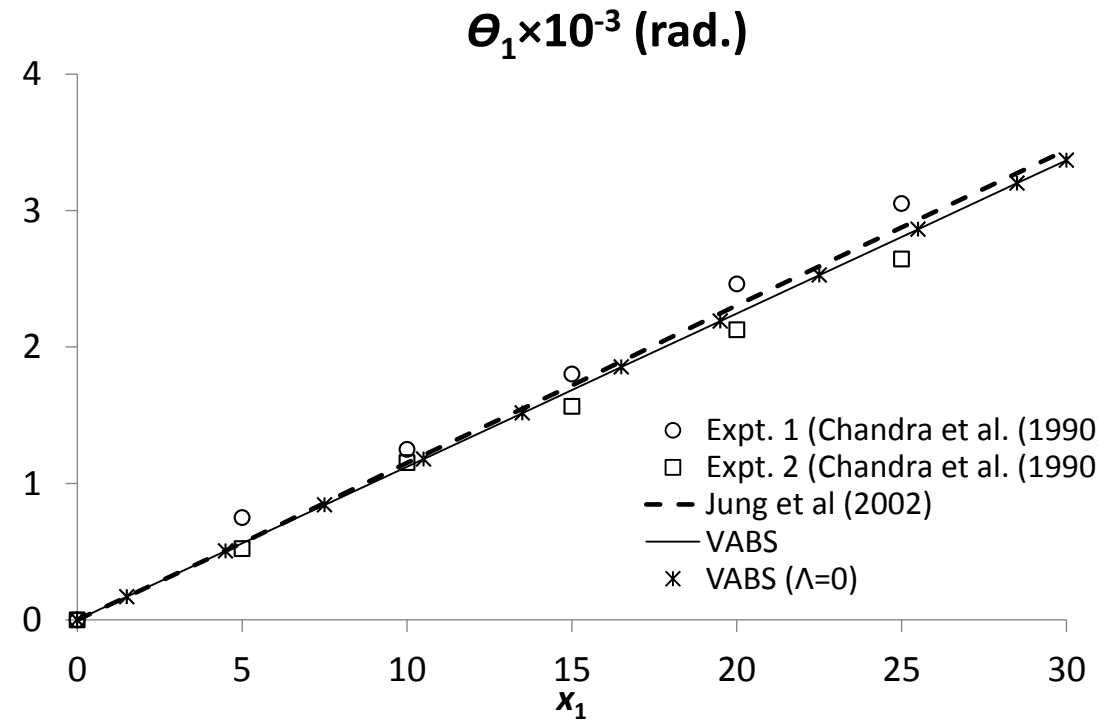

(b) M_1=1 lb-in.

Figure 56: Sectional twist for CUS, $L = 30$ in.

Table 22: Natural frequencies (Hz) for the CAS section. L=33.25 in. and rotor rotational speed about x_3 (or y_3) Ω=1002 RPM

Mode	Ref. [25]	Ref. [107]	Ref. [104]	Ref. [55]	VABS ($\Lambda = 0°$) +GEBT	VABS ($\Lambda = 15°$) +GEBT	VABS ($\Lambda = 30°$) +GEBT
Flap 1	35.20	36.00	36.87	35.64	35.58	35.58	35.59
Lag 1	53.80	57.10	62.45	56.66	56.34	56.41	56.42
Flap 2	188.00	197.30	203.00	196.20	193.25	193.40	193.51
Lag 2	–	349.30	378.90	354.30	342.62	345.64	345.73
Flap 3	–	–	–	–	519.62	520.52	521.19
Torsion 1	–	714.90	729.20	702.20	707.42	707.40	707.42

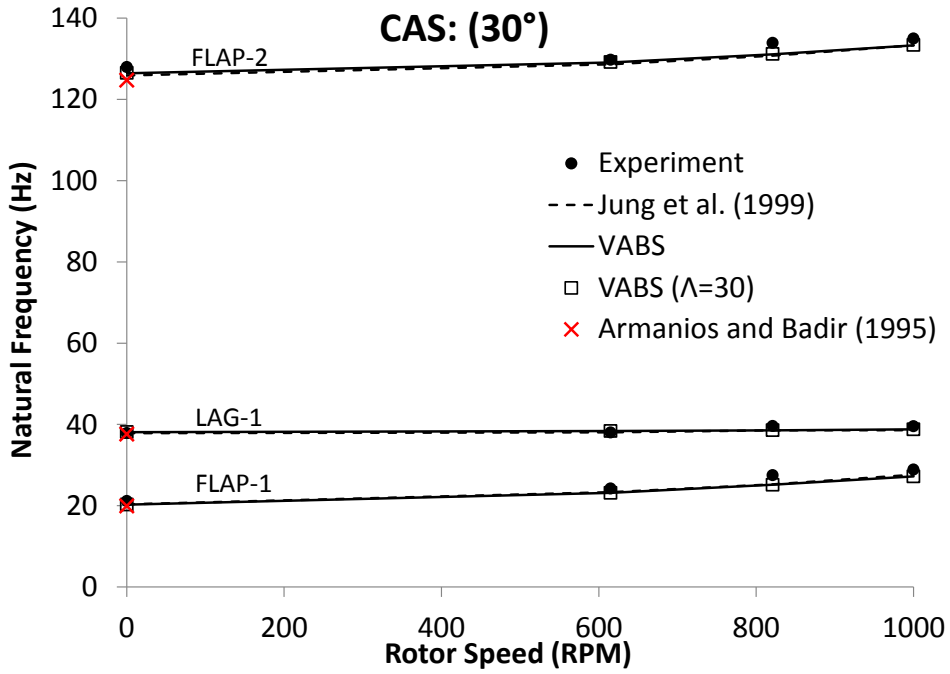

(a)

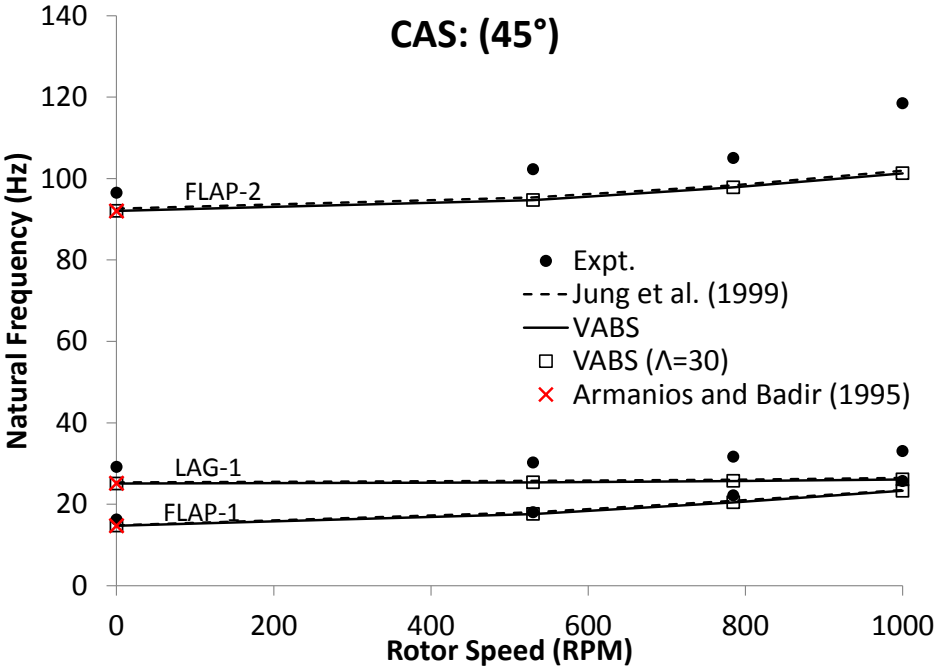

(b)

Figure 57: Variation of the first three natural frequencies vs. rotor speed for CAS with varying fiber orientations, $L = 33.25$ in.

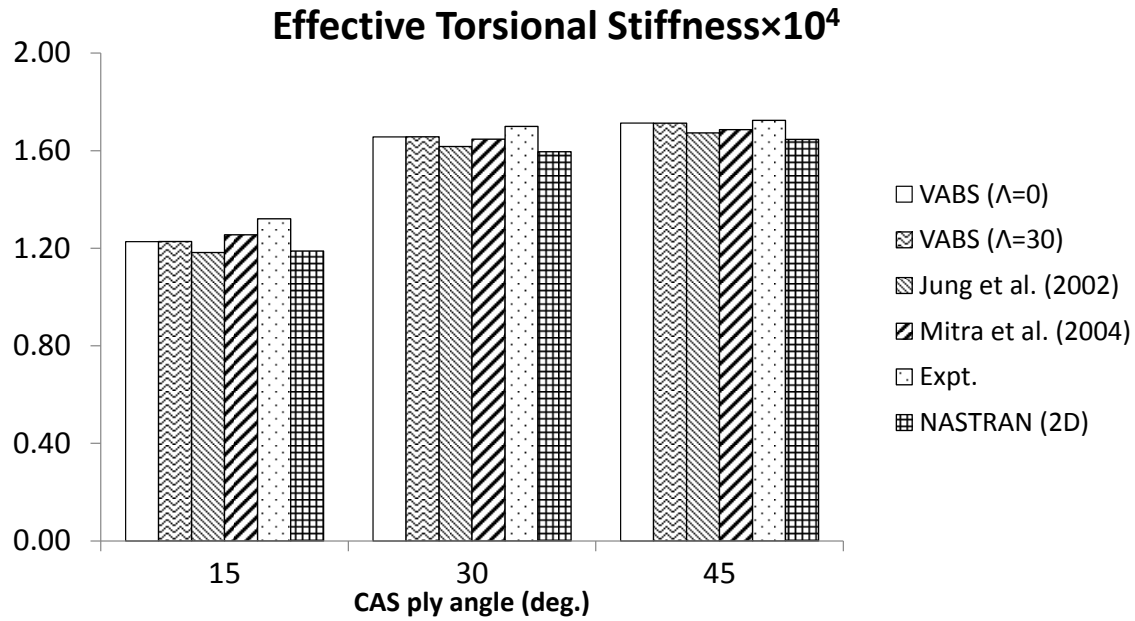

(a)

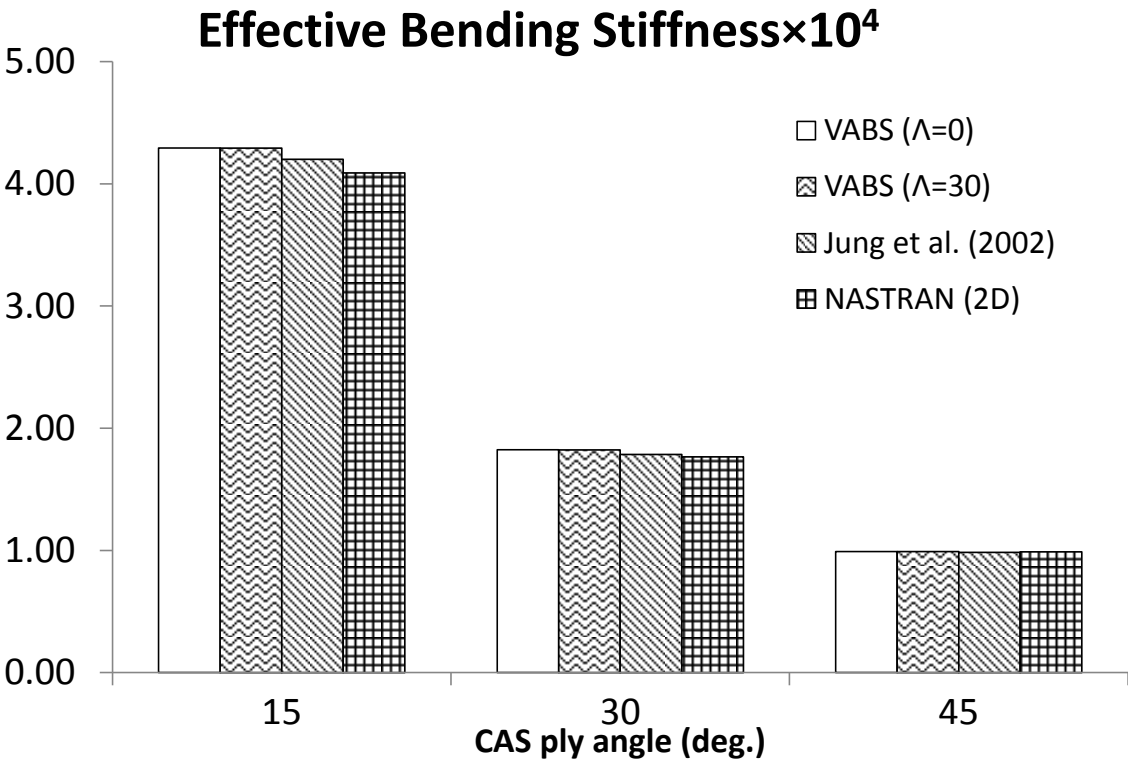

(b)

Figure 58: Effective torsional and flap bending stiffnesses for the CAS section

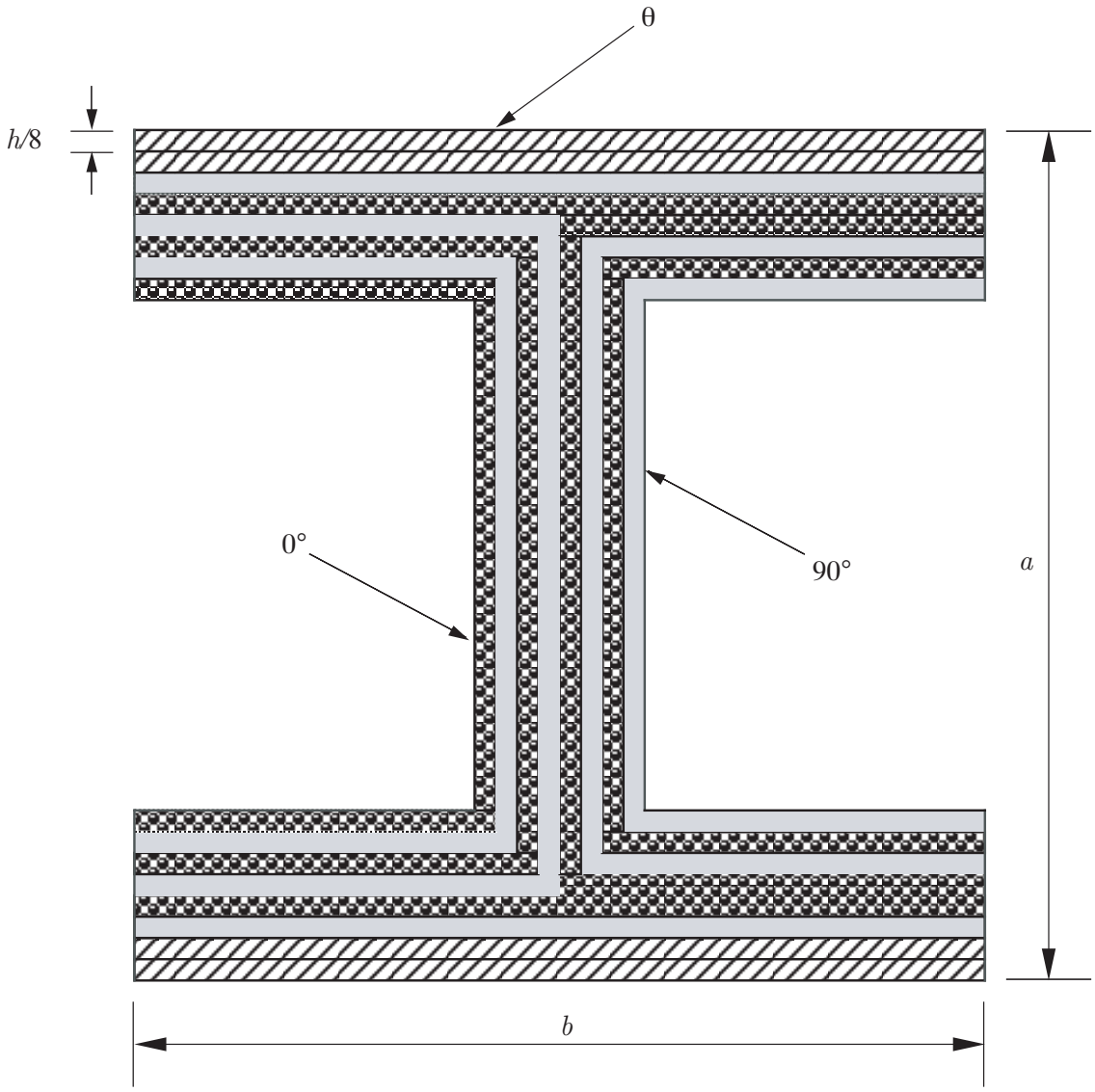

Figure 59: Orthogonal section for the anisotropic I-beam

Table 23: Section properties for the orthogonal I-beams

Geometry	Isotropic Material	Orthotropic Material
$a = 0.5$ in.	$E = 10^7$ psi	$E_l = 20.59 \times 10^6$ psi
$b = 1.0$ in.	$\nu = 0.3$	$E_t = 1.42 \times 10^6$ psi
$h = 0.04$ in.		$G_{lt} = 8.7 \times 10^5$ psi
		$G_{tn} = 6.96 \times 10^5$ psi
		$\nu_{lt} = \nu_{tn} = 0.42$

Table 24: Torsional and warping rigidities for the I-beam

Stiffness	VABS (2005)	VABS($\Lambda = 0°$)	VABS($\Lambda = 30°$)
		Isotropic	
$\hat{S}_{22}$	199.9440	200.3909	200.3914
$\hat{S}_{55}$	3553.4300	3517.2171	3521.4612
		Orthotropic	
$\hat{S}^*_{22}$	55.8658	56.4270	56.4270
$\hat{S}_{55}$	4232.1700	4398.5962	4437.5981

$$\hat{S}^*_{22} = \hat{S}_{22} - \hat{S}^2_{23}/\hat{S}_{33}$$

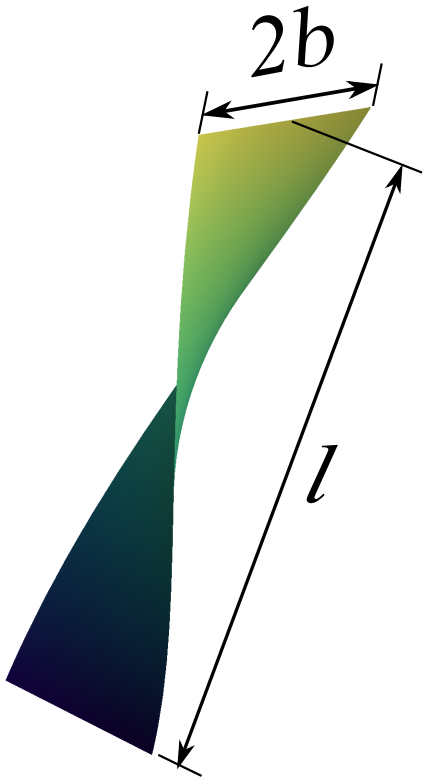

Figure 60: Initially twisted strip modeled as a initially curved and twisted beam using an oblique cross section

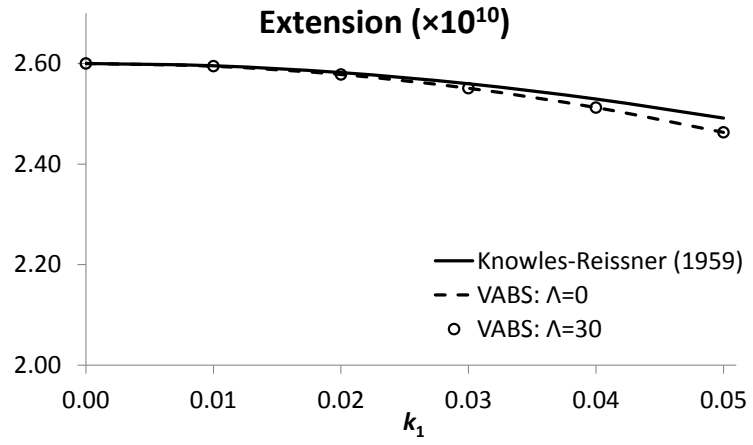

(a) A_{11}

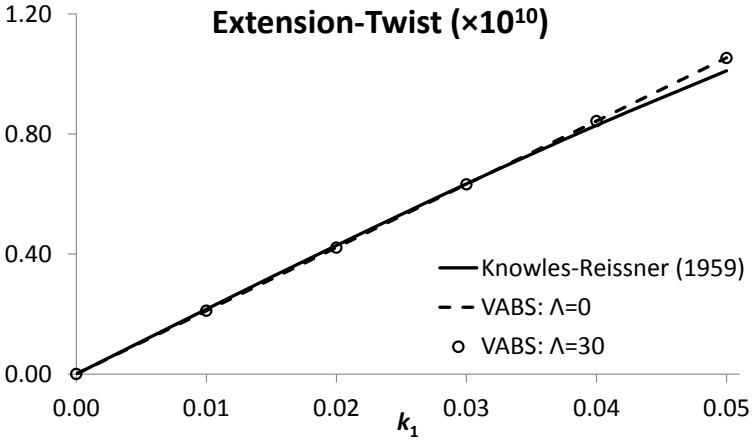

(b) A_{12}

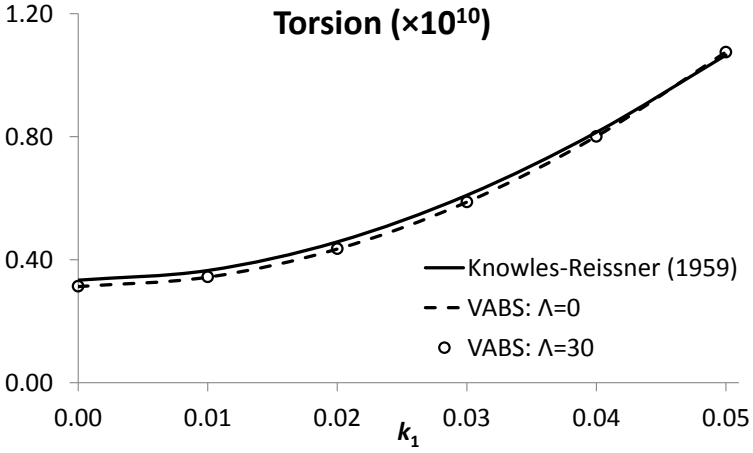

(c) A_{22}

Figure 61: Corrected classical stiffnesses for an initially twisted strip

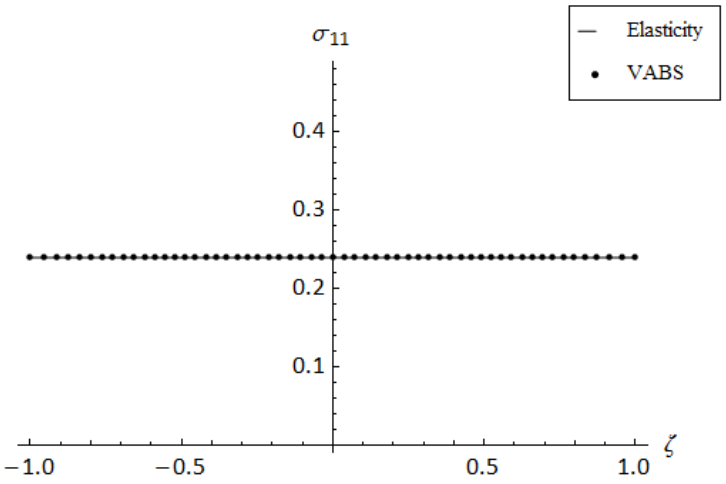

(a)

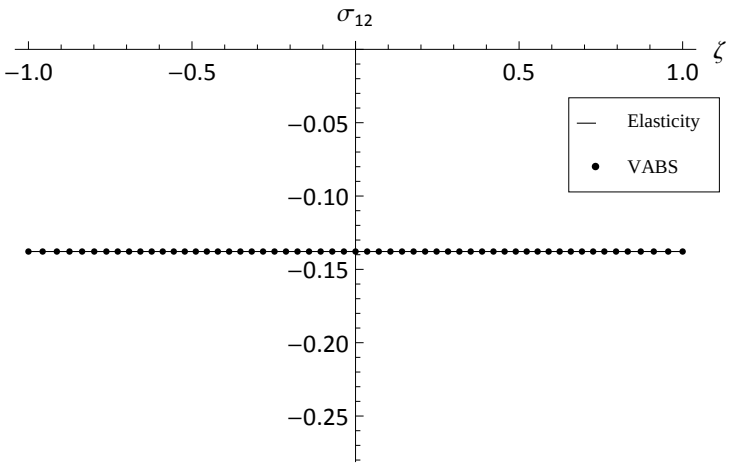

(b)

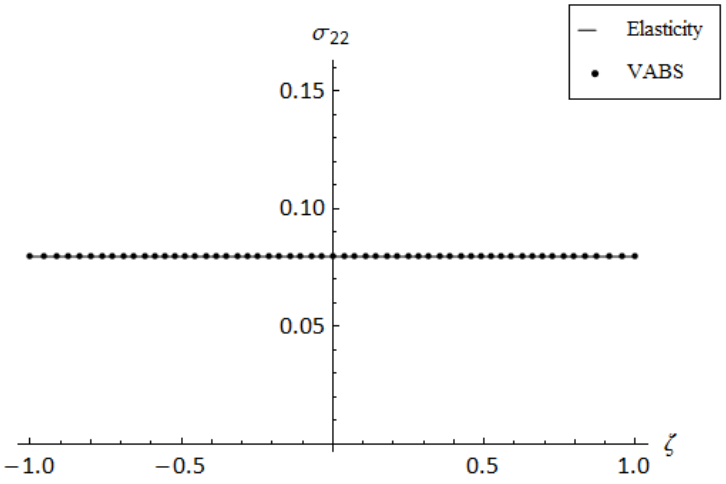

(c)

Figure 62: Stress recovery for the loading case of extension (F_1)

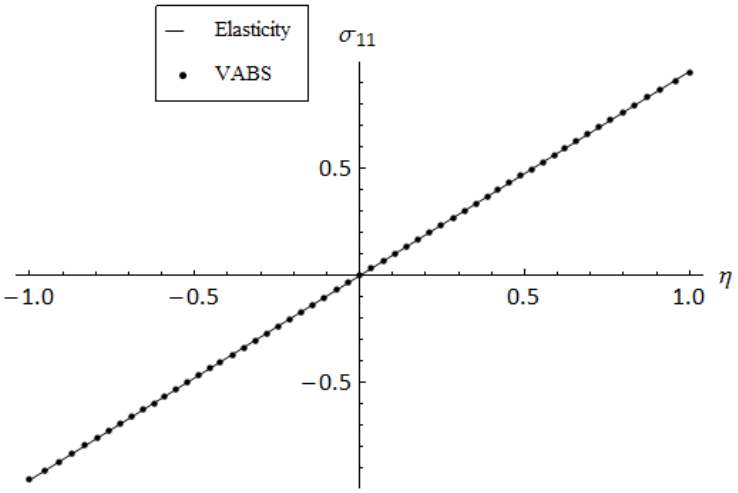

(a)

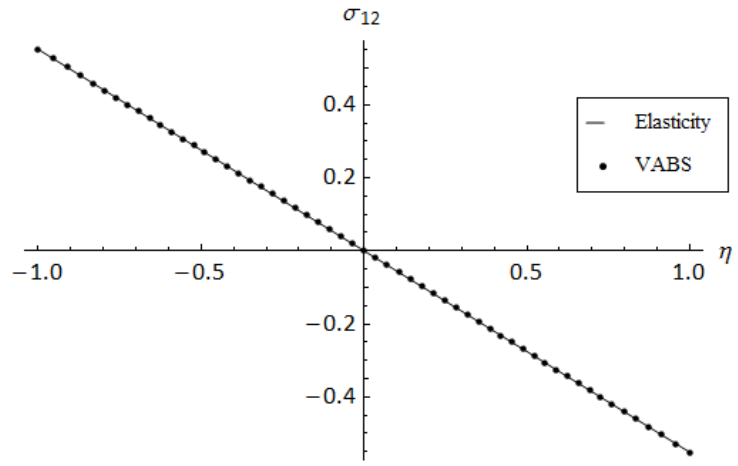

(b)

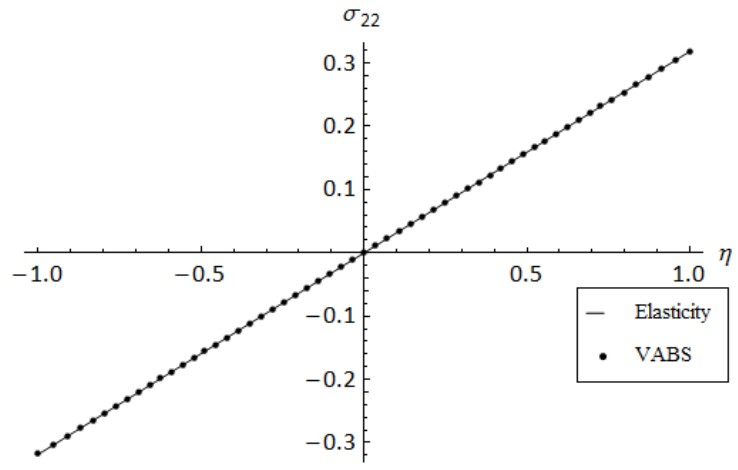

(c)

Figure 63: Stress recovery for the loading case of 2-bending (M_2)

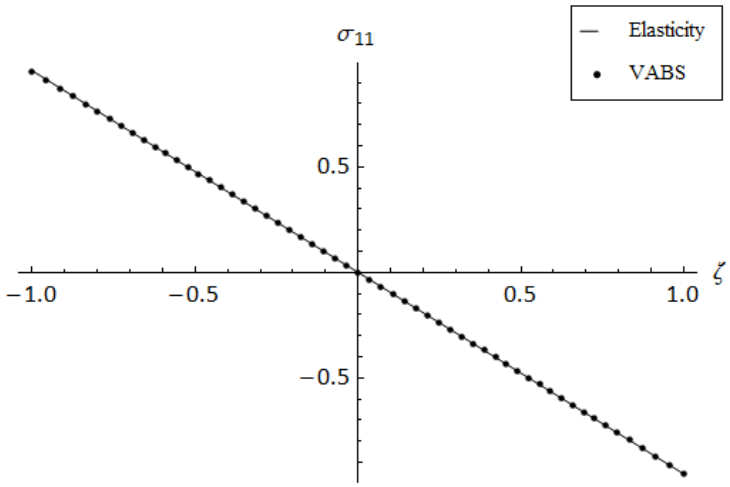

(a)

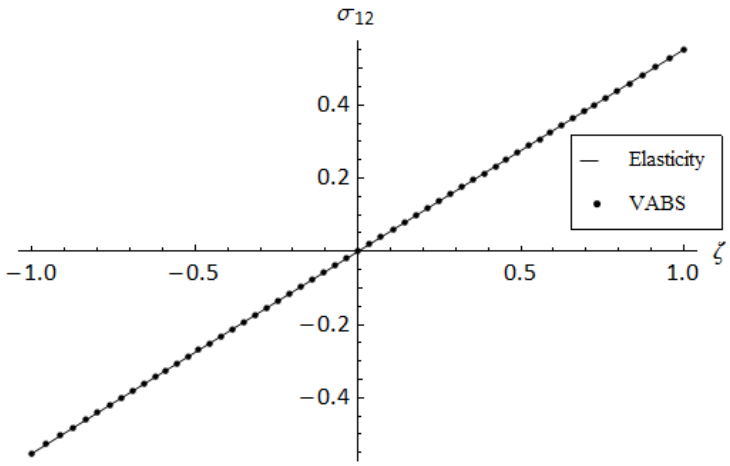

(b)

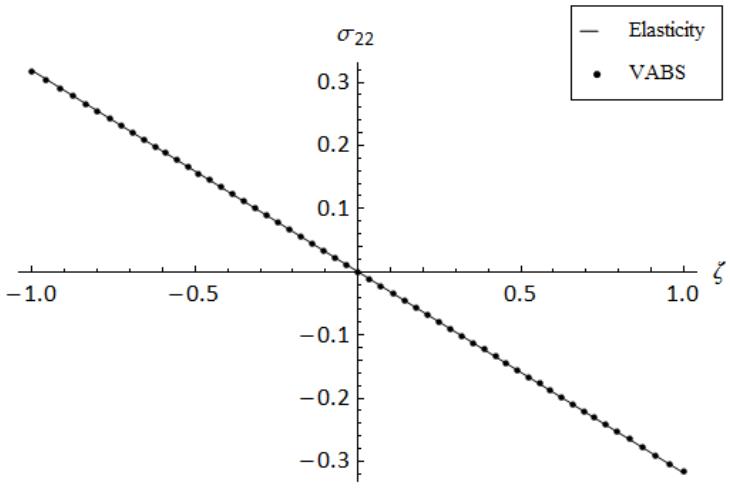

(c)

Figure 64: Stress recovery for the loading case of 3-bending (M_3)

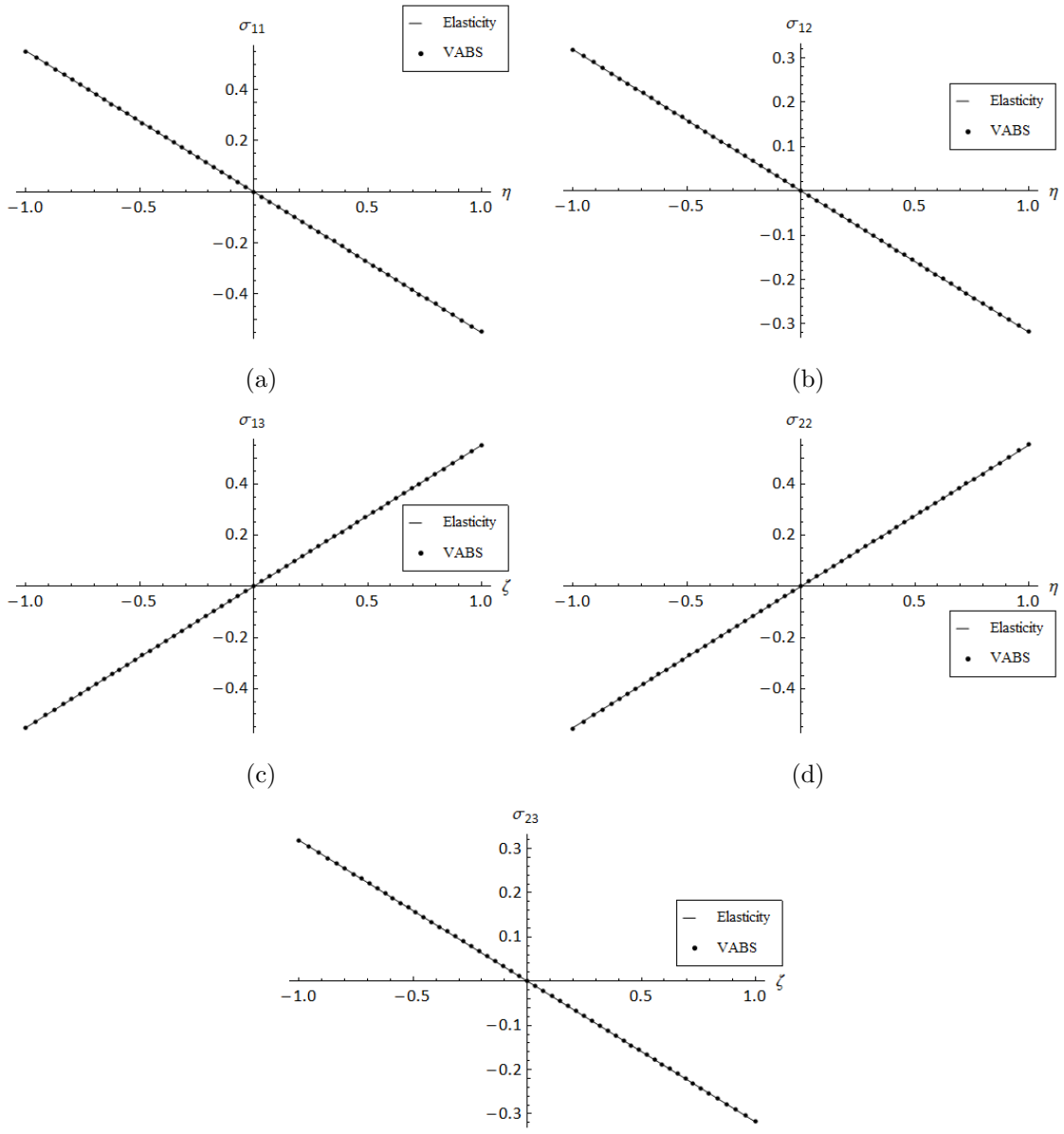

Figure 65: Stress recovery for the loading case of torsion (M_1)

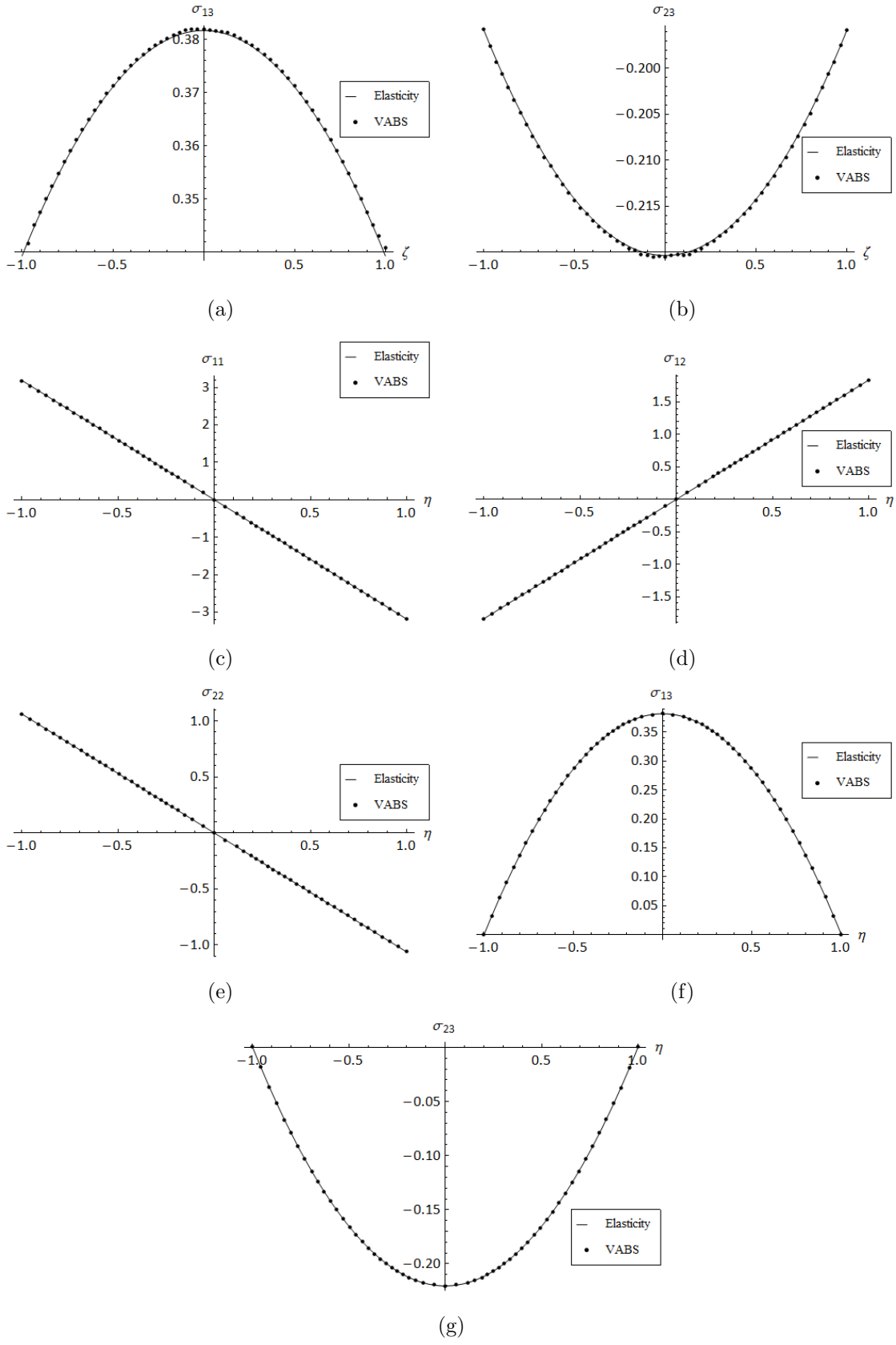

Figure 66: Stress recovery for the loading case of 3-flexure (F_3): Part I

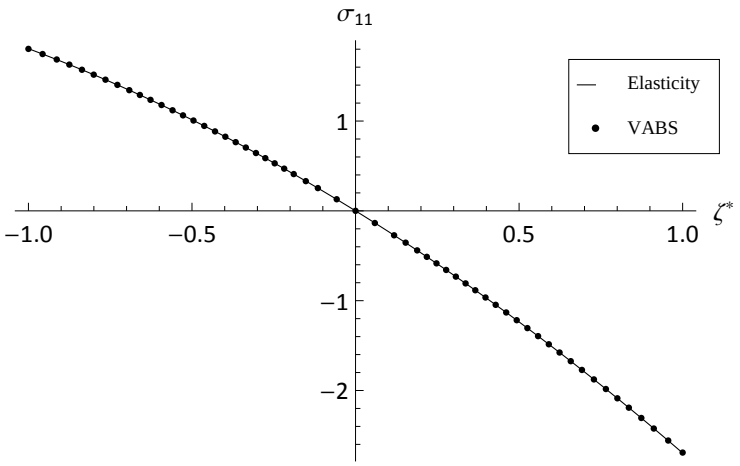

(a)

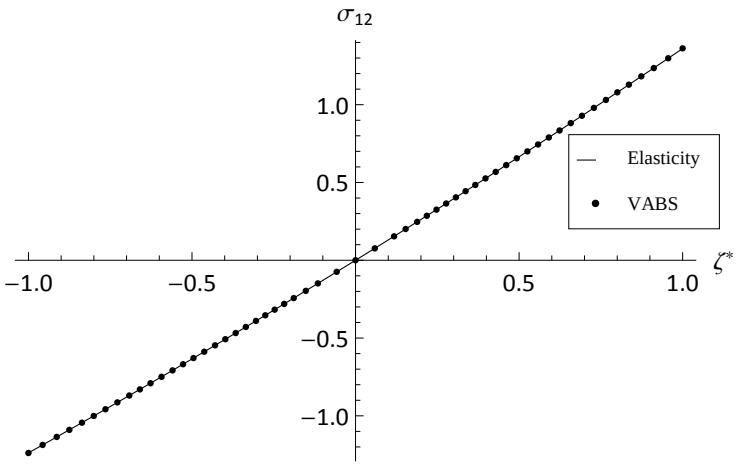

(b)

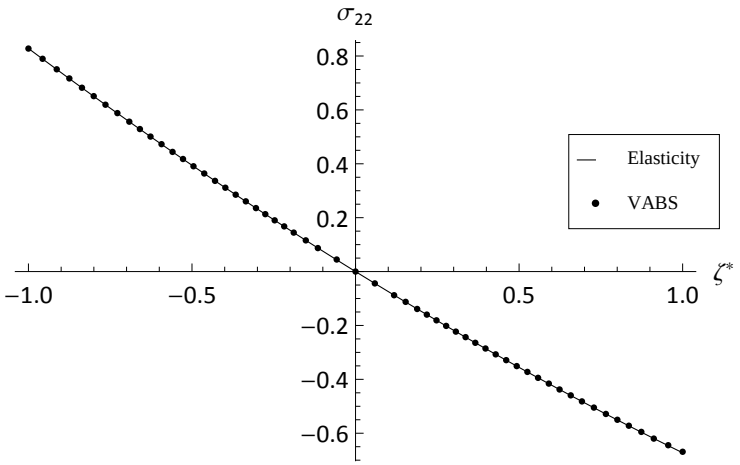

(c)

Figure 67: Stress recovery for the loading case of 3-flexure (F_3): Part II

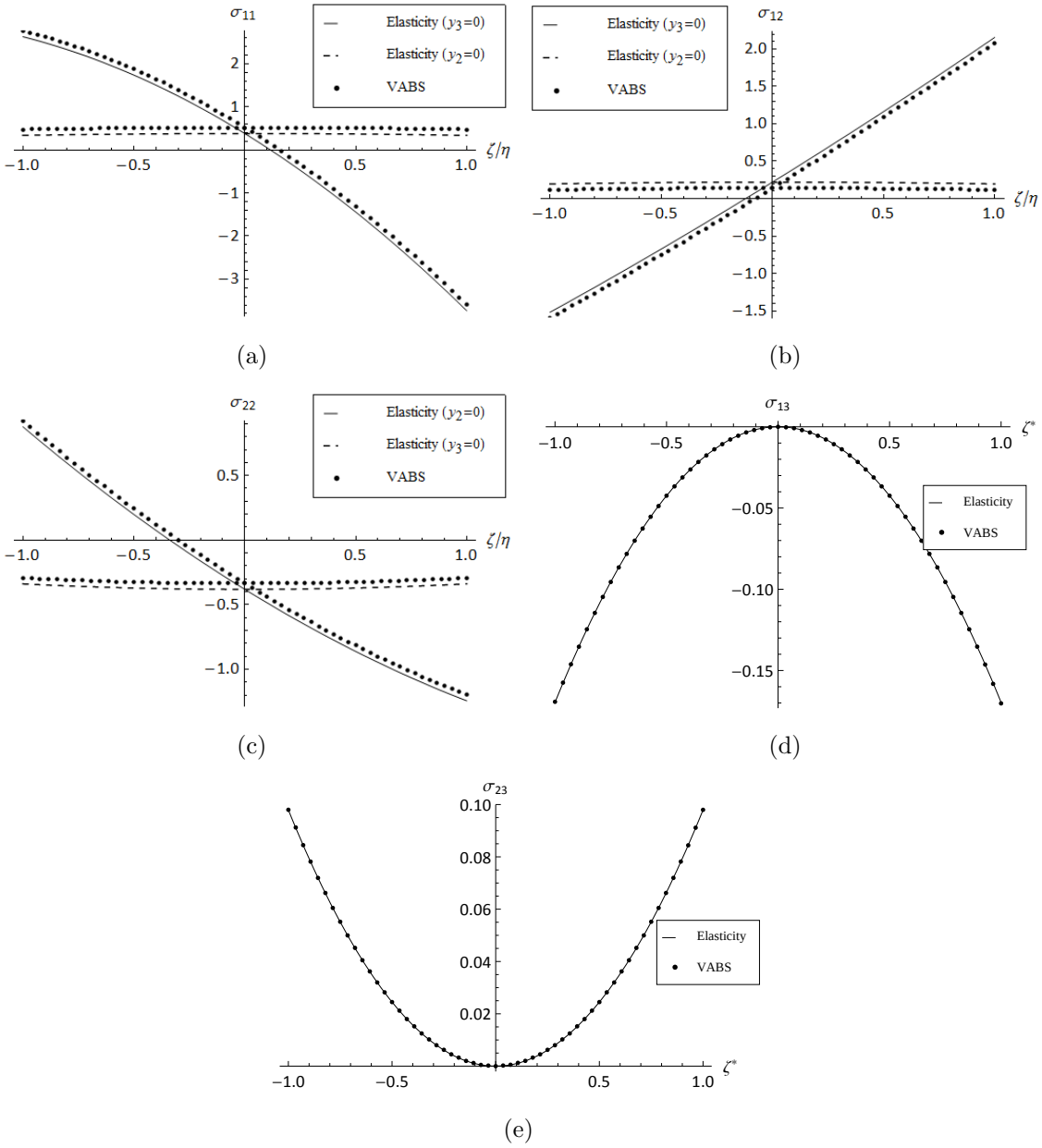

Figure 68: Stress recovery for the loading case of 2-flexure (F_2)

VII

THIN-WALLED BEAMS: INTERACTION OF SMALL PARAMETERS

One thing is that I can live with doubt and uncertainty and not knowing. I think it's much more interesting to live not knowing than to have answers which might be wrong. I have approximate answers and possible beliefs, in different degrees of certainty, about different things. But I'm not absolutely sure of anything and of many things I don't know anything about. I don't feel frightened by not knowing things, by being lost in the mysterious universe without having any purpose, which is the way it really is, as far as I can tell.

– Richard Feynman

An existing issue with VABS is the singularity of the stiffness matrices associated with thin-walled beams with moderate values of initial twist and/or curvature. This is possibly due to the fact that the asymptotic analysis does not consider a specific small parameter: the ratio of wall thickness to the the maximum cross section dimension (h/a). The theory for these kind of beams is expected to take into account this small parameter *ab initio*. This chapter demonstrates explicitly how the parameter h/a interacts with the existing small parameters of VABS to affect the solutions for the classical theory.

7.1 Euler-Lagrange Equations

The warping solution of the problems about to be considered are of a slightly different nature than the ones encountered so far. A generic mathematical result (which can be easily derived) is now stated. To determine the function $y(x)$ such that the following

(a) (b)

Figure 69: Strip with initial out-of-plane curvature (a); which is further incorporated with an initial twist (b)

functional is minimized:

$$I = \int_a^b f\left(x, y, y', y''\right)\ dx \tag{167}$$

The solution for y can be determined by solving the following equation

$$\frac{\partial f}{\partial y} - \left(\frac{\partial f}{\partial y'}\right)' + \left(\frac{\partial f}{\partial y''}\right)'' = 0 \tag{168}$$

and the corresponding boundary conditions at $x = a$ and $x = b$ (assuming y' and y are not specified at the boundaries)

$$\begin{aligned} \frac{\partial f}{\partial y''} &= 0 \\ \frac{\partial f}{\partial y'} - \left(\frac{\partial f}{\partial y''}\right)' &= 0 \end{aligned} \tag{169}$$

7.2 Pre-twisted Strip with Out-of-Plane Curvature

Consider an isotropic strip (material constants E and ν) with initial twist (k_1) and out-of-plane curvature (k_2). This is depicted in Fig. 69. The width, thickness and length of the strip are represented by $2b$, t and L; x_2 and x_3 are cross-sectional coordinates along the width and thickness respectively with the origin at the section geometric center and x_1 is the curvilinear coordinate along the axis of the beam. The small parameters of the problem are the usual b/L, bk_1 and bk_2. In addition to these, we will also consider the small parameter $\delta_h = h/b$. The fundamentals of the analysis now follow as per the development in Ref. [47], except that since the analysis here is still linear, the assumption of the smallness of the local rotation is invoked.

The expression for the 3D strain field in terms of the beam generalized strains and unknown warping $\overline{w}_i(x_1, x_2, x_3)$ can be obtained by the usual procedures outlined in Ref. [46] and repeated in Chapters 4 and 6.

$$\begin{aligned}
\Gamma_{11} =& \frac{1}{1+x_3k_2}\left[k_2\overline{w}_3 + \overline{\gamma}_{11} - x_2\overline{\kappa}_3 + x_3\overline{\kappa}_2 - k_1x_2\overline{w}_{1,3} + k_1x_3\overline{w}_{1,2} + \overline{w}_{1,1}\right] \\
2\Gamma_{12} =& \overline{w}_{1,2} + \frac{1}{1+x_3k_2}\left[-k_1\overline{w}_3 - x_3\overline{\kappa}_1 - k_1x_2\overline{w}_{2,3} + k_1x_2\overline{w}_{2,2} + \overline{w}_{2,1}\right] \\
2\Gamma_{13} =& \overline{w}_{1,3} + \frac{1}{1+x_3k_2}\left[-k_2\overline{w}_1 + k_1\overline{w}_2 + x_2\overline{\kappa_1} - k_1x_2\overline{w}_{3,3} + k_1x_3\overline{w}_{3,2} + \overline{w}_{3,1}\right] \\
\Gamma_{22} =& \overline{w}_{2,2} \\
2\Gamma_{23} =& \overline{w}_{2,3} + \overline{w}_{3,2} \\
\Gamma_{33} =& \overline{w}_{3,3}
\end{aligned} \tag{170}$$

The starting point of this theory will not be 3D elasticity but Classical Laminated Shell Theory (CLST). Therefore the next step will be the determination of the shell 2D strain measures from the plate ones. For this purpose, consider the following representation of the warping field (Greek and Latin indices go from 1 to 2 and 1 to 3 respectively):

$$\begin{aligned}
\overline{w}_\alpha(x_1, x_2, x_3) &= w_\alpha(x_1, x_2) + x_3\phi_\alpha(x_1, x_2) + \Delta_\alpha(x_1, x_2, x_3) \\
\overline{w}_3(x_1, x_2, x_3) &= w_3(x_1, x_2) + \Delta_3(x_1, x_2, x_3)
\end{aligned} \tag{171}$$

where w_i and ϕ_α's are an 'average' warping and local rotation respectively through the thickness and Δ_i's are the rest of the unknown variations. This decomposition of the warping field is motivated by the presence of the small parameter δ_h, i.e, the shell-like nature of the member shown in Fig. 69. The orders of the warping are now assumed to be

$$O(w_\alpha) = b\epsilon \quad O(w_3) = \frac{b\epsilon}{\delta_h} \tag{172}$$

where ϵ is of order of maximum strain. These can be verified once the final solution for warping is obtained. The orders of the 1D strains are as expected

$$O(\overline{\gamma}_{11}) = O(h\overline{\kappa}_\alpha) = O(b\overline{\kappa}_3) = \epsilon \tag{173}$$

Using Equation 171 in the 3D strain measures and employing a 'phantom' analysis [114] wherein terms too large to be in the strain are killed, the orders of Δ_i can be determined

$$O\left(\Delta_i\right) = b\delta_h\epsilon \tag{174}$$

Therefore if one is interested in a zeroth order analysis, Δ terms can be dropped straightaway. Another consequence of the phantom analysis are the solutions to ϕ_α of leading order:

$$\begin{aligned} \phi_1 &= -\, x_2\overline{\kappa}_1 \\ \phi_2 &= -\, w_{3,2} \end{aligned} \tag{175}$$

Again, the higher order terms in ϕ_α do not enter into the classical analysis and the above evaluation suffices. Making use of the derivation in Ref. [135], which relates 3D and shell strain measures, one discovers for the classical analysis the following simple relations

$$\Gamma_{\alpha\beta} = \epsilon_{\alpha\beta} + x_3\rho_{\alpha\beta} \tag{176}$$

Thus the measures for the shell membrane and curvtaure strain measures turn out to be

$$\begin{aligned} \epsilon_{11} &= \overline{\gamma}_{11} - x_2\overline{\kappa}_3 + k_1x_2^2\overline{\kappa}_1 + k_2w_3 \\ 2\epsilon_{12} &= -k_1w_3 + w_{1,2} + k_1x_2w_{3,2} \\ \epsilon_{22} &= w_{2,2} \\ \rho_{11} &= \overline{\kappa}_2 \\ 2\rho_{12} &= -2\overline{\kappa}_1 \\ \rho_{22} &= -w_{3,22} \end{aligned} \tag{177}$$

Again, owing to the fact that the classical shell and plate theories give the same zeroth and first order approximation to the strain energy [46], one can neglect the effects of k_1 and k_2 in the shell constitutive law, which therefore reduces to nothing

but a classical plate theory. The strain energy per unit reference-surface (chosen to be the mid-surface here) area is therefore

$$\begin{aligned}\mathcal{U}_{2D} =& \frac{1}{2}\varepsilon_{2D}^T \begin{bmatrix} A & B \\ B^T & D \end{bmatrix} \varepsilon_{2D} \\ \varepsilon_{2D} =& \lfloor \epsilon_{11} \quad 2\epsilon_{12} \quad \epsilon_{22} \quad \rho_{11} \quad 2\rho_{12} \quad \rho_{22} \rfloor^T \end{aligned} \tag{178}$$

The matrices A, B and D contain the usual plate constants and can be found in any standard plate textbook, such as Ref. [13]. To eliminate the redundancies, the usual four constraints on the warping ($\overline{w}$) are used [46]. Using the decomposition of the warping field in Eq. (171), the constraints are re-stated in terms of w_i's

$$\begin{aligned} \langle w_i \rangle &= 0 \\ \langle w_{3,2} - \phi_2 \rangle &= 0 \\ \langle \bullet \rangle &= \int_{-b}^{b} \bullet \, dx_2 \end{aligned} \tag{179}$$

Using standard variational principles, on imposing a minimization of strain energy, one obtains the following warping field (in order to obtain closed-form expressions, it is assumed that the maximum permissible order of k_2 is $\sqrt{\epsilon}/b$)

$$\begin{aligned} w_1 =& \frac{k_1}{210h^2}\Big[k_1k_2x_2\left(29b^6+35b^4x_2^2-21b^2x_2^4+5x_2^6\right)\left(1-\nu^2\right)\overline{\kappa}_1 \\ & -35\nu h^2x_2\left(x_2^2+b^2\right)\overline{\kappa}_2+k_2\left(5b^6-35b^2x_2^4+14x_2^6\right)\left(1-\nu^2\right)\overline{\kappa}_3\Big] \\ w_2 =& -\frac{\nu}{6}\left[6x_2\overline{\gamma}_{11}+2k_1x_2^3\overline{\kappa}_1+\nu k_2x_2\left(x_2^2-b^2\right)\overline{\kappa}_2+\left(b^2-3x_2^2\right)\overline{\kappa}_3\right] \\ w_3 =& \frac{1}{210h^2}\Big[k_1k_2\left(29b^6-105b^4x_2^2+35b^2x_2^4-7x_2^6\right)\left(1-\nu^2\right)\overline{\kappa}_1 \\ & -35\nu h^2\left(b^2-3x_2^2\right)\overline{\kappa}_2+7k_2x_2\left(7b^4-10b^2x_2^4+3x_2^4\right)\left(1-\nu^2\right)\overline{\kappa}_3\Big] \end{aligned} \tag{180}$$

Notice how the initial twist and curvature enter into the solution for the zeroth order warping due to the presence of δ_h in the denominator. Indeed on a perfunctory glance

one would be inclined to dismiss several of these terms as being higher order; it is only when δ_h is taken into account does one realize that they are all of the order assumed in Eq. (172). Putting these solutions back into Eq. (181), the following sectional strain energy is obtained:

$$\begin{aligned} \mathcal{U}_{1D} =& \frac{1}{2}\varepsilon^T A_{cl}\varepsilon \\ \varepsilon =& \lfloor \overline{\gamma}_{11} \quad \overline{\kappa}_1 \quad \overline{\kappa}_2 \quad \overline{\kappa}_3 \rfloor^T \end{aligned} \tag{181}$$

The non-zero components of the Matrix A_{cl} are now listed below

$$\begin{aligned} (A_{cl})_{11} &= 2Ebh \\ (A_{cl})_{12} &= \frac{2}{3}Eb^3hk_1 \\ (A_{cl})_{22} &= \frac{2}{3}Gbh^3\left[1+(1+\nu)\left(\frac{b}{h}\right)^2(bk_1)^2\left\{\frac{6}{5}-\frac{64\left(1-\nu^2\right)}{315}\left(\frac{b}{h}\right)^2(bk_2)^2\right\}\right] \\ (A_{cl})_{23} &= \frac{4\nu}{45}Eb^5hk_1k_2 \\ (A_{cl})_{33} &= \frac{1}{6}Ebh^3\left[1+\frac{4\nu}{15}\left(\frac{b}{h}\right)^2(bk_2)^2\right] \\ (A_{cl})_{44} &= \frac{2}{3}Eb^3h\left[1-\frac{8\left(1-\nu^2\right)}{105}\left(\frac{b}{h}\right)^2(bk_2)^2\right] \end{aligned} \tag{182}$$

It must be re-iterated here that all these stiffnesses are extracted from a zeroth-order strain energy. Notice several of the terms bought about by interaction of the small parameter δ_h with bk_1 and bk_2. Indeed the 'correction' term associated with the torsional stiffness due to initial twist (k_1) is comparable in magnitude to what one might colloquially consider the classical stiffness. Terms of this nature do not appear in the theory corresponding to the current classical VABS analysis [129]. Again, the fundamental cause of the appearance of such terms is the fact that the small parameter δ_h appears in the denominator of order as high as 4. This brings into play terms containing the other small parameters by changing their relative orders. This development establishes that while analyzing thin-walled rotor blade segments, the asymptotic analysis should be initiated by considering an additional small parameter

similar to δ_h. It has clearly been demonstrated that not taking into account this small parameter will result in the wrongful omission of certain terms associated with initial twist and curvature.

7.3 Shear Deformable Theory

In the previous section, the interplay of small parameters was clearly shown to produce certain terms which affect the classical stiffnesses. This section outlines the procedure for a higher fidelity theory which will produce a 6×6 cross-sectional stiffness matrix accounting for shear deformation, analogous to the current GT theory. The following considerations need to kept in mind

- While evaluating a the next higher order warping functions for w_i, the higher order terms associated with Δ_i and ϕ_α need also be considered. It is obvious that such terms cannot be obtained as a closed-form solution. Nevertheless, this does not matter as the final outcome of this procedure is to create a finite-element code for evaluating these functions.

- The simple relation of Eq. (176) does not hold; Eq. (18) of Ref. [135] gives the exact relation. This can be integrated with the latest 3D recovery from a shell theory using the VAM based plate and shell code VAPAS [125]. The shell transverse strain measures can be ignored since for thin-walled beams, the shear strain normal to the thin-walled segments is usually very small compared to the tangential shear strain.

- To determine the second order terms in the strain energy, start with the 6×6 Generalized classical model output from VAPAS. In other words, the plate strain energy will no longer work.

- While developing this higher-order theory, in addition to interacting with bk_1 and bk_2, δ_h may interact with b/L (which enter into the analysis through the

beam generalized shear strains) as well.

Though it is not possible to develop a closed-form analytical solution by this method, a finite-element formulation is adequate for the numerical solution of the warping. The solution procedure will also involve an internal run of VAPAS. This will then need to be used instead of the current VABS when the beam cross section has segments where the ratio of the wall thickness to the maximum cross section dimension becomes comparable to the other small parameters of the problem.

To summarize, in this chapter a methodology has been proposed for the analysis of thin-walled beams. It has been shown that when h/a is considered as an additional small parameter, the zeroth-order stiffness matrix is radically different from when it is performed without. It should also be noted that the development of the theory is quite different from the usual VABS procedure. An algorithm has been developed for extending the current analysis to a higher order which will yield the appropriate 6×6 stiffness matrix. Such a formulation is necessary to prevent singularities associated with the stiffness matrix which is a current concern in VABS for thin-walled beams with initial twist and curvature.

VIII

PLATES OF VARIABLE THICKNESS

These are some of the things hydrogen atoms do, given 15 billion years of cosmic evolution.

– Carl Sagan, *Cosmos*

It is a common assumption in plate theory that the effect of varying thickness on plate constants (both those associated with the membrane and curvature strains) can be simply accounted for by incorporating in the formulae obtained for a plate of uniform thickness, the thickness distribution. For example, for an isotropic and homogeneous (with material constants E and ν) plate of uniform thickness h, the well known flexural rigidity is simply $Eh^3/\left(12\left(1-\nu^2\right)\right)$. For such a plate with non-uniform thickness, the flexural rigidity is simply assumed to be $Eh(x_1,x_2)^3/\left(12\left(1-\nu^2\right)\right)$, if x_1 and x_2 denote the global coordinates. One of the aims of this chapter is to show that such an approximation is erroneous, primarily since it violates the stress-traction boundary conditions at the top and bottom surfaces of the plate. Accounting for this boundary condition will introduce into the plate potential energy a quantity which describes the variation of thickness. In the case of linearly varying thickness, these are nothing but taper constants, defined in a form similar to τ of Chapter 3.

The outline of this chapter is thus: Sec. 8.1 introduces the problem to be solved followed by the development of a VAM based theory, finally arriving at an 8×8 Generalized Reissner-Mindlin stiffness matrix and a set of stress and strain recovery expressions, both of which are shown to explicitly depend on parameters that determine the thickness distribution. Finally, Sec. 8.2 compares the results of this theory with ABAQUS for a problem similar in nature as that of Pagano's cylindrical bending

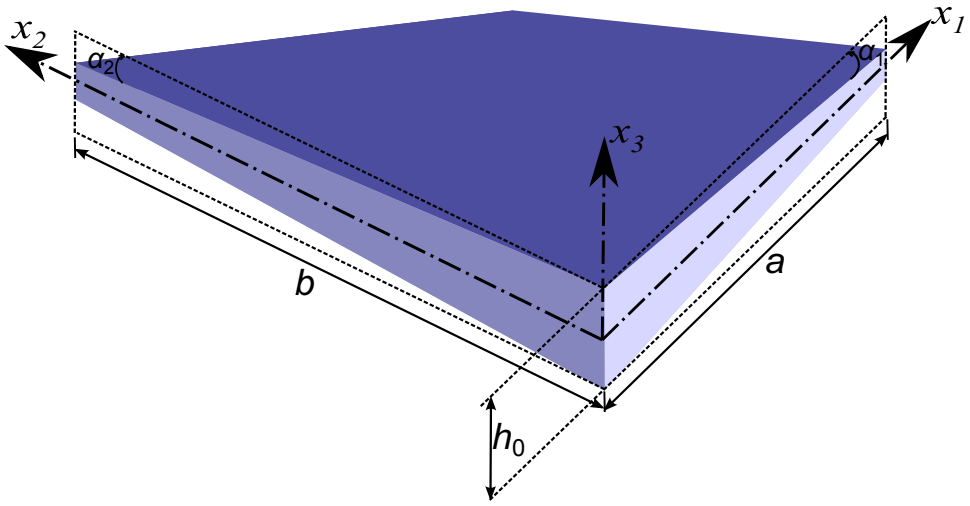

Figure 70: Isotropic prismatic plate tapered along the x_1 and x_2 directions

[82].

8.1 Isotropic, Homogeneous, Linearly Tapered Plate

Consider a plate made of isotropic, homogeneous material with a thickness distribution as follows

$$h(x_1, x_2) = h_0 - x_\alpha \zeta_\alpha \tag{183}$$

The schematic of such a plate is depicted in Fig. 70. The taper parameters ζ_1 and ζ_2 are defined in terms of the depicted angles angles α_1 and α_2 as

$$\alpha_1 = \tan^{-1}\left(\frac{\zeta_1}{2}\right) \qquad \alpha_2 = \tan^{-1}\left(\frac{\zeta_2}{2}\right) \tag{184}$$

It is now desired to develop a plate theory for such a structure. Though the methodology followed has its roots in the development of Ref. [125], to the best of the author's knowledge, no previous work based on the VAM has accounted for plates of variable thickness in a manner about to be demonstrated. The reference surface is chosen to be the mid-surface. Again, for the rest of this chapter, unless otherwise mentioned, Greek indices go from 1 to 2, while Latin indices go from 1 to 3. The index α is not to be confused with the angles shown in Fig. 70. The frames used for the development

are b, B and B^*; the latter two are employed for the classical and refined theories respectively. Each of these frames has a triad of unit vectors associated with them. For example, $\mathbf{b}_i$ $(i = 1, 2, 3)$ are a set of unit vectors along the coordinate axes x_i, so $\mathbf{b}_3$ is along the thickness direction. While $\mathbf{B}_3$ is normal to the deformed surface, $\mathbf{B}_3^*$ is along the deformed line element. Thus, while B does not accommodate 2D transverse shear strains and hence is suitable for a classical or Generalized Love-Kirchhoff theory, B^* does accommodate plate transverse shear strains and is suitable for a refined or Generalized Reissner-Mindlin theory. The position vector of a generic point in the undeformed configuration ($\hat{\mathbf{r}}$) can be written in terms of the position vector of the corresponding point on the mid-surface ($\mathbf{r}$) as

$$\hat{\mathbf{r}}\left(x_1, x_2, x_3\right) = \mathbf{r}\left(x_1, x_2\right) + x_3\mathbf{b}_3 \tag{185}$$

In a similar vein, after deformation, the point will now have a position vector which can be expressed in terms of unknown warping functions (w_i) as

$$\hat{\mathbf{R}}\left(x_1, x_2, x_3\right) = \mathbf{R}\left(x_1, x_2\right) + x_3\mathbf{B}_3 + w_i\mathbf{B}_i \tag{186}$$

The displacement field thus introduced has six redundancies. Two constraints are introduced by the definition of $\mathbf{B}_3$ above. Another is introduced by setting $\mathbf{B}_1.\mathbf{R}_{,2} = \mathbf{B}_2.\mathbf{R}_{,1}$. The final three redundancies are removed by precisely defining $\mathbf{R}$ such that

$$\begin{aligned} \langle w_i \rangle =& c_i \quad (i = 1, 2, 3) \\ \langle \bullet \rangle =& \int_{-\frac{1}{2}h(x_1,x_2)}^{\frac{1}{2}h(x_1,x_2)} \bullet \, dx_3 \end{aligned} \tag{187}$$

where the constants c_i's will be determined later so as to fit the second-order asymptotically correct strain energy into a 'best' possible Generalized Reissner-Mindlin form. Now to determine the deformation gradient tensor (χ), the same procedure as alluded to in Chapter 4 is used. In the course of doing so, the 2D strains (associated

with the B frame) are introduced into the problem [44]

$$\begin{aligned}\mathbf{R}_{,\alpha} =& \mathbf{B}_\alpha + \epsilon_{\alpha\beta}\mathbf{B}_\beta \\ \mathbf{B}_{i,\alpha} =& (-K_{\alpha\beta}\mathbf{B}_\beta \times \mathbf{B}_3 + K_{\alpha 3}\mathbf{B}_3) \times \mathbf{B}_i\end{aligned} \tag{188}$$

To summarize, the following 2D strains are introduced into the development: the membrane strains ϵ_{11}, ϵ_{12} and ϵ_{22} and the plate curvatures K_{11}, $\frac{1}{2}(K_{12} + K_{21})$ and K_{22}. For the current problem, since there are no initial curvatures, the latter three will be used interchangeably with their corresponding strain measures, κ_{11}, $\frac{1}{2}(\kappa_{12} + \kappa_{21})$ and κ_{22} respectively. A remark must be added concerning the definition of 2D strains. Plate literature is divided regarding the convention for the curvature strain measures. The current definition is based on rotation variables θ_α, which are defined to be positive when the normal tilts towards positive x_α. The notation employed in this chapter results in the classical stiffness matrix having a form that is easy on the eye. However, K_{11} is not the curvature in the x_1 direction. On the other hand, curvature definitions associated with rotation variables defined to be positive along the positive coordinate axes enables one to write the second of Eqs. (188) in a much simpler form. This difference in notation should be emphasized, particularly in the light of the fact that the beam developments till now have used the latter convention. Also, the reader is encouraged to consult Ref. [44] for an extensive discussion on the kinematics and subsequent choice (and number) of plate generalized strains required to construct a Reissner-Mindlin like plate theory.

The final expressions for the 3D strain measures are

$$\begin{aligned}
\Gamma_{11} =& \epsilon_{11} + x_3\kappa_{11} + w_{1,1} \\
2\Gamma_{12} =& 2\epsilon_{12} + x_3\left(\kappa_{12} + \kappa_{21}\right) + w_{1,2} + w_{2,1} \\
\Gamma_{22} =& \epsilon_{22} + x_3\kappa_{22} + w_{2,2} \\
2\Gamma_{13} =& w_{1,3} + w_{3,1} \\
2\Gamma_{23} =& w_{2,3} + w_{3,2} \\
\Gamma_{33} =& w_{3,3}
\end{aligned} \tag{189}$$

Using the stress-strain relationship for isotropic, homogeneous, linear elastic material ($\sigma = D\Gamma$) as in Eq. 141, the strain energy per unit reference surface is given by

$$\mathcal{U} = \frac{1}{2}\langle \Gamma^T D \Gamma \rangle \tag{190}$$

To form the total potential energy, the next logical step is to determine the potential of applied loads. The following loads are assumed to be present: body loads $\phi_i\left(x_1, x_2, x_3\right)\mathbf{B}_i$ and surface loads $\tau_i\left(x_1, x_2\right)\mathbf{B}_i$ and $\beta_i\left(x_1, x_2\right)\mathbf{B}_i$ at the top and bottom surfaces respectively. Care should be taken in recognizing that the top and bottom surfaces are not at a constant distance from the reference surface, but a variation given by Eq. 183. Following the same development as in Ref. [125], one obtains the applied load potential per unit reference area associated with warping terms (it is sufficient to consider the terms not associated with warping in the potential for the 2D analysis since they obviously do not affect warping solutions)

$$\begin{aligned}
V_w =& -\tau_i w_i^+ - \beta_i w_i^- - \langle \phi_i w_i \rangle \\
w^+ =& w|_{x_3 = h(x_1,x_2)/2} \\
w^- =& w|_{x_3 = -h(x_1,x_2)/2}
\end{aligned} \tag{191}$$

The total potential energy is therefore $\Pi = U + V_w$ and the warping functions can be solved for by setting $\delta\Pi = 0$. Following the variational formulation, the asymptotic

procedure is initiated. The usual small parameters are associated with the smallness of strain (the maximum strain is assumed to be of order ϵ) and the plate structure ($h(x_1, x_2)/a$ and $h(x_1, x_2)/b$). For this particular problem, additional small parameters arise out of taper, i.e., ζ_α. The orders of the 2D strains and loading terms (surface and body) are listed in Ref. [125]. The orders for warping are determined by equating the orders of the leading quadratic term in warping and leading bilinear term in warping and generalized plate strains in the total potential energy. This leads to the warping being $O(h\epsilon)$. The next perturbations of warping will be $O(\delta h\epsilon)$, $O(\delta^2 h\epsilon)$, etc., where the small parameters associated with the plate definition and taper are taken such that $O(h/a, h/b, \zeta_1, \zeta_2) = \delta$.

The first step in the asymptotic procedure is to discard all terms in the potential energy that are $O(\delta)$. The Euler-Lagrange equations for the extended functional (constraints on warping need to be accounted for) now yield equations which can be solved for the zeroth-order warping. The solution has the form

$$\begin{aligned} w^{(0)} =& Z\varepsilon \\ w^{(0)} =& \lfloor w_1^{(0)} \quad w_2^{(0)} \quad w_3^{(0)} \rfloor^T \end{aligned} \tag{192}$$

These warping solutions, when put back into the strain energy, yield the classical or generalized Love-Kirchhoff potential energy which corresponds to the well-known

results given by

$$
\begin{aligned}
2\Pi_0 &= \varepsilon^T \begin{bmatrix} A_{cl} & B_{cl} \\ B_{cl}^T & D_{cl} \end{bmatrix} \varepsilon \\
\varepsilon &= \lfloor \epsilon_{11} \quad 2\epsilon_{12} \quad \epsilon_{22} \quad \kappa_{11} \quad \kappa_{12}+\kappa_{21} \quad \kappa_{22} \rfloor^T \\
A_{cl} &= \frac{Eh(x_1,x_2)}{1-\nu^2} \begin{bmatrix} 1 & 0 & \nu \\ 0 & \frac{1-\nu}{2} & 0 \\ \nu & 0 & 1 \end{bmatrix} \\
B_{cl} &= 0_{3\times 3} \\
D_{cl} &= \frac{Eh(x_1,x_2)^3}{12\left(1-\nu^2\right)} \begin{bmatrix} 1 & 0 & \nu \\ 0 & \frac{1-\nu}{2} & 0 \\ \nu & 0 & 1 \end{bmatrix}
\end{aligned}
\tag{193}
$$

The next step is to perturb the warping one order higher and repeat the procedure. The first order warping functions will contain corrections associated with the applied loads, taper parameters and derivatives of the 2D strains with respect to x_1 and x_2, which cause a load vector (a term linear in strains) to appear in the potential energy, along with explicit appearance of ζ_1 and ζ_2 in the plate stiffness measures and transverse shear respectively. Thus,

$$
\begin{aligned}
w^{(1)} =& F_{S\alpha}\varepsilon_{,\alpha} + F_{T\alpha}\zeta_\alpha\varepsilon + w_L^{(1)} \\
w^{(1)} =& \lfloor w_1^{(1)} \quad w_2^{(1)} \quad w_3^{(1)} \rfloor^T
\end{aligned}
\tag{194}
$$

Note that throughout this development, the warping functions (the matrices Z, $F_{S\alpha}$, etc.) are not explicitly presented since the analytical expressions are quite lengthy, but it suffices to say that they can be determined without significant difficulty using a symbolic manipulation software such as Mathematica®. Once this warping is known, we can substitute it back into the potential energy, to obtain the second-order asymptotically correct potential energy per unit mid-surface area, which is of the form

(omitting the constant term for obvious reasons)

$$2\Pi_2 = \varepsilon^T A\varepsilon + \varepsilon_{,1}^T B\varepsilon_{,1} + 2\varepsilon_{,1}^T C\varepsilon_{,2} + \varepsilon_{,2}^T D\varepsilon_{,2} + 2\varepsilon_{,1}^T H_1\varepsilon + 2\varepsilon_{,2}^T H_2\varepsilon - 2\varepsilon^T F \tag{195}$$

where A is a quadratic function of the taper parameters and H_1 and H_2 are linear functions of the same. It is also interesting to note that there are no terms in the strain energy that can be considered to be of first order in the small parameters. All the terms are either zeroth- or second-order. Since this potential energy contains derivatives of 2D strain variables, it becomes unsuitable from an engineering perspective. Casting it into a usable form is achieved through a Generalized Reissner-Mindlin transformation. The first step involves switching to the 2D strain measures associated with the B^* system.

$$\begin{aligned}
\varepsilon &= \mathcal{R} - \mathcal{D}_\alpha \gamma_{,\alpha} \\
\mathcal{R} &= \lfloor \epsilon_{11}^* \quad 2\epsilon_{12}^* \quad \epsilon_{22}^* \quad \kappa_{11}^* \quad \kappa_{12}^* + \kappa_{21}^* \quad \kappa_{22}^* \rfloor^T \\
\gamma &= \lfloor 2\gamma_{13}^* \quad 2\gamma_{23}^* \rfloor^T \\
\mathcal{D}_1 &= \begin{bmatrix} 0 & 0 & 0 & 1 & 0 & 0 \\ 0 & 0 & 0 & 0 & 1 & 0 \end{bmatrix}^T \qquad \mathcal{D}_2 = \begin{bmatrix} 0 & 0 & 0 & 0 & 1 & 0 \\ 0 & 0 & 0 & 0 & 0 & 1 \end{bmatrix}^T
\end{aligned} \tag{196}$$

Substituting this into the expression for the asymptotically correct potential energy and discarding higher-order terms by recognizing that the trasnverse shear strains are $O(\delta\epsilon)$

$$\begin{aligned}
2\Pi_2 =& \mathcal{R}^T A\mathcal{R} \underline{- 2\mathcal{R}^T A_0 \mathcal{D}_\alpha \gamma_{,\alpha}} + \mathcal{R}_{,1}^T B\mathcal{R}_{,1} + 2\mathcal{R}_{,1}^T C\mathcal{R}_{,2} + \mathcal{R}_{,2}^T D\mathcal{R}_{,2} \\
&+ 2\mathcal{R}_{,1}^T H_1\mathcal{R} + 2\mathcal{R}_{,2}^T H_2\mathcal{R} - 2\mathcal{R}^T F
\end{aligned} \tag{197}$$

where $A_0 = A\,(\zeta_1 = \zeta_2 = 0)$. The final desired potential energy will have the following form

$$2\Pi_{\mathcal{R}} = \mathcal{R}^T X\mathcal{R} + 2\mathcal{R}^T Y\gamma + \gamma^T G\gamma - 2\mathcal{R}^T F_{\mathcal{R}} - 2\gamma^T F_\gamma \tag{198}$$

Therefore, the matrices X, Y, G, $F_{\mathcal{R}}$ and F_γ need to be determined by casting Eq. 197 into the form of Eq. 198. The stress resultants which are defined to be conjugate

to the $2D$ strains of B^* are

$$\begin{aligned}
\mathcal{F}_{\mathcal{R}} =& \frac{\partial \Pi_{\mathcal{R}}}{\partial \mathcal{R}} = X\mathcal{R} + Y\gamma - F_{\mathcal{R}} \\
\mathcal{F}_{\gamma} =& \frac{\partial \Pi_{\mathcal{R}}}{\partial \gamma} = Y^T\mathcal{R} + G\gamma - F_{\gamma} \\
\mathcal{F}_{\mathcal{R}} =& \lfloor N_{11} \quad N_{12} \quad N_{22} \quad M_{11} \quad M_{12} \quad M_{22} \rfloor^T \\
\mathcal{F}_{\gamma} =& \lfloor Q_1 \quad Q_2 \rfloor^T
\end{aligned} \tag{199}$$

where the $N_{\alpha\beta}$'s are the in-plane force stress resultants, $M_{\alpha\beta}$'s are the out-of-plane moment stress resultants and Q_α's are the transverse shear force stress resultants. The next step is to use the two moment equilibrium equations (m_α's are the plate equivalent applied and inertial loads lumped together [125]) listed below

$$\begin{aligned}
M_{11,1} + M_{12,2} - Q_1 + m_1 =& 0 \\
M_{12,1} + M_{22,2} - Q_2 + m_2 =& 0
\end{aligned} \tag{200}$$

The moment equilibrium equations can be rewritten in terms of $\Pi_{\mathcal{R}}$ as

$$\mathcal{D}_\alpha^T \left(\frac{\partial \Pi_{\mathcal{R}}}{\partial \mathcal{R}} \right)_{,\alpha} - \frac{\partial \Pi_{\mathcal{R}}}{\partial \gamma} + \begin{Bmatrix} m_1 \\ m_2 \end{Bmatrix} = 0 \tag{201}$$

The above equation will be used to solve for shear strain, and hence one can neglect all terms except those that are first-order in small parameters. Neglecting higher order terms and assuming that $X\left(\zeta_1 = \zeta_2 = 0\right) = A_0$ (which is indeed shown to be true later), the equation reduces to

$$\begin{aligned}
\mathcal{D}_\alpha^T \left(A_0 \mathcal{R} \right)_{,\alpha} - Y^T\mathcal{R} - G\gamma + \overline{F}_\gamma = 0 \\
\overline{F}_\gamma = F_\gamma + \begin{Bmatrix} m_1 \\ m_2 \end{Bmatrix}
\end{aligned} \tag{202}$$

The underlined term in Eq. 197 can now be simplified using the above relation

$$\begin{aligned}
-2\mathcal{R}^T A_0 \mathcal{D}_\alpha \gamma_{,\alpha} =& 2\left(\mathcal{R}^T A_0\right)_{,\alpha} \mathcal{D}_\alpha \gamma \quad \text{(integration by parts)} \\
=& 2\left[\left(A_0\mathcal{R}\right)_{,\alpha}\right]^T \mathcal{D}_\alpha \gamma \\
=& 2\left[\mathcal{D}_\alpha^T \left(A_0\mathcal{R}\right)_{,\alpha}\right]^T \gamma \\
=& 2\left[G\gamma + Y^T\mathcal{R} - \overline{F}_\gamma\right]^T \gamma \quad \text{(using equation 202)} \\
=& \gamma^T G\gamma + 2\mathcal{R}^T Y\gamma + \underline{\left(G\gamma - 2\overline{F}_\gamma\right)^T \gamma}
\end{aligned} \tag{203}$$

Now, Eq. 202 can be recast and used to solve for the shear strain as

$$\begin{aligned}
\gamma &= G^{-1}\left[\mathcal{D}_\alpha^T A_0 \mathcal{R}_\alpha - \overline{Y}^T\mathcal{R} + \overline{F}_\gamma\right] \\
\overline{Y} &= Y - A_{0,\alpha}\mathcal{D}_\alpha
\end{aligned} \tag{204}$$

Using the above result in the underlined term in the last of Eqs. (203)

$$\left(G\gamma - 2\overline{F}_\gamma\right)^T \gamma = \mathcal{R}_{,\alpha}^T A_0 \mathcal{D}_\alpha G^{-1} \mathcal{D}_\beta^T A_0 \mathcal{R}_\beta - 2\mathcal{R}_{,\alpha}^T A_0 \mathcal{D}_\alpha G^{-1}\overline{Y}^T\mathcal{R} + \mathcal{R}^T\overline{Y}G^{-1}\overline{Y}^T\mathcal{R} \tag{205}$$

Finally Eq. 197 can be rewritten as

$$\begin{aligned}
2\Pi_2 =& \mathcal{R}^T\left(A + \overline{Y}G^{-1}\overline{Y}^T\right)\mathcal{R} + \gamma^T G\gamma + 2\mathcal{R}^T Y\gamma - 2\mathcal{R}^T F + 2\Pi_2^* \\
2\Pi_2^* =& \mathcal{R}_{,1}^T\left(B + A_0\mathcal{D}_1 G^{-1}\mathcal{D}_1^T A_0\right)\mathcal{R}_{,1} + 2\mathcal{R}_{,1}^T\left(C + A_0\mathcal{D}_1 G^{-1}\mathcal{D}_2^T A_0\right)\mathcal{R}_{,2} \\
&+ \mathcal{R}_{,2}^T\left(D + A_0\mathcal{D}_2 G^{-1}\mathcal{D}_2^T A_0\right)\mathcal{R}_{,2} + 2\mathcal{R}_{,\alpha}^T\left(H_\alpha - A_0\mathcal{D}_\alpha G^{-1}\overline{Y}^T\right)\mathcal{R}
\end{aligned} \tag{206}$$

Therefore, if we can determine Y and G such that Π^* goes to zero, then we have a Generalized Reissner-Mindlin potential energy of the form of Eq. 198 with the following solutions:

$$\left.\begin{aligned}
B + A_0\mathcal{D}_1 G^{-1}\mathcal{D}_1^T A_0 &= 0 \\
C + A_0\mathcal{D}_1 G^{-1}\mathcal{D}_2^T A_0 &= 0 \\
D + A_0\mathcal{D}_2 G^{-1}\mathcal{D}_2^T A_0 &= 0
\end{aligned}\right\} \quad \text{Solve for G (78 equations, 9 unknowns)} \tag{207}$$

$$\left.H_\alpha - A_0\mathcal{D}_\alpha G^{-1}\overline{Y}^T = 0\right\} \quad \text{Solve for Y (72 equations, 36 unknowns)} \tag{208}$$

$$
\begin{aligned}
X &= A + \overline{Y} G^{-1} \overline{Y}^T \\
F_{\mathcal{R}} &= F \\
F_{\gamma} &= 0
\end{aligned}
\tag{209}
$$

The 30 additional unknowns come from the warping constraints in Eq. 187. Since the number of equations exceeds the number of unknowns, the solution is obtained through a least-squares approach. Thus, the second order asymptotically correct strain energy has been packaged into a form which can be directly input in plate 2D solvers. This transformation procedure described above is valid as long as the second-order asymptotically correct potential energy is of the form of Eq. 195. It is not restricted to isotropic materials. But, for the given problem at hand, we have closed-form analytical solutions for X, Y and G. The stiffnesses associated with transverse shear are

$$
G = \begin{bmatrix} \frac{5}{6} G h(x_1, x_2) & 0 \\ 0 & \frac{5}{6} G h(x_1, x_2) \end{bmatrix}
\tag{210}
$$

The coupling stiffnesses between classical and transverse shear strain measures are

$$
\begin{aligned}
Y &= \begin{bmatrix} 0 & 0 \\ 0 & 0 \\ 0 & 0 \\ Y_1\zeta_1 & Y_2\zeta_2 \\ Y_3\zeta_2 & Y_3\zeta_1 \\ Y_2\zeta_1 & Y_1\zeta_2 \end{bmatrix} \\
Y_1 &= \frac{E\left(225 - 7\nu + 171\nu^2 + 5\nu^3\right)}{72\left(1-\nu^2\right)\left(5 - 2\nu + 5\nu^2\right)} h(x_1, x_2)^2 \\
Y_2 &= \frac{E\left(15 + 70\nu + 21\nu^2 + 98\nu^3\right)}{36\left(1-\nu^2\right)\left(5 - 2\nu + 5\nu^2\right)} h(x_1, x_2)^2 \\
Y_3 &= \frac{5E\left(3 + 2\nu + 3\nu^2\right)}{16\left(1+\nu\right)\left(5 - 2\nu + 5\nu^2\right)} h(x_1, x_2)^2
\end{aligned}
\tag{211}
$$

Finally, the solution for the A matrix (from which stiffnesses associated with the classical strain measures can be obtained as per Eq. 209) is now presented. The A matrix can be decoupled into the in- and out-of-plane components as

$$A = \begin{bmatrix} A_i & 0_{3\times3} \\ 0_{3\times3} & A_o \end{bmatrix} \tag{212}$$

The in-plane part is

$$\begin{aligned}
(A_i)_{11} &= \frac{Eh(x_1,x_2)}{1-\nu^2}\left[1 - \frac{1-2\nu}{6\,(1-\nu)}\zeta_1^2 + \frac{\nu^2}{6(1-\nu)}\zeta_2^2\right] \\
(A_i)_{12} = (A_i)_{23} &= -\frac{E\zeta_1\zeta_2 h(x_1,x_2)}{12(1+\nu)} \\
(A_i)_{13} &= \frac{Eh(x_1,x_2)\nu}{1-\nu^2}\left[1 + \frac{\nu}{6(1-\nu)}\left(\zeta_1^2+\zeta_2^2\right)\right] \\
(A_i)_{22} &= \frac{Eh(x_1,x_2)\nu}{1-\nu^2}\left[1 - \frac{1}{12}\left(\zeta_1^2+\zeta_2^2\right)\right] \\
(A_i)_{33}(\zeta_1,\zeta_2) &= (A_i)_{11}(\zeta_2,\zeta_1)
\end{aligned} \tag{213}$$

while the out-of-plane part is given by

$$\begin{aligned}
(A_o)_{11} &= \frac{Eh(x_1,x_2)^3}{12\,(1-\nu^2)}\left[1 + \frac{7\nu-57}{6\,(1-\nu)}\zeta_1^2 - \frac{25\nu^2}{3(1-\nu)}\zeta_2^2\right] \\
(A_o)_{12} = (A_o)_{23} &= -\frac{E\zeta_1\zeta_2\,(57+50\nu)\,h(x_1,x_2)}{144(1-\nu^2)} \\
(A_o)_{13} &= \frac{Eh(x_1,x_2)\nu}{1-\nu^2}\left[1 + \frac{7\nu-107}{6(1-\nu)}\left(\zeta_1^2+\zeta_2^2\right)\right] \\
(A_o)_{22} &= \frac{Eh(x_1,x_2)^3\nu}{24\,(1+\nu)}\left[1 - \frac{19}{4}\left(\zeta_1^2+\zeta_2^2\right)\right] \\
(A_o)_{33}(\zeta_1,\zeta_2) &= (A_o)_{11}(\zeta_2,\zeta_1)
\end{aligned} \tag{214}$$

To recover the 3D stress and strain, one needs to evaluate the warping to second-order. This helps particularly in the determination of stresses such as σ_{33}, which is generally smaller than the other two normal stresses, but still may come into play in some cases. Therefore, the warping is further perturbed, the fourth order potential energy is taken as the functional and the solution of the second-order warping comes

out to be of the form

$$\begin{aligned} w^{(2)} =& W_{SS\alpha\beta}\varepsilon_{,\alpha\beta} + W_{ST\alpha\beta}\zeta_\alpha\epsilon_{,\beta} + W_{TT\alpha\beta}\zeta_\alpha\zeta_\beta\varepsilon + w_L^{(2)} \\ w^{(2)} =& \lfloor w_1^{(2)} \quad w_2^{(2)} \quad w_3^{(2)} \rfloor^T \end{aligned} \tag{215}$$

The zeroth, first and second order warping can be used in Eq. 189. Unlike beam problems, the generalized strain derivatives cannot be evaluated using 'global' equilibrium equations alone. Therefore, once the potential energy of Eq. 198 is input into a plate solver and the distributions of the 2D strains with respect to x_1 and x_2 are known, the derivatives can be evaluated (if the problem does not offer the luxury of an analytical solution for the generalized plate strains, the derivatives can be obtained by finite difference procedures). Once the 3D strains, are known, the 3D stresses can be obtained by the relation given in Eq. 141.

This concludes the development of a theory for plates with variable thickness. Both the solutions for an 8×8 stiffness matrix and the recovery of 3D quantities have been outlined. No assumptions were made in the development of the kinematics. Instead, the presence of naturally occurring small parameters was exploited to present a mathematically rigorous development which is valid up to second order in any of the small parameters.

8.2 Comparison with ABAQUS

In this section, the results from the plate theory developed will be compared to results from ABAQUS [1]. ABAQUS is a general purpose finite-element tool commonly used for structural analysis. The problem under consideration is the linear elasticity solution for a plate with taper in one direction (x_1). The other plate dimension, x_2 is assumed to be very long, so that the plate can be modeled in ABAQUS using plane-strain elements. The loading for this problem, depicted in Fig. 8.2, is

$$\begin{aligned} \phi_i = \tau_\alpha = \beta_\alpha = 0 \\ \tau_3 = \beta_3 = \frac{p_0}{2}\sin\left(\frac{\pi x_1}{a}\right) \end{aligned} \tag{216}$$

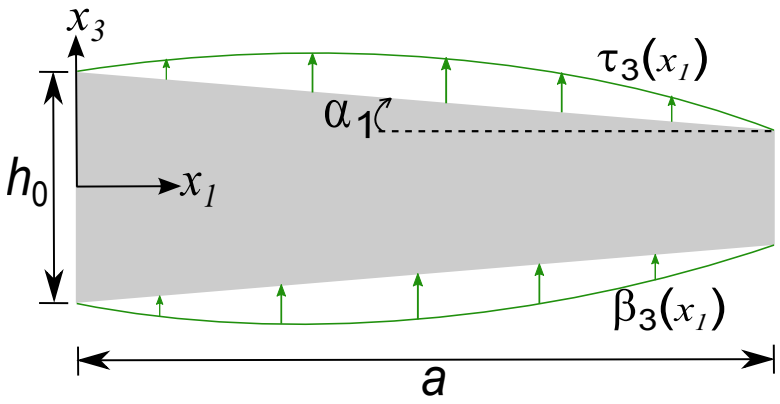

Figure 71: Plate with infinite dimension along x_2 (not shown on figure; along the normal into the plane of the paper) and linear taper along x_1; loaded at the top and bottom with sinusoidal loads

The ends of the plate at $x_1 = 0,\ a$ are assumed to be under simple support. The motivation for choosing the problem is that for plates of constant thickness, Pagano [82] gives the exact elasticity solutions under the same loading condition which is referred to as the cylindrical bending problem. For the case of varying thickness, the solutions will obviously not correspond to cylindrical bending, but nevertheless should be useful for testing the predictions of the current theory. The problem is set up with the values of ν, h_0/a and ζ_1 to be 0.3, 0.25 and 0.2 respectively. The final results are the non-dimensional 3D stresses (σ_{ij}/p_0) vs. $x_3/h(x_1)$ at $x_1 = a/2$. These are compared from three different methods, which are from ABAQUS, a VAM plate theory accounting for variable thickness as in Sec. 8.1 (VAM-corrected) and one accounting for variable thickness in the traditional way, i.e. by replacing h with $h(x_1, x_2)$ in a plate theory developed for constant-thickness plates (VAM-uncorrected). The ABAQUS model is made of 19,019 CPE8R elements (8-node bi-quadratic plane strain quadrilateral with reduced integration) and consists of a total of 57,798 nodes. The density of the mesh was chosen by refining the mesh further and further till the stress-traction boundary

conditions at $x_3 = \pm h(x_1, x_2)/2$ are satisfied with reasonable accuracy.

The solution of the problem from the plate theory of Sec. 8.1 requires the solution of the 2D problem. Before that, the load vector (the linear term $\mathcal{F}_{\mathcal{R}}$) is calculated as

$$F_{\mathcal{R}} = -\frac{\nu p_0 h(x_1, x_2)^2}{10(1-\nu)} \sin\left(\frac{\pi x_1}{a}\right) \begin{bmatrix} 0 & 0 & 0 & 1 & 0 & 1 \end{bmatrix}^T \tag{217}$$

The full list of plate equilibrium equations and linearized strain-displacement relations can be found in Refs. [124] and [94] respectively. They can be simplified since the plate is very long in the x_2 direction and hence the derivative of any quantity with respect to x_2 can be discarded. The equilibrium equations with the simple support boundary conditions yield the following solutions

$$\begin{aligned} N_{11} &= 0 \\ N_{12} &= 0 \\ M_{11} &= p_0 \left(\frac{a}{\pi}\right)^2 \sin\left(\frac{\pi x_1}{a}\right) \\ Q_1 &= p_0 \left(\frac{a}{\pi}\right) \cos\left(\frac{\pi x_1}{a}\right) \\ Q_2 &= M_{12,1} \end{aligned} \tag{218}$$

Using the plate constitutive law of Eq. 199, the 2D strains can be obtained, of which the following relations (obtained from the plate being very long in the x_2 direction) can be used to determine the remaining stress resultants

$$\begin{aligned} \epsilon^*_{22} &= 0 \\ \kappa^*_{22} &= 0 \\ 2\gamma^*_{23,1} &= \kappa^*_{12} + \kappa^*_{21} \end{aligned} \tag{219}$$

The solutions obtained are thus

$$\begin{aligned} N_{22} &= 0 \\ M_{12} &= 0 \end{aligned} \tag{220}$$

The solution for M_{22} is another lengthy expression with dependencies on both the sine and cosine of $\pi x_1/L$. These can be used to determine the final solutions for the

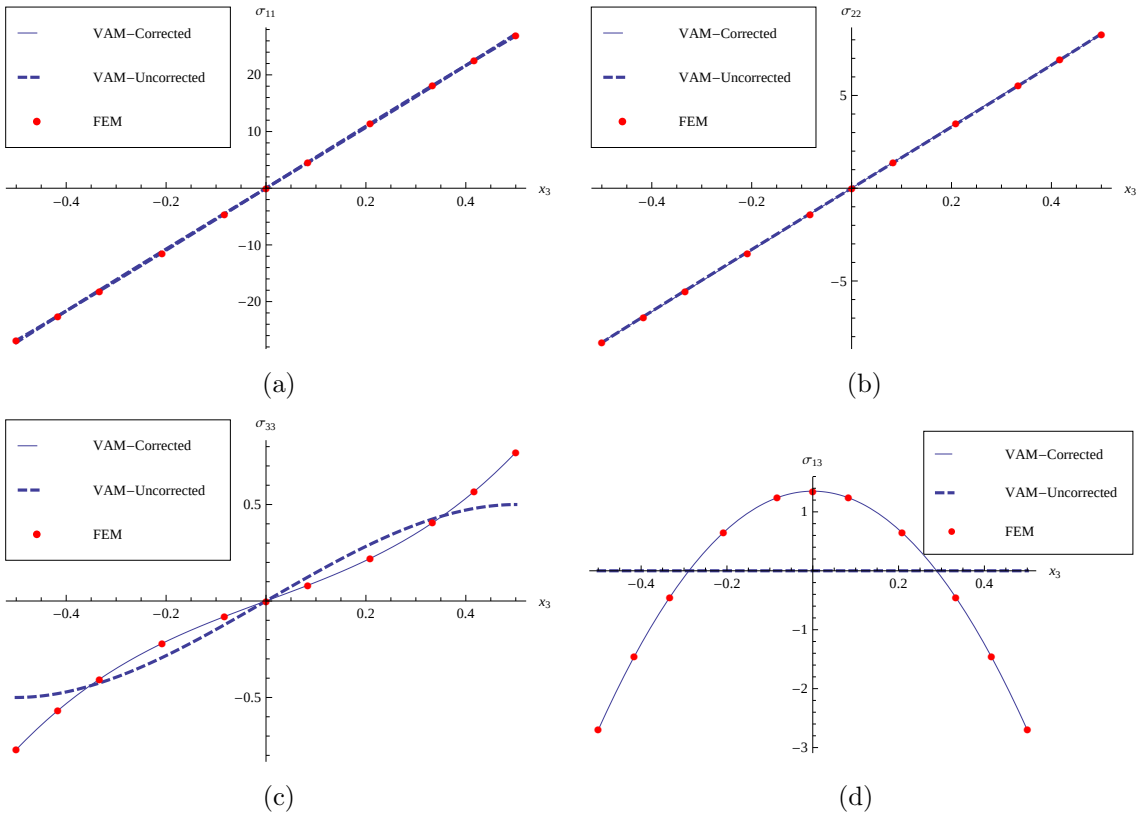

Figure 72: Stress recovery for the problem depicted in Fig. 8.2. Stress is normalized by p_0, while x_3 is by $h(x_1)$

2D strains. The solutions for the 2D strains and their derivatives can be used to determine the recovery. The results are now presented in Fig. 8.2.

It is clear from the results that while VAM-uncorrected does a good job of capturing the stresses σ_{11} and σ_{22}, the other two stress predictions are clearly in error. In fact, from the value at the ends, it is very evident that the stress-traction boundary conditions are violated as a consequence of ignoring the tilting of the outward normal. σ_{13} is predicted to vanish throughout, which is clearly not the case. On the other hand, all the stress distributions for VAM-corrected are in very good agreement with the ABAQUS results. This example clearly proves that to analyze plates of variable thickness, it is necessary to perform an analysis of the kind described in this chapter. Merely changing the thickness distributions may work for certain problems but clearly is not sufficiently general, nor can it guarantee that all aspects of the analysis

are captured with good agreement. This is because these kinds of approximations are not in tune with the mechanics of such a problem. Further as always, a theory developed using the VAM does not make any assumptions regarding the deformation and is suited to capture effects such as this, without any fundamental change in the procedure.

IX

CONCLUSIONS AND FUTURE WORK

Behind every human visage are flesh and blood, which are mortal; and ideas, which are immortal.

– V for Vendetta

The research work corresponding to the material presented in this thesis was fundamentally motivated by the need for the development of a next generation VABS. In that sense, the thesis represents a collection of problems each resulting in either an update to VABS or yielding some fundamental insight into the mechanics of the pertinent beam or plate problems. The ability to model initial curvature, obliqueness and extract a higher-fidelity recovery field have already been incorporated into VABS.

For all the problems addressed in this work, the solutions from VAM were compared with results from exact elasticity solutions (where they exist) or solutions from 3D FEM. Owing to the nature of the effects being studied (initial curvature, obliqueness etc.) the author found little sense in comparision with traditional beam theories which rely on some *ad hoc* assumptions regarding the cross-sectional deformation. For example, as has been pointed out earlier, any kind of assumptions made along the lines of traditional beam theories for the obliqueness models will produce results with very little correspondance to reality.

From the perspective of a purist, it may be argued that the plate problem does not fall under the purview of this thesis. The author however would beg to differ because possibilities such as plate elements being used to model rotorcraft flex-beams and reducing a plate model to that of a beam using the 'sequential dimensional reduction' idea (used in Sec. 4.6) as an alternative to model spanwise non-uniformity in beams

keep it under the common umbrella. Also most of the developments in this thesis are within the framework of a small strain, large dispacement analysis for dimensionally reducible structures. Therefore, they can be used in stability studies for which this assumption holds. These models cannot predict, for example, any kind of local shell buckling phenomenon as the warping variables are solved for in terms of the plate or beam generalized strains.

Most of the developments in this thesis are akin to the wheel of time, which has neither a beginning nor an end; what each development can be used to further accomplish cannot be fathomed in its entirety, but does not mean an attempt cannot be made to do so.

9.1 Accomplishments

9.1.1 Recovery for Spanwise Non-Uniform Beams

A beam theory has been presented based on the VAM for tapered strip-beam. The strip-beam is sufficiently thin that it can be assumed to be in a state of plane stress. The novel feature of the beam theory is that the effect of the taper parameter τ on the lateral-surface boundary conditions is included. This effect must be accounted for when performing a cross-sectional analysis, which gives the cross-sectional elastic constants necessary for solving the 1D beam equations, and the recovery relations necessary for accurately capturing stress, strain and displacement. To obtain accurate recovery relations, it is necessary to evaluate warping through second order in the small parameters, while only first-order warping is sufficient for obtaining accurate cross-sectional elastic constants. When the VAM-based beam theory is linearized and applied to problems for which elasticity solutions exist, such as constant axial force, constant bending moment and constant transverse shear force, the results agree quite well (within 5% of the exact elasticity ones) for all values of τ for a beam with δ up to 0.25. Beyond this value of δ, the values of τ for which the solutions are

good reduces; and, finally, for $\delta = 0.4$, the maximum value of τ is 0.26, which is satisfactory. Therefore, a VAM-based beam cross-sectional analysis can solve the problem of a tapered beam with sufficient accuracy.

Unfortunately, while extending the approach of Chapter 3 to model spanwise non-uniformity for the general case, issues with the determination of certain matrices in the second-order asymptotically correct theory and derivatives of the generalized Timoshenko stiffness matrix have stalled further development [42]. Therefore, the approach to model spanwise non-uniformity is now being pursued by a different methodology [68].

9.1.2 Analytical Verification of the Initial Curvature Effect

A beam theory has been proposed for the planar deformation of in-plane curved isotropic strips using the VAM. The beam theory was specialized for the linear case and successfully verified using classical elasticity solutions, both for its predictions of the strain energy per unit length and recovery relations for cross-sectional stress and strain. The theory was then used to compare results with VABS. The predicted behavior from VABS 3.3 and earlier versions was at variance with theory, and the problem was corrected in versions of VABS starting with 3.4. The error was caused by the way the asymptotic expansion of g and its powers was handled in the older versions of VABS. Moreover, results from the VAM-based beam theory suggest two ways of improving current VABS results. One is the pGT form, which is closer to the asymptotically correct second-order energy than the GT form. The other involves evaluation of the second-order warping to increase the accuracy of the sectional stress-strain recovery. Implementation of these two features will increase the accuracy and robustness of VABS.

Further, a beam theory has been developed for the in-plane deformation of an initially curved composite strip. The rigor in dimensional reduction from 3D elasticity

has been demonstrated using the results from the corresponding plate theory. The validity of this theory is limited to laminates whose in and out-of-plane deformations are decoupled (readers familiar with CLPT will recall that this corresponds to the vanishing of the matrix B). This is most common in the case of symmetric layup configurations. This work serves as a good validation tool for VABS and also provides analytical expressions for the stiffness matrix and stress-strain recovery, a rarity for composite structures, and consequently the author believes that this can serve as a verification tool for researchers working on slender, initially curved structural members made of composite material.

9.1.3 Higher Fidelity Stress-Strain-Displacement Recovery

The capabilities of VABS have been extended to capture a higher fidelity stress, strain and displacement recovery. The major step that is required for this functionality is to evaluate a second-order warping field. The development is valid for both the GT and GV theories of VABS and requires hardly any additional computational effort. Stress distributions over a few example cross-sections have been provided and the advantages of this feature are particularly found in the stresses σ_{22}, σ_{23} and σ_{33} for initially curved and/or twisted beams. Therefore, both the cross-sectional stiffness matrix and the recovery of 3D quantities are correct up to second-order in small parameters; bringing consistency in both aspects of VABS.

9.1.4 Oblique Cross-Sectional Analysis

Building on previous works [86, 91], this effort develops a cross-sectional model for which the user is not constrained to choose a reference cross-sectional plane that is perpendicular to the reference axis. An extensive validation of this model is preceded by the analytical development for two test cases which possess elasticity solutions, situations wherein the model comes in its own right and a brief outline of the theory. It

can be seen that the VABS results are invariant, whether the user chooses an orthogonal section or an oblique section. This is expected because the beam global behavior should be independent of the obliqueness of the reference cross-sectional plane, and the results are also in excellent agreement with other well established methods. Results grouped in four different categories (transverse shear, restrained warping, initial twist and stress recovery) were included with appropriate discussions, to demonstrate that VABS has the flexibility of modeling beams with a non-orthogonal section, an added advantage while determining the structural and aeroelastic response of a system such as a rotor blade. VABS is thus one of the few beam analysis tools that offers the user independent choices of reference line and reference cross-sectional plane.

9.1.5 Thin-Walled Beams: Interaction of Small Parameters

A theoretical framework has been provided for the problem of interaction of small parameters by considering the small parameter associated with wall thickness *ab initio*. An initially out-of-plane curved strip with initial twist was chosen as a representative problem and it was shown that in the zeroth-order analysis terms up to fourth-order in k_1 and k_2 were present in the stiffness matrix due to the presence of δ_h in the denominator. Two innovative approaches of this analysis are the splitting of the warping field motivated by the shell-like nature of the problem and a phantom step, which is used to determine certain terms and their orders in the warping field. An algorithm has been provided for the development of a shear-deformable theory and its finite-element implementation has been left for the future.

9.1.6 Plates of Variable Thickness

For plates whose thickness varies in the global directions linearly, a plate theory has been developed using the VAM. In a first of its kind development, if these linear variations along the x_1 and x_2 directions are given by ζ_1 and ζ_2, then the both the 8×8 stiffness matrix and the 3D stress and strain recovery are shown to contain these

taper parameters explicitly, as opposed to just being present by variation of the plate thickness. It is later clearly demonstrated using a problem with sinusoidal surface loads at the top and bottom that such an analysis is needed to accurately determine the stress, whose variation was compared with results from ABAQUS. In conclusion, the standard practice of simply changing the thickness in results for uniform plates will not yield the right results, since it models the mechanics of the plate wrongly, by disregarding the tilt of the outward-directed normals at the top and bottom surfaces in the boundary conditions.

9.2 Future Work

9.2.1 Principal Shear Axes in the GT Model

Ref. [34] follows up on the previous work of Ref. [33] and is clearly aimed at proving that the concept of principal shear axes is redundant. In beam theory, the idea of the principal axes of bending is well known. This is essentially the orientation of the cross-sectional axes for which the cross-bending term, i.e., the term in the stiffness matrix that couples the two bending deformations is zero. One could extend this concept to shearing deformation as well and define the principal shear to be the direction in which the term that couples the two shear deformations is zero.

This issue essentially pertains to the shear-coupling term or cross-shear term. Ref. [34] asserts on the basis of Ref. [79], that if the axes are chosen to be along the principal centroidal axes of bending, the shear coupling term vanishes. Results obtained from VABS suggest otherwise so that there seems to be no reason for the directions of principal bending and principal shear to coincide.

To decide this debate, consider the trapezoidal section, depicted in Fig. 73. The beam, of length 7.5, is cantilevered with the free end subjected to a transverse load P as shown. The material considered is isotropic with $E = 2.6 \times 10^{10}$ and $\nu = 0.3$. The reference line is chosen as the line of shear centers. Therefore, when a transverse load

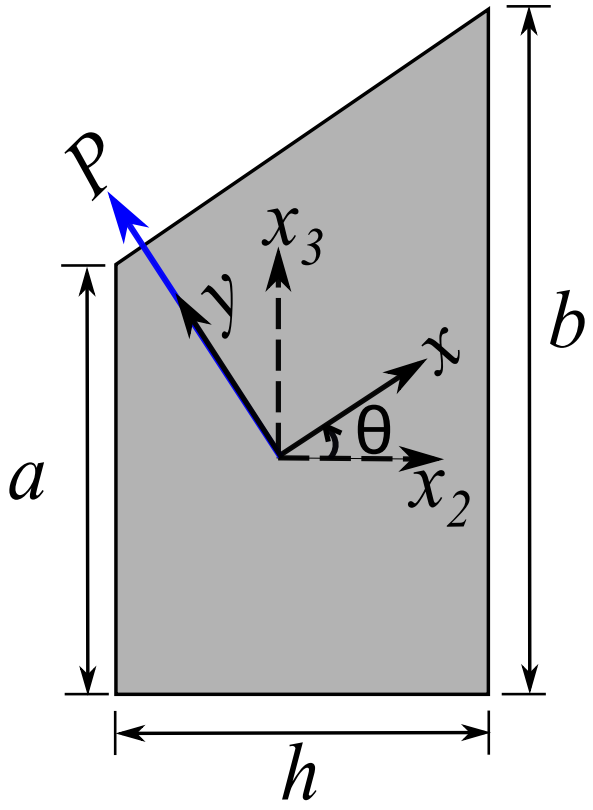

Figure 73: Trapezoidal cross section with $a = 2$; $b = 3$ and $h = 1$ with the origin at shear center

is applied at the shear center, the only deformations will be those of bending and shear. To calculate the displacements that arise purely out of shear, the bending solution can be subtracted from from the total solution. The shear displacement perpendicular to the load will determine the behavior of the cross-shear term. Consider the two methods outlined below:

1. In the first method, the refined flexibility matrix was obtained for the cross

section using VABS for the $x_2 - x_3$ coordinate axes:

$$\begin{Bmatrix} \gamma_{11} \\ 2\gamma_{12} \\ 2\gamma_{13} \\ \kappa_1 \\ \kappa_2 \\ \kappa_3 \end{Bmatrix} = \begin{bmatrix} \phi_{11} & 0 & 0 & 0 & \phi_{15} & \phi_{16} \\ 0 & \phi_{22} & \phi_{23} & 0 & 0 & 0 \\ 0 & \phi_{23} & \phi_{33} & 0 & 0 & 0 \\ 0 & 0 & 0 & \phi_{44} & 0 & 0 \\ \phi_{15} & 0 & 0 & 0 & \phi_{55} & \phi_{56} \\ \phi_{16} & 0 & 0 & 0 & \phi_{56} & \phi_{66} \end{bmatrix} \begin{Bmatrix} F_1 \\ F_2 \\ F_3 \\ M_1 \\ M_2 \\ M_3 \end{Bmatrix} \tag{221}$$

The loads at any axial coordinate can be easily determined as $F_1 = 0$, $F_2 = -P\sin(\theta)$, $F_3 = P\cos(\theta)$, $M_1 = 0$, $M_2 = -P\cos(\theta)(L - x_1)$ and $M_3 = -P\sin(\theta)(L - x_1)$. Specializing the geometrically exact strain-displacement relations of Ref. [46] for the linear case (assuming small displacements and rotations) and using the boundary conditions for the fixed end (average displacements and rotations are zero), the formula for the tip shear displacement orthogonal to P is:

$$U^{\text{shear}} = PL\left\{\phi_{23}\left[\cos(\theta)^2 - \sin(\theta)^2\right] + \sin(\theta)\cos(\theta)\left(\phi_{33} - \phi_{22}\right)\right\} \tag{222}$$

It should be noted that results recently obtained from the new SectionBuilder [14] code are identical with those obtained from VABS.

2. In the second method, the tip displacements were computed from ABAQUS using brick 3D finite elements (C3D20R) with the entire cross-sectional plane at the left end fixed (ENCASTRE boundary condition). The bending results were obtained from GEBT, using only the classical stiffness matrix from VABS (which considers only extension, torsion and bending). This solution shall be denoted for the remainder of this article as GEBT_c. The fixed boundary condition for the latter is the same as that of previous method. Using these results, the tip shear displacement perpendicular to the load can be computed.

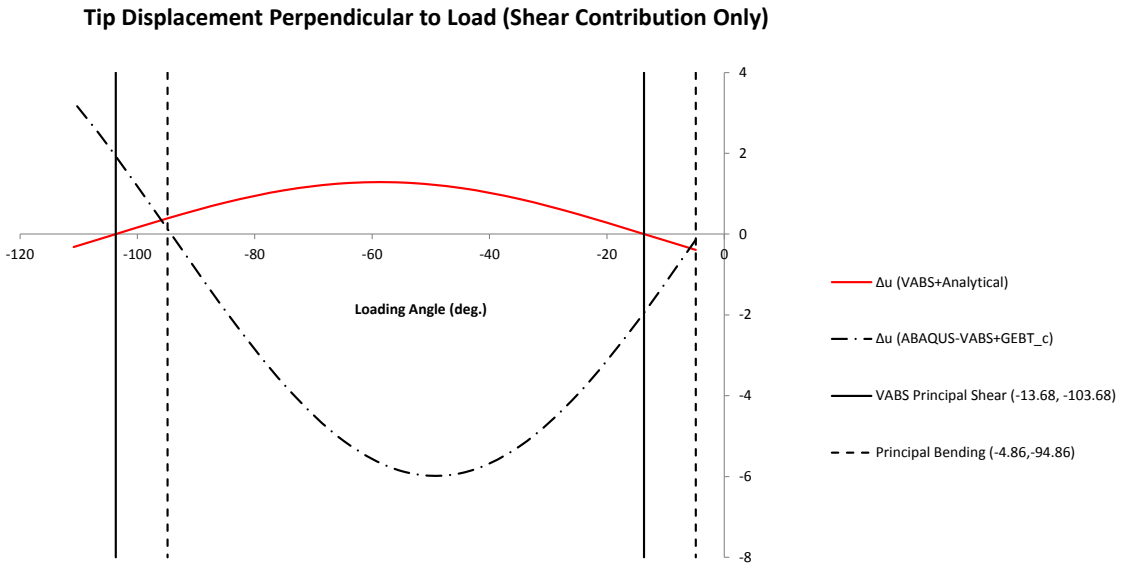

Figure 74: Tip shear displacement perpendicular to the load for varying θ as shown in Fig. 73

Plotting the results obtained from both these solution methodologies, one obtains Fig. 74. The analytical solution, which corresponds to the first method, vanishes when the load is applied at $\theta = -13.68°$, which thus occurs when the cross-shear term goes to zero and is in the direction of principal shear as predicted by VABS. However the second method's (based on 3D FEM) solutions vanish when the load is applied along the principal bending directions, which seems to suggest that Ref. [34]'s assertion is true. (All the values in this problem are assumed to be given in a consistent set of units. The load is assumed to be unity and the displacements are scaled by E). The discrepancy between the results was thought to be the difference in the application of the boundary conditions at the fixed end. While for beam theory solutions, the boundary conditions total six in number (average displacements and rotations are zero), ABAQUS models a fixed end by setting three displacements at every node of the section of the fixed end of the beam to be zero. These need not be necessarily truly equivalent but when one increases the length of the beam (and hence

by St. Venant's principle the way the boundary conditions are applied should cease to affect the solutions) to 15 and 22.5, the exact same behavior is observed. Therefore at this point it would seem that Prof. Dong's assertion concerning the principal shear is correct. A similar conclusion is obtained for another asymmetrical cross section: A thin-walled Z-section. It is evident further investigations are needed concerning the modeling of asymmetric cross-sections in VABS.

9.2.2 Unified GT-GV Model

The current Vlasov (GV) and Timoshenko (GT) models in VABS are complementary from the second order asymptotically correct energy. While the GT model offers a 6×6 stiffness matrix for 'regular' beams, the GV theory yields a 5×5 stiffness matrix for thin-walled beams with open sections. It is a well established fact that the GV theory is not valid for closed-section beams [46]. A single unified theory will no doubt be convenient for users. An approach to build a unified model was initiated by Volovoi et al. [116], who showed a decoupling only for the isotropic, prismatic case. An issue identified was the assignment of terms which contribute both to GT and GV Vlasov theories.

Therefore, the current approach [129] cannot be used to develop a unified theory. Further ambiguities which need to be addressed is the process of integration by parts before the Generalized Timoshenko transformation and definition of the Vlasov 1D variable. While integration by parts is used to remove the x_1 derivatives of warping, Ref. [127] discovered that integration by parts of the final second-order asymptotically correct strain energy results in negative shear stiffnesses. Such an ambiguity clearly does not exist for plates and shells [125].

Wempner [120] uses a warping variable $\alpha(x_1)$ not directly connected to torsion. An out-of-plane warping is introduced as

$$w_1 = \psi\left(x_2, x_3\right)\alpha\left(x_1\right) \tag{223}$$

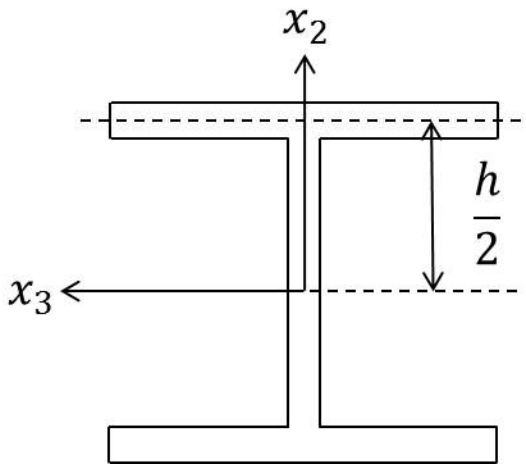

Figure 75: I-beam analyzed with a Vlasov variable: $\alpha(x_1)$

instead of the usual St. Venant assumption for torsion

$$w_1 = \psi(x_2, x_3)\,\overline{\kappa}_1(x_1) \tag{224}$$

The resulting theory developed has an 8×8 beam sectional stiffness matrix with 1D variables γ_{11}, γ_{12}, γ_{13}, κ_1, κ_2, κ_3, α and $\alpha_{,1}$. For 'regular' beams, one simply sets $\alpha = \kappa_1$. The constitutive relations of Eq. (8-100) in Ref. [120] show a theory with transverse shear and Vlasov effects. For example, for the I-beam shown in Fig. 75, the shear strains on the flanges can be written as

$$2\Gamma_{13} = 2\gamma_{13} + \frac{h}{2}(\kappa_1 - \alpha) \tag{225}$$

This equation clearly demonstrates both the usefulness of a variable such as α and the utility of a combined theory. The warping solution procedure in VABS is handicapped by the fact that it can only pick up the warping as cross-sectional variations of 1D variables that already exist in the problem. Therefore, the fundamental challenge is to revisit the beam kinematics and accommodate an α-like variable. Unlike Ref. [120], the VAM procedure never assumes warping to be of any form but rather is solved for from an asymptotic method. It should be noted that while such theories have been developed in the past by researchers [119], a fundamental understanding of

the α variable is clearly lacking. Studies in this direction are clearly promising given the utility of such a theory.

The final stiffness matrix will be an 8×8 array; from which the GT and GV model can be obtained. The study of boundary layer effects using the dispersion curves [114] should prove to be pertinent to this problem.

9.2.3 Stress Resultants from Recovery

In the beam theory of Ref. [46], the solutions to the beam force and moment resultants, F_i's and M_i's are usually obtained from the 1D analysis of the problem. In the final step, when the 3D stresses are recovered from the cross-sectional analysis, it is expected these integrate out (using the appropriate formulae) to the resultants which are used as inputs to the recovery. This serves as a good internal check for the beam analysis, i.e. verifying the consistency between the 2D and 1D parts of the problem. Therefore using these well-known formulae, the stresses can be integrated using standard Gaussian quadrature rules to obtain back the stress resultants. Without significant effort, such a feature can be added into the VABS program.

Consider the thin-walled three celled section shown in Fig. 76. The section is made of isotropic material with the following properties: $E = 0.26 \times 10^{12}$ psi and $\nu = 0.3$. The generalized shear center of the section as obtained by VABS was shown to be in excellent agreement with the results from ANSYS in Chapter 7 of Ref. [46]. Suppose the beam reference line was now taken to be the line of generalized shear centers. Further at a particular section, say the 1D analysis yields the solution for the stress resultants as all being zeros, except for $F_3 = 1 \times 10^5$ lb. For this case, the 3D stresses can be recovered from VABS.

The stress resultants obtained from the integration of the stresses are all zero except for M_1 and F_3. While F_3 is obtained as the value input (the expected value), the value for M_1 (that is expected to be zero) is 4×10^3 lb-in. The same values

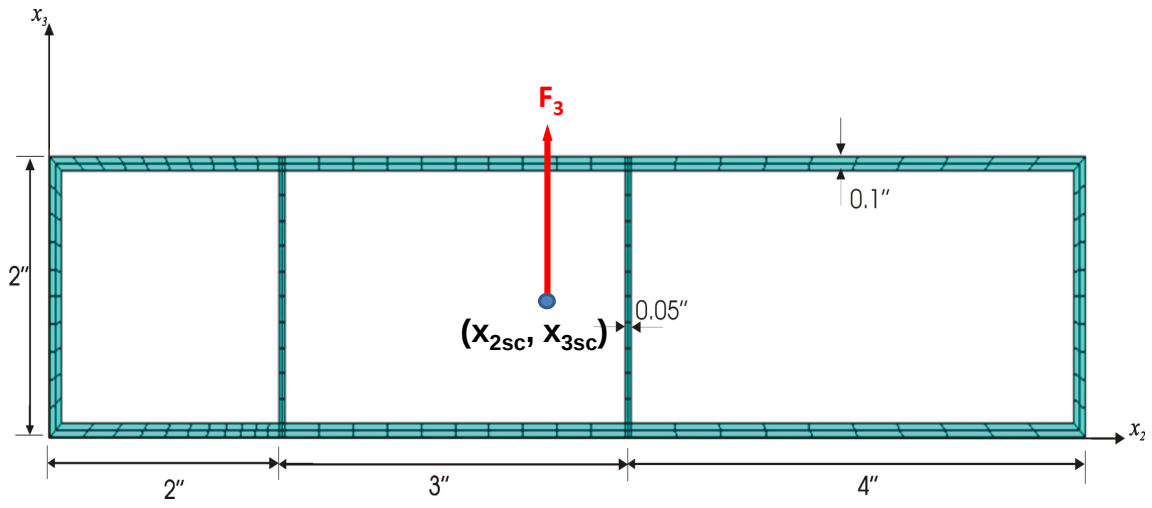

Figure 76: Cross section having three closed cells

were obtained on further refinements of the mesh indicating that these were the final converged results.

It is important to state here that the stress resultants in the beam theory of Ref. [46] are defined as those being conjugate to the 1D strain measures of the potential energy per unit length. It could be argued that the condition of the appropriate stress integrals being equal to the stress resultants is never enforced. However structural engineers expect a consistency between the stress resultants and beam forces and moments. Hence further investigation is required in relating the 1D force and moment variables in terms of the 3D stresses.

9.2.4 Miscellany

Some other avenues of fundamental and applied research in the framework of the analysis of beams and plates described in this research are listed below:

- Verification and validation of VABS is an continuous process. An essential aspect of this process is the identification of pertinent papers with new developments and exact elasticity solutions. Since VABS is a general cross-sectional analysis tool, all such solutions should fall under its purview. A sample list of

such papers has been provided in Sec. 2.1.

- The author also advocates the construction of general finite-element/ finite-difference based shell and 1D Vlasov solvers; otherwise the comparisons for any developments in these areas will be restricted to problems which have simple closed-form analytical solutions such as the works of Refs. [125] and [134].

- Another potential area of research is the development of a beam damping model similar to the development of Ref. [28]. The question to be answered is: just as the 3D elastic properties are reduced to a stiffness matrix, can the 3D viscoelastic properties be used to obtain a damping matrix? Further detailed investigation is required on this subject matter.

- One might consider moving out of the linear elastic regime and accounting for nonlinear elastic strain and metal plasticity. This will require strain measures such as the logarithmic functions introduced by Henky [4] and iteration between the local and global analyses.

- In the framework of dimensionally reducible structures, models can also developed for studies on damage and crashworthiness. There are a few studies on similar lines concerning failure predictions based on the Tsai-Wu-Hahn criterion [85].

- Avenues for applied research include structural models which account for MEMS and piezoelectric devices. Smart or intelligent structures are often designed with these devices for a variety of reasons such as wave guiding. It is expected that beam or plate modeling when accounting for such structures will have to be done with additional generalized strain measures [88].

APPENDIX A

MODIFICATION OF THE ANALYSIS FOR CURVED AND TWISTED BEAMS

In the light of the developments presented in the Chapter 4, the following equations have been modified in the VABS 3.4 code. For the original form of the equations and any further details, the reader is encouraged to consult Ref. [46]. Note that $\sqrt{g}$ is expanded as

$$\begin{aligned}
\sqrt{g} &= \beta_{11} - y_2 k_3 + y_3 k_2 = g_0 + g_1 \\
\frac{1}{\sqrt{g}} &= \frac{1}{\beta_{11}} + \frac{y_2 k_3 - y_3 k_2}{\beta_{11}^2} + \frac{(y_2 k_3 - y_3 k_2)^2}{\beta_{11}^3} + O(k_i^3) \\
&= \gamma g_0 + \gamma g_1 + \gamma g_2 + O(k_i^3)
\end{aligned} \tag{226}$$

The strain operators defined in Eqs. (3.94) – (3.99) in Ref. [46] are modified as:

$$\begin{aligned}
\Gamma_\beta &= -\frac{1}{\sqrt{g}} \left(\beta_{12} \frac{\partial}{\partial y_2} + \beta_{13} \frac{\partial}{\partial y_3} \right) \\
&= -(\gamma g_0 + \gamma g_1 + \gamma g_2) \left(\beta_{12} \frac{\partial}{\partial y_2} + \beta_{13} \frac{\partial}{\partial y_3} \right) \\
&= \Gamma_{\beta_0} + \Gamma_{\beta_1} + \Gamma_{\beta_2}
\end{aligned} \tag{227}$$

$$\Gamma_{a\beta} = \begin{bmatrix}
\Gamma_\beta & 0 & 0 \\
\frac{\partial}{\partial y_2} & \Gamma_\beta & 0 \\
\frac{\partial}{\partial y_3} & 0 & \Gamma_\beta \\
0 & \frac{\partial}{\partial y_2} & 0 \\
0 & \frac{\partial}{\partial y_3} & \frac{\partial}{\partial y_2} \\
0 & 0 & \frac{\partial}{\partial y_3}
\end{bmatrix} = \Gamma_{a\beta_0} + \Gamma_{a\beta_1} + \Gamma_{a\beta_2} \tag{228}$$

If $\beta_{1\alpha} = 0$ (cross section is chosen normal to the reference line), then $\Gamma_{a\beta} = \Gamma_{a\beta_0}$.

$$\Gamma_\epsilon = \frac{1}{\sqrt{g}} \begin{bmatrix} \beta_{11} & 0 & y_3 & -y_2 \\ \beta_{12} & -y_3 & 0 & 0 \\ \beta_{13} & y_2 & 0 & 0 \\ 0 & 0 & 0 & 0 \\ 0 & 0 & 0 & 0 \\ 0 & 0 & 0 & 0 \end{bmatrix} = \frac{1}{\sqrt{g}} \overline{\Gamma}_\epsilon \tag{229}$$

$$\Gamma_\ell = \frac{1}{\sqrt{g}} \begin{bmatrix} 1 & 0 & 0 \\ 0 & 1 & 0 \\ 0 & 0 & 1 \\ 0 & 0 & 0 \\ 0 & 0 & 0 \\ 0 & 0 & 0 \end{bmatrix} = \frac{1}{\sqrt{g}} \overline{\Gamma}_\ell \tag{230}$$

$$\Gamma_R = \frac{1}{\sqrt{g}} \begin{bmatrix} \Gamma_{hR} & -k_3 & k_2 \\ k_3 & \Gamma_{hR} & -k_1 \\ -k_2 & k_1 & \Gamma_{hR} \\ 0 & 0 & 0 \\ 0 & 0 & 0 \\ 0 & 0 & 0 \end{bmatrix} = \frac{1}{\sqrt{g}} \overline{\Gamma}_R \tag{231}$$

where

$$\Gamma_{hR} = k_1 \left(y_3 \frac{\partial}{\partial y_2} - y_2 \frac{\partial}{\partial y_3} \right) \tag{232}$$

Note above that the operator $\overline{\Gamma}_\epsilon$ contributes a zeroth-order term to the strain while $\overline{\Gamma}_\ell$ and $\overline{\Gamma}_R$ contribute to the first-order terms. Define:

$$\langle\langle \bullet \rangle\rangle = \langle \bullet \sqrt{g} \rangle \tag{233}$$

The expression for the strain energy is as given by Eq. (4.40) in Ref. [46]:

$$\begin{aligned} 2U =& V^T E V + 2V^T(D_{a\epsilon}\overline{\epsilon} + D_{aR}V + D_{a\ell}V') + \overline{\epsilon}^T D_{\epsilon\epsilon}\overline{\epsilon} + V^T D_{RR} V \\ &+ V'^T D_{\ell\ell} V' + 2V^T D_{R\epsilon}\overline{\epsilon} + 2V'^T D_{\ell\epsilon}\overline{\epsilon} + 2V^T D_{R\ell} V' \end{aligned} \tag{234}$$

The matrices defined in the above equation are now modified as:

$$\begin{aligned} E =& \langle\langle (\Gamma_{a\beta} S)^T D \Gamma_{a\beta} S\rangle\rangle \\ =& \langle (\Gamma_{a\beta} S)^T D (\Gamma_{a\beta} S)\sqrt{g}\rangle \\ =& \langle ((\Gamma_{a\beta_0} + \Gamma_{a\beta_1} + \Gamma_{a\beta_2})S)^T D ((\Gamma_{a\beta_0} + \Gamma_{a\beta_1} + \Gamma_{a\beta_2})S)\sqrt{g}\rangle \\ =& \underbrace{\langle (\Gamma_{a\beta_0} S)^T D \Gamma_{a\beta_0} S g_0\rangle}_{E_0} + \underbrace{\langle (\Gamma_{a\beta_0} S)^T D \Gamma_{a\beta_0} S g_1\rangle + 2\langle (\Gamma_{a\beta_0} S)^T D \Gamma_{a\beta_1} S g_0\rangle}_{E_1} \\ &+ \underbrace{2\langle (\Gamma_{a\beta_0} S)^T D \Gamma_{a\beta_1} S g_1\rangle + 2\langle (\Gamma_{a\beta_0} S)^T D \Gamma_{a\beta_2} S g_0\rangle + \langle (\Gamma_{a\beta_1} S)^T D \Gamma_{a\beta_1} S g_0\rangle}_{E_2} \\ =& E_0 + E_1 + E_2 \end{aligned} \tag{235}$$

$$\begin{aligned} D_{a\epsilon} &= \langle\langle (\Gamma_{a\beta} S)^T D \Gamma_\epsilon\rangle\rangle \\ &= \langle (\Gamma_{a\beta} S)^T D \overline{\Gamma}_\epsilon\rangle \\ &= \langle (\Gamma_{a\beta_0} S)^T D \overline{\Gamma}_\epsilon\rangle + \langle (\Gamma_{a\beta_1} S)^T D \overline{\Gamma}_\epsilon\rangle + \langle (\Gamma_{a\beta_2} S)^T D \overline{\Gamma}_\epsilon\rangle \\ &= D_{a\epsilon_0} + D_{a\epsilon_1} + D_{a\epsilon_2} \end{aligned} \tag{236}$$

Again, if the cross section is normal to the reference line, $D_{a\epsilon} = D_{a\epsilon_0}$.

$$\begin{aligned} D_{aR} &= \langle\langle (\Gamma_{a\beta} S)^T D (\Gamma_R S)\rangle\rangle \\ &= \langle (\Gamma_{a\beta} S)^T D \overline{\Gamma}_R S\rangle \\ &= \langle (\Gamma_{a\beta_0} S)^T D \overline{\Gamma}_R S\rangle + \langle (\Gamma_{a\beta_1} S)^T D \overline{\Gamma}_R S\rangle \\ &= D_{aR_1} + D_{aR_2} \end{aligned} \tag{237}$$

Only terms up to the second order are kept. Again, $D_{aR_2} = 0$ if $\beta_{1a} = 0$.

$$\begin{aligned} D_{a\ell} &= \langle (\Gamma_{a\beta} S)^T D \overline{\Gamma}_\ell S\rangle \\ &= \langle (\Gamma_{a\beta_0} S)^T D \overline{\Gamma}_\ell S\rangle + \langle (\Gamma_{a\beta_1} S)^T D \overline{\Gamma}_\ell S\rangle \\ &= D_{a\ell_1} + D_{a\ell_2} \end{aligned} \tag{238}$$

$$
\begin{aligned}
D_{\epsilon\epsilon} &= \langle\langle \Gamma_\epsilon^T D\Gamma_\epsilon \rangle\rangle \\
&= \langle \frac{1}{\sqrt{g}} \overline{\Gamma}_\epsilon^T D\overline{\Gamma}_\epsilon \rangle \\
&= \langle \gamma g_0 \overline{\Gamma}_\epsilon^T D\overline{\Gamma}_\epsilon \rangle + \langle \gamma g_1 \overline{\Gamma}_\epsilon^T D\overline{\Gamma}_\epsilon \rangle + \langle \gamma g_2 \overline{\Gamma}_\epsilon^T D\overline{\Gamma}_\epsilon \rangle \\
&= D_{\epsilon\epsilon_0} + D_{\epsilon\epsilon_1} + D_{\epsilon\epsilon_2}
\end{aligned}
\tag{239}
$$

$$
\begin{aligned}
D_{RR} &= \langle\langle (\Gamma_R S)^T D\Gamma_R S \rangle\rangle \\
&= \langle \frac{1}{\sqrt{g}} (\overline{\Gamma}_R S)^T D\overline{\Gamma}_R S \rangle \\
&= \langle \gamma g_0 (\overline{\Gamma}_R S)^T D\overline{\Gamma}_R S \rangle
\end{aligned}
\tag{240}
$$

$$
\begin{aligned}
D_{\ell\ell} &= \langle\langle (\Gamma_\ell S)^T D\Gamma_\ell S \rangle\rangle \\
&= \langle \frac{1}{\sqrt{g}} (\overline{\Gamma}_\ell S)^T D\overline{\Gamma}_\ell S \rangle \\
&= \langle \gamma g_0 (\overline{\Gamma}_\ell S)^T D\overline{\Gamma}_\ell S \rangle
\end{aligned}
\tag{241}
$$

$$
\begin{aligned}
D_{R\epsilon} &= \langle\langle (\Gamma_R S)^T D\Gamma_\epsilon \rangle\rangle \\
&= \langle \frac{1}{\sqrt{g}} (\overline{\Gamma}_R S)^T D\overline{\Gamma}_\epsilon \rangle \\
&= \langle \gamma g_0 (\overline{\Gamma}_R S)^T D\overline{\Gamma}_\epsilon \rangle + \langle \gamma g_1 (\overline{\Gamma}_R S)^T D\overline{\Gamma}_\epsilon \rangle \\
&= D_{R\epsilon_1} + D_{R\epsilon_2}
\end{aligned}
\tag{242}
$$

$$
\begin{aligned}
D_{\ell\epsilon} &= \langle\langle (\Gamma_\ell S)^T D\Gamma_\epsilon \rangle\rangle \\
&= \langle \frac{1}{\sqrt{g}} (\overline{\Gamma}_\ell S)^T D\overline{\Gamma}_\epsilon \rangle \\
&= \langle \gamma g_0 (\overline{\Gamma}_\ell S)^T D\overline{\Gamma}_\epsilon \rangle + \langle \gamma g_1 (\overline{\Gamma}_\ell S)^T D\overline{\Gamma}_\epsilon \rangle \\
&= D_{\ell\epsilon_1} + D_{\ell\epsilon_2}
\end{aligned}
\tag{243}
$$

$$
\begin{aligned}
D_{R\ell} &= \langle\langle (\Gamma_R S)^T D\Gamma_\ell S \rangle\rangle \\
&= \langle \frac{1}{\sqrt{g}} (\overline{\Gamma}_R S)^T D\overline{\Gamma}_\ell S \rangle \\
&= \langle \gamma g_0 (\overline{\Gamma}_R S)^T D\overline{\Gamma}_\ell \rangle
\end{aligned}
\tag{244}
$$

From Eq. (234), the zeroth-order energy can be obtained.

$$2U_0 = V^T E_0 V + 2V^T D_{a\epsilon_0}\overline{\epsilon} + \overline{\epsilon}^T D_{\epsilon\epsilon_0}\overline{\epsilon} \tag{245}$$

This along with the constraints on the warping field (to render it unique) is used to obtain the zeroth-order warping, $V_0 (= \hat{V}_0\overline{\epsilon})$. This warping is now perturbed and substituted back in the energy:

$$\begin{aligned}2U =&(V_0+V_1)^T(E_0+E_1+E_2)(V_0+V_1) + 2(V_0+V_1)^T((D_{a\epsilon_0}+D_{a\epsilon_1}+D_{a\epsilon_2})\overline{\epsilon}\\ &+ (D_{aR_1}+D_{aR_2})(V_0+V_1) + (D_{a\ell_1}+D_{a\ell_2})(V_0'+V_1')) + \overline{\epsilon}^T(D_{\epsilon\epsilon_0}+D_{\epsilon\epsilon_1}+D_{\epsilon\epsilon_2})\overline{\epsilon}\\ &+ V_0^T D_{RR} V_0 + V_0'^T D_{\ell\ell} V_0' + 2(V_0+V_1)^T(D_{R\epsilon_1}+D_{R\epsilon_2})\overline{\epsilon} + 2(V_0'+V_1')^T(D_{\ell\epsilon_1}+D_{\ell\epsilon_2})\overline{\epsilon}\\ &+ 2V_0^T D_{R\ell} V_0'\end{aligned} \tag{246}$$

From the above equation, the zeroth and first-order terms are given as:

$$\begin{aligned}2U_0 + 2U_1 =& V_0^T E_0 V_0 + 2V_0^T D_{a\epsilon_0}\overline{\epsilon} + \overline{\epsilon}^T D_{\epsilon\epsilon_0}\overline{\epsilon} + \cancel{V_0^T E_0 V_1} + V_0^T E_1 V_0 + \cancel{V_1^T E_0 V_0} + 2V_0^T D_{a\epsilon_1}\overline{\epsilon}\\ &+ \cancel{2V_1^T D_{a\epsilon_0}\overline{\epsilon}} + 2V_0^T D_{aR_1} V_0 + 2V_0^T D_{a\ell_1} V_0' + \overline{\epsilon}^T D_{\epsilon\epsilon_1}\overline{\epsilon} + 2V_0^T D_{R\epsilon_1}\overline{\epsilon} + 2V_0'^T D_{\ell\epsilon_1}\overline{\epsilon}\end{aligned} \tag{247}$$

The terms canceled above correspond to the solution of the zeroth-order warping V_0. The second-order terms are

$$\begin{aligned}2U_2 =& V_0^T E_1 V_1 + V_0^T E_2 V_0 + V_1^T E_0 V_1 + V_1^T E_1 V_0 + 2V_0^T D_{a\epsilon_2}\overline{\epsilon} + 2V_1^T D_{a\epsilon_1}\overline{\epsilon} + 2V_0^T D_{aR_1} V_1\\ &+ 2V_0^T D_{aR_2} V_0 + 2V_1^T D_{aR_1} V_0 + 2V_0^T D_{a\ell_1} V_1' + 2V_0^T D_{a\ell_2} V_0' + 2V_1^T D_{a\ell_1} V_0' + \overline{\epsilon}^T D_{\epsilon\epsilon_2}\overline{\epsilon}\\ &+ V_0^T D_{RR} V_0 + V_0'^T D_{\ell\ell} V_0' + 2V_0^T D_{R\epsilon_2}\overline{\epsilon} + 2V_1^T D_{R\epsilon_1}\overline{\epsilon} + 2V_0'^T D_{\ell\epsilon_2}\overline{\epsilon} + 2V_1' D_{\ell\epsilon_1}\overline{\epsilon} + 2V_0^T D_{R\ell} V_0'\end{aligned} \tag{248}$$

Only the terms related with V_1 are relevant in the process of the minimization of the strain energy. After performing integration by parts to get rid of the derivatives

of V_1 with respect to x_1, the relevant terms are

$$\begin{aligned}\mathcal{F} =& V_1^T E_0 V_1 + 2V_1^T(E_1 V_0 + D_{a\epsilon_1}\overline{\epsilon} + (D_{aR_1} + D_{aR_1}^T)V_0 + D_{R\epsilon_1}\overline{\epsilon}) \\ &+ 2V_1^T((D_{a\ell_1} - D_{a\ell_1}^T)V_0' - D_{\ell\epsilon_1}\overline{\epsilon}') \\ =& V_1^T E_0 V_1 + 2V_1^T(E_1\hat{V}_0 + D_{a\epsilon_1} + (D_{aR_1} + D_{aR_1}^T)\hat{V}_0 + D_{R\epsilon_1})\overline{\epsilon} \\ &+ 2V_1^T((D_{a\ell_1} - D_{a\ell_1}^T)\hat{V}_0 - D_{\ell\epsilon_1})\overline{\epsilon}' \\ =& V_1^T E_0 V_1 + 2V_1^T D_R\overline{\epsilon} + 2V_1^T D_S\overline{\epsilon}'\end{aligned} \tag{249}$$

Keeping the constraints in mind, one can use the standard procedure of the calculus of variations to solve for the warping field. Hence

$$\begin{aligned}E_0 V_1 =& (D_c(\Psi^T D_c)^{-1}\Psi^T - \Delta)(D_R\overline{\epsilon} + D_S\overline{\epsilon}') \\ V_1 =& V_{1R}\overline{\epsilon} + V_{1S}\overline{\epsilon}'\end{aligned} \tag{250}$$

where Ψ is the kernel matrix for E_0 and D_c is the constraint matrix associated with warping (i.e., $E_0\Psi = 0$ and $V^T D_c = 0$, respectively). Using this, we may now obtain the second-order asymptotically correct strain energy as

$$2U = \overline{\epsilon}^T A\overline{\epsilon} + 2\overline{\epsilon}^T B\overline{\epsilon}' + \overline{\epsilon}'^T C\overline{\epsilon}' + 2\overline{\epsilon}^T D\overline{\epsilon}'' \tag{251}$$

The matrices in the above equation are defined as

$$\begin{aligned}A =& \hat{V}_0^T D_{a\epsilon_0} + D_{\epsilon\epsilon_0} + \hat{V}_0^T E_1\hat{V}_0 + 2\hat{V}_0^T D_{a\epsilon_1} + 2\hat{V}_0^T D_{aR_1}\hat{V}_0 + D_{\epsilon\epsilon_1} + 2\hat{V}_0^T D_{R\epsilon_1} \\ &+ \hat{V}_0^T E_2\hat{V}_0 + 2\hat{V}_0^T D_{a\epsilon_2} + 2\hat{V}_0^T D_{aR_2}\hat{V}_0 + D_{\epsilon\epsilon_2} + \hat{V}_0^T D_{RR}\hat{V}_0 + 2\hat{V}_0^T D_{R\epsilon_2} + V_{1R}^T\overline{D}_R \\ B =& \hat{V}_0^T D_{a\ell_1}\hat{V}_0 + D_{\ell\epsilon_1}^T\hat{V}_0 + \hat{V}_0^T D_{a\ell_2}\hat{V}_0 + D_{\ell\epsilon_2}^T\hat{V}_0 + \hat{V}_0^T D_{R\ell}\hat{V}_0 + \frac{1}{2}(V_{1R}^T\overline{D}_S + D_R^T V_{1S}) \\ &+ (\hat{V}_0^T D_{a\ell_1} + D_{\ell\epsilon_1}^T)V_{1R} \\ C =& \hat{V}_0^T D_{\ell\ell}\hat{V}_0 + V_{1S}^T\overline{D}_S \\ D =& (\hat{V}_0^T D_{a\ell_1} + D_{\ell\epsilon_1}^T)V_{1S}\end{aligned} \tag{252}$$

where

$$\begin{aligned}\overline{D}_R =& (D_c(\Psi^T D_c)^{-1}\Psi^T + \Delta)D_R \\ \overline{D}_S =& (D_{a\ell_1} + D_{a\ell_1}^T)\hat{V}_0 + D_{\ell\epsilon_1}\end{aligned} \tag{253}$$

The generalized Timoshenko transformation now follows as that given in Ref. [41].

APPENDIX B

SOLUTION FOR THE Y MATRIX

The second-order asymptotically correct strain energy is converted into a GT form using equilibrium equations. The latest procedure for the GT transformation is outlined in Ref. [129] with which the symbols and notation used here are consistent with. The final GT form is written as

$$2\mathcal{U}_{GT} = \epsilon^T X \epsilon + 2\epsilon^T Y \gamma_s + \gamma_s^T G \gamma_s \tag{254}$$

In the zeroth-order solution, after determining G, the equations that are to be solved for Y are

$$AQG^{-1}Y^T A^{-1}Q = BA^{-1}Q \tag{255}$$

which is a system of eight equations in eight unknowns. After some matrix algebra, the solution to this equation is written as [129]

$$Y = B^T A^{-1} Q G \tag{256}$$

If one follows the therein derivation carefully, it can be observed that the solution process involved algebra with rectangular matrices, so the system goes from eight equations, eight unknowns to sixteen equations, eight unknowns and then back to eight equations, eight unknowns. Such a procedure gives incorrect results (even when the first two rows of $A^{-1}B$ are filled with zeros, as mentioned in Ref. [129]) for the obliqueness models. For example, the solution for a prismatic circular rod of Sec. 6.5 yields a non-zero extension-shear coupling in the stiffness matrix associated with the strain measures of the B frame. A better solution would be to recast Eq. (255) as

$$\begin{aligned} Ky &= r \\ y &= \begin{Bmatrix} Y_{11} & Y_{12} & Y_{13} & Y_{14} & Y_{21} & Y_{22} & Y_{23} & Y_{24} \end{Bmatrix}^T \end{aligned} \tag{257}$$

where K and r are 8×8 and 8×1 matrices respectively and obtained appropriately from Eq. (255). The best solution to this system of eight equations in eight unknowns is obtained using a Moore-Penrose pseudo-inverse based solver. This has been implemented in VABS using the well known linear algebra package LAPACK.

APPENDIX C

MOMENT VS. CURVATURE FOR A BEAM UNDER SELF-WEIGHT: ELASTICITY VS. VAM

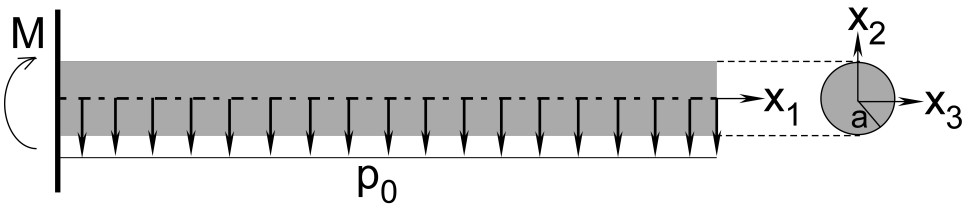

Figure 77: Isotropic, prismatic beam with a circular section loaded by self-weight

Consider a cantilevered beam loaded under its own weight ($p_0 = \rho A g$, A is the section area) as shown in Fig. 77. The beam is prismatic and made of isotropic material. The cross section of the beam is circular. All symbols have their usual meaning unless otherwise stated. The curvature of the beam centerline at the fixed end as per 3D elasticity is given by [76, 109]:

$$\frac{1}{r} = \frac{M}{EI}\left[1 - \frac{7 + 12\nu + 4\nu^2}{6(1+\nu)}\left(\frac{a}{l}\right)^2\right] \tag{258}$$

where the reaction moment at the fixed end, $M = -p_0 L^2/2$. This article demonstrates how to derive the same using the VAM of Ref. [46]. The reader is advised to refer to this text for the development of the equations used in the remainder of this article. We begin by stating the following kinematic relationship:

$$\frac{1}{r} = \overline{\kappa}_3(x_1 = L) = \kappa_3(x_1 = L) + (2\gamma_{12}(x_1))'\Big|_{x_1 = L} \tag{259}$$

The strain measures defined above are beam strains and defined as follows: $\overline{\kappa}_3$ is the curvature associated with the bending of the centerline, κ_3 and $2\gamma_{12}$ are the bending curvatures and shear strain associated with the cross section (i.e. a section perpendicular to the centerline) of the beam. The number subscripts in the strains are as usual: for example, in the case of curvatures, they denote the direction. Now employing the Generalized Timoshenko (GT) model,

$$\begin{aligned} \kappa_3(L) &= \frac{M}{EI} \\ 2\gamma_{12}(x_1) = \frac{p_0(L-x_1)}{S_2} &\implies 2\gamma'_{12}(L) = -\frac{p_0}{S_2} \end{aligned} \tag{260}$$

The shear stiffness for a cirular rod is given by

$$S_{22} = \frac{3E\pi a^2(1+\nu)}{8\nu^2+14\nu+7} \tag{261}$$

Assembling all these values

$$\frac{1}{r} = \frac{M}{EI}\left[1 - \frac{7+14\nu+8\nu^2}{6(1+\nu)}\left(\frac{a}{l}\right)^2\right] \tag{262}$$

The minor difference in the correction term, is due to the loss in the exactness of the theory while casting a mathematical model to a one usable from engineering perspective. However, the correction term is more important than the difference in the correction term as can be seen for the case of $\nu = 0.3$ in Fig. 78. The uncorrected solution refers to that from a traditional beam theory approach, wherein moment and curvature are simply related as $1/r = M/EI$.

The main purpose of this article is to demonstrate to the reader how the VAM can be used to derive such elasticity solutions for dimensionally-reducible structures. It is also to be noted that obtaining the elasticity solution for this problem is quite tedious [76]. On the other hand, to a researcher familiar with the VAM, derivation of this expression is quite simple. It is therefore the belief of this author that the VAM should be introduced to the student in advanced undergraduate/ graduate level structural analysis coursework as an efficient and elegant tool to study dimensionally reducible structures.

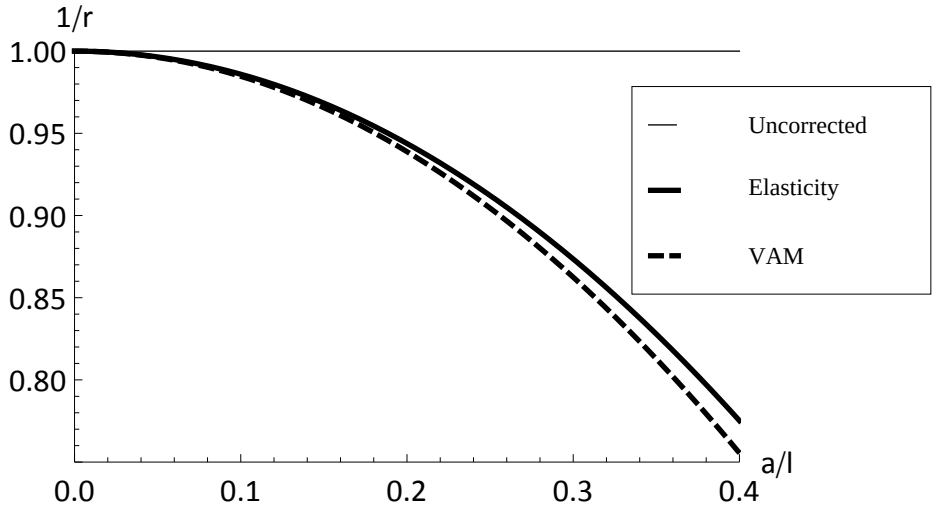

Figure 78: Comparison of Non-dimensional curvature for $\nu = 0.3$ using various approaches

APPENDIX D

RELEVANT TERMS IN WARPING CALCULATIONS

Recall from Chapter 5, the solution procedure for the nodal values of warping. The problem can be posed as: Assuming the presence of inherent small parameters in the problem, find the solution for u using an asymptotic procedure, such that the function

$$\mathcal{F}(u) = u^T A u + u^T B + C \tag{263}$$

is minimized, subject to the constraints

$$\begin{gathered} \mathcal{G}(u) = 0 \\ \text{Given,} \quad \mathcal{G}(u) = u^T D \end{gathered} \tag{264}$$

where u is a column matrix of unknowns and A (symmetric), B, C are known matrices; all of which can be expanded in terms of small parameters, i.e., $A = A_0 + A_1 + A_2 \ldots$ and so on. For simplicity it is assumed that the generalized strains and their x_1 derivatives are absorbed into the definitions of B and C, i.e., for example $B = P\overline{\epsilon} + Q\overline{\epsilon}' \ldots$, where P and Q are some known matrices extracted from the finite-element procedure. For the course of this article, the subscript denotes the order and not the component(s) of that matrix. It is well known that this problem can be posed equivalently as a single statement using a column matrix of lagrange multipliers, say λ, as a minimization of $\mathcal{H} = \mathcal{F} + \mathcal{G}\lambda$. Owing to the quadratic nature of the function, one can note that the N^{th} order solution for u will require keeping in terms up to order $2N$ in $\mathcal{F}$. This article will prove that while calculating the solution to the N^{th} order u, one needs to calculate *only* the term of order $2N$ in $\mathcal{F}$. This will be achieved using the Principle of Mathematical Induction (PMI). The steps in the proof are now sequentially listed:

1. For $n = 0$, the statement is trivially satisfied.

2. Assume the statement is true for all n such that $n \leq N$, for a general N . What this entails us is that only terms of order $2n$ need to be retained in the extended function to calculate u_n, $n = 0, 1, 2 \ldots N$. The relevant terms (superscript r) in the function to solve for are (λ_n is the Lagrange multiplier associated with the solution of u_n)

$$\mathcal{H}_n^r = u_n^T A_0 u_n + 2u_n^T \sum_{i=0}^{n} (A_i u_{n-i}) + u_n^T (B_n + D\lambda_n) \tag{265}$$

The final equations to solve for u_n and λ_n ($n = 0, 1, 2 \ldots N$) are

$$\begin{aligned} &2\sum_{i=0}^{n} (A_i u_{n-i}) + B_n + D\lambda_n = 0 \\ &u_n^T D = 0 \end{aligned} \tag{266}$$

3. It is now required to prove this statement for the solution of u_{N+1}. Again the relevant terms in the extended function are (terms which do not have u_{N+1} in the extended function can be dropped as they are constants for this problem)

$$\mathcal{H}_{N+1}^r = u_{N+1}^T A_0 u_{N+1} + u_{N+1}^T B_{N+1} + u_{N+1}^T \underbrace{\sum_{i=1}^{N} \left[2 \left(\sum_{j=0}^{N+1-i} A_j \right) u_i + B_i \right]}_{\chi} + u_{N+1}^T D\lambda_{N+1} \tag{267}$$

The term χ can be simplified as first of Eqs. (266) is valid for u_i ($i = 0, 1, 2 \ldots N$)

$$\chi = -D\sum_{k=0}^{N} (\lambda_k) + 2\sum_{j=0}^{N} (A_{N+1-j} u_j) \tag{268}$$

Replacing this back in Eq. (267), one obtains:

$$\begin{aligned} \mathcal{H}_{N+1}^r = &u_{N+1}^T A_0 u_{N+1} + u_{N+1}^T B_{N+1} + u_{N+1}^T \left[-D\sum_{k=0}^{N} (\lambda_k) + 2\sum_{j=0}^{N} (A_{N+1-j} u_j) \right] \\ &+ u_{N+1}^T D\lambda_{N+1} \end{aligned} \tag{269}$$

Now u_{N+1} is required to satisfy the warping constraint, $u_{N+1}D = 0$ and hence

$$\mathcal{H}^r_{N+1} = u^T_{N+1}A_0u_{N+1} + u^T_{N+1}B_{N+1} + u^T_{N+1}\left[2\sum_{j=0}^{N}(A_{N+1-j}u_j)\right] + u^T_{N+1}D\lambda_{N+1} \tag{270}$$

It is evident from the above expression that all the relevant terms are of order $2N + 2$ (A quick check can be carried out by adding all the indices since the index of a matrix denotes its order). This proves the statement for $N + 1$.

Hence by PMI, the statement is true.

APPENDIX E

STATIONARITY AND MINIMIZATION

The procedure to solve for the warping by determining the Euler-Lagrange equations invokes the stationarity of the total potential energy. The Euler-Lagrange equations are therefore necessary but not sufficient conditions for the minimization of the total potential energy. A simple way of establishing the minimization in the finite-element procedure (which reduces from a problem in calculus of variations to a problem in multi-variable calculus) is to check for the positive-definitiveness of E_0. However, if one wishes to check whether the solution is a minima in a problem of calculus of variations, a different set of conditions must be satisfied. This chapter will demonstrate that the warping is indeed a minima by considering the classical solution for a simple strip problem (for which the cross-sectional analysis problem is 1D).

Consider an isotropic strip as shown in Fig. 13, except with $k_3 = 0$. Following the zeroth-order analysis in Sec. 4.2, the problem can be re-stated as: Find a solution to w_1 and w_2 such that the the following functional is minimized

$$\mathcal{F} = \int_{-c}^{c} \mathcal{L}\, dx_2$$

$$\mathcal{L} = \lambda_1 w_1 + \lambda_2 w_2 + \frac{E}{2(1-\nu^2)}[(\overline{\gamma}_{11} - x_2\overline{\kappa}_3)^2 + \frac{1-\nu}{2}w_{1,2}^2 + 2\nu(\gamma_{11} - x_2\kappa_3)w_{2,2} + w_{2,2}^2] \tag{271}$$

where λ_1 and λ_2 are Lagrange multipliers associated with the constraints

$$\langle w_i \rangle = 0 \quad (i = 1, 2) \tag{272}$$

The condition that ensures stationarity yields the following solutions

$$\begin{aligned} \overline{w}_1 =& 0 \\ \overline{w}_2 =& -\nu x_2 \overline{\gamma}_{11} - \frac{1}{6}\nu(c^2 - 3x_2^2)\overline{\kappa}_3 \end{aligned} \tag{273}$$

Now for this solution to be a minima, additionally the following must be satisfied [96].

1. The warping solution must be embeddable in a field of extremals
2. The Lagrangian must be convex with respect to $w_{i,2}$
3. The Jacobi equation with vanishing end-point boundary-conditions must have only a trivial solution

The only possible parameters in the problem are those associated with the warping constraints (recall from Ref. [46], that the choice of the warping constraints are not unique). If the warping constraints were $\langle w_i \rangle = C_i$, then the solution for the warping field is:

$$\begin{aligned} w_1 =& \frac{C_1}{2c} \\ w_2 =& \frac{C_2}{2c} - \nu x_2 \overline{\gamma}_{11} - \frac{1}{6}\nu(c^2 - 3x_2^2)\overline{\kappa}_3 \end{aligned} \tag{274}$$

Therefore, one can see that the warping field is a smooth function of the set of possible parameters, thus making it embeddable in a field of extremals. The next condition is trivially satisfied as

$$\begin{aligned} \frac{\partial^2 \mathcal{L}}{\partial w_{1,2}^2} &= \frac{E}{2(1+\nu)} > 0 \\ \frac{\partial^2 \mathcal{L}}{\partial w_{2,2}^2} &= \frac{E}{(1-\nu^2)} > 0 \end{aligned} \tag{275}$$

Finally for the third condition, the functional of interest is

$$Q\left[\phi_1, \phi_2\right] = \delta^2 \mathcal{F}_{\overline{w}_1, \overline{w}_2}[\phi_1, \phi_2] \tag{276}$$

The second variation of $\mathcal{F}$ can be written as

$$\begin{aligned} \delta^2 \mathcal{F}_{w_1, w_2} &= f''(0) \\ f(\epsilon) &= \mathcal{F}\left[w_1 + \epsilon\phi_1, w_2 + \epsilon\phi_2\right] \end{aligned} \tag{277}$$

Therefore, for this specific problem the second variation with respect to the solutions of Eq. (273) is

$$Q\left[\phi_1, \phi_2\right] = \int_{-c}^{c} \left(\frac{E}{4(1+\nu)} \phi_{1,2}^2 + \frac{E}{2(1-\nu^2)} \phi_{2,2}^2 \right) dx_2 \tag{278}$$

The Euler-Lagrange equation(s) of the above functional (the Jacobi equations) are simply

$$\begin{aligned} \phi_{1,22} &= 0 \\ \phi_{2,22} &= 0 \end{aligned} \tag{279}$$

It is obvious to note that with zero endpoint boundary conditions, these equations will have only trivial solutions. Hence, the warping field solution has satisfied all the sufficient conditions for a minima.

REFERENCES

[1] ABAQUS, *Abaqus Unified FEA: Complete Solutions for Realistic Simulation*. Dassault Systemes, Vlizy-Villacoublay Cedex, France, 2013.

[2] Abdel-Jaber, M. S., Al-Qaisia, A. A., Abdel-Jaber, M., and Beale, R. G., "Nonlinear natural frequencies of an elastically restrained tapered beam," *Journal of Sound and Vibration*, vol. 313, no. 3-5, pp. 772–783, 2008.

[3] Akgoz, B. and Civalek, O., "Strain gradient elasticity and modified couple stress models for buckling analysis of axially loaded micro-scaled beams," *International Journal of Engineering Science*, vol. 49, no. 11, pp. 1268 – 1280, 2011.

[4] Anand, L., "On H. Hencky's approximate strain-energy function for moderate deformations," *Journal of Applied Mechanics*, vol. 46, pp. 78–82, March 1979.

[5] Andrade, A. and Camotim, D., "Lateral-torsional buckling of singly symmetric tapered beams: theory and applications," *Journal of Engineering Mechanics*, vol. 131, pp. 586–597, June 2005.

[6] Armanios, E. A. and Badir, A. M., "Free vibration analysis of anisotropic thin-walled closed-section beams," *AIAA Journal*, vol. 33, pp. 1905–1910, October 1995.

[7] Ashour, A. S., "The free vibration of symmetrically angle-ply laminated fully clamped skew plates," *Journal of Sound and Vibration*, vol. 323, pp. 444 – 450, 2009.

[8] Ashwill, T. D., Kanaby, G., Jackson, K., and Zuteck, M., "Development of the swept twist adaptive rotor (STAR) blade," in *Proceedings of the 48th AIAA Aerospace Sciences Meeting, Orlando, Florida*, (Reston, Virginia), AIAA, April 4 – 7, 2010. AIAA Paper 2010-1582.

[9] Barretta, R., "On the relative position of twist and shear centers in the orthotropic and fiberwise homogeneous SaintVenant beam theory," *International Journal of Solids and Structures*, vol. 49, no. 21, pp. 3038 – 3046, 2012.

[10] Barretta, R. and Diaco, M., "On the shear center in Saint-Venant beam theory," *Mechanics Research Communications*, vol. 52, pp. 52–56, 2013.

[11] Batra, R. C. and Xiao, J., "Finite deformations of curved laminated St. Venant-Kirchhoff beam using layer-wise third order shear and normal deformable beam theory (TSNDT)," *Composite Structures*, vol. 97, pp. 147 – 164, 2013.

[12] Bauchau, O. A., "DYMORE user's manual," Tech. Rep. http://dymoresolutions.com/dymore4_0/UsersManual/UsersManual.html, Dymore Solutions.

[13] Bauchau, O. A. and Craig, J. I., *Structural Analysis: With Applications to Aerospace Structures (Solid Mechanics and Its Applications)*. New York: Springer, 2010.

[14] Bauchau, O. A. and Han, S., "Three-dimensional beam theory for flexible multibody dynamics," *Journal of Computational and Nonlinear Dynamics*, 2014. http://dx.doi.org/10.1115/1.4025820.

[15] Berdichevsky, V. L., "Variational-asymptotic method of constructing a theory of shells," *PMM*, vol. 43, no. 4, pp. 664 – 687, 1979.

[16] Bhat, R. B., Laura, P. A. A., Gutierrez, R. G., Cortinez, V. H., and Sanzi, H. C., "Numerical experiments on the determination of natural frequencies of transverse vibrations of rectangular plates of non-uniform thickness," *Journal of Sound and Vibration*, vol. 138, no. 2, pp. 205 – 219, 1990.

[17] Borri, M., Ghiringhelli, G. L., and Merlini, T., "Linear analysis of naturally curved and twisted anisotropic beams," *Composites Engineering*, vol. 2, no. 5-7, pp. 433 – 456, 1992.

[18] Buannic, N. and Cartraud, P., "Higher-order effective modeling of periodic heterogeneous beams. I. asymptotic expansion method," *International Journal of Solids and Structures*, vol. 38, pp. 7139–7161, 2001.

[19] Carrera, E., Miglioretti, F., and Petrolo, M., "Computations and evaluations of higher-order theories for free vibration analysis of beams," *Journal of Sound and Vibration*, vol. 331, pp. 4269 – 4284, 2012.

[20] Carrera, E. and Petrolo, M., "On the effectiveness of higher-order terms in refined beam theories," *Journal of Applied Mechanics*, vol. 78, no. 2, 2010. article 021013.

[21] Cesnik, C. E. S., *Cross-Sectional Analysis of Initially Twisted and Curved Composite Beams*. PhD thesis, Aerospace Engineering, Georgia Institute of Technology, May 1994.

[22] Cesnik, C. E. S. and Hodges, D. H., "Stiffness constants for initially twisted and curved composite beams," *Applied Mechanics Reviews*, vol. 46, no. 11, Part 2, pp. S211 – S220, 1993.

[23] Cesnik, C. E. S. and Hodges, D. H., "VABS: a new concept for composite rotor blade cross-sectional modeling," *Journal of the American Helicopter Society*, vol. 42, pp. 27 – 38, January 1997.

[24] Cha, P. D. and Rinker, J. M., "Enforcing nodes to suppress vibration along a harmonically forced damped Euler-Bernoulli beam," *Journal of Vibration and Acoustics*, vol. 134, no. 5, p. 051010, 2012.

[25] Chandra, R. and Chopra, I., "Experimental-theoretical investigation of the vibration characteristics of rotating composite box beams," *Journal of Aircraft*, vol. 29, pp. 657 – 664, July-August 1992.

[26] Chandra, R., Stemple, A. D., and Chopra, I., "Thin-walled composite beams under bending, torsional, and extensional loads," *Journal of Aircraft*, vol. 27, no. 7, pp. 619 – 626, 1990.

[27] Chen, W., Li, L., and Xu, M., "A modified couple stress model for bending analysis of composite laminated beams with first order shear deformation," *Composite Structures*, vol. 56, pp. 2723 – 2732, 2009.

[28] Chortis, D. I., Chrysochoidis, N. A., Varelis, D. S., and Saravanos, D. A., "A damping mechanics model and a beam finite element for the free-vibration of laminated composite strips under in-plane loading," *Journal of Vibration and Acoustics*, vol. 330, no. 23, pp. 5660–5677, 2011.

[29] Danielson, D. A. and Hodges, D. H., "Nonlinear beam kinematics by decomposition of the rotation tensor," *Journal of Applied Mechanics*, vol. 54, no. 2, pp. 258 – 262, 1987.

[30] Das, D., Sahoo, P., and Saha, K., "Dynamic analysis of non-uniform taper bars in post-elastic regime under body force loading," *Applied Mathematical Modelling*, vol. 33, no. 11, pp. 4163–4183, 2009.

[31] De Rosa, M. A., Lippiello, M., Maurizi, M. J., and Martin, H. D., "Free vibration of elastically restrained cantilever tapered beams with concentrated viscous damping and mass," *Mechanics Research Communications*, vol. 37, no. 2, pp. 261–264, 2010.

[32] Dong, S. B., Kosmatka, J. B., and Lin, H. C., "On Saint-Venants problem for an inhomogeneous, anisotropic cylinder, part I: Generalized saint-venant solutions," *Journal of Applied Mechanics*, vol. 68, no. 3, pp. 376 – 381, 2001.

[33] Dong, S., Alpdogan, C., and Taciroglu, E., "Much ado about shear correction factors in timoshenko beam theory," *International Journal of Solids and Structures*, vol. 47, no. 13, pp. 1651–1665, 2010.

[34] Dong, S., Carbas, S., and Taciroglu, E., "On principal shear axes for correction factors in timoshenko beam theory," *International Journal of Solids and Structures*, vol. 50, no. 10, pp. 1681 – 1688, 2013.

[35] Ecsedi, I., "Some analytical solutions for Saint-Venant torsion of non-homogeneous anisotropic cylindrical bars," *Mechanics Research Communications*, vol. 52, pp. 95–100, 2013.

[36] Ghiringelli, G. L. and Mategazza, P., "Linear, straight and untwisted anisotropic beam section properties from solid finite elements," *Composites Engineering*, vol. 4, no. 12, pp. 1225 – 1239, 1994.

[37] Giavotto, V., Borri, M., Mantegazza, P., Ghiringhelli, G., Carmaschi, V., Maffioli, G. C., and Mussi, F., "Anisotropic beam theory and applications," *Computers and Structures*, vol. 16, no. 1-4, pp. 403 – 413, 1983.

[38] Gupta, A. P. and Bhardwaj, N., "Vibration of rectangular orthotropic elliptic plates of quadratically varying thickness resting on elastic foundation," *Journal of Vibration and Acoustics*, vol. 126, no. 1, pp. 132–140, 2004.

[39] Harursampath, D., *Non-classical non-linear effects in thin-walled composite beams*. PhD thesis, Georgia Institute of Technology, 1998.

[40] Ho, J. C., *Modeling spanwise nonuniformity in the cross-sectional analysis of composite beams*. PhD thesis, Georgia Institute of Technology, 2009.

[41] Ho, J. C., Yu, W., and Hodges, D. H., "Energy transformation to generalized timoshenko form by the variational asymptotic beam section analysis," in *Proceedings of the 51st Structures, Structural Dynamics and Materials Conference, Orlando, Florida*, (Reston, Virginia), AIAA, April 12 – 15, 2010. Paper AIAA-2010-3017.

[42] Ho, J. C., Yu, W., and Hodges, D. H., "Energy transformation to generalized Timoshenko form for nonuniform beams," *AIAA Journal*, vol. 48, no. 8, pp. 1268 – 1272, 2010.

[43] Hodges, D. H., "A mixed variational formulation based on exact intrinsic equations for dynamics of moving beams," *International Journal of Solids and Structures*, vol. 26, no. 11, pp. 1253 – 1273, 1990.

[44] Hodges, D. H., Atilgan, A. R., and Danielson, D. A., "A geometrically nonlinear theory of elastic plates," *Journal of Applied Mechanics*, vol. 60, pp. 109 – 116, March 1993.

[45] Hodges, D. H. and Dowell, E. H., "Nonlinear equations of motion for the elastic bending and torsion of twisted nonuniform rotor blades," Technical Note TN D-7818, NASA, 1974.

[46] Hodges, D. H., *Nonlinear Composite Beam Theory*. Reston, Virginia: AIAA, 2006.

[47] Hodges, D. H., Harursampath, D., Volovoi, V. V., and Cesnik, C. E. S., "Non-classical effects in non-linear analysis of pretwisted anisotropic strips," *International Journal of Non-Linear Mechanics*, vol. 34, pp. 259 – 277, March 1999.

[48] Hodges, D. H., Ho, J. C., and Yu, W., "The effect of taper on section constants for in-plane deformation of an isotropic strip," *Journal of Mechanics of Materials and Structures*, vol. 3, pp. 425 – 440, March 2008.

[49] Hodges, D. H. and Pierce, G. A., *Introduction to Structural Dynamics and Aeroelasticity*. Cambridge, U.K.: Cambridge University Press, 2nd ed., 2011.

[50] Hodges, D. H., Rajagopal, A., Ho, J. C., and Yu, W., "Stress and strain recovery for the in-plane deformation of an isotropic tapered strip-beam," *Journal of Mechanics of Materials and Structures*, vol. 5, pp. 963 – 975, June 2010.

[51] Hosseini-Hashemi, S., Taher, H. R. D., and Akhvan, H., "Vibration analysis of radially fgm sectorial plates of variable thickness on elastic foundations," *Composite Structures*, vol. 92, pp. 1734 – 1743, 2010.

[52] Houbolt, J. C. and Brooks, G. W., "Differential equations of motion for combined flapwise bending, chordwise bending and torsion of twisted nonuniform rotor blades," Report 1346, NACA, 1958. Supersedes NACA Technical Note 3905, 1957.

[53] Iesan, D., "On Saint-Venant's problem," *Archive for Rational mechanics and Analysis*, vol. 91, pp. 363–373, 1986.

[54] Jones, R. M., *Mechanics of Composite Materials*. New York, New York: McGraw Hill, 1975.

[55] Jung, S. N., Nagaraj, V. T., and Chopra, I., "A refined structural dynamics model for composite rotor blades," in *Proceedings of the 40th Structures, Structural Dynamics, and Materials Conference, St. Louis, Missouri*, (Reston, Virginia), AIAA, April 12 – 15, 1999. Paper AIAA-99-1485.

[56] Jung, S. N., Nagaraj, V. T., and Chopra, I., "Refined structural model for thin- and thick-walled composite rotor blades," *AIAA Journal*, vol. 40, pp. 105 – 116, January 2002.

[57] Kane, T. R., Likins, P. W., and Levinson, D. A., *Spacecraft Dynamics*. New York, New York: McGraw-Hill Book Company, 1983.

[58] Kargarnovin, M. H. and Joodaky, A., "Bending analysis of thin skew plates using extended Kantorovich method," in *ASME Conference Proceedings, no. 49163*, pp. 39–44, ASME, 2010.

[59] Kennedy, G. J., Hansen, J. S., and Martins, J. R. R. A., "A Timoshenko beam theory with pressure corrections for layered orthotropic beams," *International Journal of Solids and Structures*, vol. 48, pp. 2373 – 2382, 2011.

[60] Kim, C. and White, S. R., "Thick-walled composite beam theory including 3-D elastic effects and torsional warping," *International Journal of Solids and Structures*, vol. 34, no. 31–32, pp. 4237–4259, 1997.

[61] Kim, H. S. and Kim, J.-S., "A rankine-timonshenko-vlasov beam theory for anisotropic beams via an asymptotic strain energy transformation," *European Journal of Mechanics A/Solids*, vol. 40, pp. 131 – 138, 2013.

[62] Kim, J.-S. and Wang, K. W., "Vibration analysis of composite beams with end effects via the formal asymptotic method," *Journal of Vibration and Acoustics*, vol. 132, pp. 041003–1, 2010.

[63] Knowles, J. K. and Reissner, E., "Torsion and extension of helicoidal shells," *Quarterly of Applied Mathematics*, vol. 17, no. 4, pp. 400–422, 1960.

[64] Kosmatka, J. B., Lin, H. C., and Dong, S. B., "On Saint-Venants problem for an inhomogeneous, anisotropic cylinder, part II: Cross-sectional properties," *Journal of Applied Mechanics*, vol. 68, no. 3, pp. 382 – 391, 2001.

[65] Kovvali, R. K. and Hodges, D. H., "Verification of the variational asymptotic beam section (vabs) analysis for initially curved and twisted beams," *Journal of Aircraft*, vol. 49, pp. 861 – 869, May-June 2012.

[66] Krahula, J. L., "Shear formula for beams of variable cross section," *AIAA Journal*, vol. 131, pp. 1390–1391, October 1975.

[67] Kushnir, U. and Rabinovitch, O., "Nonlinear ferro-electro-elastic beam theory," *International Journal of Solids and Structures*, vol. 36, pp. 2397 – 2406, 2009.

[68] Lee, C.-Y. and Yu, W., "Variational asymptotic modeling of composite beams with spanwise heterogeneity," *Computers and Structures*, vol. 89, no. 15 – 16, pp. 1503 – 1511, 2011.

[69] Lee, S.-Y., "Finite element dynamic stability analysis of laminated composite skew plates containing cutouts based on HSDT," *Composites Science and Technology*, vol. 70, pp. 1249 – 1257, 2010.

[70] Leishman, J. G., *Principles of Helicopter Aerodynamics*. Cambridge, U.K.: Cambridge University Press, 2002.

[71] Leissa, A. W., "Vibration of plates," Tech. Rep. SP-160, NASA, January 1969.

[72] Li, J., Shi, C., Kong, X., Li, X., and Wu, W., "Free vibration of axially loaded composite beams with general boundary conditions using hyperbolic shear deformation theory," *Composite Structures*, vol. 97, pp. 1 – 14, 2013.

[73] Liew, K. M. and Lam, K. Y., "Application of two-dimensional orthogonal plate function to flexural vibration of skew plates," *Journal of Sound and Vibration*, vol. 139, no. 2, pp. 241 – 252, 1990.

[74] Liew, K. M., Xiang, Y., Kitipornchai, S., and Wang, C. M., "Vibration of thick skew plates based on Mindlin shear deformation plate theory," *Journal of Sound and Vibration*, vol. 168, no. 1, pp. 39 – 69, 1993.

[75] Lin, K. C. and Lin, C. W., "Finite deformation of 2-d laminated curved beams with variable curvatures," *International Journal of Non-Linear Mechanics*, vol. 46, pp. 1293 – 1304, 2011.

[76] Love, A. E. H., *Mathematical Theory of Elasticity*. New York, New York: Dover Publications, 4th ed., 1944.

[77] Ma, H. M., Gao, X. L., and Reddy, J. N., "A microstrcuture-dependent Timoshenko model based on a modified couple stress theory," *Journal of Mechanics and Physics of Solids*, vol. 56, pp. 3379 – 3391, 2009.

[78] Machado, S. P. and Saravia, C. M., "Shear-deformable thin-walled beams in tnternal and external resonance," *Composite Structures*, vol. 97, pp. 30 – 39, 2013.

[79] Mason, W. E. and Herrmann, L. R., "Elastic shear analysis of general prismatic beams," *J. Eng. Mech. Div.*, vol. 94, pp. 965–983, 1968.

[80] Mitra, M., Gopalakrishnan, S., and Bhat, M. S., "A new super convergent thin walled composite beam element for analysis of box beam structures," *International Journal of Solids and Structures*, vol. 41, pp. 1491 – 1518, 2004.

[81] Ogden, R. W., *Non-Linear Elastic Deformation*. Chicester: Ellis Horwood, 1984. Section 2.2.

[82] Pagano, N. J., "Exact solutions for composite laminates in cylindrical bending," *Journal of Composite Materials*, vol. 3, pp. 398 – 411, July 1969.

[83] Patil, M. J. and Hodges, D. H., "Flight dynamics of highly flexible flying wings," *Journal of Aircraft*, vol. 43, no. 6, pp. 1790–1799, 2006.

[84] Petrina, P. and Conway, H. D., "Deflection and moment data for rectangular plates of variable thickness," *Journal of Applied Mechanics*, vol. 39, no. 3, pp. 814–815, 1972.

[85] Pollayi, H., Harursampath, D., and Yu, W., "Evaluation of strength of component-laminates in strip-based mechanisms," *Composite Structures*, vol. 100, pp. 1 – 16, 2013.

[86] Popescu, B., Hodges, D. H., and Cesnik, C. E. S., "Obliqueness effects in asymptotic cross-sectional analysis of composite beams," *Computers and Structures*, vol. 76, no. 4, pp. 533 – 543, 2000.

[87] Popescu, B., *Asymptotically correct refinements in numerical cross-sectional analysis of composite beams*. PhD thesis, Georgia Institute of Technology, Atlanta, Georgia, U.S.A., 1998.

[88] Raghavan, A. and Cesnik, C. E. S., "3-D elasticity-based modeling of anisotropic piezocomposite transducers for guided wave structural health monitoring," *Journal of Vibration and Acoustics*, vol. 129, no. 6, pp. 739 – 751, 2007.

[89] Rajagopal, A., Hodges, D. H., and Yu, W., "Asymptotic beam theory for planar deformation of initially curved isotropic strips," *Thin-Walled Structures*, vol. 50, pp. 106–115, 2012.

[90] Rajagopal, A. and Hodges, D. H., "Analytical beam theory for the in-plane deformation of a composite strip with in-plane curvature," *Composite Structures*, vol. 94, pp. 3793 – 3798, 2012.

[91] Rajagopal, A. and Hodges, D. H., "Asymptotic approach to oblique cross-sectional analysis of beams," *Journal of Applied Mechanics*, vol. 81, no. 3, 2014. article 031015.

[92] Rao, B. N. and Rao, G. V., "Large amplitude vibrations of a tapered cantilever beam," *Journal of Sound and Vibration*, vol. 127, pp. 173–178, January 1988.

[93] Reissner, E., "On one-dimensional large-displacement finite-strain beam theory," *Studies in Applied Mathematics*, vol. LII, pp. 87 – 95, June 1973.

[94] Reissner, E., "On the derivation of two-dimensional strain displacement relations for small finite deformations of shear-deformable plates," *Journal of Applied Mechanics*, vol. 49, pp. 232 – 234, March 1982.

[95] Roy, S. and Yu, W., "Dimensional reduction of an end-electroded piezoelectric composite rod," *European Journal of Mechanics A/Solids*, vol. 28, no. 2, pp. 368 – 376, 2009.

[96] Sagan, H., *Introduction to the Calculus of Variations*. New York, USA: Dover, 1st ed., 1992.

[97] Santoro, R., "The line element-less method analysis of orthotropic beam for the DeSaint Venant torsion problem," *International Journal of Mechanical Sciences*, vol. 52, pp. 43 – 55, 2010.

[98] Shi, G. and Voyiadjis, G. Z., "A sixth-order theory of shear deformable beams with variational consistent boundary conditions," *Journal of Applied Mechanics*, vol. 78, no. 2, p. 021019, 2011.

[99] Silvestre, N. and Camotim, D., "First-order generalised beam theory for arbitrary orthotropic materials," *Thin-Walled Structures*, vol. 40, pp. 755–789, 2002.

[100] Silvestre, N. and Camotim, D., "Second-order generalised beam theory for arbitrary orthotropic materials," *Thin-Walled Structures*, vol. 40, pp. 791–820, 2002.

[101] Simo, J. C., "A finite strain beam formulation. the three-dimensional dynamic problem. part I," *Computer Methods in Applied Mechanics and Engineering*, vol. 49, pp. 55–70, 1985.

[102] Simo, J. C. and Vu-Quoc, L., "A three-dimensional finite-strain rod model. part II: Computational aspects," *Computer Methods in Applied Mechanics and Engineering*, vol. 58, pp. 79–116, 1986.

[103] Singh, B. and Saxena, V., "Transverse vibration of a rectangular plate with bidirectional thickness variation," *Journal of Sound and Vibration*, vol. 198, no. 1, pp. 51 – 65, 1996.

[104] Smith, E. C. and Chopra, I., "Formulation and evaluation of an analytical model for composite box-beams," *Journal of the American Helicopter Society*, vol. 36, pp. 23 – 35, July 1991.

[105] Sobuz, H. R., Ahmed, E., Sutan, N. M., Hasan, N. M. S., Uddin, M. A., and Uddin, M. J., "Bending and time-dependent responses of RC beams strengthened with bonded carbon fiber composite laminates," *Construction and Building Materials*, vol. 29, pp. 597 – 611, 2012.

[106] Steinbeck, A., Kugi, A., and Mang, H. A., "Energy-consistent shear coefficients for beams with circular cross sections and radially inhomogeneous materials," *International Journal of Solids and Structures*, vol. 48, pp. 1859 – 1868, 2011.

[107] Stemple, A. D. and Lee, S. W., "Finite element model for composite beams with arbitrary cross sectional warping," *AIAA Journal*, vol. 26, no. 12, pp. 1512 – 1520, 1988.

[108] Sutyrin, V. G., "Derivation of plate theory accounting asymptotically correct shear deformation," *Journal of Applied Mechanics*, vol. 64, pp. 905 – 915, December 1997.

[109] Timoshenko, S. P. and Goodier, J. N., *Theory of Elasticity*. Maidenhead, U.K.: McGraw-Hill, 3rd ed., 1970.

[110] Timoshenko, S. P., *History of Strength of Materials*. New York, New York: Dover Publications, 1st ed., 1953.

[111] Velazquez, E. and Kosmatka, J. B., "Stresses in half-elliptic curved beams subjected to transverse tip forces," *Journal of Applied Mechanics*, vol. 80, no. 1, 2012. article 021013.

[112] Vivio, F. and Vullo, V., "Closed form solutions of axisymmetric bending of circular plates having non-linear variable thickness," *International Journal of Mechanical Sciences*, vol. 52, pp. 1234 – 1252, 2010.

[113] Vlasov, V. Z., *Thin-Walled Elastic Beams*. National Science Foundation and Department of Commerce, 1961.

[114] Volovoi, V. V., *On End Effects in Prismatic Beams*. PhD thesis, Aerospace Engineering, Georgia Institute of Technology, January 1997.

[115] Volovoi, V. V. and Hodges, D. H., "Theory of anisotropic thin-walled beams," *Journal of Applied Mechanics*, vol. 67, pp. 453 – 459, Sept. 2000.

[116] Volovoi, V. V., Yu, W., and Hodges, D. H., "Asymptotic treatment of the Vlasov effect for composite beams," in *Proceedings of the 43rd Structures, Structural Dynamics and Materials Conference, Denver, Colorado*, (Reston, Virginia), AIAA, April 22 – 25, 2002.

[117] Wang, B., Zhao, J., and Zhou, S., "A micro scale Timoshenko beam model based on strain gradient elasticity theory," *European Journal of Mechanics A/Solids*, vol. 29, pp. 1591 – 1599, 2010.

[118] Wang, Q. and Yu, W., "Variational asymptotic modeling of the thermal problem of composite beams," *Composite Structures*, vol. 93, pp. 2330 – 2339, 2011.

[119] Weddingen, Y. V., *Evaluation of Innovative Concepts For Semi-Active And Active Rotorcraft Control*. PhD thesis, Georgia Institute of Technology, 2009.

[120] Wempner, G. A., *Mechanics of Solids with Application to Thin Bodies*. The Netherlands: Sijthoff and Noordhoff, 1981.

[121] Williams, M. D., van Keulen, F., and Sheplak, M., "Modeling of initially curved beam structures for design of multistable MEMS," *Journal of Applied Mechanics*, vol. 79, no. 1, p. 011006, 2012.

[122] Yeo, H., Truong, K., and Ormiston, R., "Assessment of 1D vs 3D methods for modeling rotor blade structural dynamics," in *Proceedings of the 51st Structures, Structural Dynamics, and Materials Conference, Orlando, Florida*, (Reston, Virginia), AIAA, April 4 – 7, 2010. Paper AIAA-2010-3044.

[123] Yin, W.-L., "Material and geometry effects on stress singularities in anisotropic heterogeneous composites," in *Proceedings of the 43rd Structures, Structural Dynamics and Materials Conference, Denver, Colarado*, (Reston, Virginia), AIAA, April 22 – 25, 1992.

[124] Yu, W., *Variational Asymptotic Modeling of Composite Dimensionally Reducible Structures*. PhD thesis, Aerospace Engineering, Georgia Institute of Technology, May 2002.

[125] Yu, W., "Mathematical construction of a reissner-mindlin plate theory for composite laminates," *International Journal of Solids and Structures*, vol. 42, pp. 6680–6699, 2005.

[126] Yu, W. and Blair, M., "GEBT: a general-purpose tool for nonlinear analysis of composite beams," *Composite Structures*, vol. 94, no. 9, pp. 2677 – 2689, 2012.

[127] Yu, W. and Hodges, D. H., "Elasticity solutions versus asymptotic sectional analysis of homogeneous, isotropic, prismatic beams," *Journal of Applied Mechanics*, vol. 71, no. 1, pp. 15 – 23, 2004.

[128] Yu, W. and Hodges, D. H., "A geometrically nonlinear shear deformation theory for composite shells," *Journal of Applied Mechanics*, vol. 71, no. 1, pp. 1 – 9, 2004.

[129] Yu, W., Ho, J. C., and Hodges, D. H., "Variational asymptotic beam sectional analysis – an updated version," *International Journal of Engineering Science*, vol. 59, pp. 40 – 64, 2012.

[130] Yu, W. and Hodges, D. H., "Generalized Timoshenko theory of the variational asymptotic beam sectional analysis," *Journal of the American Helicopter Society*, vol. 50, no. 1, pp. 46 – 55, 2005.

[131] Yu, W. and Hodges, D. H., "Best strip-beam properties derivable from classical lamination theory," *AIAA Journal*, vol. 46, pp. 1719 – 1724, July 2008.

[132] Yu, W., Hodges, D. H., and Ho, J. C., "Variational asymptotic beam sectional analysis – an updated version," *International Journal of Engineering Science*, vol. 59, pp. 40 – 64, October 2012.

[133] Yu, W., Hodges, D. H., and Volovoi, V. V., "Asymptotic construction of Reissner-like models for composite plates with accurate strain recovery," *International Journal of Solids and Structures*, vol. 39, no. 20, pp. 5185 – 5203, 2002.

[134] Yu, W., Hodges, D. H., Volovoi, V. V., and Fuchs, E. D., "A generalized Vlasov theory for composite beams," *Thin-Walled Structures*, vol. 43, pp. 1493 – 1511, 2005.

[135] Yu, W., Liao, L., Hodges, D. H., and Volovoi, V. V., "Theory of initially twisted, composite, thin-walled beams," *Thin-Walled Structures*, vol. 43, no. 8, pp. 1296 – 1311, 2005.

[136] Yu, W., Volovoi, V. V., Hodges, D. H., and Hong, X., "Validation of the variational asymptotic beam sectional (VABS) analysis," *AIAA Journal*, vol. 40, pp. 2105 – 2112, Oct. 2002.

VITA

Anurag Rajagopal was born on December 20, 1987 in Hyderabad, Andhra Pradesh, India. He received his Bachelors degree in Aerospace Engineering in 2009 from the Indian Institute of Technology Bombay (IITB). In August 2009, he entered the school of Aerospace Engineering at Georgia Institute of Technology to pursue graduate studies. This thesis is a result of more than four years of research mentored by Prof. Hodges. Parts of this work on spanwise non-uniformity and initial curvature were written up as a special problem, which was used to obtain a Masters degree from the same school in 2011.